A Study on the Mechanism of Dysregulation of Retinoic Acid Catabolism That Increases the Risk of Congenital Malformations in Embryos of Diabetic Mice

LEE, Man Yuen

A Thesis Submitted in Partial Fulfillment
of the Requirements for the Degree of
Doctor of Philosophy
in
Anatomy

The Chinese University of Hong Kong

September 2011

ProQuest LLC.
789 East Eisenhower Parkway
P.O. Box 1346
Ann Arbor, MI 48106 - 1346

Thesis/Assessment Committee

Professor SO Chan (Chair)
Professor Alisa Shum (Thesis Supervisor)
Professor KM Kwan (Committee Member)
Professor Peter McCaffery (External Examiner)
Professor SY Chan (External Examiner)

論文評審委員會

陳新安 教授 (主席)
沈秀媛 教授 (論文導師)
關健明 教授 (委員)
McCaffery 教授 (校外委員)
陳小圓 教授 (校外委員)

ACKNOWLEDGEMENTS

I would like to give my heartily thanks to my supervisor Prof. Alisa Shum whose encouragement, guidance and support from the initial to the final enabled me to develop an understanding of the project. She has provided the best environment for training me both as a scientist and as a person.

I owe special thanks to Prof. Peter McCaffery, Prof. Thomas Leung and Prof. Ronald Wang for their invaluable suggestions in designing different experiments and patience throughout the course of study. They are not just my mentors but also my friends. Whenever I needed support, they were there for me. Besides, I would also like to thank Ms. Heung Ling Choi and Dr. Maran Leung for demonstrating to me various experimental techniques during my project.

I would particularly like to thank Ms. Rachel Kwok, Mr. Alan Leung, Mr. Roy Chan, Mr. Wilson Leung, Mr. Walfred Tang who work together in the laboratory. They have all helped me through some very difficult times, and we have shared more than a few laughs along the way.

Last but not the least, thanks are never enough to my parents who have given me endless support and encouragement throughout the difficult time of study. I offer my regards and blessings to all of those who supported me in any respect during the completion of the thesis.

TABLE OF CONTENT

Title Page i
Thesis/Assessment Committee ii
Thesis/Assessment Committee (Chinese) iii
Acknowledgements iv
Table of Content v
List of Figures xi
List of Graphs xiii
List of Tables xviii
Abbreviations xxiii
Abstract xxiv
Abstract (Chinese) xxvi

Chapter 1: General Introduction

1.1 Diabetes Mellitus..... 2
1.2 Pre-existing Diabetic Pregnancy..... 3
1.2.1 Experimental animal model used for diabetic studies..... 3
1.2.1.1 Surgical method..... 4
1.2.1.2 Chemical induction of diabetes..... 4
1.2.1.3 Genetic animal model..... 6
1.2.2 Complication on pregnancy..... 7
1.2.2.1 Ovulation stage..... 7
1.2.2.2 Preimplantation embryo..... 7
1.2.2.3 Postimplantation embryo..... 9
1.2.2.4 Neonatal..... 10
1.2.3 Etiology..... 11
1.2.3.1 Depletion of myo-inositol..... 11
1.2.3.2 Alteration of protein kinase C (PKC) activity..... 12
1.2.3.3 Arachidonic acid and prostaglandin deficiency..... 13
1.2.3.4 Excess reactive oxygen species (ROS)..... 14
1.2.3.5 Folic acid depletion..... 14
1.2.3.6 Genetic predisposition..... 15
1.3 Retinoic Acid (RA)..... 16
1.3.1 RA homeostasis..... 17
1.3.2 RA signaling..... 18

1.3.3 RA teratogenicity..... 19
1.4 RA- and Maternal Diabetes-induced Malformations Share Similar Pathogenic Mechanisms..... 21
1.5 Strategy of the Thesis..... 23

Chapter 2: General Materials and Methods

2.1 Animals..... 27
2.2 Induction of Diabetes..... 28
2.3 Preparation of Retinoic Acid for Mouse Injection..... 29
2.4 RA-responsive Cell Line..... 29
2.4.1 Maintaining the cell line..... 29
2.4.2 Seeding and adding sample to 96-well plate..... 30
2.4.3 Preparation of RA standard solutions..... 31
2.4.3.1 Preparation of RA stock solution..... 31
2.4.3.2 Serial dilution of RA standard solutions..... 31
2.4.4 Staining of cells..... 32
2.5 High Pressure Liquid Chromatography (HPLC)..... 33
2.5.1 Chromatographic system..... 33
2.5.2 Preparation of standards..... 33
2.5.3 Extraction procedure..... 34
2.5.4 HPLC conditions..... 35
2.5.5 Recovery of sample..... 36
2.5.6 Protein assay..... 37
2.6 Real-Time Quantitative Reverse Transcription-Polymerase Chain Reaction (RT-PCR)..... 37
2.6.1 Collection and storage of tissues..... 37
2.6.2 Total RNA extraction..... 37
2.6.3 Reverse transcription..... 38
2.6.4 Real-time polymerase chain reaction..... 39
2.6.5 Preparation of cDNA standards..... 40
2.6.6 Mini-scale preparation of plasmid DNA..... 40
2.7 Whole mount *In Situ* Hybridization..... 41
2.7.1 Preparation of embryo sample..... 41
2.7.2 Hybridization..... 41
2.7.3 Post-hybridization wash..... 42
2.7.4 Post-antibody wash and signal development..... 43

2.7.5 Pre-absorption of antibody..... 44
2.7.6 Embryo powder preparation..... 44
2.8 Preparation of RNA Probe..... 44
2.8.1 Linearization of cDNA plasmid..... 44
2.8.2 *In vitro* transcription and labeling..... 45

Chapter 3: Analysis of *Cyp26* Expression in Embryos under Diabetic and Non-diabetic Conditions

3.1 Introduction..... 48
3.2 Experimental Design..... 52
3.3 Materials and Methods..... 54
3.3.1 Sample collection..... 54
3.3.2 Real-time quantitative RT-PCR..... 55
3.3.3 Whole mount *in situ* hybridization..... 56
3.3.4 Statistical analysis..... 57
3.4 Results..... 58
3.4.1 Expression of *Cyp26a1*, *Cyp26b1* and *Cyp26c1* at E9.0..... 58
3.4.2 Expression of *Cyp26a1* at E7.0 and E8.0..... 61
3.4.3 Changes in *Cyp26* expression in the embryo after maternal RA treatment..... 62
3.4.3.1 *Cyp26a1*..... 63
3.4.3.2 *Cyp26b1*..... 66
3.4.3.3 *Cyp26c1*..... 68
3.5 Discussion..... 72

Chapter 4: Susceptibility of *Cyp26a1* Mutant Embryos to Retinoic Acid-induced Malformations

4.1 Introduction..... 78
4.2 Experimental Design..... 83
4.3 Materials and Methods..... 86
4.3.1 Animal..... 86
4.3.2 DNA genotyping..... 86
4.3.2.1 Tissue lysis..... 86

4.3.2.2 PCR reaction..... 87
4.3.3 Whole mount *in situ* hybridization..... 88
4.3.4 Real-time quantitative RT-PCR..... 88
4.3.5 *In vitro* assay of RA degrading activity in tail bud tissue..... 89
4.3.5.1 Collection of tail bud..... 89
4.3.5.2 *In vitro* enzymatic reaction..... 90
4.3.6 Measurement of RA in the embryo after maternal treatment with RA by HPLC..... 91
4.3.7 Analysis of various types of RA-induced malformations..... 91
4.3.7.1 Cleft palate and renal malformations..... 92
4.3.7.2 Neural tube defects..... 92
4.3.8 Statistical analysis..... 93
4.4 Results..... 94
4.4.1 *Cyp26a1* expression..... 94
4.4.1.1 Expression pattern of *Cyp26a1* as determined by *in situ* hybridization..... 94
4.4.1.2 Expression level of *Cyp26a1* as determined by real-time quantitative RT-PCR..... 95
4.4.2 *In vitro* RA degrading activity in different groups of embryos... 99
4.4.3 Amount of RA in the embryo at 3 hr after maternal RA treatment as determined by HPLC..... 101
4.4.4 Susceptibility to RA teratogenicity..... 104
4.5 Discussion..... 108

Chapter 5: Normalization of *Cyp26a1* Expression in Reducing Susceptibility to Malformations

5.1 Introduction..... 115
5.2 Experimental Design..... 119
5.3 Materials and Methods..... 121
5.3.1 Determination of retinoid levels..... 121
5.3.1.1 Determination of retinol in serum of female mice by HPLC..... 121
5.3.1.2 Determination of RA in the embryo by RA-responsive cell line..... 122
5.3.2 Oral supplementation with RA..... 122
5.3.3 Real-time quantitative RT-PCR..... 123

5.3.4 *In vitro* assay of RA degrading activity in tail bud tissue..... 124
5.3.5 Induction of malformations..... 124
5.3.5.1 Caudal regression..... 124
5.3.5.2 Other malformations..... 125
5.3.6 Statistical analysis..... 125
5.4 Results..... 127
5.4.1 Serum retinol levels in female mice..... 127
5.4.2 Endogenous RA levels in E9.0 embryos..... 127
5.4.3 *Cyp26a1* expression levels in E9.0 embryos after RA supplementation..... 128
5.4.4 Teratogenicity of low dose of RA..... 130
5.4.5 RA levels in E9.0 embryos after RA supplementation..... 131
5.4.6 *In vitro* RA degrading activity in the tail bud after RA supplementation..... 132
5.4.7 Susceptibility to RA-induced caudal regression..... 133
5.4.8 *Cyp26a1* expression levels in E9.0 *Cyp26a1* mutant embryos after RA supplementation..... 135
5.4.9 Susceptibility to different types of malformations after RA supplementation..... 137
5.5 Discussion..... 143

Chapter 6: Effect of Hyperglycemia on *Cyp26a1* Expression

6.1 Introduction..... 148
6.2 Experimental Design..... 151
6.3 Materials and Methods..... 153
6.3.1 Treatment with phlorizin..... 153
6.3.2 *In vitro* culture of rat embryo..... 153
6.3.3 Preparation of rat serum..... 154
6.3.4 Whole mount *in situ* hybridization..... 155
6.3.5 Real-time quantitative RT-PCR..... 155
6.3.6 Detection of RA in the embryo by RA-responsive cell line..... 157
6.3.7 *In vitro* assay of RA degrading activity in embryonic tissues..... 158
6.3.8 Measurement of RA in embryonic tissues after maternal treatment with RA by RA-responsive cell line..... 158
6.3.9 Analysis of different types of RA-induced malformations..... 160
6.3.10 Statistical analysis..... 160

6.4 Results..... 161
6.4.1 Reduction of maternal blood glucose levels in diabetic mice after PHZ treatment.....161
6.4.2 Normalization of *Cyp26a1* expression in embryos of diabetic mice after maternal PHZ treatment..... 162
6.4.3 Normalization of endogenous RA levels in embryos of diabetic mice after maternal PHZ treatment..... 164
6.4.4 Normalization of *in vitro* RA degrading activity in embryos of diabetic mice after maternal PHZ treatment.....167
6.4.5 Normalization of RA levels in embryos of PHZ-treated diabetic mice at 3 hr after maternal injection of RA.....169
6.4.6 Reduction of susceptibility to various types of RA-induced malformations after maternal treatment with PHZ.....171
6.4.7 Dose-dependent down-regulation of *Cyp26a1* expression by glucose.....173
6.4.8 Dose-dependent reduction of endogenous RA level in rat embryos by glucose..... 177
6.5 Discussion.....178

Chapter 7: Conclusion and Future Perspectives 183

References 191

Figures

Graphs

LIST OF FIGURES

Figures	Title
3.1	Expression of 3 subtypes of *Cyp26* in E9.0 embryos of non-diabetic and diabetic mice detected by whole mount *in situ* hybridization.
3.2	Expression of *Cyp26a1* in E7.0 and E8.0 embryos of non-diabetic and diabetic mice detected by whole mount *in situ* hybridization.
3.3	Expression of *Cyp26a1* detected by whole mount *in situ* hybridization in embryos of non-diabetic and diabetic mice at different time points (0, 2, 4, 8 and 12 hr) after treatment with 50 mg/kg RA on E9.0.
3.4	Vibratome sections of the embryo of non-diabetic mouse at 2 hr after treatment with 50 mg/kg RA on E9.0 that had been subjected to whole mount *in situ* hybridization to detect *Cyp26a1*.
3.5	Vibratome sections of the embryo of non-diabetic mouse at 8 hr after treatment with 50 mg/kg RA on E9.0 that had been subjected to whole mount *in situ* hybridization to detect *Cyp26a1*.
3.6	Expression of *Cyp26b1* detected by whole mount *in situ* hybridization in embryos of non-diabetic and diabetic mice at different time points (0, 2, 4, 8 and 12 hr) after treatment with 50 mg/kg RA on E9.0.
3.7	Vibratome sections of the embryo of non-diabetic mouse at 2 hr after treatment with 50 mg/kg RA on E9.0 that had been subjected to whole mount *in situ* hybridization to detect *Cyp26b1*.
3.8	Vibratome sections of the embryo of non-diabetic mouse at 8 hr after treatment with 50 mg/kg RA on E9.0 that had been subjected to whole mount *in situ* hybridization to detect *Cyp26b1*.
3.9	Expression of *Cyp26c1* detected by whole mount *in situ* hybridization in embryos of non-diabetic and diabetic mice at different time points (0, 2, 4, 8 and 12 hr) after treatment with 50 mg/kg RA on E9.0.

LIST OF FIGURES

Figures	Title
4.1	Expression of *Cyp26a1* in *Cyp26a1* heterozygous (+/-) and wild-type (+/+) embryos of non-diabetic (ND) and diabetic (SD) mice at E9.0 detected by whole mount *in situ* hybridization.
5.1	Illustration of how the tail length and crump-rump length of a E13 mouse embryo were measured.
5.2	Gross morphology of E13 embryos of non-diabetic and diabetic mice supplemented with 1.25 mg/kg RA (1.25RA) or vehicle as control (CON).
6.1	Illustration of how the tail length and crump-rump length of a E18 fetus were measured.
6.2	Expression of *Cyp26a1* detected by whole mount *in situ* hybridization in E9.0 embryos of non-diabetic (ND) and diabetic (SD) mice treated with phlorizin (PHZ) or vehicle as control (CON).
6.3	Expression of *Cyp26a1* detected by whole mount *in situ* hybridization in rat embryos that had been cultured from head-fold stage at E9.5 for 24 hr in medium supplemented with varying concentrations of D-glucose (2, 3 and 4 mg/ml) or the solvent as control (CON).
6.4	Expression of *Cyp26a1* detected by whole mount *in situ* hybridization in rat embryos that had been cultured from head-fold stage at E9.5 for 48 hr in medium supplemented with varying concentrations of D-glucose (2, 3 and 4 mg/ml) or the solvent as control (CON).

LIST OF GRAPHS

Graphs	Title
3.1	Relative expression levels of (A) *Cyp26a1*, (B) *Cyp26b1* and (C) *Cyp26c1* in embryos of non-diabetic (ND) and diabetic (SD) mice at E9.0.
3.2	Relative expression levels of *Cyp26a1* in embryos of non-diabetic (ND) and diabetic (SD) mice at (A) E7.0 and (B) E8.0.
3.3	Relative expression levels of *Cyp26a1* in embryos of non-diabetic (ND) and diabetic (SD) mice at different time points after maternal injection of 50 mg/kg RA (RA) or vehicle as control (CON) on E9.0.
3.4	Relative expression levels of *Cyp26b1* in embryos of non-diabetic (ND) and diabetic (SD) mice at different time points after maternal injection of 50 mg/kg RA (RA) or vehicle as control (CON) on E9.0.
3.5	Relative expression levels of *Cyp26c1* in embryos of non-diabetic (ND) and diabetic (SD) mice at different time points after maternal injection of 50 mg/kg RA (RA) or vehicle as control (CON) on E9.0.
4.1	Relative expression levels of *Cyp26a1* in the tail bud of *Cyp26a1* heterozygous (+/-) and wild-type (+/+) embryos of non-diabetic (ND) and diabetic (SD) mice at E9.0.
4.2	Relative expression levels of *Cyp26a1* in the whole embryo (exclude tail bud) of *Cyp26a1* heterozygous (+/-) and wild-type (+/+) embryos of non-diabetic (ND) and diabetic (SD) mice at E9.0.
4.3	*In vitro* assay of RA degrading activity in the tail bud of *Cyp26a1* heterozygous (+/-) and wild-type (+/+) embryos of non-diabetic (ND) and diabetic (SD) mice at E9.0.

LIST OF GRAPHS

Graphs	Title
4.4	RA levels in *Cyp26a1* heterozygous (+/-) and wild-type (+/+) embryos of non-diabetic (ND) and diabetic (SD) mice at 3 hr after maternal injection of 25 mg/kg RA on E9.0 as determined by HPLC.
4.5	Incidence rates of (A) cleft palate and (B) renal malformations in E18 *Cyp26a1* heterozygous (+/−) and wild-type (+/+) fetuses of non-diabetic (ND) and diabetic (SD) mice induced by maternal injection of 40 mg/kg RA on E9.0.
4.6	Incidence rates of (A) exencephaly and (B) spina bifida in E13 *Cyp26a1* heterozygous (+/−) and wild-type (+/+) embryos of non-diabetic (ND) and diabetic (SD) mice induced by maternal injection of 25 mg/kg RA on E8.0.
5.1	Serum retinol levels in non-diabetic (ND) and diabetic (SD) mice under pregnant or non-pregnant (E9.0) status.
5.2	Endogenous RA levels in embryos at E9.0 under non-diabetic (ND) and diabetic (SD) pregnancy.
5.3	Relative expression levels of *Cyp26a1* in the tail bud of E9.0 embryos of non-diabetic (ND) and diabetic (SD) mice orally supplemented with 0.625 mg/kg RA (0.625RA) or 1.25 mg/kg RA (1.25RA) or vehicle as control (CON) on E8-22hr.
5.4	The ratio of tail length (TL) to crown-rump length (CRL) in E13 embryos of non-diabetic (ND) and diabetic (SD) mice orally supplemented with 1.25 mg/kg RA (1.25RA) or vehicle as control (CON) on E8-22hr.

LIST OF GRAPHS

Graphs	Title
5.5	RA levels in E9.0 embryos of non-diabetic (ND) and diabetic (SD) mice orally supplemented with 0.625 mg/kg RA (0.625RA) or vehicle as control (CON) on E8-22hr.
5.6	*In vitro* RA degrading activity in the tail bud of E9.0 embryos of non-diabetic (ND) and diabetic (SD) mice orally supplemented with 0.625 mg/kg RA (0.625RA) or vehicle as control (CON) on E8-22hr.
5.7	The ratio of tail length (TL) to crown-rump length (CRL) in E13 embryos of vehicle-fed control (CON) or RA-supplemented [0.625 mg/kg RA (0.625RA) or 1.25 mg/kg RA (1.25RA)] non-diabetic (ND) and diabetic (SD) mice challenged with a teratogenic dose of 25 mg/kg RA (25RA) on E9.0.
5.8	Relative expression levels of *Cyp26a1* in the tail bud of E9.0 *Cyp26a1* heterozygous (+/-) and wild-type (+/+) embryos of non-diabetic (ND) and diabetic (SD) mice orally supplemented with 0.625 mg/kg RA (0.625RA) or vehicle as control (CON) on E8-22hr.
5.9	Relative expression levels of *Cyp26a1* in the whole embryo (exclude tail bud) of E9.0 *Cyp26a1* heterozygous (+/-) and wild-type (+/+) embryos of non-diabetic (ND) and diabetic (SD) mice orally supplemented with 0.625 mg/kg RA (0.625RA) or vehicle as control (CON) on E8-22hr.
5.10	Incidence rates of cleft palate in E18 *Cyp26a1* heterozygous (+/−) and wild-type (+/+) fetuses of control (CON) or RA-supplemented [0.625 mg/kg RA (0.625RA)] non-diabetic (ND) and diabetic (SD) mice induced by maternal injection of 40 mg/kg RA on E9.0.

LIST OF GRAPHS

Graphs	Title
5.11	Incidence rates of renal malformations in E18 *Cyp26a1* heterozygous (+/−) and wild-type (+/+) fetuses of control (CON) or RA-supplemented [0.625 mg/kg RA (0.625RA)] non-diabetic (ND) and diabetic (SD) mice induced by maternal injection of 40 mg/kg RA on E9.0.
5.12	Incidence rates of exencephaly in E13 *Cyp26a1* heterozygous (+/−) and wild-type (+/+) embryos of control (CON) or RA-supplemented [0.625 mg/kg RA (0.625RA)] non-diabetic (ND) and diabetic (SD) mice induced by maternal injection of 25 mg/kg RA on E8.0.
5.13	Incidence rates of spina bifida in E13 *Cyp26a1* heterozygous (+/−) and wild-type (+/+) embryos of control (CON) or RA-supplemented [0.625 mg/kg RA (0.625RA)] non-diabetic (ND) and diabetic (SD) mice induced by maternal injection of 25 mg/kg RA on E8.0.
6.1	Maternal blood glucose levels in non-diabetic (ND) and diabetic (SD) mice after treatment with phlorizin (PHZ) or vehicle as control (CON).
6.2	Relative expression levels of the 3 subtypes of *Cyp26* in (A) tail bud and (B) whole embryo (exclude tail bud) of E9.0 embryos of non-diabetic (ND) and diabetic (SD) mice treated with phlorizin (PHZ) or vehicle as control (CON).
6.3	Endogenous RA levels in E9.0 embryos of non-diabetic (ND) and diabetic (SD) mice treated with phlorizin (PHZ) or vehicle as control (CON) as determined by RA-responsive cell line.
6.4	*In vitro* RA degrading activity in (A) tail bud and (B) whole embryo (exclude tail bud) of E9.0 embryos of non-diabetic (ND) and diabetic (SD) mice treated with phlorizin (PHZ) or vehicle as control (CON).

LIST OF GRAPHS

Graphs	Title
6.5	RA levels in (A) tail bud and (B) whole embryo (exclude tail bud) of embryos of control (CON) or phlorizin-treated (PHZ) non-diabetic (ND) and diabetic (SD) mice at 3 hr after maternal injection of 25 mg/kg RA on E9.0.
6.6	Incidence rates of (A) caudal regression, (B) cleft palate and (C) renal malformations in E18 embryos of control (CON) or phlorizin-treated (PHZ) non-diabetic (ND) and diabetic (SD) mice induced by maternal injection of 25 mg/kg RA on E9.0.
6.7	Relative expression levels of the 3 subtypes of *Cyp26* in (A) tail bud and (B) whole embryo (exclude tail bud) of rat embryos cultured for 24 hr in medium supplemented with varying concentrations of D-glucose or the solvent as control (CON).
6.8	Relative expression levels of the 3 subtypes of *Cyp26* in (A) tail bud and (B) whole embryo (exclude tail bud) of rat embryos cultured for 48 hr in medium supplemented with varying concentrations of D-glucose or the solvent as control (CON).
6.9	Endogenous RA levels in rat embryos cultured for 48 hr in medium supplemented with varying concentrations of D-glucose or the solvent as control (CON) as determined by the RA-responsive cell line.

LIST OF TABLES

Tables	Title
2.1	Procedures of preparing RA standard solutions.
2.2	Gradient conditions for elution of retinoids during HPLC.
3.1	Expression levels of *Cyp26a1, Cyp26b1* and *Cyp26c1* relative to *β-actin* in embryos of non-diabetic and diabetic mice at E9.0.
3.2	Expression levels of *Cyp26a1* relative to *β-actin* in embryos of non-diabetic and diabetic mice at E7.0 and E8.0.
3.3	Expression levels of *Cyp26* relative to *β-actin* in embryos of non-diabetic and diabetic mice at different time points after maternal injection of 50 mg/kg RA on E9.0.
3.4	Statistical analysis of relative expression levels of *Cyp26* in embryos of different treatment groups using Independent Samples t-test.
4.1	Expression levels of *Cyp26a1* relative to *β-actin* in embryos of different groups at E9.0.
4.2	Statistical analysis of relative expression levels of *Cyp26a1* between embryos of different groups using one-way ANOVA followed by Bonferroni test.
4.3	Fold difference in *Cyp26a1* expression levels between *Cyp26a1* heterozygous and wild-type embryos in diabetic and non-diabetic maternal status.
4.4	*In vitro* RA degrading activity in the tail bud tissue of E9.0 embryos of different groups.

LIST OF TABLES

Tables	Title
4.5	Statistical analysis of *in vitro* RA degrading activity between the tail bud tissue of embryos of different groups using one-way ANOVA followed by Bonferroni test.
4.6	Statistical analysis of the correlation between *Cyp26a1* expression level and *in vitro* RA degrading activity in the tail bud tissue using Pearson's correlation.
4.7	Amount of RA in embryos of different groups at 3 hr after maternal treatment with 25 mg/kg RA on E9.0 as determined by HPLC.
4.8	Statistical analysis of RA levels between embryos of different groups using one-way ANOVA followed by Bonferroni test.
4.9	Incidence rates of cleft palate and renal malformations in E18 fetuses of different groups after maternal treatment with 40 mg/kg RA on E 9.0.
4.10	Incidence rates of exencephaly and spina bifida in E13 embryos of different groups after maternal treatment with 25 mg/kg RA on E8.0.
4.11	Statistical analysis of incidence rates of various types of RA-induced malformations between embryos of different groups using one-way ANOVA followed by Bonferroni test.
5.1	Serum retinol levels in non-diabetic and diabetic mice under pregnant or non-pregnant (E9.0) status as determined by HPLC.
5.2	Endogenous RA levels in E9.0 embryos of diabetic and non-diabetic mice as determined by RA-responsive cell line.
5.3	Expression levels of *Cyp26a1* relative to *β-actin* in the tail bud of E9.0 embryos of non-diabetic and diabetic mice with or without RA supplementation on E8-22hr.

LIST OF TABLES

Tables	Title
5.4	TL/CRL ratio of E13 embryos in non-diabetic and diabetic mice with or without RA supplementation on E8-22hr.
5.5	RA levels in E9.0 embryos of non-diabetic and diabetic mice with or without RA supplementation on E8-22hr.
5.6	*In vitro* RA degrading activity in the tail bud tissue of E9.0 embryos of non-diabetic and diabetic mice with or without RA supplementation on E8-22hr.
5.7	Severity of caudal regression in terms of TL/CRL ratio in E13 embryos of non-diabetic and diabetic mice with or without RA supplementation on E8-22hr and teratogenic RA insult on E9.0.
5.8	Expression levels of *Cyp26a1* relative to *β-actin* in E9.0 embryos of different groups with or without RA supplementation on E8-22hr.
5.9	Statistical analysis of relative expression levels of Cyp26a1 between embryos of different groups using one-way ANOVA followed by Bonferroni test.
5.10	Incidence rates of cleft palate and renal malformations in different types of E18 fetuses of control or RA-supplemented non-diabetic and diabetic mice induced by maternal injection with 40 mg/kg RA on E9.0.
5.11	Incidence rate of exencephaly and spina bifida in different types of E13 embryos of control and RA-supplemented non-diabetic and diabetic mice induced by maternal injection with 25 mg/kg RA on E8.0.
5.12	Statistical analysis of incidence rates of various types of RA-induced defects between embryos of different groups using one-way ANOVA followed by Bonferroni test.

LIST OF TABLES

Tables	Title
6.1	Comparison of maternal blood glucose levels before and after treatment with PHZ in mice under diabetic and non-diabetic pregnancy.
6.2	Expression levels of *Cyp26* relative to *β-actin* in tissues of E9.0 embryos of non-diabetic and diabetic mice with or without maternal PHZ treatment.
6.3	Statistical analysis of relative expression levels of *Cyp26* between tissues of embryos of different groups using one-way ANOVA followed by Bonferroni test.
6.4	Endogenous RA levels in E9.0 embryos of non-diabetic and diabetic mice with or without maternal PHZ treatment.
6.5	Statistical analysis of endogenous RA levels between embryos of different groups using one-way ANOVA followed by Bonferroni test.
6.6	*In vitro* RA degrading activity in tissues of E9.0 embryos of non-diabetic and diabetic mice with or without maternal PHZ treatment.
6.7	Statistical analysis of *in vitro* RA degrading activity between tissues of embryos of different groups using one-way ANOVA followed by Bonferroni test.
6.8	RA levels in the tissues of embryos of PHZ-treated or control diabetic and non-diabetic mice at 3 hr after maternal injection with 25 mg/kg RA on E9.0.
6.9	Statistical analysis on the amount of RA in the tissues of embryos of different groups using one-way ANOVA followed by Bonferroni test.

LIST OF TABLES

Tables	Title
6.10	Susceptibility of fetuses of non-diabetic and diabetic mice with or without maternal PHZ treatment to various types of RA-induced malformations.
6.11	Statistical analysis on susceptibility to various types of RA-induced malformations between fetuses of different groups using one-way ANOVA followed by Bonferroni test.
6.12	Expression levels of *Cyp26a1* relative to *β-actin* in rat embryos cultured in medium supplemented with varying concentrations of D-glucose for 24 hr.
6.13	Expression levels of *Cyp26a1* relative to *β-actin* in rat embryos cultured in medium supplemented with varying concentrations of D-glucose for 48 hr.
6.14	Endogenous RA levels in rat embryos that had been cultured in medium supplemented with varying concentrations of D-glucose for 48 hr.

ABBREVIATIONS

bp	Base pairs
CON	Control
CRL	Crump-rump length
DEPC	Diethyl pyrocarbonate
ND	Non-diabetic
$ND^{+/+}$	*Cyp26a1*$^{+/+}$ embryos in non-diabetic pregnancy
$ND^{+/-}$	*Cyp26a1*$^{+/-}$ embryos in non-diabetic pregnancy
DMEM	Dulbecco's Modified Eagle's Medium
E	Day of gestation
G	Gauge
HPLC	High pressure liquid chromatography
hr	Hours
ICR	Institute of Cancer Research
min	Minutes
PBS	Phosphate buffered saline
PHZ	Phlorizin
r	rhombomere
RA	All-*trans* retinoic acid
Raldh	Retinaldehyde dehydrogenase
RAR	Retinoic acid receptors
RARE	Retinoic acid response element
RBP4	Retinol binding protein 4
rpm	Revolutions per minute
RT-PCR	Reverse transcription-polymerase chain reaction
RXR	Retinoid X receptors
SD	Diabetic
$SD^{+/+}$	*Cyp26a1*$^{+/+}$ embryos in diabetic pregnancy
$SD^{+/-}$	*Cyp26a1*$^{+/-}$ embryos in diabetic pregnancy
sec	Seconds
TL	Tail length

ABSTRACT

Offspring of diabetic mothers are more prone to have birth defects. Our laboratory previously found that there is significant down-regulation of the retinoic acid (RA) catabolizing enzyme *Cyp26a1* in the tail bud region of embryos of diabetic mice. This reduces the tail bud's ability to clear away RA, thereby increasing the embryo's susceptibility to develop caudal regression caused by ectopic RA signaling in the tail bud. The aim of this thesis was to determine whether down-regulation of *Cyp26a1* would enhance embryos' susceptibility to different types of malformations, and also investigate the underlying mechanism for down-regulation of *Cyp26a1* in diabetic pregnancy.

First, I have compared the mRNA expression level of all three subtypes of *Cyp26* (*a1*, *b1* and *c1*) in embryos of diabetic and non-diabetic mice at different developmental stages. Results show that *Cyp26a1* is the only subtype significantly affected by maternal diabetes.

Next, to test the hypothesis that down-regulation of *Cyp26a1* could increase embryos' susceptibility to various types of birth defects in diabetic pregnancy, a genetic approach was employed. *Cyp26a1*(+/-) mutant male mice were mated with diabetic or non-diabetic ICR female mice to generate embryos with different expression levels of *Cyp26a1*. Embryos were then challenged *in utero* with a teratogenic dose of RA. It was found that there is direct correlation between *Cyp26a1* expression level, RA catabolic activity and embryos' susceptibility to RA-induced birth defects, including exencephaly, spina bifida, cleft palate and renal malformations.

Cyp26a1 can be regulated by RA. I therefore hypothesized that diabetes led to down-regulation of *Cyp26a1* was due to a decrease in RA levels. RA in the embryo is synthesized from retinol taken from maternal circulation. Indeed, I found that both retinol levels in maternal serum and endogenous embryonic RA concentrations are significantly reduced in the diabetic group. Conversely, when subnormal RA levels in embryos of diabetic mice were restored by oral supplementation with a sub-teratogenic dose of RA, *Cyp26a1* expression level was normalized. Concomitantly, RA catabolizing activity was restored and embryos' susceptibility to different types of malformations upon exposure to excess RA was significantly reduced.

Finally, to test the hypothesis that glucose was a critical factor in the maternal diabetic milieu that disrupted *Cyp26a1* expressions, the blood glucose level of diabetic pregnant mice was specifically reduced by treatment with phlorizin that induced renal glucosuria. Results showed that *Cyp26a1* expression level and RA catabolic activity of the embryonic tissue were normalized upon reduction in blood glucose level. Concomitantly, the increase in embryos' susceptibility to various types of RA-induced malformations caused by diabetic pregnancy was abolished. Moreover, by culturing normal rat embryos *in vitro* in serum supplemented with varying concentrations of D-glucose, I further demonstrated a dose-dependent down-regulation of *Cyp26a1* by glucose.

To conclude, results of this thesis provide strong evidence to support that dysregulation of RA catabolism via down-regulation of *Cyp26a1* is one of the pathogenic pathways for increasing the risk of various types of birth defects in diabetic pregnancy.

撮要

糖尿病產婦的孩子容易患有先天缺陷。我們的實驗室先前發現視黃酸(RA) 降解酶基因 *Cyp26a1* 的表達水平，於糖尿病組小鼠胚胎的尾部份出現明顯下調。這減少了胚胎尾部分解視黃酸的能力，引致異常視黃酸基因訊號，從而提高胚胎出現尾椎萎縮綜合症的易感性。本論文的目的在於確定 *Cyp26a1* 下調是否提高胚胎對不同類型畸形的易感性，同時亦探討妊娠糖尿病導致胚胎 *Cyp26a1* 下調的幕後機制。

首先，我比較 *Cyp26* 三個亞型（*a1*，*b1* 和 *c1*）在糖尿病組和非糖尿病組小鼠胚胎於不同發育階段的基因表達水平。結果表明，*Cyp26a1* 是唯一的亞型於糖尿病組小鼠胚胎出現顯著影響。

接下來，我假設 *Cyp26a1* 下調會增加胚胎對不同類型先天缺陷的易感性。我利用雜交模型來測試立論，*Cyp26a1* (+/-) 雄性小鼠與糖尿病組或非糖尿病組 ICR 雌性小鼠交配會產生不同 *Cyp26a1* 表達水平的胚胎，然後胚胎在母體其間接受致畸劑量的視黃酸。結果發現， 胚胎 *Cyp26a1* 的表達水平、視黃酸在胚始組織的降解活性和視黃酸引致的先生缺陷機率，包括露腦畸形，脊柱裂，裂腭，腎畸形等缺陷均顯現直接關係。

Cyp26a1 受視黃酸水平所控制。因此，我推測 *Cyp26a1* 的下調可能是由胚胎整體視黃酸濃度減少所引致。胚胎中的視黃酸是由母體血液循環中的視黃醇轉化而成。事實上，我發現，無論孕鼠血清的視黃醇水平和胚胎內的視黃酸濃度於糖尿病組均明顯降低。相反，當糖尿病母鼠服食低劑量的視黃酸，原本低於正常濃度的視黃酸恢復正常水平，*Cyp26a1* 表達水平亦正常化。隨之而來，

視黃酸在胚始組織的降解活性恢復，胚胎對視黃酸引致先生缺陷的易感性亦顯著減少。

最後，爲了測試糖孕婦血糖升高是否擾亂胚胎 *Cyp26a1* 表達的一個關鍵因素，我爲糖尿病孕鼠注射專門降低血糖水平的根皮苷 (phlorizin)，抑制腎小管對葡萄糖的吸收。結果表明，當母體血液中的血糖水平減少，*Cyp26a1* 表達水平和視黃酸在胚始組織的降解活性回復正常。隨之而來，本應增加對視黃酸引致先天缺陷的易感性亦隨之消失。此外，把胚胎培養在不同濃度 D-葡萄糖的大鼠血清，我進一步展示了 *Cyp26a1* 的表達水平下調幅度和葡萄糖劑量成正比。

總括而言，這論文提供了強有力的證據，支持 *Cyp26a1* 下調引致視黃酸代謝失調，是一種常見因妊娠糖尿增加各類先天性缺陷風險的致病途徑。

Chapter 1

General Introduction

1.1 DIABETES MELLITUS

In 1999, the World Health Organization classified diabetes mellitus into three main types including type 1 diabetes, type 2 diabetes and gestational diabetes (World Health Organisation, 1999). These 3 types of diabetes share some similar symptoms, but with different causes and population distributions.

Type 1 diabetes accounts for about 10% of diabetic patients. Majority of type 1 diabetes mellitus is caused by autoimmune destruction of the insulin-producing pancreatic beta-cells. Different types of autoantibodies have been found in type 1 diabetic patients. Islet-cell autoantibodies and glutamic acid decarboxylase autoantibodies account for 70-80% (Schranz & Lernmark, 1998; Notkins & Lernmark, 2001), insulinoma-associated-2 autoantibodies in 50-60% (Lan et al., 1996) and insulin autoantibodies in about 40% (Yu et al., 2000) of patients diagnosed of diabetes. Expression of more than one of these autoantibodies will have high risk of developing type 1 diabetes. Type 1 diabetes usually has onset during puberty, thus, it is also called juvenile-onset diabetes. Treatment of the disease is often focused on long-term glycemic control to prevent microvascular damage including retinopathy, renal insufficiency and peripheral neuropathy.

In contrast, type 2 diabetes is the most common form of the disease, accounting for 90% of all cases. Environmental risk factors, especially obesity and physical inactivity (Chan et al., 1994; Colditz et al., 1995), play a major role in induction of type 2 diabetes. Once type 2 diabetes develops, it is characterized by increased glucose production in the liver and by insulin resistance in normally insulin-sensitive peripheral tissues (Kolterman *et al.*, 1980; Bonadonna *et al.*, 1990). Serum insulin levels are high in type 2 diabetic patients, but these levels are not

sufficient to overcome peripheral insulin resistance.

Gestational diabetes is always induced after the period of organogenesis, therefore the risk of having early embryonic defects is relatively low unless the woman has undiagnosed pregestational diabetes (Catalano et al., 1995). However, some complications induced by gestational diabetes, such as fetoplacental impairments and intrauterine programming occurring in later stage of the fetus, are similar to those induced by type 1 and type 2 diabetes (Reece et al., 2009). The ambient glucose levels are high in maternal circulation with gestational diabetes, however, insulin response per unit of glycemic stimulus is only half of that observed in normal pregnancy (Hornnes et al., 1981).

1.2 PRE-EXISTING DIABETIC PREGNANCY

Maternal diabetes provides an unfavorable environment for both embryonic and placental development. It has been widely reported that pregnancies of women or experimental animal models of type 1 or type 2 diabetes are at increased risk of miscarriage, stillbirth, congenital malformations, placental abnormalities and intrauterine malprogramming (Balsells et al., 2009; Eriksson, 2009; Michael Weindling, 2009) as a result of impaired maternal metabolism (Jensen et al., 2009).

1.2.1 Experimental animal model used for diabetic studies

To study the underlying mechanism of how diabetic pregnancy affects embryo or fetus development, we usually rely on diabetic animal models. However, the etiology of diabetes in humans and experimental diabetic models may be

different. In addition, the extent of pancreatic beta-cell dysfunction and insulin resistance, which determines the degree of maternal metabolic imbalance, severity of the complications and the rate of embryo resorption, varies between human and animal, therefore choosing an appropriate animal model is essential. Different diabetic animal models will be introduced in the following section.

Experimental models of diabetes and pregnancy can be obtained by 3 ways, including surgical procedures, chemical induction, or use of spontaneously or genetically derived animal strains.

1.2.1.1 Surgical method

Using surgical method in inducing diabetes is an old model that is seldom used nowadays. The basis of this model is to remove most of the pancreatic tissues and diminish the secretion of circulating insulin. One of the main limitations of this methodology is the expertise required to proceed with this surgery. Moreover, the postsurgical mortality rate is high, there is nonspecific reduction of the beta-cell mass, and the time that takes to develop diabetic symptoms after the surgical procedure is long, usually requires two to three months (Foglia et al., 1967).

1.2.1.2 Chemical induction of diabetes

Other than surgical method, another way to damage the pancreatic beta-cells can be achieved by administration of drugs such as streptozotocin (Junod et al., 1969) and alloxan (Lenzen & Panten, 1988). Streptozotocin is the most widely used chemical since it is more specific than alloxan (Junod et al., 1967). At the

appropriate doses, these drugs act by specifically destroying the pancreatic beta-cells. Besides, destruction of beta-cells induces a series of pro-inflammatory reactions that are highly similar to those occurring in human cases of diabetes caused by autoimmune destruction of the beta-cells (Gonzalez et al., 2001). These models are considered as type 1 diabetic model because they originate from the destruction of beta-cells rather than insulin resistance.

There are several advantages in using chemically-induced diabetic models. First of all, there is a vast amount of literature that supports the design of experimental methodology. Besides, the adverse effect generated by the animal model and the mechanism of induction of the most common complications in diabetes and pregnancy have been widely reported. Another advantage is that the induction of diabetes in animals through this method is relatively simple. Moreover, the chemically-induced diabetic model is the only model that can easily induce severe diabetes at the early age of the animal and allow the study of pre-existing diabetic pregnancy.

One of the limitations that arise, depending on the dose and rodent strains, is the difficulty in achieving reasonable pregnancy rate. Streptozotocin-induced diabetic animal models with severe hyperglycemia often stop the oestrus cycle 2 or 3 weeks after chemical administration (Tesone et al., 1983). Another disadvantage of this model is that the causes of beta-cell death between human diabetes and chemically-induced diabetes are clearly different. The genetic and immune components of the diabetic disease are not present in chemically-induced diabetic animal models.

1.2.1.3 Genetic animal model

The non-obese diabetic (NOD) mice and bio-breeding (BB) rats are the most commonly used animals that spontaneously develop type 1 diabetes. In common with the human disease, the pancreatic beta-cells are subjected to immune attack, with T cells, B cells, macrophages and natural killer cells being involved in the development of insulitis (Kay et al., 2000). However, these insulin-dependent diabetic models develop spontaneously in a low rate and a long time is required to become diabetic. For NOD mice, only 9% develop diabetes by 12 weeks and 80% by 30 weeks of age (Formby et al., 1987), so the best reproductive period has already passed. BB rats develop severe diabetes and ketoacidosis that may be fatal unless exogenous insulin is administered (Nakhooda et al., 1977).

There are many animal models of type 2 diabetes (Srinivasan & Ramarao, 2007). The db/db diabetic mouse model is the most widely studied model, resulting from an autosomal recessive point mutation in the leptin receptor gene. Since the db/db mouse is infertile (Lambin et al., 2007), to study diabetic pregnancy, the db/+ mouse has to be employed. The db/+ mouse is glucose intolerant and develops diabetes during gestation, therefore providing a good gestational diabetic experimental model (Lambin et al., 2007), but with different etiology from human gestational diabetes. Besides, most type 2 diabetic models used to analyze diabetic and pregnancy complications have a polygenic origin, such as the Cohen diabetic rat (Rosenmann et al., 1984), the Sand rat (Haines et al., 1965) and the Goto Kakizaki (GK) rat (Goto et al., 1976). An advantage of these genetic type 2 diabetic models is the wide range of phenotypes depending on the degree of obesity, hyperglycemia and insulin resistance.

However, genetic diabetic models require the analysis of the influence of maternal diabetes separately from the fetal genotype. Moreover, most of these animals are required to be obtained from special institutes or companies. The lack of availability of these strains leads to the reduced number of studies in using these genetic models when compared with the chemically-induced diabetic models.

1.2.2 Complication on pregnancy

1.2.2.1 Ovulation stage

The effect of diabetes on ovulation has long been studied. Diabetic experimental animals have reduced ovary weight and show altered response to the pregnant hormone human chorionic gonadotropin (hCG). A marked decrease of 42% in the number of hCG binding sites was found in the ovarian luteal cells of diabetic animals, which could account for the reduced sensitivity in the synthesis of progesterone (Tesone et al., 1983). Besides, women with type 1 diabetes mellitus showed a decrease in estrogen levels, which is a critical sexual hormone regulating ovulation. Reduction in estrogen secretion may cause failure in ovulation (Codner, 2008). Besides, signaling of nitric oxide, an important mediator in regulating blood-follicle barrier and ovulation, was found to be disturbed within the ovarian microvasculature in diabetic mice, which impaired ovulation (Powers et al., 1996).

1.2.2.2 Preimplantation embryo

Diabetes affecting the development of oocytes has also been well studied. Oocytes obtained from experimental models of diabetes showed delay in

development. It has been reported that when collected at day 2 of gestation, the majority of oocytes obtained from diabetic animals lagged behind at the one-cell stage, whereas oocytes were mostly at the two-cell stage in the non-diabetic group (Diamond et al., 1989; Moley et al., 1991). Moreover, when two-cell stage oocytes were collected from both diabetic and non-diabetic mice and cultured in normal media, developmental delay still occurred in the diabetic group, suggesting that the destructive effect of diabetic conditions on embryo development is permanent starting from periconceptual period (Diamond et al., 1989). A recent study has also proved that the malformation rate was increased when one-cell stage embryos obtained from superovulated streptozotocin-induced diabetic mice were transferred to control recipients (Wyman et al., 2008). Other than developmental delay, oocytes from diabetic pregnancy also show important alterations in their quality in terms of mitochondrial dysfunction (Wang & Moley, 2010).

Preimplantation embryos have also been reported to be highly susceptible to hyperglycemia-induced metabolic disorders. Embryos from diabetic animals showed a decrease in both intra-embryonic free glucose levels and glucose uptake when compared with the control group (Moley et al., 1998). Besides, preimplantation embryos from streptozotocin-induced diabetic mice showed down-regulation in mRNA and protein expressions of glucose transporters GLUT-1, GLUT-2 and GLUT-3 (Moley et al., 1998). Such decrease might be due to embryonic adaptation to the hyperglycemic maternal environment. It has been reported that reduction in glucose uptake could lead to initiation of apoptosis in other tissues (Kan et al., 1994). Indeed, apoptosis was found to be increased in preimplantation embryos obtained from NOD mice and streptozotocin-induced diabetic experimental models (Moley, 2001).

1.2.2.3 Postimplantation embryo

Diabetic pregnancy is associated with increased risk of congenital malformations. It has been reported that the malformation rate was elevated even in mildly diabetic experimental models (Mestman, 1980; Iessi et al., 2010). In diabetic pregnancy of both human cases and experimental models, malformations mainly occur in the central nervous system (such as spina bifida and exencephaly), heart (such as hypoplastic heart and ventricular septal defect) and skeleton (such as limb defect) with a 4- to 5-fold increase in the incidence rate (Otani et al., 1991; Martinez-Frias, 1994; Schaefer-Graf et al., 2000; Siman et al., 2000). The malformation that is considered to be most characteristic in infants of diabetic mothers is caudal regression syndrome, with 200 to 400 fold more frequent in diabetic pregnancy (Kucera, 1971). Although the occurrence rate of birth defects is clearly dependent on the degree of maternal glycemic control, it is very difficult to reduce the malformation rate to normal levels even in well-controlled diabetic patients (Langer & Conway, 2000).

Other than affecting the embryo, placentomegalia (enlarged or cystic placenta) is also observed in chemically-induced diabetic experimental models and in some genetic models of diabetes such as the BB rat (Capobianco et al., 2005). Structural, functional and developmental abnormalities are found in the placenta of streptozotocin-induced diabetic rodents (Padmanabhan & al-Zuhair, 1990; Schaefer-Graf et al., 2002). Besides, there are alterations in glucose transfer, transporters and metabolism in the placenta. Glucose transfer through the placenta increases linearly with the maternal glucose level in streptozotocin-induced diabetic rats (Herrera et al., 1985). It has been reported that placental GLUT3 mRNA and protein levels were increased 4 to 5 fold in near-term streptozotocin-induced diabetic

rats in comparison to non-diabetic rats. Reducing the maternal blood glucose level could normalize the increased placental GLUT3 mRNA and protein to a level similar to that of the non-diabetic group (Boileau et al., 1995).

1.2.2.4 Neonatal

The effect of maternal diabetes on the fetus can be revealed after birth. Long-term effects include increased risks for development of obesity, impaired glucose tolerance, type 2 diabetes mellitus, metabolic syndrome and minor neurological deficits (Catalano & Kirwan, 2001; Schaefer-Graf et al., 2005; Simeoni & Barker, 2009). Depending on the extent of maternal metabolic and proinflammatory derangements, macrosomia can arise in fetuses from experimental diabetic models due to excessive availability of nutrients and an increase in fetal insulin release (Goldstein et al., 1985; Khan, 2007).

Different organs of the newborn have been shown to be affected by maternal diabetes. Nephrogenesis was found impaired in fetuses of streptozotocin-induced diabetic rats (Amri et al., 1999). Both reduction in kidney weight and a decrease in nephron number were observed (Tran et al., 2008). The lung is also one of the fetal organs being affected. Reduced surfactant phospholipids (Rieutort et al., 1986) and surfactant proteins (Moglia & Phelps, 1996) were found in fetuses of streptozotocin-induced diabetic rats. Accumulation of lipid in the liver was found in fetuses and neonates of streptozotocin-induced diabetic rats and in db/+ mice (Yamashita et al., 2003).

1.2.3 Etiology

Diabetic pregnancy induces a wide spectrum of congenital malformations affecting multiple organs, indicating that its teratogenic effect is not simply mediated via a single factor or mechanism (Khoury et al., 1989), but involves a complex etiology. The teratogenic effect of diabetic pregnancy is proposed to be multi-factorial, in which both environmental and genetic predispositions are important in diabetic embryopathy (Sadler et al., 1989; Buchanan et al., 1994). By increasing the understanding on the etiology of diabetic pregnancy through basic research, new therapeutic measurements can be developed and clinically applied on pregnant diabetic patients. Some of the teratogenic processes that have been well studied in diabetic embryopathy will be briefly reviewed in the following sections.

1.2.3.1 Depletion of myo-inositol

Myo-inositol is a vital precursor of cell signaling effectors, leading to the formation of phosphoinositides and diacylglycerol through partial hydrolysis of phospholipids. Low levels of myo-inositol in tissues can result in deficiency in phospholipids turnover (Strieleman & Metzger, 1993) with a reduction in protein kinase C (PKC) activity (Wentzel et al., 2001). Details of PKC signaling will be discussed in section 1.2.3.2.

It has been reported that culturing rat embryos at mid-gestation in hyperglycemic conditions inhibited the process of myo-inositol uptake in a glucose concentration-dependent manner and reduced the myo-inositol level in the embryo (Weigensberg et al., 1990). Interestingly, myo-inositol deficiency induced by supplementation of myo-inositol uptake inhibitor, scyllo-inositol, led to failure of

rostral neural tube fusion, which is similar to abnormalities induced by hyperglycemia, suggesting that inositol depletion plays a role in diabetes-related malformations (Strieleman et al., 1992). Besides, in embryos cultured *in vitro* in hyperglycemic conditions supplemented with myo-inositol, there was a significant reduction in the risk of malformations and growth retardation (Baker et al., 1990).

1.2.3.2 Alteration of protein kinase C (PKC) activity

Other than affecting the myo-inositol level alone, hyperglycemia also affects PKC activity. In experimental diabetic pregnancy, alteration of different PKC isoforms (including PKC activities and mRNA expression) was found (Gareskog & Wentzel, 2004). PKC(delta) activity was higher in embryos cultured for 24 hr in medium with high glucose than in embryos cultured in low glucose concentrations. Supplementation of PKC(delta) specific inhibitor to high-glucose medium also normalized PKC(delta) activity and glucose-induced embryonic dysmorphogenesis was diminished (Gareskog & Wentzel, 2007).

Furthermore, over-expression of PKC(zeta) or PKC(delta) can trigger the apoptotic pathway in different cell models (Leroy et al., 2005; Santiago-Walker et al., 2005). PKC(zeta) affects apoptosis by interfering with the Fas signaling pathway and Fas ligand (FasL)-induced apoptosis (Leroy et al., 2005), while PKC(delta) stabilizes p53 proteins by inducing phosphorylation of the Ser-15 residue of p53, thereby contributing to the nitric oxide-mediated apoptosis-like cell death pathway (Lee et al., 2006). It has been reported that inhibition of PKC(delta) could also help to counteract reactive oxygen species production (Domenicotti et al., 2003), which would ultimately lead to apoptotic cell death.

1.2.3.3 Arachidonic acid and prostaglandin deficiency

Decreased arachidonic acid concentrations was shown in embryos of diabetic rats (Goldman et al., 1985). Disturbed metabolism of arachidonic acid and prostaglandins was also found in experimental diabetic pregnancy. Subcutaneous injection of arachidonic acid (200-400 mg/kg per day) into pregnant diabetic rats during the period of organogenesis, or addition of arachidonic acid to the hyperglycemic culture medium could reduce the incidence rate of different birth defects including neural tube defects, cleft palate and micrognathia (Goldman et al., 1985; Pinter et al., 1986).

Both studies of streptozotocin-induced diabetic rodents and *in vitro* hyperglycemic culture revealed that disturbed arachidonic acid-prostaglandin pathway could lead to a decrease in prostaglandin E2 (PGE2) concentrations. Measurement of PGE2 levels indicated that prostaglandin was decreased in embryos of diabetic rodents during the period of neural tube closure (Piddington et al., 1996), in rat embryos cultured in high-glucose conditions (Wentzel et al., 1999), as well as in the yolk sac of embryos of diabetic women (Schoenfeld et al., 1995). It is suggested that such alteration in prostaglandin levels is involved in the induction of neural tube defects (Goldman et al., 1985; Reece & Eriksson, 1996). In contrast, addition of PGE2 to the culture medium in turn blocked glucose-induced teratogenicity *in vitro*, as well as maldevelopment of embryos cultured in diabetic serum (Goto et al., 1992). In addition, alteration of arachidonic acid metabolism under hyperglycemia leads to altered production of prostaglandins and generation of nitric oxide, which can enhance production of reactive oxygen species (Jawerbaum et al., 2002).

1.2.3.4 Excess reactive oxygen species (ROS)

Diabetic or hyperglycemic environment can lead to formation of ROS as a consequence of either an increase in free oxygen radicals formation (Eriksson & Borg, 1993) or a decrease in the activity of ROS-scavenging enzymes (Hagay et al., 1995; Sivan et al., 1997; Weksler-Zangen et al., 2003), or both. Previous studies have demonstrated that supplementation of antioxidative agents such as copper–zinc superoxide dismutase (Eriksson & Borg, 1993), N-acetyl cysteine (Wentzel et al., 1997), vitamins E (Viana et al., 1996; Siman & Eriksson, 1997b) and C (Siman & Eriksson, 1997a; Zaken et al., 2001) and folic acid (Wentzel et al., 2005), either *in vitro* or *in vivo*, attenuated malformation rates and diminished markers of oxidative stress.

The driving cellular force behind diabetes-induced oxidative stress is associated with enhanced glucose metabolism (Fine et al., 1999) in embryonic and fetal cells exposed to increased ambient levels of glucose. One primary source of the reactive radical compounds will be the mitochondria, which receive a high influx of pyruvate and oxygen, and subsequently producing a large amount of ROS in the oxidative processes of the electron transport chain (Yang et al., 1997). The transfer of superoxide into other compartments of the mitochondria and the cytosol, and the further increase in formation of hydrogen peroxide and hydroxyl radicals, lead to mitochondrial alterations (Yang et al., 1995) as well as lipid peroxidation (Wentzel et al., 1999) and DNA damage in the embryo (Lee et al., 1999) .

1.2.3.5 Folic acid depletion

Folic acid has antioxidant properties, and its deficiency is involved in the

induction of congenital malformations in the general population and also in streptozotocin-induced diabetic animals (Wentzel et al., 2005; Oyama et al., 2009).

Rodent embryos exposed to a diabetic environment *in vivo* or *in vitro* with supplementation of folic acid showed an increase in folic acid concentrations. Diabetes or glucose-induced dysmorphogenesis, including growth retardation and maldevelopment in the offspring, was almost completely abolished (Wentzel et al., 2005).

1.2.3.6 Genetic predisposition

There are few genetic studies on human diabetic embryopathy. However, previous experimental work using animal models has suggested a number of genes that have teratological significances. DNA microarray analysis on the yolk sac of day 12 embryos from normal and diabetic rats has yielded a series of possibly teratologically active genes that are involved in insulin signaling, stress response, cell growth, calcium signaling and PKC signaling (Reece et al., 2006). Moreover, array studies have shown aberrant gene expression patterns in the placenta of streptozotocin-induced diabetic mice (Yu et al., 2008). In addition, recent work have identified altered expression of several genes related with neural tube defects and cardiac defects in embryos of streptozotocin-induced diabetic mice (Kumar et al., 2007), which may account for the increased risk of these birth defects in diabetic pregnancy. Microarray analysis of embryos of streptozotocin-induced diabetic mice show that hundreds of genes exhibit changes in expression in the whole embryo (Pavlinkova et al., 2009) and in the developing neural tube (Jiang et al., 2008). Indeed, the absence of a clear-cut pattern among the putative candidate genes further

suggests that the problem of genetic predisposition in diabetic teratogenesis may have a polygenic nature.

Another gene of teratological interest is the transcription factor *Pax3* that has been identified to have altered expressions in the mouse embryo of diabetic pregnancy and has been studied in details. Diabetes-induced down-regulation of embryonic *Pax3* is associated with neural tube defects in the offspring of diabetic mice (Phelan et al., 1997), together with over-expression of *cdc46* (Hill et al., 1998), increased *p53* expression and activated *p53*-induced apoptosis in the embryo (Pani et al., 2002). Furthermore, dietary supplementation of α-tocopherol blocked the down-regulation of *Pax3* and normalized neural tube development in the offspring of diabetic mice (Chang et al., 2003).

1.3 Retinoic Acid (RA)

RA is an active metabolite of vitamin A. Vitamin A exerts its functions through RA, a diffusible lipid-soluble hormone that regulates the expression of many target genes through receptor-mediated events (details will be discussed in section 1.3.2) (Balmer & Blomhoff, 2002). It has long been known that RA plays a crucial role in embryonic development (Ross et al., 2000; Niederreither & Dolle, 2008). Both deficiency and excess of vitamin A/RA may lead to embryonic or fetal death or a spectrum of congenital defects in a dose- and developmental stage-dependent manner.

1.3.1 RA homeostasis

Circulating maternal retinol is the source of RA in placental species. Retinol binds to retinol binding protein 4 (RBP4) and is then transferred intracellularly by the cell surface receptor STRA6 (Bouillet et al., 1997). Retinol within the cell binds to and is transported by cellular retinol binding protein (Perez-Castro et al., 1989).

Two sequential reactions are required to transform retinol into RA. The first step of RA synthesis involves oxidation of retinol to retinaldehyde, which is catalyzed by several alcohol dehydrogenases (ADHs) and retinol dehydrogenases (RDHs). There are at least three ADHs (ADH1, ADH3 and ADH4) and two RDHs (RDH1 and RDH10) that play a physiological role in RA synthesis. Expression of these retinol-oxidizing enzymes is widespread and overlapping (Ang et al., 1996; Zhang et al., 2001; Sandell et al., 2007). Among them, RDH10 plays a major role in this step (Sandell et al., 2007). The second step of RA synthesis involves irreversible oxidation of retinaldehyde to RA, which is the rate limiting step in RA synthesis. This step is catalyzed by three retinaldehyde dehydrogenases (Raldh1, Raldh2, and Raldh3), which display non-overlapping tissue-specific patterns of expression during embryogenesis (Mic et al., 2002). In the embryo, Raldh2 is the most abundant and widely expressed member of this family (Niederreither et al., 1997; Ulven et al., 2000). The expression domains of RA-synthesizing enzymes are similar to the sites of localization of RA in the embryo (Rossant et al., 1991). Homologous deletion of *Raldh2* in the mouse results in early embryonic lethality (Niederreither et al., 1999). The trunk of the mouse embryo is severely shortened and the neural tube remains open, whereas the anterior region is less affected.

When retinoid signaling needs to be turned off, RA is enzymatically catabolized into inactive metabolite such as 4-hydroxy RA or 4-oxo RA (White et al., 1997). Oxidation of RA is carried out by three cytochrome P450 (Cyp) enzymes known as Cyp26A1 (Abu-Abed et al., 2001), Cyp26B1 (Yashiro et al., 2004) and Cyp26C1 (Uehara et al., 2007). These enzymes also display unique tissue-specific patterns of expression during mouse embryogenesis. Knockdown of *Cyp26a1* and *Cyp26b1* led to developmental abnormalities that phenocopy the teratogenic effect of excess RA (Abu-Abed et al., 2001; Yashiro et al., 2004). *Cyp26a1* and *Raldh2* express in complementary but non-overlapping regions, which suggests a possible role of *Cyp26a1* in boundary formation, acting as a perimeter between regions of high RA synthesis.

1.3.2 RA signaling

RA signaling is mediated via two families of nuclear receptors: (i) the RA receptors (RARα, RARβ and RARγ) that bind to all-*trans* RA and (ii) the retinoid X receptors (RXRα, RXRβ and RXRγ) that bind to both all-*trans* RA and its isomer 9-*cis* RA (Chawla et al., 2001). RA carries out its signaling activity by binding to RAR, which form homodimers or heterodimers with RXR, and function as ligand-inducible transcriptional regulators (Leid et al., 1992; Mangelsdorf & Evans, 1995). The RA and receptors complex will bind to a regulatory DNA element called retinoic acid response element (RARE) in the promoter region of the target gene, which stimulates a cascade of events resulting in recruitment of transcriptional coactivators and initiation of transcription (Germain et al., 2002). *In vivo* studies have demonstrated that the binding of all-*trans* RA to the RAR portion of

RAR/RXR heterodimers is sufficient and essential to rescue the lethal defects in the absence of RA synthesis, suggesting that RAR is the key element in signaling (Mic et al., 2003), whereas RXR portion just functions as a scaffold protein to facilitate DNA binding (Chawla et al., 2001).

1.3.3 RA teratogenicity

The concentration of vitamin A/RA must be kept within a very narrow range in order to avoid deficiency or toxicity. The teratogenic effect of excess intake of vitamin A during pregnancy was first reported long ago in 1953 (Cohlan, 1953). Cohlan demonstrated that feeding pregnant female rats 35,000 IU/day of a "natural vitamin A" preparation (most likely a retinyl ester preparation) between gestation day 2 and 16 of pregnant rat could induce a series of fetal anomalies including exencephaly, cleft lip, cleft palate and eye defects (Cohlan, 1953). Human cases of hypervitaminosis A during pregnancy also showed same types of defects. Besides, malformations similar to those described above have been observed in cases of administration of metabolite of vitamin A, such as all-*trans* RA and 13-*cis* RA in both humans and animals (Lammer et al., 1985). The teratogenic effect of retinoids varies with species and depends on their side chain structures, rate of placental transfer and metabolism. It has been shown in mice that all-*trans* RA is the most potent teratogen with teratogenicity 4 times and 20 times higher than retinol and 13-*cis* RA respectively (Shenefelt, 1972; Soprano & Soprano, 1995). RA causes dysmorphogenesis through interference of one or more cellular events, such as cell proliferation, apoptosis, differentiation, adhesion and migration (Kochhar, 2000). For example, caudal regression is caused by apoptosis that kills off the progenitor

cell in the posterior tail bud region of the embryo (Chan et al., 2002; Vlangos et al., 2009). Recent findings showed that treatment of mouse embryos with Retinoic Acid Metabolic Blocking Agents (RAMBAs), which specifically block Cyp26 activity could raise endogenous RA levels and caused abnormalities that were similar to those found in knockout mice of RA catabolizing genes (Abu-Abed et al., 2001; McCaffery & Simons, 2007).

However, studying the teratogenic effect of RA is often not useful for determining its physiological role, given that high levels of RA may induce or repress genes not normally regulated by endogenous RA. Thus, loss-of-function studies are necessary to determine the normal function of RA during organogenesis.

There are few reports on the effect of vitamin A deficiency on human pregnancy. Hypovitaminosis A is common in the third world country (Ag Bendech et al., 1997). However, the medical backup is insufficient in these countries, so in cases of babies born with anomalies, it is difficult to make any correlation with hypovitaminosis A because the maternal vitamin A level during pregnancy has not been measured. Thus, to study the effect of hypovitaminosis A on pregnancy, animal models are commonly used. Early studies on the embryonic effect of lack of RA were performed using vitamin A deficiency (Dersch & Zile, 1993; Dickman et al., 1997; Clagett-Dame & DeLuca, 2002). These early studies indicated that RA is essential for development of several organs including the hindbrain, spinal cord, heart, eye, skeleton, forelimb buds, lung, pancreas and genitourinary tract.

More recently, the use of *Raldh* mutations (Niederreither et al., 1999) or compound *RAR* mutations (Lohnes et al., 1994; Mendelsohn et al., 1994) that completely eliminate either RA synthesis or RA signaling in specific tissues at early

stages of development has made it possible to examine the mechanism of RA action on different embryonic tissues. A loss of RA inhibits organogenesis, as shown in the *Raldh2*$^{-/-}$ embryo, which died at midgestation without undergoing axial rotation (body turning), exhibiting shortening along the anteroposterior axis and did not develop limb buds. The heart consisted of a single medial dilated cavity. The frontonasal region was truncated and the otocysts were severely reduced. On the other hand, there was near full rescue of the mutant phenotype by maternal RA administration (Niederreither et al., 1999).

1.4 RA- AND MATERNAL DIABETES-INDUCED MALFORMATIONS SHARE SIMILAR PATHOGENIC MECHANISMS

As mentioned previously, RA can induce a spectrum of congenital malformations including caudal regression, neural tube defects, heart defects and renal anomalies. Similarly, offspring of diabetic pregnancy show increased risk of these anomalies (Casson et al., 1997; Singh et al., 2005), suggesting that some common pathogenic mechanisms may exist between RA- and maternal diabetes-induced birth defects.

Our laboratory has provided the first evidence to support a link between RA- and maternal diabetes-induced malformations. We used caudal regression syndrome, the anomaly most strongly associated with maternal diabetes (Martinez-Frias, 1994), as a model for study. It was shown that administration of RA to pregnant mice at mid-gestation, which is equivalent to week 4 after conception of human pregnancy, could lead to development of caudal regression (Shum et al., 1999), with a spectrum of malformations closely resembling cases of caudal

regression associated with maternal diabetes (Singh et al., 2005). Importantly, when diabetic and non-diabetic mice were treated with the same dose of RA, embryos of diabetic group were found to be much more susceptible to RA-induced caudal regression than embryos of non-diabetic group (Chan et al., 2002), suggesting an interaction between RA and maternal diabetes in increasing the risk of caudal regression. Besides, it has previously been shown that RA induced caudal regression via down-regulating *Wnt-3a*, a gene indispensable for caudal development (Takada et al., 1994), in the tail bud region of the embryo. The tail bud mesenchyme, which contains progenitor cells for forming various caudal structures, then underwent extensive apoptosis, and terminated in further elongation, resulting in caudal regression (Shum et al., 1999). Such down-regulation of *Wnt-3a* was enhanced and cell death was exacerbated in the tail bud tissues of embryos of diabetic mice after RA treatment (Chan et al., 2002), indicating that maternal diabetes potentiates the teratogenic effect of RA.

The teratogenic effect of RA is highly dose-dependent. As discussed previously, RA concentrations can be regulated by the RA catabolizing enzyme Cyp26. Interestingly, it has been reported that mouse mutants with homologous disruption of *Cyp26a1*, the key *Cyp26* subtype, developed severe caudal regression (Abu-Abed et al., 2001), with a spectrum of abnormalities very similar to those caused by excess RA (Kochhar, 2000). This provides the hints of disturbance of RA metabolism as a pathogenic mechanism of caudal regression. In my previous study, I found that *Cyp26a1* was significantly down-regulated in the tail bud region of the mouse embryo under maternal diabetes, which led to a decrease in its RA catabolic activity. Thus, the tail bud has reduced ability to inactivate aberrant concentrations of RA, thereby increasing the embryo's susceptibility to caudal regression

commonly associated with diabetic pregnancy (Lee, 2008).

1.5 STRATEGY OF THE THESIS

The findings in my previous study give support for a causal relationship between down-regulation of *Cyp26a1* in the tail bud and maternal diabetes in inducing caudal regression. However, a number of issues were yet to be resolved: (i) whether down-regulation of *Cyp26a1* was limited to the tail bud tissue or similarly occurred in other expression domains; (ii) whether the other two subtypes, *Cyp26b1* and *Cyp26c1*, were being affected by maternal diabetes; (iii) whether disturbed RA catabolism was a general pathogenic mechanism of diabetic pregnancy in increasing various types of birth defects other than caudal regression; (iv) what caused down-regulation of *Cyp26a1*.

The aim of this thesis was to address the above mentioned issues to determine whether dysregulation of RA catabolism via down-regulation of *Cyp26a1* would increase embryonic susceptibility to various types of malformations other than caudal regression, and to investigate the underlying mechanism for down-regulated expression of *Cyp26a1* in embryos of diabetic pregnancy.

First, I have compared the mRNA expression level of the three *Cyp26* subtypes (*a1*, *b1* and *c1*) in embryos of diabetic and non-diabetic mice during the early period of organogenesis and also examined the response of different *Cyp26* genes in embryos at various time points after exposure to an exogenous dose of RA (Chapter 3). Results showed that *Cyp26a1* was the only subtype in the embryo significantly affected by maternal diabetes.

Next, I have tested whether down-regulation of *Cyp26a1* played a primary role in increasing the risk of the embryo in diabetic pregnancy to various types of birth defects (Chapter 4). To this end, *Cyp26a1*(+/-) mutant male mice were mated with diabetic or non-diabetic wild-type female mice to generate 4 types of embryos with different expression levels of *Cyp26a1*. Embryos were challenged *in utero* with teratogenic doses of RA during the stage of organogenesis, and the susceptibility of embryos of different genotypes in diabetic and non-diabetic maternal milieu to RA-induced exencephaly, spina bifida, cleft palate and renal malformations was compared.

After confirming that a direct correlation existed between *Cyp26a1* expression levels and the embryonic susceptibility to various types of RA-induced birth defects, next, I have investigated the underlying mechanism for dysregulation of *Cyp26a1* in embryos of diabetic pregnancy (Chapter 5 and Chapter 6). It was shown that *Cyp26a1* expression could be positively regulated by RA. Embryonic RA is synthesized from retinol obtained from maternal circulation. There are growing evidences that retinol levels are reduced in diabetic patients. I therefore hypothesized that subnormal retinol status in the diabetic mother might lead to an overall reduction in the RA concentration in the embryo, which caused down-regulation of *Cyp26a1*. Thus, in Chapter 5, I have first measured the retinol level in maternal serum and the endogenous RA level in the embryo, and found that indeed, there was significant reduction of these two parameters in diabetic pregnancy. To further test my hypothesis, subnormal RA levels in embryos of diabetic mice were restored by maternal oral supplementation with a sub-teratogenic dose (0.625 mg/kg) of RA in an attempt to normalize *Cyp26a1* expression level and RA catabolic activity in embryos of diabetic mice. Embryos were then maternally

challenged with teratogenic doses of RA. Embryos were examined for various malformations to determine whether the increased susceptibility to malformations caused by diabetic pregnancy could be ameliorated in *Cyp26a1*-normalized embryos of diabetic mice.

Many studies have shown that elevated glucose in maternal diabetes is responsible for the increase in incidences of congenital malformations. In Chapter 6, I have tested whether glucose was the critical factor in the maternal diabetic milieu that led to down-regulation of *Cyp26a1* in the embryo. I have first employed an *in vivo* approach to specifically reduce blood glucose levels of diabetic pregnant mice by treatment with the drug phlorizin that induced renal glucosuria. Embryos of diabetic mice with lowered blood glucose levels were examined for *Cyp26a1* expression and RA catabolic activity. They were then maternally challenged with teratogenic doses of RA to determine if a lowering of maternal blood glucose level in diabetic mice could abolish their embryos' increased susceptibility to the teratogenic effect of RA in inducing various types of malformations Next, I have employed an *in vitro* approach to test whether glucose could cause dose-dependent changes in *Cyp26a1* expression and endogenous RA levels in the embryo. This was achieved by culturing early head-fold stage rat embryos of normal pregnancy in serum supplemented with varying concentrations of D-glucose.

Finally, in Chapter 7, results of this study were concluded and future perspectives were discussed.

Chapter 2

General Materials and Methods

2.1 ANIMALS

The Institute of Cancer Research (ICR) mouse colony and the *Cyp26a1* knockout mouse colony in C57BL/6Cr background (Sakai et al., 2001) were established from breeding pairs originally obtained from Harlan Laboratories, UK and Prof. Hiroshi Hamada (Osaka University, Japan) respectively. The Sprague Dawley rat colony was established from breeding pairs obtained from the Animal Resources Centre (Perth, Australia). Both mice and rats were bred at the Laboratory Animal Services Centre (LASEC) of the Chinese University of Hong Kong. ICR mice and Sprague Dawley rats were random-bred, whereas *Cyp26a1* mutants were bred by mating between heterozygous mice, or between heterozygous and wild-type mice. All animals were fed with irradiated LabDiet for Rodents (*PMI Nutrition*) and ozone-sterilized tap water. All procedures of animal experimentation were approved by the Animal Experimentation Ethics Committee of the Chinese University of Hong Kong.

Mice were kept in a humidity- and noise-controlled room running on a 12:12 hour light-dark cycle with the dark period starting from 11:00 pm. One female mouse was paired up with one male mouse for 2 hours (hr) from 9:00 am to 11:00 am. At 11:00 am, the female mouse was examined for the presence of a copulation plug in the vagina. Fertilization was assumed to have occurred at 10:00 am, which was considered as day 0 of gestation (E0).

Rats were kept in a humidity- and noise-controlled room running on a 12:12 hour light-dark cycle with the dark period starting from 6:00 pm. Mating was set up by pairing one female rat with one male rat at 6:00 pm. The female rat was examined for the presence of a copulation plug in the following morning.

Fertilization was assumed to have occurred at midnight, i.e. the middle of the dark cycle. Noon on the day of finding the copulation plug was regarded as 0.5 day of gestation (E0.5).

At the appropriate day of gestation, pregnant mouse and rat were sacrificed by cervical dislocation for embryo collection.

2.2 INDUCTION OF DIABETES

Diabetes was chemically induced in 9 week old ICR female mice by intraperitoneal injection, using a 25 gauge (G) needle (0.50 x 16 mm; *Terumo*) fitted onto a 1 ml syringe, with 60 mg/kg body weight of streptozotocin (*ICN*) at 5:00 pm for three consecutive days. Streptozotocin was freshly prepared by dissolving in 0.01 M sodium citrate buffer (pH 4.5) prior to injection. Mice were screened for diabetes 12 days after the first day of injection. The glucose level of blood sample taken from the tail vein was measured by a glucometer (Glucometer Elite, *Bayer*). Mice with blood glucose levels equal to or higher than 16.5 mmol/L were classified as diabetic (SD), whereas mice with blood glucose levels lower than 16.5 mmol/L were discarded. In general, about 80% of induced mice would become diabetic. Untreated age-matched female mice were used as the non-diabetic (ND) control group. The blood glucose level of the diabetic pregnant mouse was remeasured on the day of sacrifice to confirm that the mouse remained diabetic during pregnancy.

2.3 PREPARATION OF RETINOIC ACID FOR MOUSE INJECTION

All-*trans* retinoic acid (RA, *Sigma*) was prepared as a stock solution at a concentration of 3.33 mg/ml. First, all-*trans* RA at a weight of 50 mg was dissolved in 1.5 ml of absolute ethanol (*BDH*) by vigorous vortexing for 2 hr. The RA solution was then suspended in peanut oil (*Sigma*) to a final volume of 15 ml by vigorous vortexing for another 2 hr. To prevent photoisomerization, RA was kept in a tube wrapped with aluminum foil throughout the process. Different concentrations of RA suspension were prepared by further dilution of the stock solution with peanut oil, such that mice being treated with different dosages of RA were injected with an equivalent volume of RA suspension. The RA suspension was stored at 4°C protected from light and used within 2 weeks. The RA suspension was warmed to room temperature before administered to the animal.

2.4 RA-RESPONSIVE CELL LINE

The RA-responsive cell line, a gift from Prof. Peter McCaffery, is derived from the F9 teratocarcinoma cell line, which is stably transfected with the *β-galactosidase* gene, with expression under the control of the RARE of RAR_β (Wagner et al., 1992). It expresses varying levels of β-galactosidase in response to different concentrations of RA.

2.4.1 Maintaining the cell line

All procedures were carried out under sterile condition in a tissue culture hood. Cells stored in sealed plastic ampoule (*Nunc*) under liquid nitrogen were

immediately thawed in a water bath at 37°C. As soon as the cell thawed, the ampule was sterilized with 70% ethanol and opened with a sterilized knife. The thawed cells were then mixed with 10 ml of Hanks' medium (*Gibco*) to dilute the toxic effect of dimethyl sulfoxide (DMSO, *Sigma*) present in the freezing medium. The cell suspension was centrifuged at 3,000 revolutions per minute (rpm) for 3 minutes (min). The supernatant was discarded and the cell pellet was resuspended in 5 ml of culture medium, composing of Dulbecco's Modified Eagle's Medium (DMEM, *Gibco*) supplemented with 10% fetal bovine serum (*Gibco*), 2 mg/ml G418 (*Sigma*), 100 units/ml penicillin G (*Sigma*) and 0.1 mg/ml streptomycin (*Sigma*). Cells were grown on a 25 cm^2 culture flask (*Nunc*) in a 5% CO_2 incubator at 37°C. To facilitate the growing of cells on the surface of the culture flask, the flask was coated with gelatin by incubating with 0.1% gelatin solution (*USB*) for half an hour at 37°C followed by washing once with Hanks' medium prior to use.

To detach cells from the surface of the culture flask, cells were incubated with 3 ml of trypsin (*Gibco*) at 37°C for 1 min. After detachment, the reaction was stopped by mixing the cell suspension with 10 ml of culture medium. The cell suspension was centrifuged at 3,000 rpm for 3 min. The supernatant was discarded and the cell pellet was resuspended in culture medium for later use. The cell density in the resuspended medium was evaluated by cell counting using a hematocytometer.

2.4.2 Seeding and adding sample to 96-well plate

To seed RA-responsive cells on the 96-well plate (*Nunc*), the plate was first incubated with 0.1% gelatin for half an hour at 37°C and then washed with Hanks'

medium. Cells were seeded onto the gelatin-coated 96-well plate at a density of 4 $x10^4$ cells in 100 µl of culture medium per well and allowed to grow until reaching 80% confluency (usually took about 16 hr of incubation after seeding).

To determine the relative amount of RA in the sample, 80 µl of the RA-containing samples were added to each well. Each sample was added in triplicate for accurate quantification. Cells were incubated in a 5% CO_2 incubator at 37°C for 25 hr to allow transcriptional activation of the *β-galactosidase* reporter gene.

2.4.3 Preparation of RA standard solutions

2.4.3.1 Preparation of RA stock solution

All procedures were carried out under sterile condition in a tissue culture hood under dim yellow light to prevent photoisomerization of RA. DMSO, at a volume of 1.66 ml, was added to 50 mg of all-*trans* RA to make a 100 mM stock solution. Aliquots of stock solution were kept in microfuge tubes wrapped with aluminium foil. The stock solution was gassed with nitrogen and then snap frozen in liquid nitrogen. It was stored at -80°C.

2.4.3.2 Serial dilution of RA standard solutions

The 100 mM RA stock solution was serially diluted to 10^{-5} M following the procedure as indicated in Table 2.1. After that, RA standard solutions from 10^{-6} M to 10^{-12} M were obtained by 10-fold serial dilution with culture medium in a stepwise manner to prevent precipitation.

Table 2.1 Procedures of preparing RA standard solutions.

Final concentration of RA	Volume of RA solution	Volume of DMSO	Volume of culture medium
10 mM	10 µl of 100 mM RA	90 µl	-----
1 mM	10 µl of 10 mM RA	90 µl	-----
500 µM	50 µl of 1 mM RA	-----	50 µl
10 µM (10^{-5} M) *	20 µl of 500 µM RA	-----	980 µl
10^{-6} - 10^{-12} M	10-fold serial dilution with culture medium		

* RA solution in 1% DMSO

Serially diluted RA standard solutions from 10^{-7} M to 10^{-12} M, at a volume of 80 µl per well, were added in duplicate to the RA-responsive cells growing on the 96-well plate in a 5% CO_2 incubator at 37°C for 25 hr. I have previously found that 25 hr was the optimal culture time for maximum response (Lee, 2008). At the end of culture, cells were stained with 5-bromo-4-chloro-3-idolyl-β-galactopyranoside (X-gal, *Gibco*) for detection of β-galactosidase activity.

2.4.4 Staining of cells

The induction level of β-galactosidase was quantified by its activity to convert the substrate X-gal into a coloured product. In brief, cells were first fixed with 1% glutaraldehyde (*Sigma*) in phosphate buffered saline (PBS) for 10 min and then washed 3 times with 200 µl of PBS. They were incubated at 37°C for 16 hr, with 90 µl per well of staining solution consisting of 3.3 mM $K_4Fe(CN)_6 \cdot 3H_2O$ (*Sigma*), 3.3 mM $K_3Fe(CN)_6 \cdot 3H_2O$ (*Sigma*), 6 mM $MgCl_2$ (*USB*) and 2 mg/ml X-gal (dissolved in dimethyl formamide as 40 mg/ml stock solution) in PBS. After incubation, the staining solution was discarded. Cells were washed three times with 200 µl of 0.1 M PBS. The stained cells could be kept in 75% glycerol at room

temperature. The level of transcriptional activation of the *β-galactosidase* reporter gene was quantified as colorimetric readings by an ELISA plate reader (Model 550 Benchmark plus microplate reader, *Biorad*) at the wavelength of 650 nm.

2.5 HIGH PRESSURE LIQUID CHROMATOGRAPHY (HPLC)

2.5.1 Chromatographic system

HPLC was performed by Alliance® HPLC System with a 2996 photodiode array detector (*Waters*). Column temperature was controlled by Alliance column heater. Empower 2 software (*Waters*) was used for instrument control, and data acquisition and processing. Analysis was performed on a 4.6 x 150 mm SunFire C18 Column containing 5 μm particles (*Waters*). The analytical column was protected by a SunFire C18, 5 μm, 4.6 x 20 mm Guard Column (*Waters*).

2.5.2 Preparation of standards

Stock solutions of various retinoids were prepared by dissolving in absolute ethanol and then gassed with nitrogen, sealed with paraffin and wrapped with aluminium foil. They were stored at -20°C. The concentration of the stock solution was determined by spectrophotometry (Lambda Bio 20, *Perkin-Elmer*), using Beer's Law with the following molar extinction coefficients and equivalent wavelength: 48305 (325 nm) for all-*trans* retinol (*Sigma*); 45300 (350 nm) for all-*trans* RA; 39750 (354 nm) for 13-*cis* RA (*Sigma*); 36900 (345 nm) for 9-*cis* RA (*Sigma*); 41400 (361 nm) for acitretin (*Fluka*) (Gundersen & Blomhoff, 2001).

Calibration standards of each retinoid were prepared in absolute ethanol yielding concentrations of 1, 2, 5 and 10 ng/ml. Calibration curves ($y = mx + b$) were constructed by linear least-squares regression analysis of peak area (y) versus concentration (x). For peak assignment, each retinoid was injected alone and the corresponding retention time was determined.

2.5.3 Extraction procedure

Embryo sample

The method for extraction of embryo sample, modified from published protocol (Suh et al., 2006), was as follow. To avoid photoisomerization, the extraction procedure was performed in the dark. The embryo was first transferred to a 15 ml centrifuge tube with 2 ml of ice-cold PBS. The ice-cold PBS was added with 33.3 nM acitretin (a type of retinoid) as internal standard for subsequent calculation of percentage of recovery (refer to section 2.5.5 for details). The embryo was homogenized by sonication with short burst of 10 seconds (sec) at 90% amplitude (Vibra-Cell VCX130, *Sonics & Materials, Inc.*) followed by 30 sec for cooling, and the procedures were repeated for 6 times. After sonication, 10 µl of sample was used for protein assay (refer to section 2.5.6). Next, 1.4 ml of acetonitrile (*BDH*):butanol (*BDH*) (1:1, v:v) with 0.01% anti-oxidant butylated hydroxytoluene (*Sigma*) were added to the homogenized embryo sample suspension. After vortexing for 60 sec, 1.2 ml of saturated (1.3 kg/L) K_2HPO_4 solution (*USB*) was added. The sample was further mixed for 30 sec, and then centrifuged at 4,000 g for 10 min at 4°C to separate the organic and aqueous phases. The upper layer of organic supernatant was collected and subsequently dried under nitrogen gas. The gas-dried extract was

reconstituted in a two-step process. The extract was first redissolved in 500 µl of methanol and then diluted with 500 µl of PBS. Each reconstitution step was aided by ultrasonification using sonicator (*Interlabs*) for 1 min. The sample was filtered by passing through a 0.22 µm nylon filter (*Quandao*), pipetted into a total recovery vial (*Waters*) and then transferred to the HPLC autosampler for analysis.

Serum sample

The serum sample was extracted following published protocol (Teerlink et al., 1997) with some modifications (refer to section 5.3.1.1). Fifty microliters of 1.0 M sodium acetate buffer (pH 4.0) and 33.3 nM acitretin as internal standard were added to 0.35 ml of serum sample. After mixing, 0.6 ml of acetonitrile was added. The sample was immediately mixed by vortexing and then centrifuged for 5 min at 3,000 rpm at 4°C. After centrifugation, 900 µl of the supernatant was transferred to a new 1.5 ml microfuge tube. Five hundred microliters of Milli-Q water and 200 µl of acetonitrile were added and the sample was mixed and centrifuged at 10,000 rpm for 1 min to remove any precipitates. The sample was filtered by passing through a 0.22 µm nylon filter, pipetted into a total recovery vial and then transferred to the HPLC autosampler for analysis.

2.5.4 HPLC conditions

Chromatographic conditions were as described by (Schmidt et al., 2003) with some modifications. A 40 mM ammonium acetate buffer (*USB*), adjusted to pH 5.75 with acetic acid, was prepared. Buffer A consisted of 40 mM ammonium

acetate buffer and methanol mixture (1:1, v:v), and Buffer B was pure methanol. The gradient conditions generated by different proportions of Buffer A and Buffer B were shown in Table 2.2.

Table 2.2 Gradient conditions for elution of retinoids during HPLC.

Time (min)	Flow (ml/min)	% Buffer A	% Buffer B
0	0.1	85	15
1	0.8	85	15
20	0.8	0	100
22	0.8	0	100
23	0.8	85	15
34	0.8	85	15

Column temperature was maintained at 30°C and detection was performed at 340 nm. Retinoids were quantified on the basis of peak area using external calibration standards (section 2.5.2).

2.5.5 Recovery of sample

Recovery of the retinoid was determined by adding known amount (33.3 nM) of acitretin (internal standard) to the serum or embryo sample at the beginning of the sample preparation procedure. After extraction and analysis, the recovery was calculated by comparing the internal standard peak areas with the peak areas obtained by direct injection of sample-free acitretin in the same amount as added to the sample. Retinoid concentrations were calculated with reference to calibration curves and corrected for the recovery ratio.

2.5.6 Protein assay

The protein concentration was determined by the Bradford assay (Bradford, 1976). Using this micro-protein assay, the sample to be measured was diluted in Milli-Q water to a final volume of 800 µl, which was then added with 200 µl of Bradford Reagent (*Bio-rad*) and then incubated for 10 min at room temperature. The absorbance of the sample was measured by spectrophotometry (UV-1601 UV Spectrophotometer, *Shimadzu*) at the wavelength of 595 nm. Bovine serum albumin (BSA; *Sigma*) was used as the protein standard and a standard curve in the range of 0-20 µg/ml BSA was plotted for quantifying the amount of protein in the sample.

2.6 Real-Time Quantitative Reverse Transcription-Polymerase Chain Reaction (RT-PCR)

2.6.1 Collection and storage of tissues

Samples were dissected out in diethyl pyrocarbonate (DEPC)-treated RNase-free ice-cold PBS. The embryonic tissue was immediately kept in 10-fold volume of RNA*later* RNA Stabilization Reagent (*Qiagen*) at 4°C overnight to allow complete penetration of the reagent into the tissue, which could inhibit RNases and protect RNA from degradation. The tissue was then stored at -20°C until extraction.

2.6.2 Total RNA extraction

Total RNA was extracted by using the RNeasy Mini Kit (*Favorgen*) according to the manufacturer's protocol. In brief, the RNA*later* RNA Stabilization Reagent was removed. The tissue was added with 350 µl of Buffer FARB and then

passed through a 25G needle fitted onto a one ml syringe for several times until the tissue was lysed completely. Subsequently, equal volume of 70% ethanol was added to the lysate and was mixed immediately by inverting up and down. The lysate mixture was added to the FARB mini column and centrifuged at 13,000 rpm for 30 sec. After discarding the flow-through, 500 µl of Wash1 buffer was applied to the FARB column and centrifuged at 13,000 rpm for 30 sec. Again, the flow-through was discarded, followed by washing twice with 700 µl of Wash2 buffer and centrifuged at 13,000 rpm for 30 sec. The flow-through was discarded and centrifuged at 13,000 rpm for 3 min to remove any carryover of Wash2 buffer. The FARB column was transferred to a new 1.5 ml microfuge tube. To elute the RNA, 50 µl of RNase-free water was added directly onto the RNeasy silica-gel membrane. After 2 min, the microfuge tube with the column was centrifuged at 13,000 rpm for 1 min to collect the RNA solution from the flow-through. The total RNA concentration was determined by measuring the optical density at the wavelength of 260 nm using a spectrophotometer (GeneQuant, *Pharmacia Biotech*) and stored at -80°C.

2.6.3 Reverse transcription

Total RNA extracted was subjected to first-strand cDNA synthesis by using the High Capacity cDNA Reverse Transcription Kit (*Applied Biosystems*). To synthesize 10 µl of cDNA solution, 500 ng of total RNA was mixed with 1x Reverse Transcription Buffer, 25 mM dNTP, 1x Reverse Transcription random primers, 25 units MultiScribe™ Reverse Transcriptase and 10 units of RNase Inhibitor. DEPC-treated water was added to the reaction mixture to obtain a final volume of 10

µl. Reverse transcription was performed in a thermal cycler (C1000 Thermal Cycler, *BioRad*) at 25°C for 10 min, followed by 37°C for 120 min and then 85°C for 5 sec. The single-stranded cDNA synthesized was kept at 4°C for short-term storage or -20°C for long-term storage.

2.6.4 Real-time polymerase chain reaction

The cDNA synthesized was subjected to quantitative polymerase chain reaction (PCR) using ABI 7900 Fast Real-Time PCR system with 384-well block module (*Applied Biosystems*). Various sets of primers specific for different genes were used. PCR amplification was performed in a reaction mixture containing 1 µl of cDNA, 0.125 µl each of 10 pmol/µl forward and reverse primers, 2.5 µl of 2X iTaq SYBR® Green PCR Master Mix (*Biorad*) and then made up with DEPC-treated water to a final volume of 5 µl. Each sample was amplified in triplicate for accurate quantification.

For each PCR, sample without addition of template was included to serve as the negative control, and a set of cDNA standards (refer to section 2.6.5) with known quantity was added in duplicate for quantifying the amount of the target gene.

The PCR started at 95°C for 10 min to activate the iTaq polymerase (*BioRad*) in the PCR Master Mix to initiate amplification, followed by 40 cycles comprising of denaturation at 95°C for 15 sec, annealing at 58°C for 30 sec and extension at 72°C for 30 sec. The quantity of the target gene was analyzed by ABI SDS 2.3 Software (*Applied Biosystems*).

2.6.5 Preparation of cDNA standards

The cDNA standard was generated by PCR amplification of serially diluted cDNA plasmids of *β-actin* or the target gene with known concentrations. The cDNA plasmid was prepared as described in section 2.6.6 and quantified by spectrophotometry at the wavelength of 260 nm. The cDNA plasmid was adjusted to a concentration of 20 ng/μl in DEPC-treated water. Finally, 10-fold serial dilution was performed to obtain a set of standards ranging from 0.02 pg to 2 ng.

2.6.6 Mini-scale preparation of plasmid DNA

Transformed bacteria were grown in 10 ml of LB Broth (*Invitrogen*) containing 80 μg/ml ampicillin (*Roche*) at 37°C overnight (about 16 hr) with vigorous shaking at 200 rpm. Bacterial cells were centrifuged down at 3,000 rpm for 15 min. The cDNA plasmid was extracted from the bacteria by using the FavorPrep™ Plasmid DNA Extraction Mini Kit (*Favorgen*) according to the manufacturer's protocol. In brief, 250 μl of Cell Suspension Buffer was added to the cell pellet to resuspend the cell by vortexing. Cells were lysed by mixing with 250 μl of Cell Lysis Solution for 5 min. The mixture was neutralized by addition of 350 μl of Neutralization Buffer. The mixture was centrifuged at 14,000 rpm for 10 min. The supernatant was loaded onto a cartridge (provided in the kit) and centrifuged again at 14,000 rpm for 1 min. The flow-through was discarded. The cartridge was washed with 700 μl of Wash Buffer and centrifuged at 14,000 rpm for 2 min. After discarding the flow-through, it was centrifuged again at 14,000 rpm for 1 min to remove any carryover of the Wash Buffer. The plasmid DNA trapped in the cartridge was finally eluted with 100 μl of autoclaved water. One microlitre of extracted

plasmid was subjected to electrophoresis in a 1% agarose gel to confirm the size of the plasmid. One microliter of plasmid was measured by spectrophotometry (GeneQuant, *Pharmacia Biotech*) at the wavelength of 260 nm for quantification. The rest of the DNA plasmid was stored at -20°C.

2.7 WHOLE MOUNT *IN SITU* HYBRIDIZATION

All procedures were carried out at room temperature unless indicated otherwise.

2.7.1 Preparation of embryo sample

Embryos at appropriate stage of gestation were dissected in DEPC-treated ice-cold PBS. They were fixed immediately in freshly-prepared ice-cold 4% paraformaldehyde in PBS overnight at 4°C. Embryos were then washed twice in PBT (PBS with 0.1% Tween-20) followed by a series of increasing concentrations of methanol in PBT starting from 25%, 50%, 70% and finally twice in 100% at 4°C for 15 min each to dehydrate the embryos. After dehydration, embryos were stored at -20°C and used within a month.

2.7.2 Hybridization

To start hybridization, embryos were first rehydrated by passing through a series of decreasing concentrations of methanol starting from 100% to 75%, 50% and 25% in PBT, followed by washing in PBT for 15 min each. After rehydration, embryos were treated with 6% hydrogen peroxide (*VWR*) in PBT for an hour to inactivate the endogenous alkaline phosphatase. Embryos were then washed three times with PBT for 15 min each and treated with 10 μg/ml proteinase K (*Roche*).

The duration of digestion should be tightly controlled, otherwise the embryos could be damaged. Normally, 3 min was enough for embryos at E9. The action of proteinase K digestion was stopped by washing with 2 mg/ml glycine (*BDH*) in PBT for 5 min, followed by washing with PBT for 15 min. Embryos were then refixed in freshly-prepared 0.2% glutaraldehyde in 4% paraformaldehyde in PBT for 20 min. After washing once with PBT for 15 min, embryos were pre-hybridized in a pre-warmed pre-hybridization solution containing 50% deionized formamide (*BDH*); SSC solution (0.75 M sodium chloride; 0.075 M sodium citrate), pH 4.5; 1% sodium dodecyl sulphate (SDS) (*Sigma*); 50 μg/ml yeast tRNA (*Invitrogen*) and 50 μg/ml heparin (*Sigma*) for 2 hr at 70°C with gentle rocking. The pre-hybridization solution was finally replaced with the pre-warmed hybridization solution that contained 1 μg of digoxigenin (DIG)-labeled RNA probes (refer to section 2.8) in 1 ml of pre-hybridization solution. Hybridization was carried out at 70°C overnight with gentle rocking.

2.7.3 Post-hybridization wash

After hybridization, the unbound RNA probes were removed by washing twice with solution 1 (50% formamide; 5X SSC, pH 4.5; 1% SDS) for 30 min each at 70°C. Holes were punched in the brain of the embryo with tungsten needle to prevent trapping of RNA probes that might lead to non-specific signal. After that, embryos were washed with a solution made up of equal volume of solution 1 and solution 2 (0.5 M NaCl; 10 mM Tris-HCl, pH 7.5; 0.1% Tween-20) for 10 min and then washed three times with solution 2 for 10 min each. The unbounded RNA probes were further digested by washing with 100 μg/ml *RNase A* (*Roche*) in

solution 2 for 30 min at 37°C. After *RNase A* digestion, embryos were washed once in solution 2 for 5 min. Afterwards, embryos were washed twice with solution 3 (50% formamide; 2X SSC, pH 4.5) for 30 min at 65°C and then three times with TBST solution [0.14 M NaCl; 2.7 mM KCl; 25 mM Tris-HCl, pH 9.5; 0.5% Tween-20; 0.5 mg/ml (-)-Tetramisole hydrochloride (*Sigma*)] for 10 min each to remove the digested RNA fragments. Embryos were then pre-blocked with 10% heat-inactivated sheep serum (*Jackson ImmunoReasearch*) in TBST for 90 min and then incubated overnight at 4°C with pre-absorbed (refer to sections 2.7.5 and 2.7.6 for details) alkaline phosphatase-conjugated anti-DIG antibody (*Roche*).

2.7.4 Post-antibody wash and signal development

The unbound antibody was removed by washing three times with TBST for 5 min each, followed by one hour washing for five times with gentle rocking. After washing, embryos were pre-conditioned in NTMT solution [100 mM NaCl; 100 mM Tris-HCl, pH 9.5; 50 mM $MgCl_2$; 0.1% Tween-20; 0.5 mg/ml (-)-Tetramisole hydrochloride] three times for 10 min each. The signal was then developed with 5 ml staining solution containing 4.5 µl of nitro blue tetratzolium (*Roche*) [75 mg/ml stock in 70% N,N-dimethyl formamide (*Sigma*)] and 3.5 µl of 5-bromo-4-chloro-3-indolyl phosphate (*Roche*) (50 mg/ml stock in N,N-dimethyl formamide) per ml of NTMT in the dark. The signal intensity was monitored occasionally under microscope until the optimal level was achieved. The staining reaction was stopped by washing embryos with PBT three times for 10 min each. Embryos were post-fixed in freshly-prepared 4% paraformaldehyde in PBS overnight at 4°C. Embryos were washed twice with PBS and cleared in graded

glycerol in increasing concentrations (50%, 75% in autoclaved water and 100%).

2.7.5 Pre-absorption of antibody

Embryo powder at a weight of 6 mg was heat-treated in 1 ml of TBST buffer for 30 min at 70°C. After chilling on ice, 10 µl of heat-treated (incubation for 30 min at 56°C) sheep serum and 2 µl of alkaline phosphatase-conjugated anti-DIG antibody (0.75 units/µl, *Roche*) were added and then shaken gently on ice for 5 hr. After centrifugation at 14,000 rpm for 5 min at 4°C, the supernatant was taken and diluted to 4 ml with 1% heat-treated sheep serum in TBST.

2.7.6 Embryo powder preparation

Embryo powder was prepared by homogenizing E13.5 mouse embryos in PBS with a sonicator (Vibra-Cell VCX130, *Sonics & Materials, Inc.*). The homogenate was incubated with ice-cold acetone on ice for 30 min, centrifuged and washed again with ice-cold acetone. After centrifugation at 10,000 rpm for 10 min, the pellet was air-dried and ground into fine powder and stored air-tight at -20°C.

2.8 PREPARATION OF RNA PROBE

2.8.1 Linearization of cDNA plasmid

To prepare single-stranded RNA probe for *in situ* hybridization, the cDNA plasmid, obtained as described in section 2.6.6, was first linearized by cutting with the appropriate restriction enzyme as described in the materials and methods section

of the relevant chapter. The reaction mixture included 5 µg cDNA plasmid, 20 units of restriction enzyme, 1X reaction buffer and made up to a final volume of 50 µl with DEPC-treated water. The reaction mixture was then incubated in a thermomixer (*Eppendrof*) for 2 hr at 37°C with gentle shaking. After digestion, the linearized plasmid DNA was extracted by adding equal volume of phenol: chloroform: isoamyl alcohol (25:24:1, v:v:v) (*Sigma*) followed by centrifugation at 14,000 rpm for 10 min at 4°C. The upper aqueous layer containing the DNA was collected and an equivalent volume of chloroform: isoamyl alcohol (24:1, v:v) (*Sigma*) was added. The reaction mixture was centrifuged again at 14,000 rpm for 10 min at 4°C. The upper aqueous layer was collected and the DNA was precipitated with 0.1 volume of 3 M sodium acetate and 2 volumes of ice-cold absolute ethanol and kept at -20°C for 2 hr. The DNA pellet was finally collected by centrifugation at 14,000 rpm for 15 min at 4°C. The supernatant was discarded and the pellet was washed with 70% ice-cold ethanol. After drying thoroughly, the DNA pellet was resuspended in 20 µl of DEPC-treated water.

To confirm that the cDNA plasmid was linearized completely, 1 µl of sample was subjected to electrophoresis in a 0.8% agarose gel to check the size. One microliter of sample was measured by spectrophotometry at the wavelength of 260 nm to quantify the concentration. The rest of the DNA solution was stored at -20°C.

2.8.2 *In vitro* transcription and labeling

Single-stranded RNA probe was synthesized by the appropriate RNA polymerase as detailed in the materials and methods section of the relevant chapter. The probe was labeled by DIG RNA Labeling Mix (*Roche*), which contained

DIG-labeled UTP and unlabeled ATP, CTP and GTP. The reaction mixture included 1X transcription buffer, 1 mM DIG RNA labeling nucleotide mix, 20 units of RNasin ribonuclease inhibitor (*Roche*), 30 units of RNA polymerase and 4 μg linearized DNA plasmid, made up to a final volume of 20 μl with DEPC-treated water. The reaction mixture was incubated in a thermomixer for 2 hr at 37°C. After *in vitro* transcription, 2 μl of *DNaseI* (10 units/μl, *Roche*) was added to digest the cDNA template by incubating for 15 min at 37°C. To precipitate the DIG-labeled RNA probe, 10 μl of 4 M lithium chloride, 100 μl of Tris-EDTA (TE) buffer (pH 7.4) and 300 μl of ice-cold absolute ethanol were added and then kept for 2 hr at -20°C. The mixture was centrifuged at 14,000 rpm for 15 min at 4°C and the pellet was washed with 700 μl of 70% ice-cold ethanol. Finally, the pellet was dissolved in 60 μl of ice-cold DEPC-treated water. The size of the RNA probe was confirmed by displaying 2 μl of the dissolved RNA using gel electrophoresis. The concentration was quantified by measuring the optical density of 2 μl of the RNA solution at the wavelength of 260 nm using a spectrophotometer. The remaining RNA solution was stored at -80°C until use.

Chapter 3

Analysis of *Cyp26* Expression in Embryos under Diabetic and Non-diabetic Conditions

3.1 INTRODUCTION

Cyp26 belongs to the family of cytochrome P450 enzymes that metabolize RA (White et al., 1996; Fujii et al., 1997; Ray et al., 1997; Hollemann et al., 1998). It has been demonstrated that cultured cells with overexpression of *Cyp26* showed reduced sensitivity to RA (White et al., 1997). Besides, microsome fractions extracted from cells that contained Cyp26 enzymes could metabolize RA *in vitro* into polar oxidative forms such as 5,8-epoxy RA, 4-hydroxy RA and 18-hydroxy RA (White et al., 1996; Fujii et al., 1997). These observations suggest that Cyp26 may be responsible for enzymatic degradation of RA *in vivo*. As mentioned previously, RA catabolism is controlled by 3 subtypes of Cyp26 enzymes, including Cyp26A1, Cyp26B1 and Cyp26C1. The three *Cyp26* genes exhibit different expression patterns at different stages of embryo development, indicating that they may be responsible for protecting different tissues from inappropriate RA signaling for development of particular organs during embryogenesis. For example, *Cyp26a1* is important for posterior development (Abu-Abed et al., 2001) while *Cyp26b1* is responsible for gonad development and sex determination (Koubova et al., 2006).

Cyp26a1 expresses in various regions in a spatially and temporally regulated manner during organogenesis. *Cyp26a1* expression initiates at E6.0 in the extraembryonic and embryonic endoderm of the mouse embryo. Its expression in the primitive streak and posterior mesoderm becomes more prominent at E6.5 (Fujii et al., 1997). Expression of *Cyp26a1* then changes dramatically, with the expression in the posterior region of the embryo rapidly disappears by E7.0. Half a day later, by E7.5, expression is found not only in anterior headfold tissues, but is also re-expressed in the tail bud mesoderm and the posterior neural plate (Fujii et al., 1997). Its expression in extraembryonic tissues also starts to be turned off at this

period. By E8.0, *Cyp26a1* is expressed in the heart tube endocardium, rostrally in the outflow tract and caudally in the atria and sinus venosus. Expression is still seen in the endocardium, but not in other vascular elements by E8.5 (Moss et al., 1998). Moreover, *Cyp26a1* is highly expressed along the maxillo-mandibular cleft and is the only *Cyp26* gene highly restricted to the tail bud region of the embryo between E9.0 to E9.5 (Fujii et al., 1997). By E10.0, *Cyp26a1* helps to generate uneven distribution of RA along the dorsoventral axis of the retina. The rich zones of RA in the dorsal and ventral retina are separated by a horizontal RA-poor stripe that contains the RA-inactivating enzyme Cyp26A1 (Wagner et al., 2000). Interestingly, the main RA catabolizing enzyme *Cyp26a1* and the main RA synthesizing enzyme *Raldh2* begin mRNA expression at the same time, and they express in complementary, but non-overlapping domains (Fujii et al., 1997; de Roos et al., 1999; Swindell et al., 1999).

The second subtype of *Cyp26* gene, *Cyp26b1*, was first identified in humans (Nelson, 1999). It is found predominantly expressed in the adult cerebellum and shows high efficiency of catabolism and substrate specificity to all-*trans* RA (White et al., 2000a). Similar to *Cyp26a1*, cells transiently transfected with *Cyp26b1* could convert all-*trans* RA to more polar metabolites including 4-oxo, 4-hydroxy and 18-hydroxy RA. The mouse ortholog of *Cyp26b1* has also been cloned and characterized by MacLean et al. (2001). *Cyp26b1* expression initiates at E8.0 of the mouse embryo in prospective rhombomeres 3 and 5. Rhombomeric expression of *Cyp26b1* further expands to specific dorso-ventral domains in rhombomeres 2 to 6 between E8.5 and E9.5 (MacLean et al., 2001). Differential expression is also seen in branchial arches, with *Cyp26a1* being mainly expressed in neural crest-derived mesenchyme (Fujii et al., 1997; de Roos et al., 1999), whereas *Cyp26b1* is observed

in both ectodermal and endodermal portions of the caudal branchial arches (MacLean et al., 2001). *Cyp26b1* is markedly expressed in the ectoderm and distal mesoderm of the limb buds from the beginning of their outgrowth. Prolonged staining revealed the presence of *Cyp26b1* expression between the developing somites and at the level of caudal branchial arches. In contrast, *Cyp26b1* is more widely expressed in the embryo than *Cyp26a1* and *Cyp26c1*, with transcripts being present in the hindbrain from E8.0 to E10.5, and in the developing limb bud, branchial arches, craniofacial structures and various organs in later stages of embryogenesis (MacLean et al., 2001; Abu-Abed et al., 2002). Recent studies have shown that *Cyp26b1* is responsible for controlling the timing of meiosis differentially between sexes, with *Cyp26b1* being completely turned off in the embryonic ovary, but is highly expressed in the embryonic testis (Koubova et al., 2006). Cyp26B1 maintains RA at low levels in the developing testis that blocks meiosis and acts as a survival factor to prevent apoptosis of male germ cells (MacLean et al., 2007).

The third subtype of *Cyp26* gene, *Cyp26c1*, has also been cloned (Tahayato et al., 2003). Sequence analysis shows that *Cyp26c1* is more closely related to *Cyp26b1* than *Cyp26a1*. However, Cyp26C1 appears to have slightly different enzymatic properties (Tahayato et al., 2003; Taimi et al., 2004). Analysis of Cyp26C1 activity *in vitro* showed that other than metabolizing all-*trans* RA, it could also hydrolyze 9-cis RA with a much greater efficiency than Cyp26A1 and Cyp26B1 (Taimi et al., 2004). *Cyp26c1* is expressed in the hindbrain between E8.0 and E9.5 mouse embryos. At E8.0, *Cyp26c1* is specifically expressed in prospective anterior rhombomeres 2 and 4, and in the rostral portion of the first branchial arch. A comparison between *Cyp26b1* and *Cyp26c1* expression shows non-overlapping

transcript distributions along rhombomeres 2 to 6, suggesting distinct roles of both enzymes in regulating RA distribution within the hindbrain (MacLean et al., 2001). By E9.0 to E9.5, *Cyp26c1* is expressed in the maxillary and mandibular components of the first branchial arch, in rhombomere 2 and in the lateral epibranchial placodes. Strong staining is also observed in the cervical mesenchyme caudal to the otic vesicle. Similarly, at this stage, *Cyp26a1* is also expressed in the cervical mesenchyme as well as in the first branchial arch, although *Cyp26c1* expression seems to be stronger.

Many of the tissues that express *Cyp26* genes are shown to be sensitive to the effect of RA. Common malformations of RA teratogenicity include exencephaly, spina bifida, caudal regression, limb truncations, cleft palate, hindbrain posteriorization, micrognanthia and other craniofacial abnormalities (Conlon & Rossant, 1992; Maden & Holder, 1992; Eichele, 1999; Shum et al., 1999). Of these malformations, spina bifida, caudal regression and subtle changes in hindbrain patterning are observed in *Cyp26a1* null mice (Abu-Abed et al., 2001; Sakai et al., 2001). Such abnormalities are also commonly found in infants of diabetic pregnancy as previously mentioned. Hence, it is worthwhile to investigate if there are any dysregulation of *Cyp26* gene expressions in embryos of diabetic pregnancy.

3.2 EXPERIMENTAL DESIGN

It is well-documented that RA is teratogenic and many tissues that express *Cyp26* genes are shown to be sensitive to the effect of RA. Our laboratory has previously found that *Cyp26a1*, which is specifically expressed in the tail bud region, was significantly down-regulated in embryos of diabetic mice (Leung, 2005). Such down-regulation led to a decrease in RA catabolic activity (Lee, 2008). As a result, upon exposure to an aberrant level of RA, the tail bud had reduced ability to clear away the unwanted RA and thereby showed increased sensitivity to the teratogenic effect of RA (Lee, 2008). These results are complementary to our previous findings that embryos of diabetic mice were more susceptible to RA-induced caudal regression (Chan et al., 2002).

Other than caudal regression, alteration in RA levels gives rise to anomalies that are strikingly similar to those observed in cases of diabetic pregnancy, such as neural tube defects, skeletal defects and genitourinary defects. Interestingly, *Cyp26a1* homozygous null mutant mouse embryos also exhibited anomalies (Abu-Abed et al., 2001; Sakai et al., 2001) similar to those caused by excess RA and diabetic pregnancy. Together, these findings implicate that some common pathogenic mechanisms may be shared among them in inducing birth defects. I therefore hypothesize that reduced RA catabolism in the developing tissue during embryonic development is a fundamental pathogenic mechanism leading to increased risk of congenital malformations in diabetic pregnancy.

To test this hypothesis, in this chapter, first, I have investigated the expression of the three subtypes of *Cyp26* genes (*a1*, *b1* and *c1*) in embryos of non-diabetic and diabetic mice at mid-gestation. Embryos were collected at E9.0, an

early stage of organogenesis. The mRNA expression level of the three *Cyp26* subtypes in both non-diabetic and diabetic groups was determined by real-time quantitative RT-PCR. Expression patterns were also studied by whole mount *in situ* hybridization in order to determine whether changes, if any, were generalized or tissue-specific.

Results in the first part of study showed that *Cyp26a1* was the only subtype in which the expression level was altered under diabetes. Since *Cyp26a1* is already expressed in primitive streak stage mouse embryos, hence, in the second part of this chapter, I have further compared *Cyp26a1* expressions in embryos of diabetic and non-diabetic mice at earlier stages (E7.0 and E8.0) to determine whether down-regulation of *Cyp26a1* expression in diabetic pregnancy was evident by then.

Although there was no significant difference in *Cyp26b1* and *Cyp26c1* expression levels between embryos of diabetic and non-diabetic mice under normal conditions, it remained to be determined whether differences between the two groups would occur in the presence of excess RA. Thus, in the last part of this chapter, I have studied the response of the three *Cyp26* genes to excess RA in diabetic and non-diabetic maternal milieu by analyzing their expressions in embryos taken at different time points (0, 2, 4, 8 and 12 hr) after maternal RA treatment.

3.3 MATERIALS AND METHODS

3.3.1 Sample collection

Diabetic or non-diabetic ICR female mice were mated with non-diabetic ICR male mice as described in section 2.1. Embryos at the desired time point (E7.0, E8.0 and E9.0) were dissected in ice-cold DEPC-treated PBS and freed from all decidual tissues and extraembryonic membranes. Embryos of the same litter were immediately fixed in 4% paraformaldehyde for whole mount *in situ* hybridization study as described in sections 2.7 and 2.8. As for quantification of gene expression by real-time RT-PCR, to minimize differences in gene expression levels due to differences in the developmental stage, only embryos at similar stages were collected. Embryos with 7-8 and 20-21 pairs of somites were collected as E8.0 and E9.0 embryos respectively. Primitive mid-streak stage embryo, identified according to the morphological landmarks as described in Downs & Davies (1993), were collected as E7.0 embryos. Embryos of the same litter at the appropriate stage were pooled as one sample. Tissues were stored in RNA*later* RNA Stabilization Reagent as described in section 2.6.1 before being processed for real-time RT-PCR quantification.

To examine the response of *Cyp26* genes to RA, on E9.0, diabetic and non-diabetic pregnant mice were intraperitoneally injected, using a 20G needle (0.90 x 38 mm; *Terumo*), with 50 mg/kg body weight of RA (RA suspension at 3.33 mg/ml) or equivalent volume of suspension vehicle (15 μl per gram of weight) as control. Pregnant mice were sacrificed prior to (0 hour) and at 2, 4, 8 and 12 hr after RA treatment. Embryos were collected for whole mount *in situ* hybridization or real-time quantitative RT-PCR studies. Again, only embryos at specific somite-stage

(17-19 somite-stage for 0 hr, 19-20 somite-stage for 2 hr, 21-22 somite-stage for 4 hr, 23-24 somite-stage for 8 hr and 26-27 somite-stage for 12 hr) were collected for analysis. Embryos of the same litter at the appropriate stage were pooled as one sample. The blood glucose level of diabetic mouse was measured prior to RA injection to ensure that the mouse remained diabetic during pregnancy.

3.3.2 Real-time quantitative RT-PCR

Extraction of total RNA from the embryo sample and first-strand cDNA synthesis by RT were performed as described in sections 2.6.2 and 2.6.3 respectively. After RT reaction, expression levels of *Cyp26a1*, *Cyp26b1* and *Cyp26c1* were determined by real-time quantitative PCR. *β-actin* was used as the internal control for normalization of PCR products. The PCR conditions were the same as described in section 2.6.4. To quantify the amount of *Cyp26* and *β-actin* genes, cDNA standards were co-amplified in each PCR. The standards were prepared as described in section 2.6.5. *Cyp26a1*, *Cyp26b1* and *Cyp26c1* mouse cDNA plasmids (particulars as described in section 3.3.3) were gifts from Prof. Hiroshi Hamada, β-actin mouse cDNA plasmid was obtained from Prof. Ronald Wang. The PCR products amplified were: a 221 base pairs (bp) sequence corresponding to nucleotide sequences 504-523 and 725-706 of mouse *Cyp26a1*, a 184 bp sequence corresponding to nucleotide sequences 2912-2931 and 3096-3077 of mouse *Cyp26b1*, a 151 bp sequence corresponding to nucleotide sequences 719-738 and 870-851 of mouse *Cyp26c1*, and a 164 bp sequence corresponding to nucleotide sequences 304-323 and 468-449 of mouse *β-actin*. The sequences of primers for amplification of partial sequence of the target gene were as follow:

Mouse *Cyp26a1*	forward primer:	5'-CAG TGC TAC CTG CTC GTG AT-3'
	reverse primer:	5'-AGA GAA GAG ATT GCG GGT CA-3'
Mouse *Cyp26b1*	forward primer:	5'-CCT GGT GAG GAT GAA TAA GG-3'
	reverse primer:	5'-TTT CCA CCT TAC CTC TCT GC-3'
Mouse *Cyp26c1*	forward primer:	5'-GGG ACC AGT TGT ATG AGC AC-3'
	reverse primer:	5'-AGC CAA CTC CTT CAG CTC TT-3'
Mouse *β-actin*	forward primer:	5'-TGT TAC CAA CTG GGA CGA CA-3'
	reverse primer:	5'-GGG GTG TTG AAG GTC TCA AA-3'

After PCR, expression levels of these genes were analyzed by ABI SDS 2.3 Software (*Applied Biosystems*).

3.3.3 Whole mount *in situ* hybridization

Embryos were processed for analysis of *Cyp26a1*, *Cyp26b1* and *Cyp26c1* mRNA expressions by whole mount *in situ* hybridization using RNA probes prepared from the following cDNA plasmids and protocols as described in sections 2.7 and 2.8. Between 5 to 7 litters of embryos were examined for each group.

Particulars of cDNA plasmids:

cDNA Plasmid	Vector	Insert size (bp)	Restriction enzyme for antisense riboprobe	RNA polymerase for antisense riboprobe
Cyp26a1	Bluescript SK	0.6 kb	*EcoRI*	T3
Cyp26b1	pGEM5	0.9 kb	*EcoRV*	T7
Cyp26c1	pBluescript II KS	0.5 kb	*BamHI*	T3

Extensive up-regulation of *Cyp26a1* and *Cyp26b1* expressions after RA treatment made the examination of expression patterns in whole embryo difficult. Detailed examination to identify the exact expression domain of the gene was performed by sectioning of the embryo using a vibratome (VT100S, *Leica*). To prepare the embryo for vibratome sectioning, the embryo, stored in glycerol, was thoroughly washed in 0.1 M phosphate buffer (PB), followed by overnight fixation in freshly-prepared 4% paraformaldehye in 0.1 M PB at 4°C. The embryo was thoroughly washed in two changes of 0.1 M PB. The portion of the embryo of interest was cut out and embedded in the desired plane in Gloop medium added with 25% glutaraldehyde (the amount of glutaraldehyde added was adjusted each time to control the speed of solidification). After solidified, the tissue block was cut into 25 μm thick vibratome sections.

The Gloop medium was prepared by dissolving 0.5 g gelatin (*USB*), 20 g sucrose (*BDH*) and 30 g chicken egg albumin (*Sigma*) in 0.1 M Phosphate buffer (pH7.4) to a final volume of 100 ml. The ingredients were mixed at room temperature for overnight with a stir bar and filtered through 4 layers of gauzes to remove bubbles. It was stored at 4°C until use.

3.3.4 Statistical analysis

The relative expression levels of *Cyp26* genes between embryos of diabetic and non-diabetic mice at different time points with or without RA treatment were compared by Independent Samples t-test. All statistical analyses were carried out using SPSS software (*SPSS*), with statistical significance level set at $p < 0.05$.

3.4 RESULTS

3.4.1 Expression of *Cyp26a1*, *Cyp26b1* and *Cyp26c1* at E9.0

The *in situ* expression patterns and relative expression levels of *Cyp26a1*, *Cyp26b1* and *Cyp26c1* in embryos of non-diabetic and diabetic mice at E9.0 were presented in Figure 3.1 and Graph 3.1 respectively. Data and results of statistical analysis were summarized in Table 3.1.

Results from *in situ* hybridization studies show that *Cyp26a1* is expressed anteriorly in the cranial and cervical mesenchyme, the maxillary and mandibular components of the first branchial arch and also along the maxillo-mandibular cleft (Figure 3.1A). Posteriorly, it is expressed in the tail bud region of the embryo. In the embryo of diabetic mouse, prominent reduction in signal intensity is observed in all expression domains (Figure 3.1B). Further quantification by real-time RT-PCR confirmed that indeed, there was a significant ($p = 0.014$) down-regulation of 22% of *Cyp26a1* expression level in embryos under diabetic pregnancy (Graph 3.1A).

Cyp26b1 shows high levels of expression in the hindbrain region at rhombomeres 2 to 6 (Figure 3.1C). Strong expression is observed in the entire rhombomere of rhombomeres 5 and 6, while expression appears to be more restricted to the basal region in rhombomeres 2 to 4. Weak *Cyp26b1* expression is also observed in the mesenchyme between developing somites, the caudal branchial arches and in the developing heart. However, no expression is observed in the tail bud region. Although the expression level of *Cyp26b1* is similar to that of *Cyp26a1*, the expression pattern of these 2 subtypes of *Cyp26* is totally non-overlapping. Unlike *Cyp26a1*, there was no significant difference in the expression level of *Cyp26b1* between embryos of non-diabetic and diabetic groups as detected by both

in situ hybridization (Figure 3.1D) and real-time quantitative RT-PCR (Graph 3.1B).

The expression pattern of *Cyp26c1* in the anterior part of the embryo (Figure 3.1E) is highly similar to that of *Cyp26a1*. It is expressed in the cranial and cervical mesenchyme, the maxillary and mandibular mesodermal components of the first branchial arch and the maxillo-mandibular cleft. It is also expressed in rhombomere 2. However, unlike *Cyp26a1*, *Cyp26c1* expression is not observed in the tail bud region of the embryo. Again, there was no significant difference in expression levels between embryos of non-diabetic and diabetic groups as determined by both *in situ* hybridization (Figure 3.1F) and real-time quantitative RT-PCR (Graph 3.1C).

To conclude, *Cyp26a1* is the only subtype of *Cyp26* gene found to be significantly altered in expression levels in embryos of diabetic pregnancy at E9.0.

Table 3.1 Expression levels of *Cyp26a1*, *Cyp26b1* and *Cyp26c1* relative to *β-actin* in embryos of non-diabetic and diabetic mice at E9.0.

Maternal status	ND	SD
No. of litters	5	5
No. of embryos	45	40
Sample size[#]	5	5
Relative expression levels of *Cyp26a1* ± SE	0.0045 ± 0.0003	0.0035 ± 0.0001
p value in comparing relative expression level of *Cyp26a1* of ND vs. SD	0.014*	
Relative expression levels of *Cyp26b1* ± SE	0.0042 ± 0.0001	0.0043 ± 0.0002
p value in comparing relative expression level of *Cyp26b1* of ND vs. SD	0.994	
Relative expression levels of *Cyp26c1* ± SE	0.0037 ± 0.0001	0.0039 ± 0.0001
p value in comparing relative expression level of *Cyp26c1* of ND vs. SD	0.384	

[#] Refer to section 3.3.1 for definition of one sample

* Statistically significant (data were analyzed by Independent Samples t-test)

3.4.2 Expression of *Cyp26a1* at E7.0 and E8.0

After confirming that *Cyp26a1* is already down-regulated in embryos of diabetic pregnancy at E9.0, next, I have examined its expression at earlier stages of development (E7.0 and E8.0). The *in situ* expression patterns and relative expression levels of *Cyp26a1* in embryos of non-diabetic (ND) and diabetic (SD) mice at E7.0 and E8.0 were presented in Figure 3.2 and Graph 3.2 respectively. Data and results of statistical analysis were summarized in Table 3.2.

At E7.0, *Cyp26a1* is expressed in the headfold mesenchyme and yolk sac endoderm of the embryo (Figure 3.2A). By E8.0, expression persists in the anterior neural fold and also begins in the posterior neural plate and tail bud mesoderm at the caudal extremity of the embryo (Figure 3.2C). In embryos of diabetic mice, prominent reduction of *Cyp26a1* signal is observed in all expression domains at both stages (Figures 3.2B and 3.2D). Further quantification by real-time RT-PCR confirmed that the reduction in expression level in the diabetic group was statistically significant [$p < 0.05$ for both E7.0 (Graph 3.2A) and E8.0 (Graph 3.2B)]. The extent of down-regulation was particularly obvious at E7.0, with 40% reduction in the expression level, while the difference became less (19%) as development proceeded to E8.0.

Taken together, results show that *Cyp26a1* is the only RA catabolizing gene that is down-regulated under diabetic pregnancy. Such down-regulation occurs in various tissues throughout the early period of organogenesis.

Table 3.2 Expression levels of *Cyp26a1* relative to *β-actin* in embryos of non-diabetic and diabetic mice at E7.0 and E8.0.

Maternal status	ND	SD
No. of litters	5	5
No. of embryos	43	39
Sample size[#]	5	5
Relative expression levels of *Cyp26a1* at E7.0 ± SE	0.0483 ± 0.0057	0.0289 ± 0.0045
p value in comparing relative expression levels of *Cyp26a1* of ND vs. SD at E7.0	0.038*	
Relative expression levels of *Cyp26a1* at E8.0 ± SE	0.0026 ± 0.0001	0.0021 ± 0.0001
p value in comparing relative expression levels of *Cyp26a1* of ND vs. SD at E8.0	0.019*	

[#] Refer to section 3.3.1 for definition of one sample

* Statistically significant (data were analyzed by Independent Samples t-test)

3.4.3 Changes in *Cyp26* expression in the embryo after maternal RA treatment

After confirming that *Cyp26a1* is the subtype with its expression level being affected in diabetic pregnancy, next, I have compared the changes in expression levels of the 3 subtypes of *Cyp26* between non-diabetic and diabetic groups at various time points after RA treatment by whole mount *in situ* hybridization and quantitative RT-PCR. Moreover, since extensive up-regulation of *Cyp26a1* and *Cyp26b1* after RA treatment made the examination of expression patterns in the whole embryo difficult, embryos at 2 hr and 8 hr after RA treatment in the non-diabetic group were cut as vibratome sections in order to have a general idea in which tissues the gene was expressed. Whole mount *in situ* expression

patterns of *Cyp26a1* were shown in Figure 3.3. Vibratome sections of embryos at 2 hr and 8 hr after RA treatment in the non-diabetic group were shown in Figure 3.4 and Figure 3.5 respectively. Whole mount *in situ* expression patterns of *Cyp26b1* were shown in Figure 3.6 and sections of embryos at 2 hr and 8 hr after RA treatment in the non-diabetic group were shown in Figure 3.7 and Figure 3.8 respectively. Whole mount *in situ* expression patterns of *Cyp26c1* were shown in Figure 3.9. The expression levels of *Cyp26a1*, *Cyp26b1* and *Cyp26c1* were quantified by real-time RT-PCR, with the data summarized in Table 3.3 and presented in Graphs 3.3, 3.4 and 3.5 respectively. Results of statistical analyses were shown in Table 3.4.

3.4.3.1 *Cyp26a1*

As described in section 3.4.1, without RA treatment, expression of *Cyp26a1* was found in the cranial and cervical mesenchyme, and in the first branchial arch (Figure 3.3A). Restricted signal was also seen along the maxillo-mandibular cleft. Posteriorly, it was strongly expressed in the tail bud region of the embryo. Embryos of the diabetic group showed reduced signal intensity (Figure 3.3F). Two hours after RA treatment, the expression level of *Cyp26a1* (Graph 3.3) was significantly up-regulated in both diabetic ($p = 0.003$) and non-diabetic ($p = 0.007$) groups, with the expression in the cranial and cervical mesenchyme expanded to a much broader domain in the head region (Figure 3.3B). However, expression was totally excluded from the forebrain, midbrain, hindbrain and optic vesicle of the embryo, but was strongly expressed in the surface ectoderm overlying these structures as observed in vibratome sections of stained embryos (Figures 3.4B and 3.4C). Intense signal was

also observed in the epithelial lining of the maxillo-mandibular cleft, with lower level of expression in the mesenchymal component of the first branchial arch. There was also weak expression in the heart region (Figure 3.4D). Intense signal was observed along the ventral body wall of the trunk (Figure 3.4E) and in the ventral part of the hindgut diverticulum (Figure 3.4F). In the posterior region of the embryo, intense signal was observed in the posterior neural plate, the underlying mesoderm and the dorsal hindgut endoderm, with lower level of expression in ventral structures (Figure 3.4G). *Cyp26a1* was strongly and uniformly expressed in the entire tail bud (Figure 3.4H). In embryos of diabetic pregnancy, there was noticeably lesser extent of up-regulation of *Cyp26a1* (Figure 3.3G). Quantification by real-time RT-PCR further confirmed that the expression level of *Cyp26a1* was significantly ($p = 0.030$) lower in the RA-treated embryos of diabetic mice in comparison to the RA-treated embryos of non-diabetic mice. Moreover, the difference in the expression level of *Cyp26a1* between embryos of diabetic and non-diabetic mice exacerbated from 20% prior to RA treatment to 36% at 2 hr after RA treatment. At 4 hr after RA treatment, the level of expression of *Cyp26a1* in the usual and ectopic domains was further intensified (Figures 3.3C and 3.3H) in both diabetic and non-diabetic groups. Similar to the 2 hr time point, the difference in the expression level of *Cyp26a1* between embryos of diabetic and non-diabetic groups was about 37%. The up-regulation of *Cyp26a1* reached a peak level at 8 hr after RA treatment. Expression in all domains was further intensified as observed in both whole mount embryos (Figure 3.3D) and in vibratome sections cut in transverse plane (Figures 3.5B and 3.5C). Expression was observed in the spinal neural tube with variations along the body axis. In the upper trunk, expression was restricted to the neural crest (Figure 3.5D). In the middle trunk, other than intense expression in the neural crest

at the dorsal midline, there were patches of cells along the neural tube that expressed *Cyp26a1* (Figure 3.5G). In the lower trunk, distinct patterns of *Cyp26a1* expression were observed along the dorsoventral axis of the neural tube except the floor plate (Figure 3.5H). Strong expression was also observed in the heart (Figure 3.5E). Detailed examination of the heart found that the expression was on the pericardial lining (Figure 3.5D). After removing the lining, high expression was found at the aortic sac and bulbus cordis region, whereas only weak level of expression was found in the ventricular chamber of the heart (Figures 3.5D and 3.5F). Strong expression persisted in the ventral body wall (Figures 3.5G and 3.5H), the posterior neuropore and the tail bud (Figure 3.5I). Similar expression patterns were observed in embryos of diabetic group, but with obvious reduction in signal intensity (Figure 3.3I). Measurement by quantitative RT-PCR further confirmed that there was significant (p = 0.046) difference in the expression level of *Cyp26a1* between embryos of diabetic and non-diabetic mice. Four hours later, i.e. at 12 hr after RA treatment, the expression of *Cyp26a1* in the embryo was dramatically reduced to such an extent that the level was significantly ($p < 0.001$ for non-diabetic group; p = 0.046 for diabetic group) lower than that of the control embryo at the same time point. Expression of *Cyp26a1* in all ectopic sites had switched off (Figure 3.3E and Figure 3.3J). Very low level of expression was observed anteriorly in the cranial and cervical mesenchyme and in the maxillo-mandibular cleft. Expression in the posterior neural plate and the tail bud was also prominently reduced. Interestingly, at this time point, the expression of *Cyp26a1* in the diabetic group (Figure 3.3J) was, on the other hand, significantly (p = 0.043) higher than the non-diabetic group (Figure 3.3E), suggesting that the down-regulation of *Cyp26a1* was slower in the diabetic group.

3.4.3.2 *Cyp26b1*

For *Cyp26b1*, as mentioned in section 3.4.1, expression was mainly located in the hindbrain region at rhombomeres 2 to 6 (Figure 3.6A). Weak expression was also observed in the developing heart, the caudal branchial arch and in intersomitic tissues. No difference in expression patterns or expression levels of *Cyp26b1* could be found between embryos of non-diabetic and diabetic groups by *in situ* hybridization (Figure 3.6F) nor by the more sensitive method of real-time quantitative RT-PCR (Graph 3.4). Two hours after RA injection, similar to *Cyp26a1*, *Cyp26b1* was significantly up-regulated in the non-diabetic ($p = 0.001$, Figure 3.6B) and diabetic ($p = 0.029$, Figure 3.6G) groups. Weak expression was found in the cranial mesenchyme but not in the forebrain, midbrain and optic vesicles (Figures 3.7A and 3.7B). Expression in rhombomeres 2-4 was located in a strip of cells in the mid-ventral part of the neural tube (Figure 3.7B), whereas expression in rhombomeres 5-6 spanned the entire neural tube except the roof plate and the floor plate (Figure 3.7C). Intense expression was found in the endocardial lining of the heart (Figure 3.7D) and the dorsal aorta. In the trunk region below the heart, expression was observed in patches of cells lining the periphery of the neural tube (Figure 3.7E). Expression was intense in the dorsal aorta and in the cardinal vein. In the posterior region, strong expression was observed in the caudal extremity of the intracoelomic cavity, in the vitelline artery and also in the allantois of the embryo (Figure 3.7F). In embryos of diabetic pregnancy, the extent of up-regulation was not as much as the non-diabetic group, except rhombomeric expression was more or less unchanged (Figure 3.6G). Overall, there was significant ($p = 0.028$) difference in the expression level of *Cyp26b1* between embryos of non-diabetic and diabetic groups. At 4 hr after RA treatment, expression was further up-regulated, especially obvious

in the cranial mesenchyme, the first branchial arch and also at the region connecting the umbilical vein (Figure 3.6C). Ectopic expression was also found at the posterior somitic region, which was later identified to be the early developing somite (Figure 3.8F). The expression level of *Cyp26b1* in embryos of diabetic mice at 4 hr after RA treatment was obviously lower (Figure 3.6H) than that of embryos of the non-diabetic group, with statistically significant difference ($p = 0.017$) between them. At 8 hr, the expression was generally further intensified (Figure 3.6D). The tissue location of the strong signal at the head and cervical regions were examined by sections. Results showed that most of the intense staining was located in by the epithelial lining of blood vessels rather than in the mesenchymal layer (Figures 3.8B and 3.8C). On the other hand, down-regulation of the gene in rhombomeric region became obvious (Figure 3.8D) when compared with the embryo at 2 hr after RA treatment (Figure 3.7C). Besides, when examining the embryo at the forelimb bud level, high level of expression was found at the ventral half of the neural tube, in the forelimb bud and in the midgut endoderm (Figure 3.8E). In the differentiating somite, expression was restricted to the dermomyotome in the lateral portion, with no expression in the medial portion. However, in more posterior region at the level of the allantois, expression was found in the entire somite (Figure 3.8F). Again, similar to more anterior regions, intense signal was observed in the endothelial lining of the blood vessels, such as the dorsal aorta, vitelline artery and the allantois (Figure 3.8F). In the tail bud region, *Cyp26b1* only showed expression in discrete patches of cells (Figure 3.8G). Unlike the 2 hr and 4 hr time points where significant differences in expression levels of *Cyp26b1* were observed between embryos of diabetic and non-diabetic mice, by 8 hr after RA treatment, expression intensity of *Cyp26b1* in embryos of diabetic mice (Figure 3.6I) was much more similar to

embryos of non-diabetic mice (Figure 3.6D), with no statistically significant difference between the two as determined by real-time RT-PCR. Twelve hours after RA injection, the expression of *Cyp26b1* was dramatically reduced, with most of the expression found at 8 hr time point completely disappeared (Figure 3.6E). Even the normal rhombomeric expression was severely reduced to uneven expression in rhombomeres 2, 3 and 5, such that in the non-diabetic group, the expression level of *Cyp26b1* in RA-treated embryos was significantly ($p < 0.001$) less than control embryos at equivalent time points. Similar to *Cyp26a1*, down-regulation of *Cyp26b1* in embryos of the diabetic group (Figure 3.6J) was less rapid than embryos of the non-diabetic group (Figure 3.6E), such that the expression level of embryos of diabetic group was significantly ($p = 0.018$) higher.

3.4.3.3 *Cyp26c1*

As mentioned previously, the expression pattern of *Cyp26c1* is similar to that of *Cyp26a1*. It is expressed in the cranial and cervical mesenchyme, the maxillary and mandibular components of the first branchial arch, and the maxillo-mandibular cleft (Figure 3.9A). However, the level of *Cyp26c1* expression in these anterior domains appeared to be higher than that of *Cyp26a1* (Figure 3.3A), particularly at rhombomere 2. Moreover, expression was not observed in the tail bud region. No difference in *Cyp26c1* expression levels between diabetic and non-diabetic group could be detected by *in situ* hybridization (Figure 3.9F) nor real-time quantitative RT-PCR (Graph 3.5). Following RA treatment, the change of *Cyp26c1* expression was totally different from *Cyp26a1* and *Cyp26b1*. Instead of up-regulation, *Cyp26c1* was down-regulated in RA-treated embryos. At 2 hr after RA treatment, although the *in situ* expression pattern of *Cyp26c1* did not change

dramatically for both embryos of non-diabetic (Figure 3.9B) and diabetic groups (Figure 3.9G), a significant ($p = 0.020$) decrease in expression level was found in the non-diabetic group as determined by real-time RT-PCR. By 4 hr after RA treatment, significant down-regulation of *Cyp26c1* was found in embryos of both non-diabetic ($p < 0.001$) and diabetic groups ($p < 0.001$). While reduction occurred in most domains, it was most prominent in the cervical mesenchyme, with expression almost completely disappeared (Figures 3.9C and 3.9H). Expression continued to diminish as observed in embryos at 8 hr after RA treatment (Figures 3.9D and 3.9I). Expression in the cranial mesenchyme, and in the maxillary and mandibular components of the first branchial arch was very low. Only expression in rhombomere 2 was still clearly seen. By 12 hr after RA treatment, even expression in rhombomere 2 was severely inhibited (Figures 3.9E and 3.9J). However, except the 2 hr time point, there was no significant difference between embryos of diabetic and non-diabetic groups as determined by both *in situ* hybridization and real-time RT PCR.

Table 3.3 **Expression levels of *Cyp26* relative to *β-actin* in embryos of non-diabetic and diabetic mice at different time points after maternal injection of 50 mg/kg RA on E9.0.**

Treatment groups	ND (CON)					SD (CON)					ND (RA)				SD (RA)			
Length of time after RA injection	0 hr	2 hr	4 hr	8 hr	12 hr	0 hr	2 hr	4 hr	8 hr	12 hr	2 hr	4 hr	8 hr	12 hr	2 hr	4 hr	8 hr	12 hr
No. of litters	3	3	3	3	3	3	3	3	3	3	3	3	3	3	3	3	3	3
No. of embryos	19	21	18	19	18	16	19	17	17	19	17	18	16	17	16	16	18	17
Sample size[#]	3	3	3	3	3	3	3	3	3	3	3	3	3	3	3	3	3	3
Relative expression levels of *Cyp26a1*± SE	0.0049 ± 0.0003	0.0045 ± 0.0003	0.0047 ± 0.0003	0.0046 ± 0.0001	0.0030 ± 0.0001	0.0039 ± 0.0002	0.0034 ± 0.0002	0.0038 ± 0.0002	0.0033 ± 0.0002	0.0024 ± 0.0001	0.0097 ± 0.0010	0.0158 ± 0.0011	0.0207 ± 0.0013	0.0008 ± 0.0001	0.0062 ± 0.0003	0.0099 ± 0.0002	0.0171 ± 0.0005	0.0012 ± 0.0001
Relative expression levels of *Cyp26b1*± SE	0.0042 ± 0.0002	0.0033 ± 0.0001	0.0036 ± 0.0001	0.0042 ± 0.0002	0.0042 ± 0.0001	0.0043 ± 0.0002	0.0036 ± 0.0006	0.0038 ± 0.0002	0.0043 ± 0.0004	0.0046 ± 0.0002	0.0090 ± 0.0003	0.0126 ± 0.0004	0.0149 ± 0.0009	0.0020 ± 0.0001	0.0060 ± 0.0008	0.0104 ± 0.0004	0.0139 ± 0.0008	0.0027 ± 0.0002
Relative expression levels of *Cyp26c1*± SE	0.0042 ± 0.0003	0.0039 ± 0.0004	0.0036 ± 0.0002	0.0042 ± 0.0001	0.0039 ± 0.0005	0.0047 ± 0.0001	0.0037 ± 0.0003	0.0038 ± 0.0002	0.0043 ± 0.0003	0.0046 ± 0.0003	0.0024 ± 0.0001	0.0017 ± 0.0001	0.0011 ± 0.0001	0.0006 ± 0.0002	0.0030 ± 0.0001	0.0017 ± 0.0001	0.0010 ± 0.0001	0.0004 ± 0.0001

[#] Refer to section 3.3.1 for definition of one sample

Table 3.4 **Statistical analysis of relative expression levels of *Cyp26* in embryos of different treatment groups using Independent Samples t-test.**

Groups for comparison	ND (CON) vs. SD (CON)					ND (CON) vs. ND (RA)				SD (CON) vs. SD (RA)				ND (RA) vs. SD (RA)			
Length of time after RA injection	0 hr	2 hr	4 hr	8 hr	12 hr	2 hr	4 hr	8 hr	12 hr	2 hr	4 hr	8 hr	12 hr	2 hr	4 hr	8 hr	12 hr
p value in comparing relative expression levels of *Cyp26a1*	0.014 *	0.028 *	0.024 *	0.001 *	0.008 *	0.007 *	< 0.001 *	< 0.001 *	< 0.001 *	0.003 *	< 0.001 *	< 0.001 *	0.046 *	0.030 *	0.005 *	0.046 *	0.043 *
p value in comparing relative expression levels of *Cyp26b1*	0.663	0.587	0.252	0.988	0.282	0.001 *	< 0.001 *	< 0.001 *	< 0.001 *	0.029 *	< 0.001 *	< 0.001 *	0.212	0.028 *	0.017 *	0.439	0.018 *
p value in comparing relative expression levels of *Cyp26c1*	0.139	0.693	0.384	0.707	0.099	0.020 *	< 0.001 *	< 0.001 *	< 0.001 *	0.095	< 0.001 *	< 0.001 *	< 0.001 *	0.011 *	0.804	0.410	0.567

* Statistically significant

3.5 DISCUSSION

There are some variations in the expression of individual subtype of *Cyp26* genes between different vertebrate species. However, the combined expression domains of all three subtypes overall are very similar among different species including mice (Fujii et al., 1997; MacLean et al., 2001; Tahayato et al., 2003), chick (Blentic et al., 2003; Reijntjes et al., 2003; Reijntjes et al., 2004) and xenopus (de Roos et al., 1999), revealing the importance of *Cyp26* in vertebrate development.

In this study, I have demonstrated that *Cyp26a1* is the only subtype of *Cyp26* gene being altered in embryos under diabetic pregnancy. In contrast, expressions of the other two subtypes, *Cyp26b1* and *Cyp26c1*, are not affected, indicating that altered expression of *Cyp26a1* in diabetic conditions is not due to global disruption of gene regulation in the embryo, but specific to *Cyp26a1*. All three *Cyp26* genes are expressed in the anterior part of the embryo, particularly in the facial and cervical regions, hindbrain rhombomeres and the branchial arch region, in overlapping and non-overlapping domains, which suggest that they may work tightly together to maintain RA at a low level for normal anterior development. However, in the posterior region, Cyp26A1 is the dominant subtype of RA catabolizing enzymes to protect the tail bud region of the embryo from excessive RA signaling, suggesting that the posterior region of the embryo at the stage of organogenesis is much more susceptible to aberrant levels of RA than the anterior region. Thus, significant down-regulation of *Cyp26a1* may render the tail bud region of the embryo in diabetic pregnancy highly susceptible to the deleterious effect of ectopic RA signaling. These findings may give insight on the strong association between caudal regression and diabetic pregnancy (Martinez-Frias, 1994).

Without RA treatment, all the 3 *Cyp26* subtypes, *Cyp26a1*, *Cyp26b1* and *Cyp26c1*, showed similar expression levels at E9.0. Upon challenge with a teratogenic dose of RA, both *Cyp26a1* and *Cyp26b1* showed significant up-regulation with expression at multiple ectopic sites For example, there were high levels of expression of both *Cyp26a1* and *Cyp26b1* in the heart after the teratogenic RA insult. In the caudal region of the embryo where *Cyp26a1* is predominantly expressed, upon challenged with RA, expression of *Cyp26b1* was induced in there. Sections of the embryo revealed that *Cyp26a1* and *Cyp26b1* were expressed in non-overlapping regions. For example, in the cranial region of the embryo, *Cyp26a1* was expressed in the cranial mesenchyme and outer ectodermal layer. In contrast, *Cyp26b1* was expressed specifically in the developing blood vessels. In the heart region, *Cyp26a1* was expressed in the outer pericardial lining, but *Cyp26b1* was expressed in the endocardial layer of the heart. Moreover, their expression patterns were highly site-specific. For instance, in the neural tube, *Cyp26a1* was specifically expressed at the neural crest, and in discrete patches of cells in the middle and ventral region of the neural tube. These results suggest that *Cyp26a1* and *Cyp26b1* play different roles in organogenesis and protect different tissues against ectopic RA signaling.

In my MPhil project, I have focussed on studying the role of *Cyp26a1* in increasing the risk of caudal regression in diabetic pregnancy (Lee, 2008). I have shown that the significantly lower expression level of *Cyp26a1* in the tail bud region of embryos of diabetic mice results in reduced ability to clear away RA. Thus, when embryos are exposed to aberrant levels of RA, there is a local build-up of a higher concentration of RA in the tail bud region in the diabetic group. Such higher RA concentrations in the tail bud may exert molecular and cellular actions, such as

enhancing down-regulation of *Wnt3a* (Shum et al., 1999), a gene indispensible for caudal development (Takada et al., 1994), and exacerbating cell death. As a result, the teratogenic effect of RA is increased in embryos of diabetic mice in comparison to embryos of non-diabetic mice, leading to a greater extent of caudal regression.

In the anterior region of the embryo, *Cyp26a1* co-expresses with *Cyp26c1* (Uehara et al., 2007), together with the expression of *Cyp26b1* in rhombomeres 2 to 6 (MacLean et al., 2001). Thus, unlike the tail bud region where *Cyp26a1* is predominantly expressed, in the anterior region, all 3 subtypes of *Cyp26* may play a role in protecting tissues against RA. The effect of down-regulation of *Cyp26a1* in the anterior region of embryos of diabetic mice may be diluted out, and therefore, the susceptibility to ectopic RA may not be as high as the caudal region of the embryo. This may be one of the reasons why caudal regression is the most characteristic malformation associated with diabetic pregnancy with 250 times more common (Kucera, 1971; Martinez-Frias, 1994), while defects in the anterior region such as cleft palate and exencephaly only show 3 to 4- fold increases in incidence in diabetic pregnancy. *Cyp26* is highly expressed in hindbrain rhombomeres, which is closely related to *Hox* gene expression. *Hox* gene expression in the hindbrain of E8.0 RA-treated mouse embryos exhibited transformation of rhombomeres 2/3 to rhombomeres 4/5 identity (Conlon, 1995). Both *Hox* and *RAR* loss-of-function mutants show anterior vertebral homeotic transformations similar to those observed in embryos exposed to excess RA (Kessel & Gruss, 1991; Krumlauf, 1994).

As mentioned previously, RA can induce a spectrum of malformations including caudal regression, neural tube defects, heart defects and renal anomalies. Concomitantly, babies of diabetic pregnancy also show increased risk of these malformations (Casson et al., 1997; Singh et al., 2005). Interestingly, these defects

are also observed in *Cyp26a1* homozygous null mutants (Abu-Abed et al., 2001). These findings give support to our hypothesis that common pathogenic mechanisms may exist between *Cyp26a1*- and maternal diabetes-induced birth defects.

In this study, it was found that upon challenged with RA, both *Cyp26a1* and *Cyp26b1* were highly up-regulated, which helped to eliminate unwanted RA in the tissues. In contrast, for *Cyp26c1*, even though it co-expresses with *Cyp26a1* at the facial and cervical regions of the embryo (Uehara et al., 2007), upon challenged with a teratogenic dose of RA, its expression was significantly down-regulated and was nearly switched off after 8 hr, suggesting that *Cyp26c1* is not the critical enzyme to protect tissues against exogenous RA in embryos at E9. Knockdown of *Cyp26c1* showed no effects on embryo development (Uehara et al., 2007). It is possible that the function of *Cyp26c1* can be totally replaced by *Cyp26a1*, as they may be functionally redundant. This is supported by the findings that embryos with homologous disruption of both *Cyp26a1* and *Cyp26c1* manifested more pronounced anterior truncation of the brain than embryos with single knockout of *Cyp26a1*, due to failure in producing migratory cranial neural crest cells in the forebrain and midbrain (Uehara et al., 2007).

I have previously found that exogenously-applied RA could reach the embryo as soon as the first hour after maternal intraperitoneal injection (Lee, 2008). Indeed, results of this chapter showed that a significant up-regulation of *Cyp26a1* and *Cyp26b1* was already detectable at 2 hr after RA treatment. *Cyp26a1* is shown to contain two RAREs, R1 and R2 (Loudig et al., 2000; Loudig et al., 2005). Hence, *Cyp26a1* expression can be induced by RA through direct binding of the RA-RAR/RXR complex. However, no RARE has been identified in *Cyp26b1* even though it was found to be up-regulated upon RA exposure (Reijntjes et al., 2005).

Thus, it is possible that up-regulation of *Cyp26a1* and *Cyp26b1* by RA may be mediated via different mechanisms. In this study, it was found that the expression levels of *Cyp26a1* and *Cyp26b1* were significantly lower at 12 hr after RA treatment. This could be explained by the fact that rapid increase in *Cyp26a1* and *Cyp26b1* levels during the first few hr would result in rapid decline in RA concentrations. As the RA level dropped, *Cyp26a1* and *Cyp26b1* expressions might start to down-regulate. Moreover, since *Cyp26a1* and *Cyp26b1* were up-regulated to a greater extent in the non-diabetic group than the diabetic group, catabolic removal of RA was faster in the former. This would lead to a more rapid decline in RA levels, which may explain the significantly lower expression levels of both *Cyp26a1* and *Cyp26b1* in the non-diabetic group than the diabetic group observed at 12 hr after RA treatment.

Results of this study agree with findings in other species. For example, in zebrafish embryos, the expression of *Cyp26a1* in the presumptive anterior neural ectoderm can be positively induced by RA, whereas *Raldh2* expression is repressed by RA, suggesting that development of this tissue require an absence of RA signaling (Dobbs-McAuliffe et al., 2004). These results are also in agreement with findings by Reijntjes et al. (2005), which showed that exogenous RA could up-regulate the expressions of *Cyp26a1* and *Cyp26b1* in the posterior region of chick embryos, while expressions of *Cyp26c1* were unaffected.

To conclude, results of this chapter show that expression of *Cyp26a1* in the embryo is specifically reduced in maternal diabetes. Whether this reduction might play an important role in diabetic embryopathy and the underlying mechanism for this dysregulation were examined in the following chapters.

Chapter 4

Susceptibility of *Cyp26a1* Mutant Embryos to Retinoic Acid-induced Malformations

4.1 INTRODUCTION

To study the functional role of RA on embryo development, one of the ways is to challenge the embryo with teratogenic doses of RA. Regions that are susceptible to RA teratogenesis may implicate that RA signaling is prohibited there. However studying the teratogenic effect of RA is often not useful for determining its physiological role, as high levels of RA may induce or repress genes that are normally not regulated by endogenous RA. On the other hand, loss-of-function studies are the most common ways to determine the normal function of RA during organogenesis.

Various mutants with knockout of multiple *RAR* isoforms have been used to demonstrate the importance of RA signaling. Offspring with knockdown of all isoforms of either *RARα* or *RARγ* exhibited a high postnatal lethality rate (Lohnes et al., 1993; Lufkin et al., 1993). *RARα* null mice displayed webbed digits on both forelimbs and hindlimbs (Lufkin et al., 1993), while $RAR\gamma^{-/-}$ mice exhibited different congenital malformations, including tracheal cartilage malformations and homeotic transformations along the cervical axial skeleton (Lohnes et al., 1993). Compound knockout of *RARα* and *RARβ*, or *RARα* and *RARγ*, together exhibited severe disruption in early hindbrain patterning (Dupe et al., 1999; Werner & DeLuca, 2001). Nearly all characteristic features of *RAR* knockout mice (Lohnes et al., 1994; Lohnes et al., 1995; Luo et al., 1996) are associated with syndromes of embryonic vitamin A deficiency, and also in many ways mirror the defects seen in both RA-insufficient rat embryos and vitamin A-deficient (VAD) rat embryos (White et al., 1998; White et al., 2000b). These mutants reveal the significance of RAR in RA signaling in different embryonic tissues.

To study RA homeostasis, various knockout mice of RA synthesizing and degrading enzymes have been generated (MacLean et al., 2001; Sakai et al., 2001; Martin et al., 2005). Raldh2 is the most dominant RA synthesizing enzyme in the embryo. Embryos of *Raldh2* homozygous null mutant mice, with perturbed retinoid signaling, displayed severe abnormalities including disruption of hindbrain patterning, impaired body turning (axial rotation), a lack of heart looping and heart chamber morphogenesis, incomplete neural tube closure, shortening of the trunk region and absence of limb buds (Niederreither et al., 1999). Some of these anomalies are similar to those observed in *RAR* knockout mutants. On the other hand, in my project, I have employed *Cyp26a1* knockout mice to investigate the association between *Cyp26a1* and diabetic embryopathy. *Cyp26a1*$^{-/-}$ mutants died at mid-gestation (Abu-Abed et al., 2001). Morphological abnormalities first appeared in the mutant embryo at day 9.5 of gestation. Posterior truncation was found in all embryos and 75% of them also exhibited exencephaly. Some embryos also manifested additional defects in hindbrain, vertebral and limb patterning, irregular folding of the neural tube, improper head development, incomplete axial turning and heart abnormalities (Abu-Abed et al., 2001; Sakai et al., 2001; Ribes et al., 2007). Upon exposure to a low dose of exogenous RA (1 mg/kg), *Cyp26a1*$^{-/-}$ mutants exhibited head truncation but unaffected forelimb bud, while *Cyp26a1*$^{+/-}$ and *Cyp26a1*$^{+/+}$ embryos appeared normal (Ribes et al., 2007). This experiment demonstrated that embryos with down-regulation of *Cyp26a1* were more susceptible to RA teratogenesis and in particular, the anterior region of the embryo might probably be more susceptible to the effect of a transient increase in RA levels.

Caudal agenesis, one of the major malformations in *Cyp26a1*$^{-/-}$ mutant mouse embryos (Sakai et al., 2001), is phenotypically similar to that induced by

administration of excess RA during early embryonic axis extension (Shum et al., 1999). It is also the most characteristic malformations associated with diabetic pregnancy (Martínez-Frías, 1994). In all cases, there is disorganized neural tissue outgrowth within the truncated tail rudiments. It has been reported that loss of *Cyp26a1* resulted in an increase in the endogenous RA level in the tail bud of mutant embryos when compared with that of wild-type embryos (Sakai et al., 2001). Such alteration affected the expression of RA-regulated genes in the caudal end of the embryo, including *Wnt3a*, *Cdx4* and *Brachyury* (Iulianella et al., 1999), which are genes critical for normal caudal development. It has been reported that *Wnt3a*$^{-/-}$ and *Brachyury*$^{-/-}$ mutant embryos exhibit caudal truncation accompanied by excessive neural tube formation at the expense of mesoderm (Wilkinson et al., 1990; Takada et al., 1994; Yoshikawa et al., 1997; Yamaguchi et al., 1999). Similarly, expressions of both *Wnt3a* and *Brachyury* were down-regulated upon administration of exogenous RA (Iulianella et al., 1999). Taken together, increase in endogenous RA concentrations in *Cyp26a1*$^{-/-}$ embryos could down-regulate *Wnt3a* and *Brachyury* expression in the tail bud, which in turn impaired the proliferation of mesodermal cells and transformed mesoderm into a neural fate, causing severe axial truncation with terminal neural tissues apparent in the mutant. These experiments clearly implicate the importance of *Cyp26a1* and the signaling pathway involved in caudal regression.

Moreover, in order to study the functional role of RA, it is important to determine their RA levels in different tissues. The most common method employed to detect retinoid is by high pressure liquid chromatography (HPLC). This technique has been used in many studies for analyzing RA concentrations in tissues of different organs (Pappas et al., 1993) and embryonic tissues (Maden et al., 1998; Sakhi et al.,

1998). The advantage of using HPLC in detecting retinoids is that the procedures are simple and time efficient. Using HPLC, it has been reported that endogenous concentrations of all-*trans* RA and all-*trans* retinol in the E9.5 mouse embryo were 75.8 pg and 279 pg per embryo respectively (Sakhi et al., 1998). However, because of detection limit, determination of retinoids in embryos at earlier stages using HPLC is much more difficult. A more powerful technique is high pressure liquid chromatography/mass spectrometry (HPLC/MS), which has higher sensitivity and specificity for retinoids, with sensitivity to RA approximately down to 0.7 pmole (McCaffery et al., 2002). However, this method is not cost-effective.

Another method to detect RA is based on bioassay in which RA binds to the RARE that drives the expression of a reporter gene. This method has been employed in RARE-lacZ transgenic mice (Rossant et al., 1991; Koubova et al., 2006) and RA-responsive cell lines (Wagner et al., 1992; McCaffery & Drager, 1997; Iulianella et al., 1999). The RARE-lacZ mouse will show the site of RA distribution in the embryo upon staining for β-galactosidase. For instance, it has been shown that there were distinct temporal and spatial distribution patterns of lacZ activity along the anterior-posterior axis of the mouse embryo (Mendelsohn et al., 1991; Balkan et al., 1992). RA-responsive cell lines have also been widely used for detecting and quantifying RA levels in mouse embryos with sensitivity much higher than HPLC (down to 10^{-12}M of RA).

Another way to study the level of endogenous RA in the embryo is by determining RA synthesis and degradation in tissues. Study on RA production and degradation in the embryonic chick retina has been conducted using the RA-responsive cell line (Mey et al., 2001). It was found that there was a high level of RA synthesizing activity in the retinal pigment epithelium, and in the ventral and

dorsal poles of the retina, while RA degradation occurred in a horizontal region in the middle of the retina.

To conclude, most of the malformations found in *Cyp26a1*$^{-/-}$ embryos are similar to those caused by excess RA and diabetic pregnancy. It is therefore possible that there is an inverse relationship between the expression level of *Cyp26a1* and the concentration of RA, such that the lower the *Cyp26a1* expression level in the tissue, the higher the RA concentration and thus the greater the teratogenicity. In this chapter, I have employed a *Cyp26a1* knockout mouse model together with different RA detection methods to investigate the relationship between *Cyp26a1* expression level, RA concentration and the embryo's susceptibility to various types of RA-induced anomalies in diabetic pregnancy.

4.2 EXPERIMENTAL DESIGN

In Chapter 3, I have shown that *Cyp26a1* is the only subtype of RA catabolizing enzyme being down-regulated in the mouse embryo under diabetic pregnancy. As mentioned, *Cyp26a1* expresses in different tissues at different developmental stages. For instance, *Cyp26a1* is expressed in the cranial neural fold and posterior neural plate at E8.0, thus dysregulation of RA catabolism at this stage may cause exencephaly and spina bifida. Similarly, down-regulation of *Cyp26a1* in the maxillo-mandibular cleft in the branchial arch region at E9.0 may lead to cleft palate. In this chapter, I have further investigated whether down-regulation of *Cyp26a1* was directly involved in affecting RA degradation and increasing embryos' susceptibility to malformations other than caudal regression in diabetic pregnancy. To this end, I have used a genetic approach by employing the *Cyp26a1* knockout mouse as a model and compared the susceptibility of *Cyp26a1*$^{+/-}$ heterozygous embryos with their *Cyp26a1*$^{+/+}$ wild-type littermates to various types of RA-induced malformations in diabetic and non-diabetic pregnancies. If down-regulation of *Cyp26a1* was directly involved in the pathogenic pathway, it was expected that *Cyp26a1*$^{+/-}$ embryos, with haploinsufficiency of Cyp26A1, would be more susceptible to the teratogenic effect of RA than their *Cyp26a1*$^{+/+}$ littermates, and the difference between these two genotypes would further be exaggerated in diabetic conditions.

To achieve this, *Cyp26a1* heterozygous male mice were mated with non-diabetic or diabetic ICR female mice to generate 4 types of embryos with different genotype and maternal environment combinations, including *Cyp26a1*$^{+/+}$ embryos in non-diabetic pregnancy (ND$^{+/+}$), *Cyp26a1*$^{+/-}$ embryos in non-diabetic pregnancy (ND$^{+/-}$), *Cyp26a1*$^{+/+}$ embryos in diabetic pregnancy (SD$^{+/+}$) and

Cyp26a1$^{+/-}$ embryos in diabetic pregnancy (SD$^{+/-}$). The aim of this chapter was to decipher the relationship between maternal diabetes, *Cyp26a1* expression level and RA catabolic activity in affecting the embryo's susceptibility to different types of RA-induced malformations.

First, the difference in expression patterns of *Cyp26a1* in the 4 types of embryos mentioned above was determined by whole mount *in situ* hybridization. Further quantification of the expression level was achieved by real-time quantitative RT-PCR. However, to avoid the high expression level of *Cyp26a1* in the tail bud region from mastering over differences in *Cyp26a1* expression in anterior domains, the embryo was divided into two parts: one part containing the tail bud region only and the other part containing the rest of the embryo. *Cyp26a1* expression levels in these two parts were considered separately. This experiment aimed to determine whether a direct relationship existed between maternal diabetes and the *Cyp26a1* expression level.

Next, I have compared the RA degrading activity in the tail bud region of the 4 types of embryos with different expression levels of *Cyp26a1*. By using an *in vitro* assay, the ability of the tail bud tissue excised from ND$^{+/+}$, ND$^{+/-}$, SD$^{+/+}$ and SD$^{+/-}$ embryos to degrade a known amount of RA added into the culture medium was compared. After a fixed period of time for reaction, the amount of RA remained in the medium was measured by the RA-responsive cell line. Next, to compare the amount of RA that the 4 types of embryos were actually exposed to when maternally challenged with the same dose of RA, pregnant mice were injected with a teratogenic dose of RA, and the amount of RA present in the embryo at 3 hr after RA treatment was determined by HPLC.

Finally, the susceptibility of the 4 types of embryos to the teratogenic effect of RA in inducing various types of malformations, including exencephaly, spina bifida, cleft palate and renal malformations, was determined by being maternally challenged with a teratogenic dose of RA on appropriate gestational day because the teratogenic effect of RA in inducing different types of defects was highly dose- and developmental stage-dependent. To induce exencephaly and spina bifida, pregnant mice were treated with 25 mg/kg RA on E8.0. To induce cleft palate and renal malformations, pregnant mice were treated with 40 mg/kg RA on E9.0.

4.3 MATERIALS AND METHODS

4.3.1 Animal

ICR female mice were induced diabetic by receiving injections of streptozotocin as described in section 2.2. Non-diabetic and diabetic ICR female mice were time-mated with *Cyp26a1* heterozygous male mice following the description in section 2.1. Such mating combinations generated *Cyp26a1*$^{+/-}$ and *Cyp26a1*$^{+/+}$ littermates developing in non-diabetic and diabetic maternal conditions. Embryos of the 4 different genotype-maternal environment combinations were collected for various analyses as described in sections 4.3.3, 4.3.4, 4.3.5, 4.3.6 and 4.3.7. The yolk sac of the embryo or the tail tip of the fetus was used for DNA genotyping as described in section 4.3.2.

As mentioned previously, *Cyp26a1*$^{-/-}$ embryos die in mid-gestation due to severe malformations, whereas *Cyp26a1*$^{+/-}$ mutants appear morphologically normal and are fertile. Thus, the *Cyp26a1* mouse colony was maintained by mating between heterozygous mice or between heterozygous and wild-type mice. The tail tip of the mouse was used for DNA genotyping as described in section 4.3.2.

4.3.2 DNA genotyping

4.3.2.1 Tissue lysis

To genotype the adult mouse or the embryo/fetus, 5 mm of the tail tip of the adult mouse or the E18 fetus, or the yolk sac of the embryo was digested using 150 µl of PCR lysis buffer containing 50 mM KCl (*BDH*), 10 mM Tris-HCl in pH 8.0 (*Invitrogen*), 2 mM $MgCl_2$ (*BDH*), 0.1 mg/ml gelatin (*USB*), 0.45% (v/v) NP40

(*Sigma*), 0.45% (v/v) Tween 20 (*Sigma*) and 0.1 mg/ml proteinase K (*Roche*). The digestion was carried out at 55°C with vigorous shaking by a thermomixer (*Eppendorf*) until the tissues were completely digested, which normally took 4 hr and 2 hr for the tail tip and the yolk sac respectively. The lysate was then boiled at 95°C for 30 min to denature proteinase K. After that, the lysate containing genomic DNA was directly used for PCR.

4.3.2.2 PCR reaction

Two microlitres of the lysate was added to a PCR reaction mixture containing 2 µl of 10x PCR buffer (*Bioneer*), 1.6 µl of 2.5 mM dNTP (*Bioneer*), 1.5 µl of 20 mM $MgCl_2$ (*Bioneer*), 0.5 µl of each primers, 1 µl of 5 U/µl Taq polymerase (*Bioneer*) and made up to a total volume of 20 µl using autoclaved water.

Primers used are as followings:

Primer 1: 5'- GGT AAC GTG GGC AGT AAC CTG -3'

Primer 2: 5'- TCC ATG AGC CGA GTT CTG TAG -3'

Primer 3: 5'- TCC GTT CAG TCA GTC TCA TAC -3'

Primer 2 and 3 were used to detect wild-type *Cyp26a1* with 235 bp amplified PCR product, while primer 1 and 3 amplified the mutated *Cyp26a1* with 371 bp PCR product. Thirty cycles of PCR were performed in a thermal cycler (*Biorad*) with denaturing temperature at 95°C for 2 min, annealing temperature at 58°C for 30 sec and extension at 72°C for 30 sec. The reaction was ended with final extension at 72°C for 8 min. PCR products were detected in a 3% agarose gel with gel-red stain (*Biorad*) using 12 µl of the PCR product. The size of the PCR product

was determined by a 50 kb DNA ladder (*Fermentas*). *Cyp26a1*$^{+/+}$ embryos got a single PCR product of 235 bp in size, whereas *Cyp26a1*$^{+/-}$ embryos got PCR products of 235 bp and 371 bp together.

4.3.3 Whole mount *in situ* hybridization

Different groups of embryos at E9.0 were dissected in DEPC-treated ice-cold PBS and fixed in 4% paraformaldehye overnight at 4 °C and then processed for whole mount *in situ* hybridization to detect the expression of *Cyp26a1* following the description in sections 2.7 and 2.8. Particulars of the mouse *Cyp26a1* cDNA plasmid used for generating anti-sense riboprobes were the same as described in section 3.3.3. About 30 embryos from 3 litters were examined for each group.

4.3.4 Real-time quantitative RT-PCR

At E9.0, embryos were collected in DEPC-treated ice-cold PBS. To reduce variation in gene expression levels due to differences in developmental stage, only embryos at 19-21 somite-stage were collected. The body was cut in the presomitic region at a level one-somite length caudal to the last somite. The caudal part was defined as the tail bud of the embryo and the rest of the embryo was defined as the whole embryo (exclude tail bud). The tail bud and the whole embryo (exclude tail bud) were individually stored in the RNA*later* RNA stabilization solution as described in section 2.6.1. The yolk sac of the embryo was used for genotyping as described in section 4.3.2. After genotyping, tissues of embryos of the same genotype in the same litter were pooled as one sample.

To compare *Cyp26a1* expressions between *Cyp26a1*$^{+/+}$ and *Cyp26a1*$^{+/-}$ embryos of non-diabetic and diabetic groups, mRNA levels were measured by real-time quantitative RT-PCR following the procedures as described in 2.6. *β-actin* was used as the internal control for normalization of PCR products. The cDNA standards used for quantifying the amount of *Cyp26a1* and *β-actin* genes were prepared from cDNA plasmids of mouse *Cyp26a1* and *β-actin*. The sequences of primer pairs for amplification of partial sequence of mouse *Cyp26a1* and *β-actin* were the same as listed in section 3.3.2

After PCR, expression levels of these genes were analyzed by ABI SDS2.3 Software (*Applied Biosystems*).

4.3.5 *In vitro* assay of RA degrading activity in tail bud tissue

4.3.5.1 Collection of tail bud

Embryos of diabetic and non-diabetic mice at E9.0 were dissected out in L15 medium (*Gibco*). The tail bud was excised from the embryo at a level as described in section 4.3.4. To minimize differences in the size of the excised tail bud, only embryos at 19-21 somite-stage were used for experiments. The tail bud was individually collected in a microfuge tube with excess medium being removed. It was snap frozen in liquid nitrogen and then stored at -80°C until analysis. The yolk sac of the embryo was used for DNA genotyping as described in section 4.3.2. To conduct the assay, four tail buds from embryos of the same litter were pooled as one sample and were collected in 5 μl of DMEM in a microfuge tube. The tail buds were lysed by triturating with a 10 μl pipette tip, followed by freezing in liquid nitrogen and then thawing in a water bath at 37°C for 1 min in each step. The freeze-thaw

procedures were repeated for 5 times.

4.3.5.2 *In vitro* enzymatic reaction

The enzymatic reaction was performed as follow. All procedures, where necessary, were conducted in the dark under dim yellow light to prevent photoisomerization of RA. Lysed tail bud sample in a microfuge tube was incubated in 50 µl of reaction mixture containing 1.6 mg/ml nicotinamide adenine dinucleotide phosphate (NADPH; *Sigma*), 0.3 mg/ml dithiothreitol (DTT; *Sigma*) and 50 nM all-*trans* RA in culture medium (refer to section 2.4.1 for composition of culture medium for the RA-responsive cell line). Incubation was carried out in a 5% CO_2 incubator at 37°C for 2 hr, protected from light by loosely covering the microfuge tube (with lid open) with aluminum foil. During incubation, the exogenous RA in the medium was degraded by the RA catabolizing enzyme in the tail bud sample.

To test if degradation of RA was mediated via Cyp26 enzyme, the reaction mixture was added with 100 nM R115866 (1 µl of 5 µM stock solution in DMEM, a gift from *Johnson and Johnson*), a highly potent Cyp26 specific inhibitor (Stoppie et al., 2000), to check if the enzymatic degrading activity could be inhibited.

After incubation, the reaction mixture was diluted 30-fold with culture medium (refer to section 2.4.1 for composition of culture medium for the RA-responsive cell line) to minimize the toxic effect of NADPH and DTT. The amount of RA in the diluted reactive mixture was then measured by the RA-responsive cell line as described in section 2.4.

4.3.6 Measurement of RA in the embryo after maternal treatment with RA by HPLC

RA suspension was prepared as described in section 2.3 and diluted to the desired dosage with peanut oil. On E9.0, non-diabetic and diabetic pregnant mice were intraperitoneally injected with 25 mg/kg body weight of RA (RA suspension at 1.67 mg/ml) or equivalent volume of suspension vehicle (15 μl per gram of body weight) as the control. At 3 hr after RA treatment, embryos were dissected out in ice-cold PBS in the dark under dim yellow light to prevent photoisomerization of RA. Only embryos at 20-22 somite-stage were used for experiment. After thorough washing with PBS for 3 times, embryos were individually collected in a microfuge tube with excess PBS being removed. It was gassed with nitrogen, sealed with parafilm and then wrapped in aluminum foil. It was snap frozen in liquid nitrogen and stored at -80°C until analysis. Embryos were collected within half an hour to minimize the diffusion of RA. The yolk sac of the embryo was collected for DNA genotyping as described in section 4.3.2.

After all samples were collected, the amount of RA in the sample was determined by HPLC as described in section 2.5.

4.3.7 Analysis of various types of RA-induced malformations

To compare the susceptibility of the 4 types of embryos to various types of RA-induced malformations, embryos were maternally challenged with a teratogenic dose of RA at a specific developmental stage. The dosage and developmental stage of treatment were dependent on the malformation type to be induced.

4.3.7.1 Cleft palate and renal malformations

To induce cleft palate and renal malformations in the embryo, pregnant mice received an intraperitoneal injection of RA at a dose of 40 mg/kg body weight (RA suspension at 2.66 mg/ml) on E9.0. The occurrence rate of malformation was examined in near-term fetuses at E18. Cleft palate was determined by direct observation of the palate with the mouth of the fetus opened. This defect is characterized by failure of fusion of the lateral palatine processes, the nasal septum, and/or the median palatine processes, forming an opening on the roof of the mouth. Renal malformations were observed by opening up the abdomen of the fetus to expose the kidneys. There are different kinds of renal malformations including hypoplastic, dysplastic, polycystic and horseshoe kidneys, and renal agenesis. The tail tip of the fetus was used for genotyping as described in section 4.3.2. The occurrence rate was determined by the % of fetuses per litter with the malformation concerned.

4.3.7.2 Neural tube defects

To induce neural tube defects in the embryo, pregnant mice received an intraperitoneal injection of RA at a dose of 25 mg/kg body weight (RA suspension at 1.67 mg/ml) on E8.0. Embryos were dissected out at E13 for direct observation of open neural tube defects including exencephaly and spina bifida. Exencephaly is characterized by persistently opened cranial neural folds, while spina bifida is characterized by failure of closure of the spinal neural tube. The yolk sac of the embryo was used for genotyping as described in section 4.3.2.

4.3.8 Statistical analysis

The expression level of *Cyp26a1*, the *in vitro* RA degrading activity, the amount of RA in the embryo and the occurrence rate of different types of malformations among embryos of the 4 types ($ND^{+/+}$, $ND^{+/-}$, $SD^{+/+}$, $SD^{+/-}$) were compared by one-way Analysis of Variance (ANOVA) followed by Bonferroni test. Correlation between *Cyp26a1* expression level and RA degrading activity was tested by Pearson's correlation. All statistical analyses were carried out using SPSS software (*SPSS*), with statistical significance level set at $p < 0.05$.

4.4 RESULTS

4.4.1 *Cyp26a1* expression

4.4.1.1 Expression pattern of *Cyp26a1* as determined by *in situ* hybridization

The 4 types of embryos in different genotype and maternal environment combinations at E9.0 were subjected to *in situ* hybridization study. Results were shown in Figure 4.1. Similar to the result in Chapter 3 (Figure 3.1), for *Cyp26a1*$^{+/+}$ embryo in non-diabetic pregnancy (ND$^{+/+}$; Figure 4.1A), *Cyp26a1* is expressed in the cranial and cervical mesenchyme in the anterior region (Figure 4.1C). Caudally, it is specifically expressed in the posterior neural plate and tail bud mesoderm in the tail bud region of the embryo (Figure 4.1B). For *Cyp26a1*$^{+/-}$ embryo in non-diabetic pregnancy (ND$^{+/-}$; Figure 4.1D), reduced expression of *Cyp26a1* can be observed in the tail bud region, especially in the tail bud mesoderm (Figure 4.1E). However, the most obvious reduction in signal intensity is found in the anterior domains (Figure 4.1F). For *Cyp26a1*$^{+/+}$ embryo in the diabetic group (SD$^{+/+}$; Figure 4.1G), the expression of *Cyp26a1* is reduced in both the anterior (Figure 4.1I) and posterior domains (Figure. 4.1H) in comparison to ND$^{+/+}$ embryo (Figures 4.1A, 4.1B and 4.1C), which has the same genotype, but in non-diabetic maternal environment. This is in agreement with the findings in Chapter 3 that *Cyp26a1* expression is down-regulated under maternal diabetes (Figure 3.1). However, the signal intensity, especially in the anterior domains of SD$^{+/+}$ embryos (Figure 4.1I), is clearly higher than in the ND$^{+/-}$ embryo (Figure 4.1F), implying that the effect of maternal diabetes in down-regulating *Cyp26a1* expression is less than the effect of heterozygous deletion of *Cyp26a1*. In the *Cyp26*$^{+/-}$ embryo of diabetic mouse (SD$^{+/-}$; Figure 4.1J), with the combined genetic effect of heterozygous deletion of *Cyp26a1* and maternal

effect of diabetes, *Cyp26a1* expression in the anterior domains is hardly observed (Figure 4.1L) and the signal intensity in the tail bud region is obviously the lowest (Figure 4.1K) in comparison to the other 3 types of embryos (Figures 4.1B, 4.1E and 4.1H).

4.4.1.2 Expression level of *Cyp26a1* as determined by real-time quantitative RT-PCR

Although a difference in *Cyp26a1* expression can be observed in embryos with different combinations of genotype and maternal status, the more sensitive method of real-time RT-PCR was employed to quantitate the expression level of *Cyp26a1* in the tail bud and in the whole embryo (exclude tail bud).

Tail bud

The expression level of *Cyp26a1* in the tail bud of embryos in different groups was summarized in Table 4.1 and presented in Graph 4.1. Results of statistical analysis were shown in Table 4.2. Results showed that the expression level of *Cyp26a1* in the tail bud of *Cyp26a1* heterozygous embryos was significantly lower than that of their wild-type littermates in both non-diabetic ($p < 0.001$, $ND^{+/+}$ vs. $ND^{+/-}$) and diabetic maternal status ($p = 0.013$, $SD^{+/+}$ vs. $SD^{+/-}$). Moreover, when comparing the expression level between non-diabetic and diabetic groups, both $Cyp26a1^{+/-}$ and $Cyp26a1^{+/+}$ embryos in diabetic pregnancy showed a significantly lower level of *Cyp26a1* expression in the tail bud in comparison to embryos of the same genotype in non-diabetic pregnancy ($p = 0.001$, $ND^{+/+}$ vs. $SD^{+/+}$; $p = 0.015$, $ND^{+/-}$ vs. $SD^{+/-}$). When both maternal and genetic factors were considered, the

expression level of *Cyp26a1* was the lowest in the tail bud of *Cyp26a1*$^{+/-}$ embryos in diabetic pregnancy, but highest in that of *Cyp26a1*$^{+/+}$ embryos in non-diabetic pregnancy. These variations in *Cyp26a1* expression levels between embryos of different genotype and maternal environment combinations agree with the findings obtained by *in situ* hybridization (Figures 4B, 4E, 4H and 4K).

Whole embryo (exclude tail bud)

The expression level of *Cyp26a1* in the whole embryo (exclude tail bud) in different groups of embryos was summarized in Table 4.1 and presented in Graph 4.2. Results of statistical analysis were shown in Table 4.2. Variations in the expression level of *Cyp26a1* in the whole embryo (exclude tail bud) amongst the 4 groups of embryos showed a similar trend as the tail bud. There were significant differences between different maternal status ($p < 0.001$, ND$^{+/+}$ vs. SD$^{+/+}$ and ND$^{+/-}$ vs. SD$^{+/-}$) and different genotypes ($p < 0.001$, ND$^{+/+}$ vs. ND$^{+/-}$ and SD$^{+/+}$ vs. SD$^{+/-}$). These variations in *Cyp26a1* expression levels between embryos of different genotype and maternal environment combinations agree with the findings obtained by *in situ* hybridization (Figures 4.1C, 4.1F, 4.1I and 4.1L).

One point worth noticing is that the extent of difference in *Cyp26a1* expression levels between embryos of the two genotypes was not the same in comparing non-diabetic and diabetic maternal status. Results were compared in Table 4.3. It was clearly shown that the difference in *Cyp26a1* expression levels between wild-type and heterozygous genotypes was about 2-fold in the non-diabetic group, but the difference was about 3-fold in the diabetic group in both the tail bud and the whole embryo (exclude tail bud). This implied that the difference in

Cyp26a1 expression levels between the two genotypes in diabetic pregnancy was larger than that in non-diabetic pregnancy, suggesting a synergistic down-regulation of *Cyp26a1* by genetic and maternal factors.

In summary, the mating combination of *Cyp26a1* heterozygous male mice with ICR diabetic or non-diabetic female mice could generate embryos that expressed different levels of *Cyp26a1*.

Table 4.1 Expression levels of *Cyp26a1* relative to *β-actin* in embryos of different groups at E9.0.

Maternal status	ND		SD	
Genotype of *Cyp26a1* mutant embryos	+/+	+/–	+/+	+/–
No. of litters	4		4	
No. of embryos	18	16	14	15
Sample size[#]	4	4	4	4
Relative expression levels of *Cyp26a1* in tail bud ± SE	0.237 ± 0.025	0.120 ± 0.004	0.128 ± 0.014	0.044 ± 0.002
Relative expression levels of *Cyp26a1* in whole embryo (exclude tail bud) ± SE	0.0073 ± 0.0002	0.0037 ± 0.0004	0.0053 ± 0.0002	0.0017 ± 0.0002

[#] Refer to section 4.3.4 for definition of one sample

Table 4.2 Statistical analysis of relative expression levels of *Cyp26a1* between embryos of different groups using one-way ANOVA followed by Bonferroni test.

Groups for comparison	$ND^{+/+}$ vs. $ND^{+/-}$	$ND^{+/+}$ vs. $SD^{+/+}$	$SD^{+/+}$ vs. $SD^{+/-}$	$ND^{+/-}$ vs. $SD^{+/-}$
p value in comparing relative expression levels of *Cyp26a1* in tail bud	< 0.001*	0.001*	0.013*	0.015*
p value in comparing relative expression levels of *Cyp26a1* in whole embryo (exclude tail bud)	< 0.001*	< 0.001*	< 0.001*	< 0.001*

* Statistically significant

Table 4.3 Fold difference in *Cyp26a1* expression levels between *Cyp26a1* heterozygous and wild-type embryos in diabetic and non-diabetic maternal status.

Maternal status	ND		SD	
Genotype of *Cyp26a1* mutant embryos	+/+	+/–	+/+	+/–
Relative expression levels of *Cyp26a1* in tail bud ± SE	0.237 ± 0.025	0.120 ± 0.004	0.128 ± 0.014	0.044 ± 0.002
Fold difference between +/+ and +/– in tail bud	1.98		2.91	
Relative expression levels of *Cyp26a1* in whole embryo (exclude tail bud) ± SE	0.0073 ± 0.0002	0.0037 ± 0.0004	0.0053 ± 0.0002	0.0017 ± 0.0002
Fold difference between +/+ and +/– in whole embryo (exclude tail bud)	1.97		3.12	

4.4.2 *In vitro* RA degrading activity in different groups of embryos

Results in Chapter 3 show that among the 3 subtypes of *Cyp26*, only *Cyp26a1* is predominantly expressed in the tail bud region, whereas all 3 subtypes are expressed in anterior domains (Figures 3.1, 3.2 and 3.3). Thus, to avoid the RA degrading effect of other subtypes of *Cyp26*, only the tail bud region was used for testing the relationship between *Cyp26a1* expression level and RA degrading activity in the 4 types of embryos in different genotype and maternal environment combinations.

The *in vitro* RA degrading activity in the tail bud of the 4 types of embryos was summarized in Table 4.4 and presented in Graph 4.3. Results of statistical analysis were shown in Table 4.5. The *in vitro* RA degrading activity was measured in terms of the % of RA in the medium being degraded by the tail bud lysate. To confirm that the RA degrading activity was mediated via Cyp26 enzymes, a Cyp26 specific inhibitor was added to the medium as a control. Indeed, the RA degrading activity was almost completely inhibited in the presence of Cyp26 inhibitor.

Results showed that there were significant differences in the RA degrading activity in the tail bud caused by genotype ($p = 0.003$, $ND^{+/+}$ vs. $ND^{+/-}$; $p < 0.001$, $SD^{+/+}$ vs. $SD^{+/-}$) and maternal environment ($p = 0.004$, $ND^{+/+}$ vs. $SD^{+/+}$ and $ND^{+/-}$ vs. $SD^{+/-}$). The tail bud of *Cyp26a1* wild-type embryos in non-diabetic pregnancy, which expressed the highest level of *Cyp26a1*, exhibited the greatest RA degrading activity. On the other hand, *Cyp26a1* heterozygous embryos in diabetic pregnancy, which exhibited the lowest level of *Cyp26a1*, exhibited the weakest RA degrading activity. The other two groups exhibited medium levels of degrading activity. To test whether there was significant correlation between *Cyp26a1* expression level and RA

degrading activity, data were analyzed by Pearson's Correlation. This test is used to compare the strength of association between two variables. It will generate a Pearson's correlation coefficient (*r*) with values ranging from +1 to -1. If the value is close to +1, it means that there is a strong positive linear relationship between the 2 variables. In contrast, if the value is close to -1, it means that there is a strong negative linear relationship between the 2 variables. A value equals to zero means that there is no linear correlation between the 2 variables. Moreover, the *p* value of the correlation can indicate how significant the result is. Results showed that there was a direct ($r = +0.715$) and significant ($p < 0.001$) relationship between *Cyp26a1* expression level and the RA degrading activity, such that the higher the *Cyp26a1* expression level, the greater the RA degrading activity in the tail bud.

Table 4.4 ***In vitro*** **RA degrading activity in the tail bud tissue of E9.0 embryos of different groups.**

Maternal status	ND		SD		ND
Genotype of *Cyp26a1* mutant embryos	+/+	+/–	+/+	+/–	+/+
Cyp26 inhibitor	Nil	Nil	Nil	Nil	Yes
No. of litters	7		8		5
No. of embryos	52	40	48	48	32
Sample size[#]	13	10	12	12	8
% RA in medium being degraded ± SE	61.14 ± 1.83	43.46 ± 1.96	47.02 ± 1.40	25.99 ± 1.18	3.59 ± 1.46

[#] Refer to section 4.3.5.1 for definition of one sample

Table 4.5 Statistical analysis of *in vitro* RA degrading activity between the tail bud tissue of embryos of different groups using one-way ANOVA followed by Bonferroni test.

Groups for comparison	$ND^{+/+}$ vs. $ND^{+/-}$	$ND^{+/+}$ vs. $SD^{+/+}$	$SD^{+/+}$ vs. $SD^{+/-}$	$ND^{+/-}$ vs. $SD^{+/-}$
p value in comparing relative RA levels in tail bud	0.003*	0.004*	< 0.001*	0.004*

* Statistically significant

Table 4.6 Statistical analysis of the correlation between *Cyp26a1* expression level and *in vitro* RA degrading activity in the tail bud tissue using Pearson's correlation.

Groups for comparison	ND^{++}	$ND^{+/-}$	$SD^{+/+}$	$SD^{+/-}$
Relative expression levels of *Cyp26a1* in tail bud ± SE	0.237 ± 0.025	0.120 ± 0.004	0.128 ± 0.014	0.044 ± 0.002
% RA in medium being degraded ± SE	61.14 ± 1.83	43.46 ± 1.96	47.02 ± 1.40	25.99 ± 1.18
Pearson's correlation coefficient (*r*)	+0.715			
p value of Pearson's correlation	< 0.001*			

* Statistically significant

4.4.3 Amount of RA in the embryo at 3 hr after maternal RA treatment as determined by HPLC

The teratogenic effect of RA is dose-dependent. To determine whether

differences in expression levels of *Cyp26a1* would affect the effective concentration of RA in the embryo, diabetic and non-diabetic pregnant mice were injected with the same dose of RA (25 mg/kg) and the amount of RA in the embryo at 3 hr after treatment was compared among embryos with different *Cyp26a1* expression levels. I have previously conducted a detailed study to compare the amount of RA in the embryo of diabetic and non-diabetic mice at hourly intervals after maternal RA injection. It was found that peak accumulation of RA in the embryo occurred at 3 hr after RA injection and it was also the time point at which difference in RA levels between embryos of diabetic and non-diabetic groups was the greatest (Lee, 2008). Thus, this time point was adopted for the present study. Since the aim of this chapter was to determine if there was any correlation between *Cyp26a1* expression levels and different types of malformations other than caudal regression, thus, the effective concentration of RA in the whole embryo, rather than the tail bud, was determined by HPLC.

The amount of RA in embryos of different groups at 3 hr after maternal injection of 25 mg/kg RA on E9.0 was summarized in Table 4.7 and presented in Graph 4.4. Results of statistical analyses were shown in Table 4.8.

Results showed that *Cyp26a1*$^{+/-}$ embryos with lower *Cyp26a1* expression levels had significantly higher RA levels than their *Cyp26a1*$^{+/+}$ littermates, no matter whether they were under non-diabetic (p = 0.007, ND$^{+/+}$ vs. ND$^{+/-}$) or diabetic (p = 0.001, SD$^{+/+}$ vs. SD$^{+/-}$) pregnancy. In comparing different maternal status, the diabetic group had significantly higher RA levels than the non-diabetic group in *Cyp26a1* heterozygous embryos (p = 0.013, ND$^{+/-}$ vs. SD$^{+/-}$). Similar differences between diabetic and non-diabetic groups occurred in *Cyp26a1* wild-type embryos

although not yet reaching a statistically significant level. Together, the data showed that there was an inverse relationship between *Cyp26a1* expression level and the effective concentration of RA in the embryo after RA treatment, such that *Cyp26a1* wild-type embryos in non-diabetic pregnancy, which expressed the highest level of *Cyp26a1* (Table 4.1), were exposed to the least amount of RA. On the hand, *Cyp26a1* heterozygous embryos in diabetic pregnancy, which expressed the lowest level of *Cyp26a1*, were exposed to the largest amount of RA.

Table 4.7 Amount of RA in embryos of different groups at 3 hr after maternal treatment with 25 mg/kg RA on E9.0 as determined by HPLC.

Maternal status	ND		SD	
Genotype of *Cyp26a1* mutant embryos	+/+	+/–	+/+	+/–
No. of litters	6		6	
No. of embryos	30	31	30	27
Sample size[#]	6	6	6	6
Amount of RA in embryos (ng/mg protein) ± SE	106.62 ± 3.07	173.07 ± 16.63	145.35 ± 6.39	234.31 ± 17.68

[#] Refer to section 4.3.5.1 for definition of one sample

Table 4.8 Statistical analysis of RA levels between embryos of different groups using one-way ANOVA followed by Bonferroni test.

Groups for comparison	$ND^{+/+}$ vs. $ND^{+/-}$	$ND^{+/+}$ vs. $SD^{+/+}$	$SD^{+/+}$ vs. $SD^{+/-}$	$ND^{+/-}$ vs. $SD^{+/-}$
p value in comparing RA concentrations in whole embryo	0.007*	0.136	0.001*	0.013*

* Statistically significant

4.4.4 Susceptibility to RA teratogenicity

After confirming that there was an inverse relationship between *Cyp26a1* expression level and the effective concentration of RA that the embryo was exposed to after maternal injection with a teratogenic dose of RA, studies were conducted to determine whether there was any corresponding susceptibility to various types of RA-induced malformations.

Cleft palate and kidney malformations were induced by maternal injection with 40 mg/kg RA on E9.0. Exencephaly and spina bifida were induced by maternal injection with 25 mg/kg RA on E8.0. The incidence rates of cleft palate and kidney malformations, expressed in terms of % of fetuses per litter with the defect, were summarized in Table 4.9 and presented in Graph 4.5. The incidence rates of exencephaly and spina bifida were summarized in Table 4.10 and presented in Graph 4.6. Results of statistical analysis were shown in Table 4.11.

Results showed that *Cyp26a1*$^{+/-}$ embryos with lower *Cyp26a1* expression levels had significantly higher incidence rates of cleft palate than their *Cyp26a1*$^{+/+}$ littermates when being challenged with RA, no matter whether they were developed in non-diabetic ($p < 0.001$, ND$^{+/+}$ vs. ND$^{+/-}$) or diabetic maternal environment ($p < 0.001$, SD$^{+/+}$ vs. SD$^{+/-}$). In comparing the effect of maternal status, the diabetic group, which expressed lower levels of *Cyp26a1*, had significantly higher incidence rates of cleft palate than the non-diabetic groups for both *Cyp26a1* heterozygous ($p < 0.001$; ND$^{+/-}$ vs. SD$^{+/-}$) and *Cyp26a1* wild-type embryos ($p = 0.001$; ND$^{+/+}$ vs. SD$^{+/+}$). As for renal malformations, exencephaly and spina bifida, similar trends were observed. Maternal diabetes significantly increased the incidence rates of these 3 types of malformations in both *Cyp26a1* heterozygous and wild-type embryos.

Genotype also significantly affected incidence rates of exencephaly and spina bifida in both diabetic and non-diabetic groups. However, for renal malformations, significant difference was only found between *Cyp26a1*$^{+/+}$ and *Cyp26a1*$^{+/-}$ embryos in diabetic pregnancy (p = 0.001, SD$^{+/+}$ vs. SD$^{+/-}$), whereas difference between embryos of the two genotypes had not yet reached statistically significant level in non-diabetic pregnancy.

Results also showed that although maternal diabetes increased the incidence rate of defects, the extent of increase was dependent on the malformation type. For example, maternal diabetes caused 3.5-fold and 5.5-fold increase in the incidence rate of renal malformations in *Cyp26a1*$^{+/-}$ (from 21% to 74%) and *Cyp26a1*$^{+/+}$ (from 7% to 39%) embryos respectively. However, for cleft palate, maternal diabetes only caused 1.5-fold increase in incidence rate in both *Cyp26a1*$^{+/-}$ (from 59% to 92%) and *Cyp26a1*$^{+/+}$ (from 36% to 54%) embryos.

Together, the data showed that susceptibility of embryos to the teratogenic effect of RA was inversely correlated with *Cyp26a1* expression levels, such that *Cyp26a1* wild-type embryos in non-diabetic pregnancy, which expressed the highest level of *Cyp26a1* (Table 4.1), exhibited the lowest incidence rate of cleft palate, renal malformations, exencephaly and spina bifida when exposed to teratogenic doses of RA. In contrast, *Cyp26a1* heterozygous embryos in diabetic pregnancy, which expressed the lowest level of *Cyp26a1*, developed the highest incidence of these defects.

Table 4.9 Incidence rates of cleft palate and renal malformations in E18 fetuses of different groups after maternal treatment with 40 mg/kg RA on E 9.0.

Maternal status	ND		SD	
Genotype of *Cyp26a1* mutant embryos	+/+	+/–	+/+	+/–
No. of litters	10		10	
No. of fetuses	68	60	54	46
% of fetuses per litter with cleft palate ± SE	35.6 ± 3.7	59.0 ± 2.2	54.2 ± 3.8	92.3 ± 3.3
% fetuses per litter with renal malformations ± SE	7.1 ± 3.4	21.3 ± 5.1	38.8 ± 6.3	73.3 ± 7.7

Table 4.10 Incidence rates of exencephaly and spina bifida in E13 embryos of different groups after maternal treatment with 25 mg/kg RA on E8.0.

Maternal status	ND		SD	
Genotype of *Cyp26a1* mutant embryos	+/+	+/–	+/+	+/–
No. of litters	9		9	
No. of embryos	36	26	27	27
% of embryos per litter with exencephaly ± SE	5.4 ± 3.6	36.1 ± 6.6	31.9 ± 5.2	71.3 ± 5.5
% of embryos per litter with spina bifida ± SE	3.7 ± 2.5	30.6 ± 5.7	37.4 ± 5.9	75.0 ± 7.5

Table 4.11 Statistical analysis of incidence rates of various types of RA-induced malformations between embryos of different groups using one-way ANOVA followed by Bonferroni test.

Groups for comparison	$ND^{+/+}$ vs. $ND^{+/-}$	$ND^{+/+}$ vs. $SD^{+/+}$	$SD^{+/+}$ vs. $SD^{+/-}$	$ND^{+/-}$ vs. $SD^{+/-}$
p value in comparing cleft palate	< 0.001*	0.001*	< 0.001*	< 0.001*
p value in comparing renal malformations	0.611	0.005*	0.001*	< 0.001*
p value in comparing exencephaly	0.047*	0.016*	0.002*	< 0.001*
p value in comparing spina bifida	0.003*	0.012*	< 0.001*	0.001*

* Statistically significant

4.5 DISCUSSION

It has been reported that *Cyp26a1* null mutants could be rescued by heterozygous disruption of *Raldh2* responsible for RA synthesis (Niederreither et al., 2002a), suggesting that a number of phenotypes exhibited in *Cyp26a1* null mutants was caused by exposure to excess RA. Haploinsufficiency of Raldh2 prevented the occurrence of spina bifida and rescued development of posterior structures. These findings are in agreement with results of the present study that the lower the *Cyp26a1* expression level, the higher the amount of RA found in the embryo after RA treatment and the greater the disruption of development. Based on these findings, it is therefore expected that if RA or *Cyp26a1* expression in the embryo of diabetic pregnancy can be maintained to normal levels, it is possible to reduce the risk of caudal regression, or even other types of congenital malformations.

The aim of this chapter was to investigate whether there was any correlation between maternal diabetes, *Cyp26a1* expression level and RA catabolic activity, and whether these factors would affect the embryo's susceptibility to various types of malformations other than caudal regression as demonstrated in my previous findings (Lee, 2008). Results of this chapter clearly show that indeed there are causal relationships among them. Heterozygous embryos with haploinsufficiency of Cyp26A1 developing in a diabetic milieu were most susceptible to RA-induced malformations. The lower the *Cyp26a1* expression level, the lower the RA catabolic activity, the higher the effective concentration of RA in the tissue after RA treatment, and thereby, the higher the susceptibility to malformations.

Ectopic RA can alter thousands of genes. Different RA signaling pathways can be involved in controlling different tissues. Mutation of over 150 genes is

known to cause neural tube defects in mice. Among which about 70% of the genes only cause exencephaly, 5% only cause spina bifida, 5% cause craniorachischisis, whereas the remaining 20% have increased risk of either exencephaly or spina bifida or sometimes both (Greene et al., 2009). It has been shown that there is a change of *RAR* expression from *RARγ* in the open posterior neuropore to *RARβ* in the closed neural tube region, suggesting a role of RA in spinal neurulation. However, how RA signaling participates in neural tube closure at the cellular level remains to be determined (Copp and Greene, 2010). RA has long been studied as a potent teratogen in rodents, with neural tube defects among the most commonly observed malformations. It has been reported that anomalies exhibited in *Cyp26a1*$^{-/-}$ mutant embryos closely resemble those caused by RA teratogenic effects, such as exencephaly and spina bifida. The locations of these two defects correlate with the two major sites of *Cyp26a1* expression during early organogenesis, i.e. the rostral neural plate and posterior neuropore, as shown in Figure 3.2. The occurrence rate of exencephaly in *Cyp26a1*$^{-/-}$ embryos is much lower than spina bifida. This may be due to coexpression of *Cyp26c1* and *Cyp26a1* in the anterior, but not posterior region (Uehara et al., 2007). Interestingly, *RARγ*$^{-/-}$ mutant embryos were resistant to exencephaly and spina bifida caused by RA (Lohnes et al., 1994; Iulianella & Lohnes, 1997), supporting that RA teratogenicity in inducing these two types of defects is mediated via *RARγ*. Moreover, co-knockdown of *RARγ* could rescue anomalies originally found in *Cyp26a1*$^{-/-}$ embryos, especially malformations in the caudal region (Abu-Abed et al., 2003). It has been reported that RARγ mediated the deleterious effects of RA on caudal development by down-regulating the critical signaling activities of Wnt3A (Takada et al., 1994) and FGF8 (Sun et al., 1999). These findings further support that the teratogenic effect of RA is mediated via

genes downstream of *RARγ*.

Some mechanisms involving genes downstream of *RARγ* have been proposed by Abu-Abed et al. (2003). *Cyp26a1* maintains cells in a RA-depleted state for the normal function of downstream genes including *Fgf8*, *Wnt3a*, *Brachyury*, *Tbx6* and *Cdx1*. In contrast, in the presence of excess RA, such as in cases of *Cyp26a1* knockout or being challenged with exogenous RA, RARγ mediates RA signaling in inhibiting *Wnt3a* and *Fgf8* expression, leading to spina bifida. However, there is no significant difference in the expression level of *RARα*, *RARγ* and *RXRα* between embryos of diabetic and non-diabetic pregnancy (Leung, 2005), suggesting that the difference in RA teratogenicity is not dependent on the difference in the expression level of RA receptors but the level of RA in the tissues.

Alternatively, RA deficiency can also lead to neural tube defects. *Raldh2* knockout mouse embryos show consistent occurrence of spina bifida, but not exencephaly (Niederreither et al., 2002b). While co-knockdown of *RARα* (expressed in the closed neural tube) and *RARγ* (expressed in the open neural tube) showed consistent occurrence of exencephaly only, but not spina bifida (Lohnes et al., 1994). These results suggest that RA deficiency leads to exencephaly and spina bifida through 2 different molecular pathways. The molecular pathway leading to exencephaly is less well reported, the most possible pathway would involve Sonic hedgehog (*Shh*) signaling. *Shh* is highly cooperative with RA in embryonic development. For instance, *Shh* is misregulated in RA-deficient embryonic forebrain (Halilagic et al., 2007). The presence of RA is also necessary for the proper induction of *Shh* in limb bud cells to regulate antero-posterior patterning and digit specification (Niederreither et al., 2002b). *Shh* is highly expressed in the notochord underneath the neural plate, which gives out signal for induction of median hinge

point and also controlling dorsolateral hinge points formation that is necessary for neural tube closure (Ybot-Gonzalez et al., 2002). It has been well documented that over-activation of *Shh* leads to exencephaly (Echelard et al., 1993). Besides, loss of function of other *Shh* inhibitory genes, including *Gli3*, *Rab23* and *Tulp3*, also produce neural tube defects.

For renal malformations, our laboratory has established a RA-induced renal agenesis mouse model via injection of 125 mg/kg RA on E9.0 (Tse et al., 2005). It has been demonstrated that renal agenesis is mediated via RA deficiency during early formation of the metanephros. RA deficiency is possibly established after strong up-regulation of RA catabolizing genes *Cyp26a1* and *Cyp26b1*, together with prolonged down-regulation of RA synthesizing gene *Raldh2*. *Wt1* and *c-Ret* are genes critical for kidney development, with both of them being known to be regulated by RA (Tse et al., 2005; Rosselot et al., 2010). *Wt1* was found to be significantly down-regulated in our RA-induced renal agenesis mouse model (Tse et al., 2005). In *Raldh2*$^{-/-}$ knockout mouse embryos, there was total loss of *c-Ret* expression in the ureteric bud at E12.5. Furthermore, in metanephric explants cultured in the absence of RA, *c-Ret* expression was found to be down-regulated and ureteric bud branching was not observed (Batourina et al., 2001). It has been shown that double knockout mutants of *RARα* and *RARβ* had down-regulated *c-Ret* expression. There were fewer ureteric bud branches and mutant embryos developed renal malformations (Mendelsohn et al., 1999). Other than *Wt1* and *c-Ret*, *Midkine* (*MK*), a heparin-binding growth factor essential for regulation of kidney development (Vilar et al., 2002), is found to be RA responsive. *In utero* exposure to vitamin A deficiency could significantly down-regulate *MK* expression in the metanephros of E14 rat embryos. *In vitro* culture of E14 rat metanephros in medium

added with 100 nM RA could successfully stimulate expression of *MK*. Besides, *in vitro* nephrogenesis was strongly inhibited (reduction of nephron number by 50%) in the presence of neutralizing antibodies for *MK* without changes in ureteric bud branching morphogenesis. These results indicate that *MK* is implicated in the regulation of kidney development by RA.

For cleft palate, it is well known that transforming growth factor-beta (TGF-β) is essential for sending critical instructions to neural crest cells, which form the bony part of the upper palate. Homozygous knockout of *TGF-β3* in mice could induce 100% cleft palate among 200 offspring examined (Koo et al., 2001). Besides, *TGF-β3* can be disrupted by RA. It has been shown that maternal exposure to exogenous RA could disrupt the spatio-temporal patterns of expression of *TGF-β3* in the mouse embryonic palatal processes, which is suggested to be involved in RA-induced cleft palate (Degitz et al., 1998; Huang et al., 2003). Other than TGFβ, it has been reported that human cleft palate disorder is significantly correlated to the fibroblast growth factor receptor 2 (*FGFR2*) mutations. Indeed, *FGFR2* is co-expressed with *TGF-β3*. They work together throughout the stages of human palatal fusion to control apoptosis and epithelio-mesenchymal trans-differentiation at the palatal medial edge epithelium (Britto et al., 2002). It has also been reported that RA could inhibit the cell proliferating activity and the expression of *FGFR2* in the palatal mesenchyme of E12 and E13 mouse embryos (critical period for palate development). These might delay the elevation of palatal shelves, causing cleft palate (Bae et al., 2001). Interestingly, the teratogenic effect of RA in inducing cleft palate can be overcome by *RXRα* knockout. It has been reported that treatment with a teratogenic dose of RA on E11 or E12 induced cleft palate at a lower frequency in *RXRα* knockout mouse embryos than in wild-type embryos (Nugent et al., 1999),

suggesting that RA-induced teratogenicity may be mediated via *RXRα*.

To conclude, this chapter provides evidence for a direct relationship between *Cyp26a1* expression, RA degrading activity and susceptibility to various RA-induced malformations. Such alteration in RA catabolism may affect a series of genes down-stream of RA and leads to birth defects.

Chapter 5

Normalization of *Cyp26a1* Expression in Reducing Susceptibility to Malformations

5.1 INTRODUCTION

In Chapter 3, I have found that the main RA catabolizing enzyme *Cyp26a1*, which is expressed in specific tissues in the embryo to protect against inappropriate exposure to RA, was significantly down-regulated in diabetic pregnancy. In Chapter 4, I have proved that down-regulation of *Cyp26a1* in embryos under diabetic pregnancy reduced the RA degrading activity, increased the RA level in the embryo and enhanced the teratogenic effect of RA in inducing different types of malformations. However, the underlying mechanism of dysregulation of *Cyp26a1* expression in embryos of diabetic pregnancy remains to be determined.

In this chapter, I have investigated how *Cyp26a1* is being altered in diabetic pregnancy. As previously mentioned, *Cyp26a1* has two RAREs in the promoter region, therefore, it is highly sensitive to tiny changes in RA levels and can be directly regulated by RA (Loudig et al., 2000). RA in the embryo is synthesized from retinol obtained from maternal circulation. It is well-documented that the plasma retinol level of type 1 diabetic patients and streptozotocin-induced diabetic rats is significantly lower than normal (Wako et al., 1986; Martinoli et al., 1993; Tuitoek et al., 1996b). Moreover, retinol binding protein 4 (RBP4), which is responsible for transport of retinol in the plasma, is also found to be decreased in type 1 diabetes (Basu et al., 1989; Tuitoek et al., 1996a). Hence, I hypothesized that reduction in maternal plasma retinol levels in diabetic pregnancy might lead to a decrease in the endogenous level of RA in the embryo, thereby causing down-regulation of *Cyp26a1*, as the expression of *Cyp26a1* has been shown to be regulated by RA/retinol levels (Yamamoto et al., 2000).

Retinol is stored in the liver in the form of retinyl esters by the enzyme lecithin:retinol acyltransferase (LRAT). To release retinol from the liver to blood circulation, retinyl ester is converted back to retinol by the enzyme retinyl ester hydrolases. The mammalian fetus acquires retinol from maternal circulation, in which retinol is transported in association with RBP4 (Soprano et al., 1994). To reach the fetal circulation, maternal retinol must traverse the placenta. However, it has been demonstrated that maternal retinol-RBP complex cannot cross the placenta directly (Quadro et al., 2004). To enter the fetal circulation, maternal retinol bound to RBP4 must first be released at the maternal-fetal interface. In the rodent placenta, 2 proteins are responsible for the uptake of retinol. RBP4 is localized on the maternal side in the decidua basalis and the embryonic yolk sac endoderm starting from E7. Circulating retinol binds to RBP4 in the yolk sac and can be released into the fetal circulation (Quadro et al., 1999; Quadro et al., 2004). STRA6, another protein indentified to be critical for retinol uptake (Blaner, 2007; Kawaguchi et al., 2007), is strongly expressed in the innermost cells of the uterine wall, encircling the entire implantation site, as well as in the primitive endoderm, which will later give rise to the yolk sac at E7. Later, at E9, the decidua, yolk sac membrane and chorionic zone also found to express *Stra6* transcripts (Bouillet et al., 1997).

There are evidences for the importance of retinol supply for endogenous embryonic RA levels and embryonic development. Mouse embryos cultured at presomitic stage, with yolk-sac injection of antisense oligodeoxynucleotides for RBP4 to block the expression of RBP4 and also the uptake of retinol from the environment, showed deprivation of RA. Such deficiency resulted in malformations of the vitelline vessels, cranial neural tube and eye etc. (Bavik et al., 1996). In contrast, addition of RA to the culture medium together with antisense injection

could obviously restore normal embryonic development, revealing the critical role of RBP4 in embryonic RA synthesis (Bavik et al., 1996). In humans, mutation in *Stra6* is associated with Matthew-Wood syndrome, manifested with multisystem developmental malformations (Chassaing et al., 2009). Loss-of-function analysis in zebrafish embryos also revealed that *Stra6* deficiency caused retinol deprivation in the developing eyes (Isken et al., 2008).

Furthermore, it has been proved that embryonic RBP4 plays a key role in distributing retinol to the developing tissues particularly under conditions of inadequate maternal retinol intake (Quadro et al., 2005). Experiment demonstrated that RBP4 null mice with dietary retinol deprivation showed reduction in the amount of retinol delivered from the maternal circulation to the fetus. As a result, less retinol is available to the developing tissues such as eye, limb, skin and spinal cord for conversion to RA to maintain normal development.

Induction of RA deficiency using antisense oligodeoxynucleotides for RBP4 resulted in alteration of expression of many genes (Chen et al., 2002). In particular, the most important ones included early down-regulation of the developmentally essential genes including *TGF-β1* and *Shh* (Bavik et al., 1996), of which their importance in causing cleft palate and neural tube defects respectively have already been discussed in the previous chapter. Moreover, in the case of excessive maternal dietary retinol intake as shown in rats, some of the RA-related genes including *LRAT*, *Cyp26a1* and *Stra6* showed significant up-regulation (Quadro et al., 2005), suggesting that these genes are essential in maintaining adequate levels of retinoids in embryonic and extraembryonic tissues. Thus, alteration in retinol levels will definitely affect RA homeostasis. In contrast, the pathway of RA synthesis does not contribute significantly to regulating retinoid

homeostasis during mammalian development, except under conditions of severe maternal retinoid deficiency (Kim et al., 2008).

Other than embryos, RA metabolism was found to be significantly dysregulated in the kidney of *db/db* mice, a type 2 diabetic mouse model, at 20 weeks of age after development of hyperglycemia for 12 weeks (Starkey et al., 2010). *Raldh1*, which is localized at the proximal tubule in the renal cortex, was found to be significantly up-regulated in the diabetic mice, suggesting that a shift in RA metabolism is a novel feature in type 2 diabetic renal diseases. Preliminary results of our laboratory also show that there is an increased expression of *Raldh1* in the kidney of our streptozotocin-induced type 1 diabetic mouse model (data not shown). Together, these findings give support to our hypothesis that diabetic conditions alter RA homeostasis.

5.2 EXPERIMENTAL DESIGN

This chapter aimed to investigate whether there were subnormal maternal retinol levels and endogenous embryonic RA levels in diabetic pregnancy, which might lead to down-regulation of *Cyp26a1*, thereby predisposing embryos to various types of malformations. To begin with, all-*trans* retinol levels in the serum of diabetic and non-diabetic pregnant and non-pregnant mice were determined by HPLC. Because of the minute size of the embryo, the RA-responsive cell line, with detection limit down to 10^{-10} M RA, was used to determine the endogenous level of RA in embryos of diabetic and non-diabetic mice. Indeed, retinol levels from maternal supply and embryonic RA concentrations were found to be significantly reduced in the diabetic group.

Next, I have tested whether increasing the RA level in the embryo of diabetic mouse could normalize the *Cyp26a1* expression level. A single low dose of all-*trans* RA (0.625 or 1.25 mg/kg body weight), or the suspension vehicle as control, was orally fed to pregnant diabetic and non-diabetic mice at 2 hr before E9.0 (E8-22hr). These dosages were chosen based on the fact that for mouse mutants with homologous deletion of the key RA synthesizing gene *Raldh2*, maternal supplementation with 2.5-5 mg/kg of RA was sufficient to rescue these embryos from most of the congenital malformations (Niederreither et al., 1999). Thus, I have used a fraction of these dosages in an attempt to restore the subnormal level of RA in embryos of diabetic mice found in the first part of study. The RA level and *Cyp26a1* expression level were determined in embryos at E9.0 by the RA-responsive cell line and real-time quantitative RT-PCR respectively. Embryos were examined at E13 to determine if the low dose of RA itself would exert any teratogenic effect. Results showed that there was a direct dose-dependent relationship between RA and the

Cyp26a1 expression level, with the dose of 0.625 mg/kg RA being able to normalize *Cyp26a1* expression to a level similar to that of the non-diabetic group.

After working out the dose effect, I have examined whether up-regulation of *Cyp26a1* by oral supplementation with a sub-teratogenic dose of RA might in turn normalize RA catabolism by testing the RA degrading activity in the tail bud tissue using the *in vitro* assay as employed in Chapter 4. Next, the embryo's susceptibility to RA-induced caudal regression was determined by being maternally challenged with a teratogenic dose of RA to see whether normalization of *Cyp26a1* expression and RA degrading activity would protect the tail bud tissue of embryos of diabetic mice against RA teratogenicity.

To follow on, I have extended the study to investigate the effect of normalizing *Cyp26a1* expression in reducing the embryo's susceptibility to different types of birth defects, including exencephaly, spina bifida, cleft palate and renal malformations. Following the design of Chapter 4, *Cyp26a1* heterozygous male mice were mated with diabetic or non-diabetic ICR female mice to generate 4 types of embryos with different *Cyp26a1* expression levels. The effect of supplementation with a sub-teratogenic dose of RA prior to teratogenic RA insult was tested. Similar to the previous experiment, *Cyp26a1* expression levels in the tail bud and in the rest of the embryo of different groups were compared by real-time quantitative RT-PCR. Next, 2 hr after oral supplementation with a sub-teratogenic dose of RA, embryos were maternally challenged with a teratogenic dose of RA at appropriate gestational day, as employed in Chapter 4, to determine their susceptibility to different types of malformations.

5.3 MATERIALS AND METHODS

5.3.1 Determination of retinoid levels

5.3.1.1 Detection of retinol in serum of female mice by HPLC

Non-pregnant mice at 2 weeks after the first day of injection of streptozotocin to induce diabetes or non-pregnant age-matched uninduced normal mice, and diabetic or non-diabetic pregnant mice at E9.0 were subjected to cardiac puncture for taking blood samples. Before blood extraction, mice received an intraperitoneal injection of 200 µl anaesthetic agents of ketamine/xylazine mixture (10:1, w:w). When the animal became unconscious (usually took a few min), a 25G needle (0.50 x 16 mm; *Terumo*) fitted onto a 1 ml syringe was pierced through the skin and inserted directly into the heart of the animal (cardiac puncture). Blood was slowly drawn up into the syringe until the heart stopped beating. The mouse was immediately killed by cervical dislocation. About 1 ml of blood could be taken from each mouse and was put into a 1.5 ml microfuge tube. The blood sample was immediately centrifuged at 3,000 g for 15 min at 4°C to remove blood cells and fibrinogen. The serum was transferred to a new 1.5 ml microfuge tube, gassed with nitrogen, sealed with parafilm and then wrapped in aluminum foil. It was snap frozen in liquid nitrogen and stored at -80°C for not more than 3 months. All procedures described above were performed in the dark under dim yellow light. Extraction of retinoids from the serum sample was carried out according to section 2.5.3. HPLC was carried out as described in section 2.5.4 to determine the level of all-*trans* retinol and all-*trans* RA.

5.3.1.2 Detection of RA in the embryo by RA-responsive cell line

To determine the endogenous concentration of RA in the embryo of diabetic and non-diabetic mice either treated or untreated with a sub-teratogenic dose of RA, embryos were collected at E9.0 using ice-cold L15 medium in the dark under dim yellow light. Five embryos from the same litter with somite-stage between 18 to 20 were pooled as one sample and collected in a new 1.5 ml microfuge tube, gassed with nitrogen, sealed with parafilm and then wrapped in aluminum foil. It was snap frozen in liquid nitrogen and stored at -80°C for not more than 3 months.

To determine the endogenous concentration of RA, embryo samples were first immersed in 500 µl of culture medium (refer to section 2.4.1 for composition of culture medium for RA-responsive cell line) containing 100 nM CYP26 specific inhibitor R115866 and subjected to lysis by pipetting up and down through a 100 µl pipette tip. Embryo samples were incubated at 37°C in a 5% CO_2 incubator protected from light by loosely covering the microfuge tube (with lid open) with aluminum foil for 5 hr to allow the release of RA from the embryonic tissue into the medium. The sample was then centrifuged at 3,000 rpm for 10 min at room temperature to remove large particles. All procedures were conducted in the dark under dim yellow light to prevent photoisomerization of RA in the sample. The concentration of RA in the medium was then determined by the RA-responsive cell line as described in section 2.4.

5.3.2 Oral supplementation with RA

RA suspension was prepared according to the description in section 2.3. Desired concentrations were further prepared by serial dilution with peanut oil. Two

hours before E9.0, diabetic and non-diabetic pregnant mice, which had been mated with ICR male or *Cyp26a1*$^{+/-}$ male mice, were orally fed with 0.625 mg/kg (RA suspension at 0.17 mg/ml) or 1.25 mg/kg RA (RA suspension at 0.33 mg/ml) by using a gavage feeding needle of 22G, 1.25 mm in diameter and 25 mm in length (*Fine Science Tools*). Mice fed with equivalent volume of suspension vehicle (15 μl per gram of weight) served as the control. Two hours afterwards, embryos were collected for determination of *Cyp26a1* expression level by real-time quantitative RT-PCR (section 5.3.3), RA level by RA-responsive cell line (section 5.3.1.2) or RA degrading activity by using an *in vitro* assay (section 5.3.4). To check whether the dose of RA applied had any teratogenic effect, embryos were examined at E13 for morphological abnormalities and caudal regression was determined by the ratio of tail length to crown-rump length (Figure 5.1). To determine the susceptibility of *Cyp26a1*-normalized embryos of diabetic mice to RA teratogenicity, 2 hr after oral supplementation with the sub-teratogenic dose of RA, pregnant mice were intraperitoneally injected with a teratogenic dose of RA at various gestational days and then examined for the incidence or severity of different types of malformations (section 5.3.5).

5.3.3 Real-time quantitative RT-PCR

At E9.0, embryos of different groups were collected in DEPC-treated ice-cold PBS. Embryos at 17-19 somite-stage were divided into two parts: the tail bud and the whole embryo (exclude tail bud) according to the morphological landmark as described in section 4.3.4. For embryos obtained by mating of ICR female with ICR male, tissues of embryos from the same litter were pooled as one

sample and stored in RNA*later* solution as described in section 2.6.1. For embryos obtained by mating of ICR female with *Cyp26a1*$^{+/-}$ male, tissues were first stored individually in RNA*later* solution at -20°C. After the genotype of the embryo was confirmed by DNA genotyping of the yolk sac as described in section 4.3.2, tissues of embryos of the same genotype were pooled as one sample. The mRNA expression level of *Cyp26a1* was measured by real-time quantitative RT-PCR as described in sections 2.6 and 3.3.2., with *β-actin* used as the internal control for normalization of PCR products.

5.3.4 *In vitro* assay of RA degrading activity in tail bud tissue

To determine the RA degrading activity in the tail bud of embryos obtained by mating of ICR female with ICR male, 2 hr after maternal supplementation with 0.625 mg/kg RA or the suspension vehicle as control, the tail bud of embryos at 17-19 somite-stage was excised at a level as described in section 4.3.4. Four tail buds of embryos from the same litter were pooled as one sample. The RA degrading activity was determined by the *in vitro* assay as described in section 4.3.5.

5.3.5 Induction of malformations

5.3.5.1 Caudal regression

ICR male mice were mated with non-diabetic or diabetic ICR female mice. At E8-22hr, pregnant mice received oral supplementation with 0.625 or 1.25 mg/kg body weight of RA to up-regulate *Cyp26a1* expression. Two hours afterwards, i.e. at E9.0, pregnant mice received an intraperitoneal injection a teratogenic dose of 25

mg/kg body weight of RA. At E13, embryos were examined for caudal regression, with the severity being determined by the ratio of tail length to crown-rump length.

5.3.5.2 Other malformations

Cyp26a1$^{+/-}$ male mice were mated with non-diabetic or diabetic ICR female mice. For induction of cleft palate and renal malformations, E9.0 pregnant mice, which had been orally supplemented with a sub-teratogenic dose of 0.625 mg/kg body weight of RA at E8-22hr, received an intraperitoneal injection of a teratogenic dose of 40 mg/kg body weight of RA (RA suspension at 2.66 mg/ml). At E18, near-term fetuses were examined for the incidence rate of cleft palate or renal malformations as described in section 4.3.7.1. The tail tip of the fetus was used for DNA genotyping as described in section 4.3.2.

For induction of neural tube defects, pregnant mice were orally supplemented with 0.625 mg/kg body weight of RA at E7-22hr, and 2 hr later, i.e. at E8.0, pregnant mice received an intraperitoneal injection of 25 mg/kg body weight of RA (RA suspension at 1.67 mg/ml). Embryos were examined at E13 for the incidence rate of exencephaly and spina bifida as described in section 4.3.7.2. The yolk sac was used for DNA genotyping as described in section 4.3.2.

5.3.6 Statistical analysis

Comparison of serum retinol, embryonic RA and *Cyp26a1* expression levels, and TL/CRL ratio between diabetic and non-diabetic groups with or without RA supplementation was performed by Independent Samples t-test. Expression

levels of *Cyp26a1* and the occurrence rate of different malformations among the 4 types of embryos (*Cyp26a1*$^{+/-}$ and *Cyp26a1*$^{+/+}$ embryos in diabetic or non-diabetic pregnancies) were compared by one-way ANOVA followed by Bonferroni test. Correlation between the dose of supplemented RA and the expression level of *Cyp26a1* or TL/CRL ratio was analyzed by Pearson's correlation. All statistical analyses were carried out using SPSS software (*SPSS*), with statistical significance level set at $p < 0.05$.

5.4 RESULTS

5.4.1 Serum retinol levels in female mice

Results of serum retinol levels as determined by HPLC were summarized in Table 5.1 and presented in Graph 5.1. In non-pregnant state, the retinol level of non-diabetic mice is 223.92 ng/ml of serum. There was a significant reduction (p = 0.013) by 10% to 200.79 ng/ml of serum in retinol levels in diabetic mice. When mice became pregnant, at E9.0, the retinol levels were significantly ($p < 0.001$) dropped by more than half and the difference in retinol levels between diabetic and non-diabetic mice were significantly ($p < 0.001$) exaggerated to 20%. These results suggest that supply from maternal serum under diabetic pregnancy may be subnormal especially when the animal becomes pregnant.

Table 5.1 Serum retinol levels in non-diabetic and diabetic mice under pregnant or non-pregnant (E9.0) status as determined by HPLC.

Pregnancy status	Non-pregnant		Pregnant	
Diabetic status	ND	SD	ND	SD
No. of animals	14	14	26	32
Amount of retinol in serum (ng/ml) ± SE	223.92 ± 6.51	200.79 ± 4.45	96.57 ± 5.04	75.61 ± 3.47
p value of ND vs. SD	0.013*		< 0.001*	
p value of ND (Non-pregnant) vs. ND (Pregnant)	< 0.001*			
p value of SD (Non-pregnant) vs. ND (Pregnant)	< 0.001*			

* Statistically significant (data were analyzed by Independent Samples t-test)

5.4.2 Endogenous RA levels in E9.0 embryos

The endogenous RA level in E9.0 embryos was summarized in Table 5.2

and Graph 5.2. Results showed that the endogenous RA level in embryos of diabetic mice was significantly (p = 0.004) reduced by about 35% in comparison to that of the non-diabetic group. To sum up, results of the first part showed that indeed in diabetic pregnancy, there was a significant reduction in both maternal retinol supply and endogenous embryonic RA concentrations.

Table 5.2 Endogenous RA levels in E9.0 embryos of diabetic and non-diabetic mice as determined by RA-responsive cell line.

Maternal status	ND	SD
No. of litters	5	3
No. of embryos	50	20
Sample size[#]	10	4
Amount of RA per embryo (pg) ± SE	8.96 ± 0.20	5.79 ± 0.33
p value of ND vs. SD	0.004*	

[#] Refer to section 5.3.1.2 for definition of one sample

* Statistically significant (data were analyzed by Independent Samples t-test)

5.4.3 *Cyp26a1* expression levels in E9.0 embryos after RA supplementation

Next, I have increased the RA level in the embryo by supplementation with low doses of RA to determine whether this would normalize the *Cyp26a1* expression level. Results of real-time quantification of *Cyp26a1* in the tail bud region of embryos were summarized in Table 5.3 and Graph 5.3. As shown before, in comparing control embryos of non-diabetic and diabetic mice, the *Cyp26a1* expression level was significantly (p = 0.001) down-regulated in diabetic pregnancy. Feeding a low dose of 0.625 mg/kg RA to non-diabetic animals could significantly

($p = 0.001$) increased the expression level of *Cyp26a1*. The expression level further significantly ($p < 0.001$) increased as the dose of RA raised to 1.25 mg/kg, suggesting that the *Cyp26a1* expression could be significantly ($p < 0.001$) positively regulated by RA in a dose-dependent manner ($r = +0.943$). Similar findings were obtained in diabetic pregnancy ($r = +0.926$, $p < 0.001$), such that oral supplementation to the diabetic group with 0.625 mg/kg RA could normalize *Cyp26a1* expression to a level similar to that of the control non-diabetic group without RA supplementation. Results showed that normalization of RA content could significantly restore *Cyp26a1* expressions in embryos of diabetic mice to a level similar to that of embryos of non-diabetic mice.

Table 5.3 Expression levels of *Cyp26a1* relative to *β-actin* in the tail bud of E9.0 embryos of non-diabetic and diabetic mice with or without RA supplementation on E8-22hr.

Maternal status	ND			SD		
Dose of RA supplementation (mg/kg)	CON	0.625	1.25	CON	0.625	1.25
No. of litters	4	4	4	4	4	4
No. of embryos	32	31	32	27	26	29
Sample size[#]	4	4	4	4	4	4
Relative expression levels of *Cyp261* ± SE	0.184 ± 0.005	0.276 ± 0.015	0.523 ± 0.027	0.132 ± 0.007	0.205 ± 0.012	0.450 ± 0.032
p value vs. ND (CON)	-	0.001*	< 0.001*	0.001*	0.151	-
p value vs. SD (CON)	-	-	-	-	0.002*	< 0.001*
Pearson's correlation coefficient (*r*)	+0.943			+0.926		
p value of Pearson's correlation	< 0.001[α]			< 0.001[α]		

[#] Refer to section 5.3.3 for definition of one sample

* Statistically significant (data were analyzed by Independent Samples t-test)

[α] Statistically significant (data were analyzed by Pearson's correlation)

5.4.4 Teratogenicity of low dose of RA

After proving that *Cyp26a1* expression level was correlated with endogenous RA level, and increasing RA concentration with a low dose of RA could normalize *Cyp26a1* expression level, next, I have examined whether the low dose of RA would cause any teratogenic effect on the embryo. As shown in Figure 5.1, there was no observable difference between E13 embryos of control non-diabetic (Figure 5.2A) and diabetic (Figure 5.2B) mice. Feeding with the dose of 1.25 mg/kg RA also did not cause any observable malformations in both groups of embryos (Figures 5.2C and 5.2D). Besides, the teratogenicity of this dose of RA in inducing caudal regression, measured in terms of the ratio of tail length to crown-rump length (TL/CRL ratio) in E13 embryos, was summarized in Table 5.4 and presented in Graph 5.4. Results showed that there was no significant difference in the TL/CRL ratio in control embryos between non-diabetic and diabetic groups. The dose of 1.25 mg/kg RA also did not cause any reduction in the TL/CRL ratio of embryos. Together, these findings indicated that the low dose of RA used in this experiment was non-teratogenic or referred as "sub-teratogenic" to the embryo.

Table 5.4 TL/CRL ratio of E13 embryos in non-diabetic and diabetic mice with or without RA supplementation on E8-22hr.

Treatment groups	CON		1.25 mg/kg RA	
Maternal status	ND	SD	ND	SD
No. of litters	3	3	3	3
No. of embryos	34	24	35	30
Sample size[#]	34	24	35	30
TL/CRL ratio ± SE	0.451 ± 0.004	0.436 ± 0.005	0.456 ± 0.004	0.430 ± 0.005
p value vs. ND (CON)	-	1.000	1.000	1.000
p value vs. SD (CON)	-	-	-	1.000

[#] Refer to section 5.3.5.1 for definition of one sample

5.4.5 RA levels in E9.0 embryos after RA supplementation

The effect of supplementation with sub-teratogenic dose of RA on endogenous RA level was examined. Results were summarized in Table 5.5 and presented in Graph 5.5. The endogenous RA level in embryos of the control diabetic group was significantly (p = 0.004) lower than the control non-diabetic group. Supplementation with sub-teratogenic dose of RA (0.625 mg/kg) could significantly increase the endogenous RA level in embryos in both diabetic (p = 0.030) and non-diabetic groups (p < 0.001). Besides, the low dose of RA could normalize the amount of RA in embryos of diabetic mice to a level similar to that of embryos of non-diabetic mice [p = 0.233, ND (CON) vs. SD (RA)].

Table 5.5 RA levels in E9.0 embryos of non-diabetic and diabetic mice with or without RA supplementation on E8-22hr.

Treatment groups	CON		0.625 mg/kg RA	
Maternal status	ND	SD	ND	SD
No. of litters	5	3	6	6
No. of embryos	50	20	35	30
Sample size	10	4	7	6
Amount of RA per embryo (pg) ± SE	8.96 ± 0.20	5.79 ± 0.33	31.32 ± 3.0	11.41 ± 0.97
p value vs. ND (CON)	-	0.004*	< 0.001*	0.233
p value vs. SD (CON)	-	-	-	0.030*

Refer to section 5.3.1.2 for definition of one sample

* Statistically significant (data were analyzed by Independent Samples t-test)

5.4.6 *In vitro* RA degrading activity in the tail bud after RA supplementation

Next, I tested for the *in vitro* RA degrading activity in the tail bud to determine whether up-regulation of *Cyp26a1* could indeed increase its ability to degrade RA. The *in vitro* RA degrading activity, expressed in terms of % of RA in the medium being degraded, was summarized in Table 5.6 and presented in Graph 5.6. Similar to the previous finding in Chapter 4, the RA degrading activity was significantly ($p < 0.001$) reduced in the control diabetic group in comparison to the control non-diabetic group. Supplementation with a low dose of RA (0.625 mg/kg) significantly increased the RA degrading activity in embryos of both non-diabetic ($p = 0.002$) and diabetic groups ($p < 0.001$), such that the RA degrading activity of the diabetic group was normalized to a level similar to that of the control non-diabetic group [$p = 0.1117$, ND (CON) vs. SD (RA)].

Table 5.6 ***In vitro* RA degrading activity in the tail bud tissue of E9.0 embryos of non-diabetic and diabetic mice with or without RA supplementation on E8-22hr.**

Treatment groups	CON		0.625 mg/kg RA	
Maternal status	ND	SD	ND	SD
No. of litters	3	5	3	5
No. of embryos	25	25	25	25
Sample size[#]	5	5	5	5
% RA in medium being degraded ± SE	62.69 ± 2.62	43.52* ± 1.00	85.79* ± 2.75	68.99[#] ± 2.53
p value vs. ND (CON)	-	< 0.001*	0.002*	0.117
p value vs. SD (CON)	-	-	-	< 0.001*

[#] Refer to section 5.3.4 for definition of one sample

* Statistically significant (data were analyzed by Independent Samples t-test)

5.4.7 Susceptibility to RA-induced caudal regression

To test whether supplementation with *sub-teratogenic* doses (0.625 mg/kg or 1.25 mg/kg) of RA to normalize *Cyp26a1* expression and RA degrading activity in the tail bud could reduce the embryo's susceptibility to RA teratogenesis, embryos were maternally challenged with a *teratogenic* dose of RA (25 mg/kg) following RA supplementation and their susceptibility to RA-induced caudal regression was determined. Results of severity of caudal regression, measured in terms of TL/CRL ratio, in embryos of different treatment groups at E13 were summarized in Table 5.7 and presented in Graph 5.7. There was no significant difference in the TL/CRL ratio between embryos of non-diabetic and diabetic mice without the teratogenic RA insult. However, when subjected to challenge with a teratogenic dose of RA, there was a significant ($p < 0.001$) reduction in TL/CRL ratio in embryos of the control diabetic group than that of the control non-diabetic group, which agreed with our previous findings that embryos of diabetic mice were more susceptible to RA-induced caudal regression than embryos of non-diabetic mice (Chan et al., 2002). In contrast, supplementing sub-teratogenic doses of RA to non-diabetic mice could significantly cause a dose-dependent increase in TL/CRL ratio of the embryos ($r = +0.961$; $p < 0.001$), implying that the teratogenic effect of RA in inducing caudal regression was ameliorated. This significant dose-dependent rescue effect similarly occurred in diabetic groups ($r = +0.945$; $p < 0.001$), such that supplementation with 0.625 mg/kg RA to diabetic mice to normalize *Cyp26a1* expression levels could increase the TL/CRL ratio of embryos to a level similar to that of embryos of control non-diabetic mice.

Table 5.7 Severity of caudal regression in terms of TL/CRL ratio in E13 embryos of non-diabetic and diabetic mice with or without RA supplementation on E8-22hr and teratogenic RA insult on E9.0.

Maternal status	ND				SD			
Dose of RA supplementation (mg/kg)	CON	CON	0.625	1.25	CON	CON	0.625	1.25
Dose of teratogenic RA insult (mg/kg)	-	25	25	25	-	25	25	25
No. of litters	3	5	5	5	3	5	3	5
No. of embryos	34	59	53	54	24	54	30	51
Sample size[#]	34	59	53	54	24	54	30	51
TL/CRL ratio ± SE	0.451 ± 0.004	0.249 ± 0.008	0.283 ± 0.008*	0.358 ± 0.008*	0.436 ± 0.005	0.282 ± 0.008*	0.255 ± 0.016[#]	0.334 ± 0.009[#]
p value vs. ND (CON)	-	< 0.001 *	< 0.001 *	< 0.001 *	1.000	-	-	-
p value vs. SD (CON)	-	-	-	-	-	< 0.001 *	< 0.001 *	< 0.001 *
p value vs. ND (CON) + 25 mg/kg RA	-	-	< 0.001 *	< 0.001 *	-	< 0.001 *	1.000	-
p value vs. SD (CON) + 25 mg/kg RA	-	-	-	-	-	-	< 0.001 *	< 0.001 *
Pearson's correlation coefficient (*r*)	-	+0.961			-	+0.945		
p value of Pearson's correlation	-	< 0.001[α]			-	< 0.001[α]		

[#] Refer to section 5.3.2 for definition of one sample

* Statistically significant (data were analyzed by Independent Samples t-test)

[α] Statistically significant (data were analyzed by Pearson's correlation)

5.4.8 *Cyp26a1* expression levels in E9.0 *Cyp26a1* mutant embryos after RA supplementation

To further determine whether up-regulation of *Cyp26a1* expression levels in embryos of diabetic mice could ameliorate/abolish their increased susceptibility to various types of birth defects, I have employed the *Cyp26a1* mutant model (*Cyp26a1* heterozygous male mice mated with ICR diabetic or non-diabetic female mice) to generate embryos with different expression levels of *Cyp26a1*. Before testing for their susceptibility to different types of RA-induced birth defects, *Cyp26a1* expression in the tail bud and the whole embryo (exclude tail bud) at 2 hr after maternal oral supplementation with 0.625 mg/kg RA was determined. Results were summarized in Table 5.8, and presented in Graphs 5.8 and 5.9. As shown previously, embryos in different genotype and maternal environment combinations exhibited different levels of *Cyp26a1*. With supplementation of sub-teratogenic dose of RA (0.625 mg/kg), the expression level of *Cyp26a1* in all 4 types of embryos was significantly up-regulated in both the tail bud and the whole embryo (exclude tail bud), such that the expression level of *Cyp26a1* in $Cyp26a1^{+/-}$ and $Cyp26a1^{+/+}$ embryos in diabetic mice supplemented with RA showed no significant difference from embryos of the sample genotype in control non-diabetic mice.

Table 5.8 **Expression levels of *Cyp26a1* relative to *β-actin* in E9.0 embryos of different groups with or without RA supplementation on E8-22hr.**

Treatment group	CON			
Maternal status	ND		SD	
Genotype	+/+	+/-	+/+	+/-
No. of litters	4	4	3	3
No. of embryos	16	18	14	12
Sample size[#]	4	4	3	3
Relative expression levels of *Cyp26a1* in tail bud ± SE	0.237 ± 0.025	0.120 ± 0.004	0.128 ± 0.014	0.044 ± 0.002
Relative expression levels of *Cyp26a1* in whole embryo (exclude tail bud) ± SE	0.0073 ± 0.0002	0.0037 ± 0.0004	0.0053 ± 0.0002	0.0017 ± 0.0002
Treatment group	0.625 mg/kg RA			
Maternal status	ND		SD	
Genotype	+/+	+/-	+/+	+/-
No. of litters	4	4	4	4
No. of embryos	17	16	16	15
Sample size[#]	4	4	4	4
Relative expression levels of *Cyp26a1* in tail bud ± SE	0.354 ± 0.026	0.207 ± 0.028	0.195 ± 0.011	0.134 ± 0.007
Relative expression levels of *Cyp26a1* in whole embryo (exclude tail bud) ± SE	0.0089 ± 0.0006	0.0051 ± 0.0003	0.0071 ± 0.0004	0.0040 ± 0.0003

[#] Refer to section 5.3.3 for definition of one sample

Table 5.9 Statistical analysis of relative expression levels of *Cyp26a1* between embryos of different groups using one-way ANOVA followed by Bonferroni test.

Groups for comparison	*p* value in comparing CON embryos in different genotype-maternal status combinations			
	$ND^{+/+}$(CON) vs. $ND^{+/-}$(CON)	$ND^{+/+}$(CON) vs. $SD^{+/+}$(CON)	$SD^{+/+}$(CON) vs. $SD^{+/-}$(CON)	$ND^{+/-}$(CON) vs. $SD^{+/-}$(CON)
Tail bud	0.002*	0.002*	0.043*	0.029*
Whole embryo (exclude tail bud)	< 0.001*	< 0.001*	< 0.001*	0.001*
Groups for comparison	*p* value in comparing CON and RA-supplemented embryos of the same genotype in the same maternal status			
	$ND^{+/+}$(CON) vs. $ND^{+/+}$(RA)	$ND^{+/-}$(CON) vs. $ND^{+/-}$(RA)	$SD^{+/+}$(CON) vs. $SD^{+/+}$(RA)	$SD^{+/-}$(CON) vs. $SD^{+/-}$(RA)
Tail bud	0.002*	0.040*	0.047*	0.018*
Whole embryo (exclude tail bud)	0.015*	0.049*	0.009*	< 0.001*
Groups for comparison	*p* value in comparing CON and RA-supplemented embryos of the same genotype in different maternal status			
	$ND^{+/+}$(CON) vs. $SD^{+/+}$(RA)	$ND^{+/-}$(CON) vs. $SD^{+/-}$(RA)		
Tail bud	1.000	1.000		
Whole embryo (exclude tail bud)	1,000	1.000		

* Statistically significant

5.4.9 Susceptibility to different types of malformations after RA supplementation

After confirming that there was up-regulation of *Cyp26a1* in the 4 types of embryos following RA supplementation with low dose of RA, embryos were

maternally challenged with a teratogenic dose of RA at appropriate developmental stage to determine their susceptibility to various types of birth defects.

Incidence rates of RA-induced cleft palate and renal malformations in fetuses maternally treated with 40 mg/kg RA on E9.0 were summarized in Table 5.10, and presented in Graph 5.10 and Graph 5.11 respectively. Incidence rates of RA-induced exencephaly and spina bifida in embryos maternally treated with 25 mg/kg RA on E8.0 were summarized in Table 5.11, and presented in Graph 5.12 and Graph 5.13. Results of statistical analyses were shown in Table 5.12.

Table 5.10 Incidence rates of cleft palate and renal malformations in different types of E18 fetuses of control or RA-supplemented non-diabetic and diabetic mice induced by maternal injection with 40 mg/kg RA on E9.0.

Treatment group	CON			
Maternal status	ND		SD	
Genotype	+/+	+/-	+/+	+/-
No. of litters	11	11	10	10
No. of fetuses	68	60	54	46
% of fetuses per litter with cleft palate ± SE	35.6 ± 3.7	59.0 ± 2.2	54.2 ± 3.8	92.3 ± 3.3
% of fetuses per litter with renal malformations ± SE	7.1 ± 3.4	21.3 ± 5.1	38.8 ± 6.3	73.3 ± 7.7
Treatment group	0.625 mg/kg RA			
Maternal status	ND		SD	
Genotype	+/+	+/-	+/+	+/-
No. of litters	9	9	9	9
No. of fetuses	63	47	50	46
% of fetuses per litter with cleft palate ± SE	6.4 ± 2.6	22.4 ± 4.8	24.4 ± 5.6	55.9 ± 7.1
% of fetuses per litter with renal malformations ± SE	4.4 ± 2.2	15.3 ± 5.5	11.3 ± 3.9	34.5 ± 6.0

Upon challenged with a teratogenic dose of RA, as mentioned in Chapter 4, the incidence rate of cleft palate, renal malformations, exencephaly and spina bifida in the control diabetic group was significantly higher than the control non-diabetic group for both *Cyp26a1* heterozygous embryos and their wild-type littermates. When embryos were pre-fed with sub-teratogenic dose of RA, the incidence rate of RA-induced cleft palate was significantly reduced in both genotypes in diabetic and non-diabetic groups. For renal malformations, exencephaly and spina bifida, significant reduction in the incidence rate after pre-feeding with sub-teratogenic dose of RA was only found in the diabetic group of both genotypes. In the non-diabetic group, there was slight reduction in the incidence rate in both genotypes, but without any statistical significance. The most important finding was that there were no longer any significant differences in the incidence rate of cleft palate, renal malformations, exencephaly and spina bifida between embryos of both genotypes in the diabetic group supplemented with low dose of RA and embryos of corresponding genotypes in the control non-diabetic group. This result implied that after RA supplementation, the increased susceptibility of *Cyp26a1*$^{+/-}$ embryos and their *Cyp26a1*$^{+/+}$ littermates to RA-induced cleft palate, renal malformations, exencephaly and spina bifida caused by diabetic pregnancy was ameliorated to a level similar to that of the control non-diabetic group.

Statistical analyses by two-way ANOVA were further performed to investigate the contribution of the 3 factors to birth defects including: 1) maternal factor, 2) genetic factor and 3) sub-teratogenic RA treatment. Results showed that all malformations showed significant differences between diabetic and non-diabetic pregnancy ($p < 0.05$ for all defects). Besides renal malformations, the other threes types of malformations all showed significant differences between genotypes,

suggesting that these malformations are highly dependent on *Cyp26a1* expression levels ($p < 0.05$ for all defects except renal malformations). With oral supplementation of low dose RA, the risk of all malformations in diabetic pregnancy was significantly reduced to a level similar as non-diabetic pregnancy.

Table 5.11 Incidence rates of exencephaly and spina bifida in different types of E13 embryos of control and RA-supplemented non-diabetic and diabetic mice induced by maternal injection with 25 mg/kg RA on E8.0.

Treatment group	CON			
Maternal status	ND		SD	
Genotype	+/+	+/-	+/+	+/-
No. of litters	9	9	9	9
No. of embryos	36	26	27	27
% of embryos per litter with exencephaly ± SE	5.4 ± 3.6	30.6 ± 5.7	37.4 ± 6.5	75.0 ± 8.3
% of embryos per litter with spina bifida ± SE	3.7 ± 2.5	36.1 ± 7.3	31.9 ± 5.7	71.3 ± 6.1
Treatment group	0.625 mg/kg RA			
Maternal status	ND		SD	
Genotype	+/+	+/-	+/+	+/-
No. of litters	8	8	9	9
No. of embryos	28	29	33	30
% of embryos per litter with exencephaly ± SE	2.5 ± 2.5	8.3 ± 5.5	22.9 ± 4.9	40.7 ± 4.13
% of embryos per litter with spina bifida ± SE	2.5 ± 2.4	20.8 ± 6.2	13.9 ± 6.2	39.1 ± 9.0

Table 5.12 Statistical analysis of incidence rates of various types of RA-induced defects between embryos of different groups using one-way ANOVA followed by Bonferroni test.

Groups for comparison	*p* value in comparing CON embryos in different genotype-maternal status combinations			
	$ND^{+/+}$(CON) vs. $ND^{+/-}$(CON)	$ND^{+/+}$(CON) vs. $SD^{+/+}$(CON)	$SD^{+/+}$(CON) vs. $SD^{+/-}$(CON)	$ND^{+/-}$(CON) vs. $SD^{+/-}$(CON)
Cleft palate	0.002*	0.046*	< 0.001*	< 0.001*
Renal malformations	1.000	0.002*	< 0.001*	< 0.001*
Exencephaly	0.047*	0.003*	< 0.001*	< 0.001*
Spina bifida	0.010*	0.046*	< 0.001*	0.003*
Groups for comparison	*p* value in comparing CON and RA-supplemented embryos of the same genotype in the same maternal status			
	$ND^{+/+}$(CON) vs. $ND^{+/+}$(RA)	$ND^{+/-}$(CON) vs. $ND^{+/-}$(RA)	$SD^{+/+}$(CON) vs. $SD^{+/+}$(RA)	$SD^{+/-}$(CON) vs. $SD^{+/-}$(RA)
Cleft palate	< 0.001*	< 0.001*	< 0.001*	< 0.001*
Renal malformations	1.000	1.000	0.023*	< 0.001*
Exencephaly	1.000	0.182	1.000	0.001*
Spina bifida	1.000	1.000	1.000	0.001*
Groups for comparison	*p* value in comparing CON and RA-supplemented embryos of the same genotype in different maternal status			
	$ND^{+/+}$(CON) vs. $SD^{+/+}$(RA)	$ND^{+/-}$(CON) vs. $SD^{+/-}$(RA)		
Cleft palate	1.000	1.000		
Renal malformations	1.000	1.000		
Exencephaly	0.708	1.000		
Spina bifida	1.000	1.000		

* Statistically significant (data were analyzed by one-way ANOVA followed by Bonferroni test).

To summarize, results showed that in diabetic pregnancy, there was a significant reduction in endogenous RA levels which might lead to down-regulation of *Cyp26a1* and increased RA teratogenicity. By increasing RA level in the embryo, it could normalize *Cyp26a1* expression and RA degrading activity, concomitantly, abolishing the increase in susceptibility to various types of malformations exhibited by embryos of diabetic pregnancy.

5.5 DISCUSSION

Results in section 5.4.2 showed that the endogenous RA level in embryos of diabetic mice was significantly reduced by about 35% in comparison to that of the non-diabetic group. This reduction is comparable with the extent of down-regulation of *Cyp26a1* (22%) in embryos of diabetic pregnancy (Table 3.1), suggesting that reduction of endogenous RA in the embryo may be one of the mechanisms that causes down-regulation of *Cyp26a1*. Indeed, preliminary study has showed that there is already a decrease in RA level in the embryo as early as E7.0 (data not shown), which coincides with the time of initiation of *Cyp26a1* expression. Moreover, a decrease in endogenous RA level is further supported by our laboratory's recent findings that expressions of all 3 subtypes of RA synthesizing enzymes, *Raldh1*, *Raldh2* and *Raldh3*, were significantly down-regulated in E9.0 embryos under diabetic conditions (Chan, 2011). Moreover, the enzymatic activity of Raldh2, the most abundant RA synthesizing enzyme in the embryo, is also significantly reduced (Chan, 2011). Together, these results support that there is subnormal level of RA in the mouse embryo under diabetic conditions.

In this chapter, I have demonstrated that *Cyp26a1* expression level in the embryo was significantly up-regulated after supplementation with a low dose of RA (0.625 mg/kg) (Table 5.8). Concomitantly, there was reduced severity of different types of malformations, including caudal regression, cleft palate, renal malformations, spina bifida and exencephaly, upon being challenged with a teratogenic dose of RA. These results therefore give evidence that up-regulation of *Cyp26a1*, by administration of low doses of RA, can provide protective effect to the embryo against RA teratogenesis in diabetic pregnancy. Taken together, findings of this chapter support the hypothesis that subnormal level of RA will down-regulate

Cyp26a1 expression in the embryo, but maternal supplementation with low doses of RA to restore embryonic RA levels can normalize *Cyp26a1* expression, thereby reducing the risk of birth defects.

Indeed, the altered endogenous RA level and *Cyp26a1* expression involve complex feedback mechanism. It is predicted that a global decrease in endogenous RA levels occurring in embryos of diabetic pregnancy will down-regulate *Cyp26a1* expression locally in specific tissues, e.g. cranial and cervical mesenchyme and tail bud region in E9.0 embryos. The reduction in *Cyp26a1* expression may lead to the local build up of RA in specific tissues, thus increasing the risk of various birth defects. However, the increase in RA levels in local tissues may not be able to compensate the global decrease of RA levels, leading to a persisted down-regulation of *Cyp26a1*. In my previous study, it was found that when embryos were maternally challenged with a teratogenic dose of RA (25 mg/kg), there was a 8-fold difference of RA levels in the tail bud between *Cyp26a1* wild-type embryos in non-diabetic pregnancy and *Cyp26a1* heterozygous embryos in diabetic pregnancy at 3 hr after RA treatment (Lee, 2008). This difference found in the tail bud was much greater than the 2.5-fold difference found in the whole embryo (Graph 4.4). Together, these results suggest that there is a local variation of RA levels in the embryo.

Besides, a direct relationship between the maternal retinol level and the embryonic RA level is yet to be determined. Several lines of evidence showed that maternal vitamin A deficiency may only affect embryonic RA levels in severe cases. Mice fed with vitamin A-deficient diet for 7 weeks before pregnancy could still give birth to normal offspring (Quadro et al., 2005). Loss of RBP4 will cause embryonic abnormalities typical of vitamin A deficiency. However, when maintained on a vitamin A-sufficient diet, even $RBP4^{-/-}$ mice could yield embryos that only displayed

relatively mild and transient cardiac embryonic developmental anomalies (Quadro et al., 1999; Wendler et al., 2003). It was found that in mice lacking retinol-RBP4, high levels of retinyl ester was incorporated into maternal circulating chylomicrons and very low-density lipoprotein particles, which served as an alterative source to supply embryos with sufficient amount of vitamin A to enable relatively normal development of most embryonic tissues (Quadro et al., 2004). These results suggest that even in very limited vitamin A conditions, retinyl ester can serve as alternative source of retinol supply to the embryo. Thus, the actual role of reduction of retinol level in down-regulating *Cyp26a1* is still unknown.

Besides, the RBP4 level in type 2 diabetes is significantly increased, which is opposite to type 1 diabetes (Cho et al., 2006; Graham et al., 2006; Polonsky, 2006). A potential link between RBP4 and human diabetes was suggested by a report, which revealed that RBP4 levels were elevated in insulin-resistant mice (Yang et al., 2005) and humans with obesity and type 2 diabetes mellitus (Graham et al., 2006). On the other hand, when RBP4 levels were normalized by rosiglitazone, insulin sensitivity was restored (Yang et al., 2005). Studies in transgenic rodent models showed that overexpression of human RBP4 or injection of recombinant RBP4 could induce insulin resistance in mice, whereas RBP4 knockout mice showed enhanced insulin sensitivity (Yang et al., 2005). Recent studies have attempted to inhibit RBP4 to reduce the effect of diabetes (Craig et al., 2007). RBP4 is the carrier protein for retinol, whether up-regulation of RBP4 will increase retinol circulation is still unknown. If so, subnormal levels of RA in the embryo may only be a pathogenic mechanism for type 1 diabetic embryopathy.

Moreover, I have shown that embryos in non-diabetic pregnancy showed a higher endogenous RA concentration than embryos in diabetic pregnancy at 2 hr

after treatment with a sub-teratogenic dose of RA. Similar observation was found when non-diabetic and diabetic pregnant mice were treated with a teratogenic dose of RA (50 mg/kg) on E9.0 (data not shown). Thus, it is speculated that the uptake of RA into embryos of non-diabetic pregnancy is much faster than that of diabetic pregnancy. To test this hypothesis, the major cellular retinoic acid binding protein (Crabp), *Crabp1* and *Crabp2* in embryonic tissues of non-diabetic and diabetic pregnancy should be examined. My preliminary result shows that there is no significant difference in the expression level of *Crabp1* and *Crabp2* in the embryo proper between the two groups. However, expressions of both *Crabp1* and *Crabp2* are significantly down-regulated in the ectoplacental cone of the embryo in diabetic pregnancy. *Crabp1* is also significantly down-regulated in the decidual tissues of diabetic pregnancy. The down-regulation of *Crabps* in extraembryonic and decidual tissues in diabetic pregnancy may account for the reduction in RA uptake into the embryo. Difference in RA uptake may in turn accounts for the difference in up-regulation of *Cyp26a1* in the embryo upon RA treatment and may also account for the difference in endogenous embryonic RA levels between diabetic and non-diabetic status.

Chapter 6

Effect of Hyperglycemia on *Cyp26a1* Expression

6.1. INTRODUCTION

It is well-known that maternal diabetes is associated with increased frequency of congenital anomalies in the offspring. Despite considerable advances in diabetic management, congenital malformation rate associated with diabetic pregnancy remains two to three times higher than in the general population (Casson et al., 1997; Hawthorne et al., 1997). However, the teratogenic mechanism of diabetic pregnancy is not completely understood.

Many studies have shown that the risk of diabetic embryopathy is correlated with maternal blood glucose levels or glycosylated hemoglobin (HbA1c) levels. Women with early maternal HbA1c concentrations over 7% showed a three- to five-fold increase in fetal malformation rates than women with normal pregnancy (Galindo et al., 2006). In contrast, effective glycemic control during preconception and early gestation has generally led to a lower frequency of malformations (Fuhrmann et al., 1983; Kitzmiller et al., 1991). In several studies using animal models, culture of postimplantation rat embryos in the presence of elevated glucose resulted in multiple defects such as exencephaly, spina bifida, torsion defects and growth retardation, which were similar to those occurring in diabetic pregnancy (Sadler et al., 1989; Eriksson et al., 1991; Strieleman & Metzger, 1993). The critical period of vulnerability to glucose is the stage of organogenesis. Moreover, β-hydroxybutyrate and somatomedin inhibitors, which were found to be increased in diabetic animals, could also synergize with glucose to cause maldevelopment (Sadler et al., 1989). These results suggest that metabolic disturbances that are secondary to hyperglycemia may also have embryopathogenic potential.

Pax3 is one of the genes well known to be altered under diabetic pregnancy

and hyperglycemia (Phelan et al., 1997; Pani et al., 2002; Loeken, 2006). It is expressed in the neural tube, neural crest and somitic mesoderm during early embryonic development (Epstein et al., 1991; Conway et al., 1997) and is indispensible for neural tube development. *Splotch* mice, a spontaneously occurred mouse mutant with disrupted *Pax3* show 100% occurrence of neural tube defects (Goulding et al., 1991). Both non-diabetic mice made transiently hyperglycemic by receiving repeated injections of D-glucose and *in vitro* whole embryo culture of mouse embryos in high glucose medium showed inhibition of *Pax3* expression (Phelan et al., 1997), via elevation in oxidative stress levels (Li et al., 2005). Conversely, injection of phlorizin, a drug that inhibits renal tubular reabsorption of glucose, to diabetic mice could normalize *Pax3* expression level and reduced adverse consequences in the embryos of diabetic pregnancy (Fine et al., 1999). Alteration of *Pax3* expression provides the first insight that high concentration of glucose can affect gene expression. Besides, similar to *Cyp26a1*, *Pax3* possesses got a RARE located in the promoter region (Kennedy et al., 2009), it is possible that enhanced oxidative stress under hyperglycemic condition may cause a lowering in endogenous RA level in the embryo, which in turn reduces the expression of both *Pax3* and *Cyp26a1*.

RA, an bioactive metabolite of vitamin A is the first morphogen identified (Thaller & Eichele, 1987) and a key signaling molecule that governs many embryonic developmental processes. However, it is also a teratogen when it is present in excess during development. Using the mouse as a model, our laboratory has reported that embryos of mice in diabetic or hyperglycemic conditions showed increased susceptibility to caudal regression induced by RA (Chan et al., 2002). Both diabetic and hyperglycemic conditions enhanced RA-induced down-regulation

of *Wnt-3a*, a gene indispensable for development of the embryonic caudal region (Takada et al., 1994), suggesting that the underlying cellular and molecular changes induced by the two conditions are very similar. On the other hand, reduction in blood glucose levels of diabetic mice could completely abolish the embryo's increased susceptibility to RA (Leung et al., 2004). These results suggest that elevated glucose is the critical factor in maternal diabetes responsible for potentiating the teratogenic effect of RA. I, therefore, hypothesized that elevated glucose may be one of the factors affecting *Cyp26a1* expression in embryos of diabetic pregnancy.

6.2. EXPERIMENTAL DESIGN

In previous chapters, I have found that the expression of *Cyp26a1*, the main catabolizing enzyme for controlling RA homeostasis in the embryo, was significantly down-regulated in embryos of diabetic mice, thereby increasing the embryo's susceptibility to malformations caused by disrupted RA levels. As mentioned in section 6.1, embryos in both diabetic and hyperglycemic conditions showed increased susceptibility to birth defects induced by RA (Chan et al., 2002). This chapter therefore aimed to test whether elevated glucose was the critical factor in the maternal diabetic milieu that down-regulated *Cyp26a1*.

First, streptozotozin-induced diabetic and non-diabetic pregnant mice were treated with phlorizin (PHZ), a drug that can cause renal glucosuria by inhibiting glucose reabsorption in the proximal renal tubule (Rossetti et al., 1987) and thus specifically reduces blood glucose concentrations. Mice treated with equivalent volume of suspension vehicle served as the control. Embryos were collected for analysis of: (i) *Cyp26a1* expression by *in situ* hybridization and real-time quantitative RT-PCR; (ii) endogenous RA levels by using the RA-responsive cell line, (iii) the RA degrading activity by using the *in vitro* assay; (iv) amount of RA in the tissue at 3 hr after exposure to an exogenous dose of RA; (v) susceptibility to develop different types of malformations after being maternally challenged with a teratogenic dose of RA. These analyses were aimed to determine whether lowering of maternal blood glucose levels alone in diabetic mice could lead to normalization of *Cyp26a1* expression, endogenous RA level, and RA catabolism in their embryos, resulting in amelioration or abolishment of increased embryonic susceptibility to malformations caused by diabetic pregnancy. Results showed that elevated glucose was indeed the critical factor in the maternal diabetic milieu that caused changes in

*Cyp26*1 expression levels and predisposed embryos to malformations.

To further prove that glucose could cause dose-dependent effect on *Cyp26a1* expression, an *in vitro* approach was employed. Early head-fold stage rat embryos of normal pregnancy were cultured *in vitro* in serum supplemented with varying concentrations of D-glucose (2 mg/ml, 3 mg/ml and 4 mg/ml dissolved in DMEM, which is equivalent to blood glucose levels of 17.5 mmol/L, 22.5 mmol/L and 27.5 mmol/L respectively). Unlike *in vivo* study where maternal blood glucose levels showed great variations in different mice, the *in vitro* method has the advantage that the concentration of glucose could be precisely determined. Rat, instead of mouse embryos were employed in this study because of several reasons: (i) rat embryos developed better than mouse embryos when cultured *in vitro* from early head-fold to early stage of organogenesis; (ii) rat embryos developed *in vitro* showed more consistent response to glucose than mouse embryos; (iii) there were less variations in the developmental stage of rat embryos within a litter, so more embryos per litter were at the correct developmental stage (head-fold stage) that could be used for culture. At the end of 24 or 48 hr in culture, embryos were collected for analysis of *Cyp26a1* expressions by *in situ* hybridization and real-time quantitative RT-PCR, and endogenous RA levels by using the RA-responsive cell lines. These analyses aimed to determine whether glucose could induce dose-dependent changes in *Cyp26a1* expression and endogenous RA levels in the embryo.

6.3. MATERIALS AND METHODS

6.3.1 Treatment with phlorizin

Phlorizin (PHZ; Sigma) was suspended in 40% propylene glycol in autoclaved water to make a stock at the concentration of 0.04 g/ml. It was vortexed vigorously for an hour before use. Starting from E8-14hr, diabetic and non-diabetic ICR pregnant mice, which had been mated with ICR male mice, received intraperitoneal injections of 0.4 g/kg body weight of PHZ, using a 25G needle (0.50 x 16 mm; *Terumo*), for a total of three doses given at 4 hour-interval to ensure continuous inhibition of renal tubular glucose reabsorption. Mice injected with equivalent volume of suspension vehicle (10 μl per gram of body weight) served as control. Glycemic level of tail vein blood measured with a glucometer was recorded prior to each injection and also prior to dissection. At E9.0, i.e. 10 hr after the first dose of PHZ or suspension vehicle, embryos were collected for different types of analysis, including determination of (i) *Cyp26* expression levels (sections 6.3.4 and 6.3.5), (ii) endogenous RA levels (section 6.3.6) and (iii) *in vitro* RA degrading activity (section 6.3.7). Mice were injected with a teratogenic dose of RA for determining the effective concentration of RA in the embryo (section 6.3.8) and the susceptibility of embryos to different types of malformations (section 6.3.9).

6.3.2 *In vitro* culture of rat embryo

Sprague Dawley rats in normal pregnancy were sacrificed by cervical dislocation at E9.5 (equivalent to E7.5 of mouse pregnancy). The uterus was dissected in pre-warmed PB1 medium (Cockroft, 1990) containing 10% fetal bovine serum (*Gibco*). Embryos were freed from decidual tissues and Reichert's membrane,

but the ectoplacental cone and the yolk sac were left intact. To minimize differences in embryos' responses to glucose due to variations in developmental stages, only embryos at the early head-fold stage were used for culture. Rat embryos were cultured *in vitro* in rat serum (prepared as described in section 6.3.3) at a volume of 1 ml per embryo. Normally 3 embryos were placed in each culture bottle. In experimental groups, the culture medium was supplemented with varying concentrations (2 mg/ml, 3 mg/ml and 4 mg/ml) of D-glucose (*BDH*; prepared as a stock of 0.5 g/ml dissolved in DMEM) for either 24 or 48 hr. Equivalent volume of DMEM (8 µl per ml of serum) was added as the control group. Culture bottles were fitted onto a rotating culture unit inside an incubator (*BTC Engineering*) at 38°C. The culture bottles were continuously aerated with a gas mixture composed of 5% O_2, 5% CO_2 and 90% N_2 for the first 24 hr; 20% O_2, 5% CO_2 and 75% N_2 for the next 8 hr; 40% O_2, 5% CO_2 and 55% N_2 for the remaining 16 hr. After *in vitro* culture, embryos were collected for different types of analysis, including determination of *Cyp26a1* expression (sections 6.3.4 and 6.3.5) and endogenous RA levels (section 6.3.6).

6.3.3 Preparation of rat serum

Rat serum was prepared according to the method as described by Cockroft (1990). In brief, adult male Sprague Dawley rat was anaesthetized by ether. The abdominal wall was cut open and blood was collected from the dorsal aorta using a 20 ml syringe fitted with a 19G needle (1.1 x 38 mm; *Terumo*) until the heart stopped beating. The rat was immediately sacrificed by cutting open the diaphragm to stop breathing followed by cervical dislocation. Blood sample was immediately

centrifuged for 5 min at 4,000 rpm. After standing for 1 hr, the serum was transferred to a new tube in a culture hood. The serum was heat-inactivated at 56°C in a water bath for 40 min, during which the serum was gassed with a gentle stream of N_2 to drive away any residual ether. The serum was stored at -80°C until use.

6.3.4 Whole mount *in situ* hybridization

Mouse and rat embryos (collected as described in sections 6.3.1 and 6.3.2 respectively) were dissected free from all extraembryonic membranes in ice-cold DEPC-treated PBS and fixed in 4% paraformaldehyde in PBS at 4°C overnight. They were processed for analysis of *Cyp26a1* mRNA expression by whole mount *in situ* hybridization according to the protocol as described in section 2.7. Particulars of the *Cyp26a1* mouse cDNA plasmid, used for generating antisense riboprobes as described in section 2.8, were detailed in section 3.3.3. Since mouse and rat *Cyp26a1* share about 95% homology, the *Cyp26a1* mouse cDNA plasmid was used for detecting *Cyp26a1* expression in both mouse and rat embryos. Between three to four litters of embryos were examined for each group.

6.3.5 Real-time quantitative RT-PCR

Mouse embryos at 19-21 somite-range (collected as described in section 6.3.1.) were freed from all decidual tissues and extraembryonic membranes in ice-cold DEPC-treated PBS. They were divided into two parts: the tail bud and the whole embryo (exclude tail bud) according to the landmark as described in section 4.3.4. Tissues of embryos from the same litter were pooled as one sample. As for rat

embryos (collected as described in section 6.3.2), either the tail bud or the whole embryo was collected. The three embryos cultured in the same bottle were pooled as one sample. Both mouse and rat samples were stored in RNA*later* RNA Stabilization Reagent at -20°C before being processed for measurement of the expression level of the 3 subtypes of *Cyp26* by real-time quantitative RT-PCR as described in section 2.6.

The sequence of primer pairs for amplification of partial sequence of mouse *Cyp26a1*, *Cyp26b1*, *Cyp26c1* and *β-actin* were the same as listed in section 3.3.2. The sequences for rat samples were as follow:

Rat *Cyp26a1*	forward primer:	5'-GTG CCA GTG ATT GCT GAA GA-3'
	reverse primer:	5'-AGA GAA GAG ATT GCG GGT CA-3'
Rat *Cyp26b1*	forward primer:	5'-CAC ATC CTT GAT CAT GCA AC-3'
	reverse primer:	5'-AGC CTC ATG ACC TCC TTG AT-3'
Rat *Cyp26c1*	forward primer:	5'-ATC CCT TAT CCT GCT GCT TC-3'
	reverse primer:	5'-AGC ACC TCC TTC ACT ACG GC-3'
Rat *β-actin*	forward primer:	5'-GGA AAT CGT GCG TGA CAT TA-3'
	reverse primer:	5'-AGG AAG GAA GGC TGG AAG AG-3'

The standards used for quantifying the amount of rat *Cyp26a1*, *Cyp26b1*, *Cyp26c1* and *β-actin* were prepared from genomic DNA (gDNA) extracted from rat liver using FavorPrep tissue genomic DNA extraction kit (*Favorgen*) according to the manufacturer's protocol. In brief, 20 mg of rat liver was grinded into small pieces by a micropestle in 200 µl of FATG1 Buffer. Twenty microliters of proteinase K (10 mg/ml) were added and then incubated at 60°C with vortexing for 2 hr until

complete lysis of the tissue. After incubation, 200 µl of FATG2 Buffer was added and further incubated at 70°C for 10 min. The mixture was then mixed with 200 µl of absolute ethanol followed by vortexing and transferred to a FATG Mini Column, which was fitted with a collection tube, and centrifuged for 1 min at 14,000 rpm. With the flow-through discarded, the cartridge was washed with 700 µl of W1 Buffer and centrifuged at 14,000 rpm for 1 min. The cartridge was then washed with 750 µl Wash Buffer and centrifuged at 14,000 rpm for 1 min. After discarding the flow-through, the FATG Mini Column was further centrifuged for 3 min to remove any carryover of the Wash Buffer. The column was then placed into a new microfuge tube. The gDNA trapped in the cartridge was finally eluted with 200 µl of autoclaved water by centrifugation for 2 min at 14,000 rpm. The concentration of gDNA was quantified by spectrophotometry at the wavelength of 260 nm and stored at -20°C. The gDNA standard was generated by PCR amplification of serially diluted gDNA with known concentrations. The gDNA was subjected to 3-fold serial dilution with DEPC-treated water to obtain a set of external standards ranging from 1 ng to 27 ng.

6.3.6 Detection of RA in the embryo by RA-responsive cell line

To determine the endogenous concentration of RA, mouse and rat embryos (collected as described in sections 6.3.1 and 6.3.2 respectively) were dissected free of all extraembryonic membranes in ice-cold PBS in the dark under dim yellow light. Four embryos at somite range 19-21 from the same litter were pooled as one sample. It was gassed with nitrogen, sealed with parafilm and then wrapped in aluminum foil. It was snap frozen in liquid nitrogen and stored at -80°C for not more than 3 months. After all samples were collected, RA concentration in the sample was determined by

using the RA-responsive cell line according to the procedures as described in sections 5.3.1.2 and 2.4.

6.3.7 *In vitro* assay of RA degrading activity in embryonic tissues

Mouse embryos of different groups (as collected in section 6.3.1) were dissected in ice-cold L15 medium. Only embryos at 19-21 somite ranges were collected. The embryo was divided into 2 parts: the tail bud and the whole embryo (exclude tail bud) according to the landmark as described in section 4.3.4. Four tail buds of embryos from the same litter were pooled as one sample, whereas the whole embryo (exclude tail bud) was individually analyzed. The tissue sample collected in a microfuge tube was gassed with nitrogen, sealed with parafilm and then wrapped in aluminum foil. It was snap frozen in liquid nitrogen and stored at -80°C until use. To conduct the analysis after all samples were collected, the tail bud or the whole embryo (exclude tail bud) sample was first subjected to lysis by triturating with either a 10 µl pipette tip for the tail bud sample or 100 µl pipette tip for the whole embryo (exclude tail bud) sample respectively, followed by freezing in liquid nitrogen and then thawing in a water bath at 37°C for 1 min in each step. The RA degrading activity of the lysed sample was determined by the *in vitro* assay using the RA-responsive cell line as described in sections 4.3.5.2 and 2.4.

6.3.8 Measurement of RA in embryonic tissues after maternal treatment with RA by RA-responsive cell line

Diabetic and non-diabetic pregnant mice were treated with PHZ or

suspension vehicle as control according to section 6.3.1. On E9.0, pregnant mice received an intraperitoneal injection of 25 mg/kg body weight of RA. Embryos were dissected out in L15 medium in the dark under dim yellow light at 3 hr after RA treatment, which was previously found to be the time point where accumulation of RA in the embryo reached the peak level (Lee, 2008). Only embryos at 20-22 somite-stage were collected. After through washing with L15 medium, the embryo was divided into 2 parts: the tail bud and the whole embryo (exclude tail bud) according to the landmark as described in section 4.3.4. The tail bud and whole embryo (exclude tail bud) were individually collected in a microfuge tube. After removal of excess medium, it was gassed with nitrogen, sealed with parafilm and then wrapped in aluminum foil. It was snap frozen in liquid nitrogen and stored at -80°C for less than 3 months.

To conduct the analysis after all samples were collected, the single tail bud or whole embryo (exclude tail bud) was immersed in 300 µl of culture medium (refer to section 2.4.1 for composition of culture medium for RA-responsive cell line) for 20 hr (as tested in my previous study which showed the maximum release of RA into the medium) to allow the diffusion of RA from the sample into the medium. One hundred nanomolar of Cyp26 specific inhibitor R115866 was added to prevent degradation of RA by Cyp26 enzyme present in the sample. The sample was then centrifuged at 3,000 rpm for 10 min at room temperature to remove any large particles. All procedures were carried out in the dark under dim yellow light to prevent photo-degradation of RA. The concentration of RA in the medium was then determined by the RA-responsive cell line as described in section 2.4.

6.3.9 Analysis of different types of RA-induced malformations

Diabetic and non-diabetic pregnant mice were treated with PHZ or suspension vehicle as control according to section 6.3.1. On E9.0, mice were challenged by receiving an intraperitoneal injection of a teratogenic dose of 25 mg/kg body weight of RA. At E18, near-term fetuses were examined for the severity of caudal regression in terms of the ratio of TL to CRL (landmark for measuring TL and CRL in E18 fetus was illustrated in Figure 6.1). The incidence rate of other types of defects including cleft palate and renal malformations was determined as mentioned in section 4.3.7.1.

6.3.10 Statistical analysis

The maternal blood glucose level before and after treatment was compared by Paired Samples t-test. The blood glucose level between different groups was compared by Independent Samples t-test. Embryonic *Cyp26a1* expression level, endogenous RA concentration, *in vitro* RA degrading activity, RA concentration following maternal RA treatment and susceptibility to various types of RA-induced malformations between different groups were analyzed by one-way ANOVA followed by Bonferroni test. Correlation between glucose concentration and *Cyp26a1* expression level or endogenous RA concentration in rat embryos were analyzed by Pearson's Correlation. All statistical analyses were carried out using *SPSS* software (*SPSS*), with statistical significance level set at $p < 0.05$.

6.4. RESULTS

6.4.1 Reduction of maternal blood glucose levels in diabetic mice after PHZ treatment

Results of blood glucose levels before and after PHZ treatment in diabetic and non-diabetic pregnant mice were summarized in Table 6.1 and presented in Graph 6.1. Injection of vehicle alone (CON) did not affect maternal blood glucose levels in both diabetic and non-diabetic mice. Streptozotocin-induced diabetic mice showed a non-reversible increase in blood glucose levels at an average of 28 mmol/L. After 3 doses of PHZ injection, the blood glucose level of diabetic mice was significantly lowered by half ($p < 0.001$) to a non-diabetic level. In contrast, non-diabetic mice did not show any response to PHZ and maintained a normal blood glucose level.

Table 6.1 Comparison of maternal blood glucose levels before and after treatment with PHZ in mice under diabetic and non-diabetic pregnancy.

Maternal status	ND			SD		
Treatment groups	Before treatment	CON	PHZ	Before treatment	CON	PHZ
No. of mice	12	6	6	12	6	6
Blood glucose levels (mmol/L) ± SE	6.08 ± 0.12	5.88 ± 0.09	5.80 ± 0.09	28.07 ± 0.56	26.11 ± 1.06	13.36 ± 1.42
p value vs. ND (CON)	1.000	-	1.000	-	< 0.001*	< 0.001*
p value vs. SD (CON)	-	-	-	1.000	-	< 0.001*

* Statistically significant (data were analyzed by Independent Samples t-test)

6.4.2 Normalization of *Cyp26a1* expression in embryos of diabetic mice after maternal PHZ treatment

Expression levels of *Cyp26* relative to *β-actin* in embryos treated with PHZ or equivalent volume of vehicle were summarized in Table 6.2 and presented in Graph 6.2. Results of statistical analysis were reported in Table 6.3. *In situ* hybridization of *Cyp26a1* was shown in Figure 6.2. Similar to the finding in Chapter 3, results of real-time quantification confirmed that *Cyp26a1* was the predominant RA degrading enzyme that highly expressed in the tail bud region of the embryo, whereas *Cyp26b1* and *Cyp26c1* were only detectable at very low levels (Graph 6.2A), implying that RA level in the tail bud region was controlled by *Cyp26a1*. For animals treated with vehicle alone, *Cyp26a1* expression in the tail bud region of embryos in the diabetic group (Figure 6.2F) was found to be significantly down-regulated (p = 0.009) when compared with the non-diabetic group (Figure 6.2B). With reduced maternal blood glucose levels by injection of PHZ, the expression level of *Cyp26a1* in embryos of diabetic mice (Figure 6.2H) was significantly increased (p = 0.004) and restored to a level similar as the non-diabetic group (Figure 6.2B). Concomitant with unaltered maternal blood glucose levels, *Cyp26a1* expression did not show any variation in the non-diabetic group treated with PHZ (Figure 6.2D). Real-time quantification results showed that *Cyp26b1* and *Cyp26c1* did not show any significant changes in all 4 groups of embryos (Graph 6.2A), suggesting that normalization of *Cyp26a1* in embryos of diabetic mice treated with PHZ was highly specific.

In the anterior region of the embryo, the expression level of *Cyp26a1*, *Cyp26b1* and *Cyp26c1* was more comparable (Graph 6.2B). Similar to the tail bud region, in embryos of diabetic mice treated with vehicle only, there was significant

down-regulation (p = 0.001) of *Cyp26a1* in the anterior region (Figure 6.2E) in comparison to that in the non-diabetic group (Figure 6.2A). However, upon reduction of maternal blood glucose levels by PHZ, embryos of diabetic mice showed significant (p = 0.005) up-regulation of *Cyp26a1* expression in the anterior region (Figure 6.2G) to a level similar as the non-diabetic group (Figures 6.2A and 6.2C). For *Cyp26b1* and *Cyp26c1*, similar to the finding of the tail bud, no significant difference in expression levels was found in the rest of the embryo between non-diabetic and diabetic groups with or without PHZ treatment (Graph 6.2B), further supporting that normalization of *Cyp26a1* in embryos of PHZ-treated diabetic mice was specific.

Table 6.2 Expression levels of *Cyp26* relative to *β-actin* in tissues of E9.0 embryos of non-diabetic and diabetic mice with or without maternal PHZ treatment.

Tissue type	Tail bud			
Maternal status	ND		SD	
Treatment groups	CON	PHZ	CON	PHZ
No. of litters	5	5	5	5
No. of embryos	30	32	27	26
Sample size[#]	5	5	5	5
Relative expression levels of *Cyp26a1* ± SE	0.198 ± 0.009	0.194 ± 0.009	0.155 ± 0.008	0.203 ± 0.004
Relative expression levels of *Cyp26b1* ± SE	0.009 ± 0.003	0.006 ± 0.002	0.006 ± 0.002	0.006 ± 0.001
Relative expression levels of *Cyp26c1* ± SE	0.002 ± 0.001	0.002 ± 0.001	0.004 ± 0.005	0.002 ± 0.001
Tissue type	Whole embryo (exclude tail bud)			
Maternal status	ND		SD	
Treatment groups	CON	PHZ	CON	PHZ
Relative expression levels of *Cyp26a1* ± SE	0.0048 ± 0.0001	0.0044 ± 0.0002	0.0034 ± 0.0002	0.0045 ± 0.0002
Relative expression levels of *Cyp26b1* ± SE	0.0061 ± 0.0004	0.0066 ± 0.0007	0.0063 ± 0.0007	0.0070 ± 0.0006
Relative expression levels of *Cyp26c1* ± SE	0.0063 ± 0.0003	0.0069 ± 0.0005	0.0066 ± 0.0009	0.0066 ± 0.0007

[#] Refer to section 6.3.5 for definition of one sample

Table 6.3 Statistical analysis of relative expression levels of *Cyp26* between tissues of embryos of different groups using one-way ANOVA followed by Bonferroni test.

Groups for comparison	Tail bud			
	ND (CON) vs. ND (PHZ)	ND (CON) vs. SD (CON)	SD (CON) vs. SD (PHZ)	ND (CON) vs. SD (PHZ)
p value in comparing *Cyp26a1*	1.000	0.009*	0.004*	1.000
p value in comparing *Cyp26b1*	0.948	0.785	1.000	0.368
p value in comparing *Cyp26c1*	1.000	1.000	1.000	1.000
Groups for comparison	Whole embryo (exclude tail bud)			
	ND (CON) vs. ND (PHZ)	ND (CON) vs. SD (CON)	SD (CON) vs. SD (PHZ)	ND (CON) vs. SD (PHZ)
p value in comparing *Cyp26a1*	1.000	0.001*	0.005*	1.000
p value in comparing *Cyp26b1*	1.000	1.000	0.608	0.258
p value in comparing *Cyp26c1*	1.000	1.000	1.000	1.000

* Statistically significant

6.4.3 Normalization of endogenous RA levels in embryos of diabetic mice after maternal PHZ treatment

After confirming that *Cyp26a1* could be normalized in embryos of diabetic mice by lowering maternal blood glucose to non-diabetic levels, I further examined the endogenous RA level in embryos. The endogenous RA level in embryos of different groups was summarized in Table 6.4 and presented in Graph 6.3. Results of

statistical analysis were shown in Table 6.5. Results clearly showed that in treatment with vehicle alone, the endogenous RA level in embryos under diabetic pregnancy remained significantly ($p = 0.005$) lower than embryos of non-diabetic pregnancy by 33%. For embryos in diabetic pregnancy with PHZ treatment, the endogenous RA level increased significantly ($p = 0.037$) to such an extent that there was no longer any significant difference from embryos of the control group in non-diabetic pregnancy.

Table 6.4 Endogenous RA levels in E9.0 embryos of non-diabetic and diabetic mice with or without maternal PHZ treatment.

Maternal status	ND		SD	
Treatment groups	CON	PHZ	CON	PHZ
No. of litters	4	4	5	5
No. of embryos	30	30	30	30
Sample size[#]	6	6	6	6
Amount of RA per embryo (pg) ± SE	0.446 ± 0.035	0.456 ± 0.033	0.300* ± 0.015	0.412[#] ± 0.018

[#] Refer to section 6.3.6 for definition of one sample

Table 6.5 Statistical analysis of endogenous RA levels between embryos of different groups using one-way ANOVA followed by Bonferroni test.

Groups for comparison	ND (CON) vs. ND (PHZ)	ND (CON) vs. SD (CON)	SD (CON) vs. SD (PHZ)	ND (CON) vs. SD (PHZ)
p value in comparing endogenous RA levels	1.000	0.005*	0.037*	1.000

* Statistically significant

6.4.4 Normalization of *in vitro* RA degrading activity in embryos of diabetic mice after maternal PHZ treatment

The *in vitro* RA degrading activity in the tail bud and the whole embryo (exclude tail bud) was summarized in Table 6.6 and Graph 6.4. Results of statistical analysis were shown in Table 6.7. As shown previously, Cyp26A1 is the predominant RA degrading enzyme in the tail bud region (Graph 6.2A), therefore, any RA degrading activity detected in the tail bud should be contributed mainly by Cyp26A1. The *in vitro* RA degrading activity in the tail bud tissue (Graph 6.4A) was found to be significantly (p = 0.002) diminished in the diabetic group treated with vehicle only when compared with the non-diabetic group. Upon lowering of blood glucose levels in diabetic mice with PHZ, the *in vitro* RA degrading activity in the tail bud tissue was significantly (p = 0.006) increased to a level similar to that of the control non-diabetic group.

For the whole embryo excluding the tail bud (Graph 6.4B), the situation was more complicated since *Cyp26a1*, *Cyp26b1* and *Cyp26c1* co-expressed in the anterior region of the embryo as shown in Chapter 3 (Figures 3.1, 3.2 and 3.3). Yet, similar trend as the finding of the tail bud tissue was observed. Besides, the *in vitro* RA degrading activity in the whole embryo (exclude tail bud) was much faster, with about 80% of RA in the medium being degraded as compared with about 60% in the tail bud tissue. Diabetic group treated with vehicle only showed significantly (p = 0.009) lower *in vitro* RA degrading activity than the non-diabetic group. However, there was a significant (p = 0.027) increase in the diabetic group after PHZ treatment, such that it was normalized to a level similar as the control non-diabetic group. These results were complementary with the finding of *Cyp26a1* expression, i.e. once the *Cyp26a1* expression level was normalized, there was a corresponding

normalization of the *in vitro* RA degrading activity.

Table 6.6 ***In vitro*** **RA degrading activity in tissues of E9.0 embryos of non-diabetic and diabetic mice with or without maternal PHZ treatment.**

Maternal status	ND		SD	
Treatment groups	CON	PHZ	CON	PHZ
No. of litters	4	4	3	3
No. of embryos	24	24	20	20
Sample size for tail bud[#]	6	6	5	5
Sample size for whole embryo (exclude tail bud)[#]	18	18	18	18
% RA in medium being degraded by tail bud sample ± SE	67 ± 3	62 ± 4	39 ± 2	59 ± 4
% RA in medium being degraded by whole embryo (exclude tail bud) sample ± SE	78 ± 4	78 ± 3	61 ± 4	76 ± 3

[#] Refer to section 6.3.7 for definition of one sample

Table 6.7 **Statistical analysis of** ***in vitro*** **RA degrading activity between tissues of embryos of different groups using one-way ANOVA followed by Bonferroni test.**

Groups for comparison	ND (CON) vs. ND (PHZ)	ND (CON) vs. SD (CON)	SD (CON) vs. SD (PHZ)	ND (CON) vs. SD (PHZ)
p value in comparing % RA in medium being degraded by tail bud	1.000	0.002*	0.006*	1.000
p value in comparing % RA in medium being degraded by whole embryo (exclude tail bud)	1.000	0.009*	0.027*	1.000

* Statistically significant

6.4.5 Normalization of RA levels in embryos of PHZ-treated diabetic mice at 3 hr after maternal injection of RA

The amount of RA present in the tissues of embryos of different groups at 3 hr after maternal injection of 25 mg/kg RA on E9.0 was summarized in Table 6.8 and presented in Graph 6.5. Results of statistical analysis were shown in Table 6.9. Embryos in diabetic pregnancy treated with vehicle only had a significantly higher amount of RA than embryos of non-diabetic group at 3 hr after treatment with 25 mg/kg RA in both the tail bud (p = 0.03; Graph 6.5A) and the whole embryo (exclude tail bud) (p = 0.006; Graph 6.5B), suggesting that embryos of diabetic pregnancy were exposed to a higher effective concentration of RA after maternal administration of an exogenous dose of RA. With normalization of *Cyp26a1* expression by reduction of blood glucose level using PHZ, the amount of RA present in embryonic tissues of diabetic pregnancy was significantly [p = 0.033 for tail bud; $p < 0.001$ for whole embryo (exclude tail bud)] reduced to a level similar to the control non-diabetic group. This result agreed with the finding on the *in vitro* RA degrading activity, supporting the notion that normalization of *Cyp26a1* expression and *in vitro* RA degrading activity by reducing maternal blood glucose levels in diabetic pregnancy could offer a protective effect to defend against aberrant build up of RA in embryonic tissues.

Table 6.8 RA levels in the tissues of embryos of PHZ-treated or control diabetic and non-diabetic mice at 3 hr after maternal injection with 25 mg/kg RA on E9.0.

Maternal status	ND		SD	
Treatment groups	CON	PHZ	CON	PHZ
No. of litters	2	2	3	3
No. of embryos	11	12	12	12
Sample size[#]	11	12	12	12
Amount of RA in tail bud (nM) ± SE	0.28 ± 0.06	0.26 ± 0.03	0.52 ± 0.07	0.28 ± 0.07
Amount of RA in whole embryo (exclude tail bud) (nM) ± SE	121 ± 9	117 ± 7	166 ± 11	94 ± 8

[#] Refer to section 6.3.8 for definition of one sample

Table 6.9 Statistical analysis on the amount of RA between tissues of embryos of different groups using one-way ANOVA followed by Bonferroni test.

Groups for comparison	ND (CON) vs. ND (PHZ)	ND (CON) vs. SD (CON)	SD (CON) vs. SD (PHZ)	ND (CON) vs. SD (PHZ)
p value in comparing RA in tail bud	1.000	0.030*	0.033*	1.000
p value in comparing RA in whole embryo (exclude tail bud)	1.000	0.006*	< 0.001*	0.247

* Statistically significant

6.4.6 Reduction of susceptibility to various types of RA-induced malformations after maternal treatment with PHZ

To further investigate whether prior treatment with PHZ to prevent aberrant build up of RA in embryos of diabetic mice could indeed reduce embryos' susceptibility to RA teratogenesis, pregnant mice were challenged with a teratogenic dose of 25 mg/kg RA on E9.0 to induce different types of malformations, including caudal regression, cleft palate and renal malformations.

The incidence rate, expressed in terms of the % of embryos per litter with the malformation, was summarized in Table 6.10 and presented in Graph 6.6. Results of statistical analysis were shown in Table 6.11. Embryos of control diabetic group treated with vehicle had significantly reduced TL/CRL ratio ($p < 0.001$; Graph 6.6A), that means more severe caudal regression, and showed higher incidence rates of cleft palate ($p < 0.001$; Graph 6.6B) and renal malformations ($p = 0.001$; Graph 6.6C) in comparison to embryos of control non-diabetic group. In contrast, lowering of maternal blood glucose levels by PHZ treatment could significantly ($p < 0.001$) ameliorate the severity of caudal regression, as shown by an increase in the TL/CRL ratio, and reduced the incidence rates of cleft palate ($p < 0.001$) and renal malformations ($p = 0.022$). Together, results of this part showed that the susceptibility of *Cyp26a1*-normalized embryos of diabetic mice to various types of malformations was significantly reduced to such an extent that the increase in embryonic susceptibility to RA teratogenicity caused by diabetic pregnancy was totally abolished.

Table 6.10 Susceptibility of fetuses of non-diabetic and diabetic mice with or without maternal PHZ treatment to various types of RA-induced malformations.

Maternal status	ND		SD	
Treatment groups	CON	PHZ	CON	PHZ
No. of litters	8	8	7	7
No. of fetuses	75	94	52	64
TL/CRL ratio ± SE	0.19 ± 0.01	0.17 ± 0.01	0.06 ± 0.01	0.17 ± 0.01
% of fetuses per litter with cleft palate ± SE	33 ± 5	31 ± 4	72 ± 6	28 ± 6
% of fetuses per litter with renal malformations ± SE	19 ± 5	14 ± 4	50 ± 7	27 ± 3

Table 6.11 Statistical analysis on susceptibility to various types of RA-induced malformations between fetuses of different groups using one-way ANOVA followed by Bonferroni test.

Groups for comparison	ND (CON) vs. ND (PHZ)	ND (CON) vs. SD (CON)	SD (CON) vs. SD (PHZ)	ND (CON) vs. SD (PHZ)
p value in comparing TL/CRL ratio	1.000	< 0.001*	< 0.001*	1.000
p value in comparing incidence rate of cleft palate	1.000	< 0.001*	< 0.001*	1.000
p value in comparing incidence rate of renal malformations	1.000	0.001*	0.022*	1.000

* Statistically significant

6.4.7 Dose-dependent down-regulation of *Cyp26a1* expression by glucose

To further determine if glucose could regulate *Cyp26a1* expression in a dose-dependent manner, whole embryo culture, which allowed accurate control of glucose concentrations in the culture medium, was employed. The expression level of *Cyp26a1*, *b1* and *c1* in rat embryos after culturing in medium supplemented with varying concentrations of D-glucose for 24 and 48 hr was summarized in Table 6.12 and Table 6.13 and presented in Graph 6.7 and Graph 6.8 respectively. *In situ* expression patterns of *Cyp26a1* were shown in Figures 6.3 and 6.4 respectively. After *in vitro* culture for 24 hr from head-fold stage, rat embryos in the control group had developed normally into early somite stage. Results of *in situ* hybridization study showed that *Cyp26a1* was normally expressed in the posterior neural plate and the tail bud mesoderm in the caudal region (Figures 6.3A and 6.3B). There was weak expression in the anterior region near the optic primordium (Figure 6.3A). For embryos cultured in medium supplemented with 2 mg/ml D-glucose, reduction in *Cyp26a1* expression was observed in both the tail bud region and in the anterior domain (Figures 6.3B and 6.3D). For embryos cultured in 3 mg/ml D-glucose, *Cyp26a1* expression in the posterior neural plate appeared to have diminished, and *Cyp26a1* expression was shifted to more ventral part at the caudal limit (Figures 6.3E and 6.3F). In 4 mg/ml D-glucose group, the signal intensity of *Cyp26a1* was further reduced (Figures 6.3G and 6.3H).

After cultured for 48 hr, embryos in the control group showed normal development. *Cyp26a1* was highly expressed in the tail bud region (Figures 6.4A and 6.4B). Embryos cultured in medium supplemented with 2 mg/ml D-glucose showed minor caudal regression with diminished *Cyp26a1* expression (Figures 6.4C and 6.4D). For embryos cultured in medium supplemented with 3 mg/ml (Figures

6.4E and 6.4F) and 4 mg/ml D-glucose (Figures 6.4G and 6.4H), there was an increase in severity of caudal regression as the concentration of D-glucose increased. The signal intensity of *Cyp26a1* also showed further reduction.

Quantification of *Cyp26a1* expression levels by real-time RT-PCR showed that indeed there was significant negative linear correlation between the concentration of D-glucose supplemented in the medium and *Cyp26a1* expression level in the tail bud (Graph 6.7A, $r = -0.911$ and $p < 0.001$ for 24 hr; Graph 6.8A, $r = -0.931$ and $p < 0.001$ for 48 hr) and in the whole embryo (exclude tail bud) (Graph 6.7B, $r = -0.693$ and $p < 0.001$ for 24 hr; Graph 6.8B, $r = -0.791$ and $p < 0.001$ for 48 hr). These results implied that when the concentration of D-glucose increased, there was a corresponding linear decrease in *Cyp26a1* expression. However, no correlation was found between *Cyp26b1* and *Cyp26c1* expression with D-glucose concentration, which further supported that the effect of D-glucose was specific to *Cyp26a1*.

Table 6.12 Expression levels of *Cyp26a1* relative to *β-actin* in rat embryos cultured in medium supplemented with varying concentrations of D-glucose for 24 hr.

Tissue type	Tail bud (24 hr)			
D-Glucose concentrations	CON	2 mg/ml	3 mg/ml	4 mg/ml
No. of embryos	15	15	15	15
Sample size[#]	5	5	5	5
Relative expression levels of *Cyp26a1* ± SE	0.3463 ± 0.0107	0.2945 ± 0.0100	0.2529 ± 0.0084	0.1813 ± 0.0184
Pearson's correlation coefficient (*r*)	-0.911			
p value of Pearson's correlation	< 0.001*			
Relative expression levels of *Cyp26b1* ± SE	0.0015 ± 0.0001	0.0016 ± 0.0002	0.0019 ± 0.0002	0.0013 ± 0.0003
Pearson's correlation coefficient (*r*)	-0.322			
p value of Pearson's correlation	0.224			
Relative expression levels of *Cyp26c1* ± SE	0.0085 ± 0.0029	0.0074 ± 0.0020	0.0069 ± 0.0066	0.0059 ± 0.0029
Pearson's correlation coefficient (*r*)	+0.288			
p value of Pearson's correlation	0.349			
Tissue type	Whole embryo (exclude tail bud) 24 hr			
D-Glucose concentrations	CON	2 mg/ml	3 mg/ml	4 mg/ml
Relative expression levels of *Cyp26a1* ± SE	0.0059 ± 0.0005	0.0049 ± 0.0003	0.0036 ± 0.0003	0.0028 ± 0.0003
Pearson's correlation coefficient (*r*)	-0.693			
p value of Pearson's correlation	< 0.001*			
Relative expression levels of *Cyp26b1* ± SE	0.0034 ± 0.0003	0.0034 ± 0.0001	0.0033 ± 0.0002	0.0039 ± 0.0003
Pearson's correlation coefficient (*r*)	-0.068			
p value of Pearson's correlation	0.773			
Relative expression levels of *Cyp26c1* ± SE	0.0053 ± 0.0005	0.0051 ± 0.0013	0.0056 ± 0.0004	0.0060 ± 0.0005
Pearson's correlation coefficient (*r*)	+0.417			
p value of Pearson's correlation	0.085			

[#] Refer to section 6.3.2 for definition of one sample

* Statistically significant

Table 6.13 Expression levels of *Cyp26a1* relative to *β-actin* in rat embryos cultured in medium supplemented with varying concentrations of D-glucose for 48 hr.

Tissue type	Tail bud (48 hr)			
D-Glucose concentrations	CON	2 mg/ml	3 mg/ml	4 mg/ml
No. of embryos	15	15	15	15
Sample size#	5	5	5	5
Relative expression levels of *Cyp26a1* ± SE	0.1063 ± 0.0083	0.0833 ± 0.0033	0.0581 ± 0.0038	0.0391 ± 0.0036
Pearson's correlation coefficient (*r*)	-0.931			
p value of Pearson correlation	< 0.001*			
Relative expression levels of *Cyp26b1* ± SE	0.0019 ± 0.0004	0.0021 ± 0.0005	0.0017 ± 0.0006	0.0016 ± 0.0004
Pearson's correlation coefficient (*r*)	-0.173			
p value of Pearson's correlation	0.508			
Relative expression levels of *Cyp26c1* ± SE	0.0031 ± 0.0018	0.0031 ± 0.0013	0.0030 ± 0.0011	0.0036 ± 0.0012
Pearson's correlation coefficient (*r*)	+0.189			
p value of Pearson's correlation	0.500			
Tissue type	Whole embryo (exclude tail bud) 48 hr			
D-Glucose concentrations	CON	2 mg/ml	3 mg/ml	4 mg/ml
Relative expression levels of *Cyp26a1* ± SE	0.0047 ± 0.0001	0.0044 ± 0.0002	0.0035 ± 0.0002	0.0033 ± 0.0002
Pearson's correlation coefficient (*r*)	-0.791			
p value of Pearson's correlation	< 0.001*			
Relative expression levels of *Cyp26b1* ± SE	0.0047 ± 0.0005	0.0045 ± 0.0002	0.0046 ± 0.0003	0.0049 ± 0.0005
Pearson's correlation coefficient (*r*)	+0.069			
p value of Pearson's correlation	0.773			
Relative expression levels of *Cyp26c1* ± SE	0.0042 ± 0.0006	0.0042 ± 0.0004	0.0048 ± 0.0005	0.0059 ± 0.0003
Pearson's correlation coefficient (*r*)	+0.317			
p value of Pearson's correlation	0.185			

Refer to section 6.3.2 for definition of one sample

* Statistically significant

6.4.8 Dose-dependent reduction of endogenous RA level in rat embryos by glucose

The endogenous RA level in rat embryos cultured in varying concentrations of D-glucose for 48 hr was summarized in Table 6.14 and presented in Graph 6.9. Results showed that similar to the finding on the effect of D-glucose on *Cyp26a1* expression levels, there was a significant inverse correlation between glucose concentration in the medium and endogenous RA level in the embryo by using Pearson's correlation (r = -0.700, p < 0.001), such that the higher the glucose concentration, the lower the endogenous RA level in the embryo.

Table 6.14 Endogenous RA levels in rat embryos that had been cultured in medium supplemented with varying concentrations of D-glucose for 48 hr.

D-glucose concentrations	CON	2 mg/ml	3 mg/ml	4 mg/ml
No. of embryos	28	28	28	28
Sample size[#]	7	7	7	7
Amount of RA per embryo (pg) ± SE	0.507 ± 0.030	0.366 ± 0.045	0.300 ± 0.045	0.234 ± 0.048
Pearson's correlation coefficient (r)	-0.700			
p value of Pearson's correlation	< 0.001*			

[#] Refer to section 6.3.6 for definition of one sample

* Statistically significant

6.5. DISCUSSION

This chapter aimed to investigate whether elevated blood glucose was the critical factor by which maternal diabetes disturbed the expression of the RA catabolizing gene *Cyp26a1* in embryos, leading to increased risk of birth defects. By ameliorating the hyperglycemic level in diabetic mice using PHZ, *Cyp26a1* expression in the embryo was up-regulated and normalized to a level similar to that of embryos of non-diabetic mice. Such normalization of *Cyp26a1* expression could successfully increase the RA degrading activity in the embryo, resulting in a reduction of susceptibility to different types of RA-induced malformations that showed a higher risk in diabetic pregnancy. As a control, non-diabetic pregnant animals treated with PHZ did not show any changes in the maternal blood glucose level, or any changes in embryonic *Cyp26a1* expression and RA degrading activity, supporting that glucose, but not PHZ, was the factor regulating *Cyp26a1*expression. Furthermore, rat embryos cultured in serum containing different concentrations of D-glucose, at levels similar to those occurring in diabetic pregnancy, caused a dose-dependent inhibition on the expression of *Cyp26a1*. In both *in vivo* and *in vitro* experiments, expressions of *Cyp26b1* and *Cyp26c1* were unaffected. These results demonstrate that the expression of *Cyp26a1*, but not *Cyp26b1* and *Cyp26c1*, in the embryo is correlated with glucose concentration. Taken together, findings in this chapter have provided evidences to support that hyperglycemia is the critical factor in the maternal diabetic milieu leading to increase in embryo's susceptibility to various malformations, via specific down-regulation of *Cyp26a1* and disruption of RA homeostasis.

Real-time quantitative RT-PCR study shows that *Cyp26a1* is the subtype of *Cyp26* gene family predominantly expressed in the tail bud region of the embryo.

Specific dysregulation of *Cyp26a1* in diabetic pregnancy will therefore render the caudal region highly sensitive to ectopic RA. However, in the anterior region of the embryo, *Cyp26a1* is co-expressed with *Cyp26c1* (Uehara et al., 2007), together with the presence of *Cyp26b1* (MacLean et al., 2001). Since *Cyp26b1* and *Cyp26c1* may also play a role in protecting anterior tissues against RA, thus, in comparing the RA-degrading activity in the whole embryo excluding the tail bud, the difference between diabetic and non-diabetic groups might be masked by these 2 subtypes. Indeed, results showed that while there was about 40% reduction in the *in vitro* RA degrading activity in the tail bud tissue of embryos of diabetic mice in comparison to that of embryos of non-diabetic mice (Graph 6.4A), only 20% reduction was found in the whole embryo excluding the tail bud (Graph 6.4B).

In this chapter, it was demonstrated that reduction of glucose levels in the diabetic milieu restored the low RA level in the embryo to normal, concomitantly, *Cyp26a1* expression was normalized. These results may suggest that the primary effect of diabetes is to decrease RA levels while the change in *Cyp26a1* expression is secondary. As discussed in Chapter 4, RA deficiency can also lead to birth defects, therefore, the primary effect of reduction in RA synthesis (by Raldh1, Raldh2 and Raldh3) (Chan, 2011) and RA levels may also be one of the causes accounting for the increased risk of malformations in diabetes. Thus, the rescue effect of subteratogenic dose of RA described in Chapter 5 may be mediated via correcting both RA deficiency and reduced *Cyp26a1* expression levels rather than just affecting *Cyp26a1*.

It has been reported that embryos at early somitic stage or early organogenesis have no vascular system to deliver oxygen. The developing embryo is relatively anaerobic and glucose is the major source of energy during early

embryogenesis. Any interruption in glucose utilization may initiate a cascade of events that leads to congenital defects (Shepard et al., 1997). Some experiments show that organogenesis is the stage that utilizes the highest amount of glucose (Shepard et al., 1997). In rat embryos, glucose transporters (Glut) 1 and 3 have been identified. Both of them are expressed in the amnion and yolk sac. In addition, Glut 1 is localized in the neuroepithelium while Glut 3 is expressed in the endoderm, suggesting that glucose is essential for normal development (Takao et al., 1993; Trocino et al., 1994). How does glucose regulate *Cyp26a1*? In Chapter 5, I have demonstrated that the expression of *Cyp26a1* could be controlled by endogenous RA levels, possibly via direct binding to the RAREs in the promoter region of the *Cyp26a1* gene (Loudig et al., 2005). In this chapter, I have further showed that glucose could also regulate *Cyp26a1* in a dose-dependent manner. Moreover, results of this chapter also showed that other than *Cyp26a1* expression, reduction in maternal blood glucose levels could normalize endogenous RA levels in embryos of diabetic mice, and D-glucose could induce dose-dependent reduction of endogenous RA levels in rat embryos, suggesting a link between glucose, endogenous RA and *Cyp26a1* expression.

Glucose is well-known in inducing oxidative stress. It has been shown that maternal diabetes induced by streptozotocin or transient induction of hyperglycemia by injection of glucose to head-fold stage mouse embryos could lead to hypoxia (Li et al., 2005). It is because O_2 delivery is limited at this stage of development, and excess glucose metabolism can accelerate the rate of O_2 consumption, thereby exacerbating the hypoxic state (Li et al., 2005). Hypoxia appears to be the result of increased production of mitochondrial superoxide, as indicated by assay of lipid peroxidation, reduced glutathione and H_2O_2, suggesting that excessive hypoxia may

contribute to oxidative stress. There is much evidence implicating oxidative stress in the pathogenesis of diabetic embryopathy (Eriksson & Siman, 1996; Wentzel et al., 1997; Baynes & Thorpe, 1999; Chang et al., 2003). Some evidences for mechanistic links between hyperglycemia, oxidative stress and RA signaling have been shown in the cortical neurons in diabetic rats (Guleria et al., 2006). It has been reported that exposing neurons to elevated glucose level *in vitro* could induce oxidative stress, which in turn inhibited the activation of a RA-induced gene, *Rac1*, and differentiation of cortical neurons. In contrast, application of RA at physiological levels could in turn reverse the oxidative stress and minimized the apoptotic effect on neurons generated by hyperglycemia. Some studies have reported that oxidative stress can suppress RA synthesis. Inhibition of embryonic RA synthesis by aldehydes of lipid peroxidation was previously demonstrated (Chen & Juchau, 1998). Aldehydes of lipid peroxidation, including trans-2-nonenal, nonyl aldehyde and 4-hydroxy-2-nonenal, could inhibit all-*trans* RA synthesis from retinal. However, addition of reduced glutathione that conjugated with aldehydes could prevent the inhibition, suggesting that these aldehydes may compete with the RA synthesizing enzyme Raldh, resulting in a mutual inhibition between oxidations of retinal and other aldehydes, leading to a deficiency of endogenous RA in the embryo (Chen & Juchau, 1998). In Chapter 5, I have shown that endogenous RA level was significantly reduced in embryos of diabetic mice. In this chapter, I have further demonstrated that elevated glucose in maternal diabetes or *in vitro* addition of glucose could affect endogenous RA levels in the embryo. Taken together, it is tempting to suggest that hyperglycemia in maternal diabetes will increase aldehydes of lipid peroxidation, which will inhibit RA synthesis and thus leads to an overall reduction in the endogenous level of RA in the embryo. As *Cyp26a1* expression in

the embryo can be regulated by RA, a reduction in RA level in the embryo of diabetic pregnancy may lead to down-regulation of *Cyp26a1* gene. Tissues that express *Cyp26a1* will therefore have reduced ability to clear away RA and become more susceptible to malformations caused by ectopic RA signaling. Take caudal regression, the most characteristic anomaly associated with diabetic pregnancy as an example. During embryogenesis, RA distribution is tightly controlled by the combined actions of Raldh family of RA synthesizing enzymes and the Cyp26 family of RA catabolizing enzymes. Both types of enzymes are expressed in a dynamic and spatially restricted manner, such that they are often expressed in complementary but non-overlapping domains. In the caudal region, RA synthesized by Raldh2 in the somitic mesoderm can diffuse posteriorly to the tail bud region. *Cyp26a1*, which expresses specifically in the tail bud region, will catabolically remove the RA to prevent ectopic RA signaling that has been shown to cause apoptosis of tail bud cells and lead to caudal regression (Shum et al., 1999). Thus, in cases of diabetic pregnancy, although there is reduced RA synthesis in the somitic mesoderm, down-regulation of *Cyp26a1* in the tail bud region may also result in reduced ability to clear away RA diffused from anterior tissues, making this region more prone to the deleterious effect of aberrant levels of RA, thus increasing the risk of caudal regression. This mechanism may similarly occur in other tissues where *Cyp26a1* is expressed, resulting in increased risk of malformations such as exencephaly, spina bifida and cleft palate.

Chapter 7

Conclusion and Future Perspectives

7.1 CONCLUSION AND FUTURE PERSPECTIVES

In Chapter 1, I have mentioned that RA- and maternal diabetes-induced malformations share similar phenotypes, suggesting that some common pathogenic mechanisms may exist between RA and maternal diabetes in inducing birth defects. Our laboratory has previously found that the expression of the RA catabolizing enzyme, *Cyp26a1*, is significantly down-regulated in the mouse embryo under maternal diabetes (Leung, 2005). This leads to our speculation that alteration of RA degradation may be one of the pathogenic mechanisms in diabetic embryopathy. The aim of this thesis was to test the hypothesis that alteration of RA catabolism would increase the embryo's susceptibility to different anomalies commonly associated with diabetic pregnancy and also to decipher the underlying mechanism for the alteration in RA catabolism.

To begin with, in Chapter 3, I have conducted a detailed investigation on the mRNA expression of the major RA degrading enzymes in the embryo, *Cyp26*, which have 3 subtypes including *Cyp26a1*, *Cyp26b1* and *Cyp26c1*. Results showed that *Cyp26a1* was the only subtype found to be altered in embryos under diabetic pregnancy, while the expression of the other two subtypes, *Cyp26b1* and *Cyp26c1*, was not affected. Besides, the up-regulation of *Cyp26a1* upon exposure to exogenously applied RA in the diabetic group was found to be significantly less than the non-diabetic group. These results suggest that alteration of RA catabolism via dysregulation of *Cyp26a1* expression may be one of the pathogenic mechanisms of diabetic embryopathy.

To follow on, in Chapter 4, I have studied the relationship between maternal diabetes, *Cyp26a1* expression level and RA degrading activity in increasing the susceptibility of the embryo to different types of RA-induced malformations. This was achieved by comparing the response of *Cyp26a1*$^{+/-}$ mutant embryos with their *Cyp26a1*$^{+/+}$ wild-type littermates to RA teratogenicity under diabetic and non-diabetic pregnancies. Results showed that *Cyp26a1*$^{+/-}$ heterozygous embryos in diabetic pregnancy had the lowest expression level of *Cyp26a1*, whereas *Cyp26a1*$^{+/+}$ embryos in non-diabetic pregnancy had the highest. Concomitant with exhibiting the lowest expression level of *Cyp26a1*, embryonic tissues of *Cyp26a1*$^{+/-}$ embryos of diabetic mice demonstrated the lowest RA degrading activity and developed the highest incidence rate of malformations. These results support a primary role of *Cyp26a1* in diabetic embryopathy.

Although results of Chapter 4 have provided evidences that significant down-regulation of *Cyp26a1* in the embryo is directly involved in increasing the risk of birth defects in diabetic pregnancy, the underlying mechanism of how maternal diabetes affects the expression level of *Cyp26a1* in the embryo is still a question. In Chapter 5, I have focused on addressing this question. Since *Cyp26a1* has two RAREs (Yamamoto *et al.*, 2000; Wang *et al.*, 2002) and thus can be positively regulated by the RA level, I started the study by examining the endogenous RA level of the embryo and demonstrated that indeed, embryos of diabetic pregnancy had significant reduction in RA levels. However, low dose of RA supplementation (0.625 mg/kg body weight) could normalize *Cyp26a1* expression level in embryos of diabetic pregnancy. Concomitantly, there was reduction in the severity of different types of malformations, including caudal regression, cleft palate, renal malformations, spina bifida and exencephaly, when embryos were challenged with a

teratogenic dose of RA. Taken together, these findings support the hypothesis that subnormal level of RA may down-regulate *Cyp26a1* expression in the embryo, but maternal supplementation with a low dose of RA to restore embryonic RA level can normalize *Cyp26a1* expression, thereby reducing the risk of birth defects.

Besides, our laboratory has previously shown that embryos that were made transiently hyperglycemic by repeated glucose injections exhibited an increased susceptibility to caudal regression upon treatment with RA (Leung et al., 2004). On the other hand, normalization of blood glucose levels in diabetic mice by PHZ could in turn reduce the susceptibility (Leung et al., 2004). These results suggest that hyperglycemia and diabetes may act via similar pathogenic pathways to affect the embryo. Hence, in Chapter 6, I have investigated whether elevated blood glucose is the critical factor by which maternal diabetes affects *Cyp26a1* expression First of all, by lowering the blood glucose level in diabetic mice using PHZ, I found that *Cyp26a1* expression in embryos was normalized to a level similar to that of non-diabetic mice, and such normalization of expression could increase the RA degrading activity in the embryo, causing reduction in the risk of different types of RA-induced malformations. Moreover, culturing rat embryos in serum containing different concentrations of D-glucose could cause a dose-dependent inhibition on the expression level of *Cyp26a1*, demonstrating that *Cyp26a1* expression level in the embryo is correlated with glucose concentration. Results presented in this chapter provide experimental evidences to support that hyperglycemia is the critical factor leading to increased susceptibility of the embryo to various types of malformations via down-regulation of *Cyp26a1* and thus disruption of RA homeostasis. However, the following two questions remain unsolved in this thesis.

Question 1

In Chapter 5, I have shown that the serum retinol level is significantly reduced in maternal circulation of diabetic pregnancy, which may account for the significant reduction in the endogenous level of RA found in the embryo, thereby causing down-regulation of *Cyp26a1*, as expression of *Cyp26a1* has been shown to be regulated by RA/retinol levels (Zhang et al., 2010). However, a direct relationship between maternal retinol level and embryonic RA level remains to be established. To further test the hypothesis, it is possible to make use of fenretinide, a drug which can lower plasma retinol and RBP4 levels (Formelli et al., 1989; Smith et al., 1992; Schaffer et al., 1993). It has been shown that oral feeding of 5 mg/kg body weight of fenretinide to rat could induce severe retinol deficiency after 12 hr (Schaffer et al., 1993). Using this method, retinol-deficient serum can be obtained for *in vitro* whole embryo culture. Culturing rodent embryos in retinol-deficient serum can be a good method to test the effect of retinol deficiency on embryo development, embryonic endogenous RA levels and also gene expressions. Furthermore, we can investigate the effect of maternal retinol deficiency using an *in vivo* approach. It may be possible to prolong retinol deficiency for 2 days in pregnant rodents, by multi-dosing of 5 mg/kg of fenretinide at 12-hr interval, and then examined the effect on embryo development, endogenous RA levels and gene expressions. The expression of different retinoid binding proteins, such as cellular retinol binding proteins and cellular retinoic acid binding proteins, which regulate the availability of retinol and RA to the embryo, can also be examined.

Question 2

In Chapter 6, the underlying mechanism of how glucose reduces endogenous RA levels in the embryo remains to be determined. I have previously mentioned that glucose-induced oxidative stress is the cause of many types of congenital malformations in diabetic pregnancy (Eriksson et al., 1990). Animal studies have shown that *in vivo* or *in vitro* supplementation with free radical scavenging enzymes such as copper zinc superoxide dismutase, and antioxidants such as butylated hydroxytoluene, vitamin C and vitamin E, can rescue embryos in diabetic or hyperglycemic conditions from developing malformations (Eriksson & Borg, 1991; Hagay et al., 1995; Siman & Eriksson, 1997a; Siman & Eriksson, 1997b), suggesting that excess oxidative stress plays an important role in diabetic embryopathy. Besides, glucose-generated lipid peroxidation produces different aldehydes in diabetes, which has been reported to inhibit RA synthesis in embryonic tissues (Chen & Juchau, 1998). It is therefore hypothesized that elevation of glucose levels under diabetes may generate different aldehydes, which inhibit RA synthesis and thus affect the RA signaling pathway. Our laboratory has previously shown that the expression level and activity of RA synthesizing enzyme *Raldh2* was significantly reduced (Chan, 2011). These findings therefore lend support to my hypothesis. To prove that there is a direct relationship between oxidative stress, RA synthesis and *Cyp26a1* expression in embryos of diabetic pregnancy, diabetic pregnant mice can be administered with antioxidants (Eriksson & Siman, 1996; Siman & Eriksson, 1997a; Siman & Eriksson, 1997b). If *Cyp26a1* expression is acting downstream of oxidative stress, it is envisaged that alleviation of oxidative stress should normalize endogenous RA and *Cyp26a1* expression levels in embryos of diabetic mice.

Question 3

In this thesis, although I have provided evidence that dysregulation of *Cyp26a1* increases embryo's susceptibility to various types of birth defects attributed to aberrant RA levels, the down-stream effectors involved in causing these malformations in diabetic pregnancy are yet to be investigated. Moreover, If reduction in endogenous RA levels and down-regulation of *Cyp26a1* are the pathogenic mechanisms of diabetic pregnancy, disrupted endogenous RA levels may affect various RA-responsive genes, particularly those with RARE. Thus, the expression of genes that are known to be affected by RA, e.g. *Shh*, *Pax3*, *Hb9*, *BMP4* and *Cdx1*, should be compared between embryos of diabetic and non-diabetic pregnancy.

Undoubtedly, there are other developmentally important genes that are affected by maternal diabetes, thereby leading to embryonic malformations. Hence, by understanding the molecular mechanisms by which maternal diabetes inhibits expression of *Cyp26a1*, we may gain insight into the general mechanisms by which diabetic pregnancy leads to malformations. Diabetes mellitus is one of the most common diseases and the global prevalence of diabetes is increasing at an alarming rate. Moreover, there is a growing trend towards earlier onset of diabetes. It is therefore of utmost importance to understand the underlying mechanism of increased susceptibility to congenital malformations associated with diabetic pregnancy. Results of this thesis support the hypothesis that elevated glucose, via alteration of RA-associated mechanisms, is responsible for the molecular, cellular and developmental defects observed in a mouse model of diabetic pregnancy. Investigation of the biochemical pathways by which glucose triggers transcriptional

responses in embryonic cells will provide further understanding into the molecular mechanisms by which diabetic pregnancy causes congenital malformations. It is hoped that findings obtained in this thesis may pave the way for deriving preventive measures to reduce the risk of adverse pregnancy outcome associated with diabetic pregnancy.

References

Abu-Abed S, Dolle P, Metzger D, Beckett B, Chambon P & Petkovich M (2001) The retinoic acid-metabolizing enzyme, CYP26A1, is essential for normal hindbrain patterning, vertebral identity, and development of posterior structures. *Genes Dev* **15**, 226-240.

Abu-Abed S, Dolle P, Metzger D, Wood C, MacLean G, Chambon P & Petkovich M (2003) Developing with lethal RA levels: genetic ablation of Rarg can restore the viability of mice lacking Cyp26a1. *Development* **130**, 1449-1459.

Abu-Abed S, MacLean G, Fraulob V, Chambon P, Petkovich M & Dolle P (2002) Differential expression of the retinoic acid-metabolizing enzymes CYP26A1 and CYP26B1 during murine organogenesis. *Mech Dev* **110**, 173-177.

Abu-Abed SS, Beckett BR, Chiba H, Chithalen JV, Jones G, Metzger D, Chambon P & Petkovich M (1998) Mouse P450RAI (CYP26) expression and retinoic acid-inducible retinoic acid metabolism in F9 cells are regulated by retinoic acid receptor gamma and retinoid X receptor alpha. *J Biol Chem* **273**, 2409-2415.

Ag Bendech M, Malvy DJ & Chauliac M (1997) [Vitamin A deficiency: epidemiological aspects and control methods]. *Sante* **7**, 309-316.

Amri K, Freund N, Vilar J, Merlet-Benichou C & Lelievre-Pegorier M (1999) Adverse effects of hyperglycemia on kidney development in rats: in vivo and in vitro studies. *Diabetes* **48**, 2240-2245.

Ang HL, Deltour L, Hayamizu TF, Zgombic-Knight M & Duester G (1996) Retinoic acid synthesis in mouse embryos during gastrulation and craniofacial development linked to class IV alcohol dehydrogenase gene expression. *J Biol Chem* **271**, 9526-9534.

Bae ST, Kim H & Kim KR (2001) Effects of Retinoic Acid on the Cell Proliferating Activity and the Expression of Fibroblast Growth Factor 2, Fibroblast Growth Factor Receptor 2 during Palatal Development of Mice. *Korean J Anat.* **34(1)**, 41-55.

Baena RM, Campoy C, Bayes R, Blanca E, Fernandez JM & Molina-Font JA (2002) Vitamin A, retinol binding protein and lipids in type 1 diabetes mellitus. *Eur J Clin Nutr* **56**, 44-50.

Baker L, Piddington R, Goldman A, Egler J & Moehring J (1990) Myo-inositol and prostaglandins reverse the glucose inhibition of neural tube fusion in cultured mouse embryos. *Diabetologia* **33**, 593-596.

Balkan W, Colbert M, Bock C & Linney E (1992) Transgenic indicator mice for studying activated retinoic acid receptors during development. *Proc Natl Acad Sci U S A* **89**, 3347-3351.

Balmer JE & Blomhoff R (2002) Gene expression regulation by retinoic acid. *J Lipid Res* **43**, 1773-1808.

Balsells M, Garcia-Patterson A, Gich I & Corcoy R (2009) Maternal and fetal outcome in women with type 2 versus type 1 diabetes mellitus: a systematic review and metaanalysis. *J Clin Endocrinol Metab* **94**, 4284-4291.

Basu TK, Tze WJ & Leichter J (1989) Serum vitamin A and retinol-binding protein in patients with insulin-dependent diabetes mellitus. *Am J Clin Nutr* **50**, 329-331.

Batourina E, Gim S, Bello N, Shy M, Clagett-Dame M, Srinivas S, Costantini F & Mendelsohn C (2001) Vitamin A controls epithelial/mesenchymal interactions through Ret expression. *Nat Genet* **27**, 74-78.

Bavik C, Ward SJ & Chambon P (1996) Developmental abnormalities in cultured mouse embryos deprived of retinoic by inhibition of yolk-sac retinol binding protein synthesis. *Proc Natl Acad Sci U S A* **93**, 3110-3114.

Baynes JW & Thorpe SR (1999) Role of oxidative stress in diabetic complications: a new perspective on an old paradigm. *Diabetes* **48**, 1-9.

Blaner WS (2007) STRA6, a cell-surface receptor for retinol-binding protein: the plot thickens. *Cell Metab* **5**, 164-166.

Blentic A, Gale E & Maden M (2003) Retinoic acid signaling centres in the avian embryo identified by sites of expression of synthesising and catabolising enzymes. *Dev Dyn* **227**, 114-127.

Boileau P, Mrejen C, Girard J & Hauguel-de Mouzon S (1995) Overexpression of GLUT3 placental glucose transporter in diabetic rats. *J Clin Invest* **96**, 309-317.

Bonadonna RC, Groop L, Kraemer N, Ferrannini E, Del Prato S & DeFronzo RA (1990) Obesity and insulin resistance in humans: a dose-response study. *Metabolism* **39**, 452-459.

Bouillet P, Sapin V, Chazaud C, Messaddeq N, Decimo D, Dolle P & Chambon P (1997) Developmental expression pattern of Stra6, a retinoic acid-responsive gene encoding a new type of membrane protein. *Mech Dev* **63**, 173-186.

Bradford MM (1976) A rapid and sensitive method for the quantitation of microgram quantities of protein utilizing the principle of protein-dye binding. *Anal Biochem* **72**, 248-254.

Britto JA, Evans RD, Hayward RD & Jones BM (2002) Toward pathogenesis of Apert cleft palate: FGF, FGFR, and TGF beta genes are differentially expressed in sequential stages of human palatal shelf fusion. *Cleft Palate Craniofac J* **39**, 332-340.

Buchanan TA, Denno KM, Sipos GF & Sadler TW (1994) Diabetic teratogenesis. In vitro evidence for a multifactorial etiology with little contribution from glucose per se. *Diabetes* **43**, 656-660.

Capobianco E, Jawerbaum A, Romanini MC, White V, Pustovrh C, Higa R, Martinez N, Mugnaini MT, Sonez C & Gonzalez E (2005) 15-Deoxy-Delta12,14-prostaglandin J2 and peroxisome proliferator-activated receptor gamma (PPARgamma) levels in term placental tissues from control and diabetic rats: modulatory effects of a PPARgamma agonist on nitridergic and lipid placental metabolism. *Reprod Fertil Dev* **17**, 423-433.

Casson IF, Clarke CA, Howard CV, McKendrick O, Pennycook S, Pharoah PO, Platt MJ, Stanisstreet M, van Velszen D & Walkinshaw S (1997) Outcomes of pregnancy in insulin dependent diabetic women: results of a five year population cohort study. *BMJ* **315**, 275-278.

Catalano PM, Drago NM & Amini SB (1995) Maternal carbohydrate metabolism and its relationship to fetal growth and body composition. *Am J Obstet Gynecol* **172**, 1464-1470.

Catalano PM & Kirwan JP (2001) Maternal factors that determine neonatal size and body fat. *Curr Diab Rep* **1**, 71-77.

Chan BW, Chan KS, Koide T, Yeung SM, Leung MB, Copp AJ, Loeken MR, Shiroishi T & Shum AS (2002) Maternal diabetes increases the risk of caudal regression caused by retinoic acid. *Diabetes* **51**, 2811-2816.

Chan JM, Rimm EB, Colditz GA, Stampfer MJ & Willett WC (1994) Obesity, fat distribution, and weight gain as risk factors for clinical diabetes in men. *Diabetes Care* **17**, 961-969.

Chan WL (2011) Dysregulation of retinoic acid synthesis in mouse embryos under diabetic or hyperglycemic conditions. *MPhil thesis submitted to The Chinese University of Hong Kong*.

Chang TI, Horal M, Jain SK, Wang F, Patel R & Loeken MR (2003) Oxidant regulation of gene expression and neural tube development: Insights gained from diabetic pregnancy on molecular causes of neural tube defects. *Diabetologia* **46**, 538-545.

Chassaing N, Golzio C, Odent S, Lequeux L, Vigouroux A, Martinovic-Bouriel J, Tiziano FD, Masini L, Piro F, Maragliano G, Delezoide AL, Attie-Bitach T, Manouvrier-Hanu S, Etchevers HC & Calvas P (2009) Phenotypic spectrum of STRA6 mutations: from Matthew-Wood syndrome to non-lethal anophthalmia. *Hum Mutat* **30**, E673-681.

Chawla A, Repa JJ, Evans RM & Mangelsdorf DJ (2001) Nuclear receptors and lipid physiology: opening the X-files. *Science* **294**, 1866-1870.

Chen H & Juchau MR (1998) Inhibition of embryonic retinoic acid synthesis by aldehydes of lipid peroxidation and prevention of inhibition by reduced glutathione and glutathione S-transferases. *Free Radic Biol Med* **24**, 408-417.

Chen MH, Antoni L, Tazi-Ahnini R, Cork M, Ward SJ & Bavik CO (2002) Identification of known and novel genes whose expression is regulated by endogenous retinoic acid during early embryonic development of the mouse. *Mech Dev* **114**, 205-212.

Cho YM, Youn BS, Lee H, Lee N, Min SS, Kwak SH, Lee HK & Park KS (2006) Plasma retinol-binding protein-4 concentrations are elevated in human subjects with impaired glucose tolerance and type 2 diabetes. *Diabetes Care* **29**, 2457-2461.

Clagett-Dame M & DeLuca HF (2002) The role of vitamin A in mammalian reproduction and embryonic development. *Annu Rev Nutr* **22**, 347-381.

Cockroft DL (1990) Dissection and culture of postimplantation embryos. Copp AJ and Cockroft DL eds. In: Postimplantation Mammalian Embryos. A Practical Approach. *IRL Press. Oxford*, 15-40.

Codner E (2008) Estrogen and type 1 diabetes mellitus. *Pediatr Endocrinol Rev* **6**, 228-234.

Cohlan SQ (1953) Excessive intakes of vitamin A as a cause of congential anomalies in the rat. *Science* **117**, 535-536.

Colditz GA, Willett WC, Rotnitzky A & Manson JE (1995) Weight gain as a risk factor for clinical diabetes mellitus in women. *Ann Intern Med* **122**, 481-486.

Conlon RA (1995) Retinoic acid and pattern formation in vertebrates. *Trends Genet* **11**, 314-319.

Conlon RA & Rossant J (1992) Exogenous retinoic acid rapidly induces anterior ectopic expression of murine Hox-2 genes in vivo. *Development* **116**, 357-368.

Conway SJ, Henderson DJ & Copp AJ (1997) Pax3 is required for cardiac neural crest migration in the mouse: evidence from the splotch (Sp2H) mutant. *Development* **124**, 505-514.

Copp AJ & Greene ND (2010) Genetics and development of neural tube defects. *J Pathol* **220**, 217-230.

Craig RL, Chu WS & Elbein SC (2007) Retinol binding protein 4 as a candidate gene for type 2 diabetes and prediabetic intermediate traits. *Mol Genet Metab* **90**, 338-344.

de Roos K, Sonneveld E, Compaan B, ten Berge D, Durston AJ & van der Saag PT (1999) Expression of retinoic acid 4-hydroxylase (CYP26) during mouse and Xenopus laevis embryogenesis. *Mech Dev* **82**, 205-211.

Degitz SJ, Morris D, Foley GL & Francis BM (1998) Role of TGF-beta in RA-induced cleft palate in CD-1 mice. *Teratology* **58**, 197-204.

Dersch H & Zile MH (1993) Induction of normal cardiovascular development in the vitamin A-deprived quail embryo by natural retinoids. *Dev Biol* **160**, 424-433.

Diamond MP, Moley KH, Pellicer A, Vaughn WK & DeCherney AH (1989) Effects of streptozotocin- and alloxan-induced diabetes mellitus on mouse follicular and early embryo development. *J Reprod Fertil* **86**, 1-10.

Dickman ED, Thaller C & Smith SM (1997) Temporally-regulated retinoic acid depletion produces specific neural crest, ocular and nervous system defects. *Development* **124**, 3111-3121.

Dobbs-McAuliffe B, Zhao Q & Linney E (2004) Feedback mechanisms regulate retinoic acid production and degradation in the zebrafish embryo. *Mech Dev* **121**, 339-350.

Domenicotti C, Marengo B, Verzola D, Garibotto G, Traverso N, Patriarca S, Maloberti G, Cottalasso D, Poli G, Passalacqua M, Melloni E, Pronzato MA & Marinari UM (2003) Role of PKC-delta activity in glutathione-depleted neuroblastoma cells. *Free Radic Biol Med* **35**, 504-516.

Downs KM & Davies T (1993) Staging of gastrulating mouse embryos by morphological landmarks in the dissecting microscope. *Development* **118**, 1255-1266.

Dupe V, Ghyselinck NB, Wendling O, Chambon P & Mark M (1999) Key roles of retinoic acid receptors alpha and beta in the patterning of the caudal hindbrain, pharyngeal arches and otocyst in the mouse. *Development* **126**, 5051-5059.

Echelard Y, Epstein DJ, St-Jacques B, Shen L, Mohler J, McMahon JA & McMahon AP (1993) Sonic hedgehog, a member of a family of putative signaling molecules, is implicated in the regulation of CNS polarity. *Cell* **75**, 1417-1430.

Eichele G (1999) A vital role for vitamin A. *Nat Genet* **21**, 346-347.

Epstein DJ, Vekemans M & Gros P (1991) Splotch (Sp2H), a mutation affecting development of the mouse neural tube, shows a deletion within the paired homeodomain of Pax-3. *Cell* **67**, 767-774.

Eriksson UJ (2009) Congenital anomalies in diabetic pregnancy. *Semin Fetal Neonatal Med* **14**, 85-93.

Eriksson UJ & Borg LA (1991) Protection by free oxygen radical scavenging enzymes against glucose-induced embryonic malformations in vitro. *Diabetologia* **34**, 325-331.

Eriksson UJ & Borg LA (1993) Diabetes and embryonic malformations. Role of substrate-induced free-oxygen radical production for dysmorphogenesis in cultured rat embryos. *Diabetes* **42**, 411-419.

Eriksson UJ, Borg LA, Forsberg H & Styrud J (1991) Diabetic embryopathy. Studies with animal and in vitro models. *Diabetes* **40 Suppl 2**, 94-98.

Eriksson UJ & Siman CM (1996) Pregnant diabetic rats fed the antioxidant butylated hydroxytoluene show decreased occurrence of malformations in offspring. *Diabetes* **45**, 1497-1502.

Fine EL, Horal M, Chang TI, Fortin G & Loeken MR (1999) Evidence that elevated glucose causes altered gene expression, apoptosis, and neural tube defects in a mouse model of diabetic pregnancy. *Diabetes* **48**, 2454-2462.

Foglia VG, Cattaneo de Peralta R, Ibarra R & Rivera Cortes L (1967) [Fetal and placental characteristics of pregnancy in pancreatectomized rats]. *Rev Soc Argent Biol* **43**, 187-198.

Formby B, Schmid-Formby F, Jovanovic L & Peterson CM (1987) The offspring of the female diabetic "nonobese diabetic" (NOD) mouse are large for gestational age and have elevated pancreatic insulin content: a new animal model of human diabetic pregnancy. *Proc Soc Exp Biol Med* **184**, 291-294.

Formelli F, Carsana R, Costa A, Buranelli F, Campa T, Dossena G, Magni A & Pizzichetta M (1989) Plasma retinol level reduction by the synthetic retinoid fenretinide: a one year follow-up study of breast cancer patients. *Cancer Res* **49**, 6149-6152.

Fuhrmann K, Reiher H, Semmler K, Fischer F, Fischer M & Glockner E (1983) Prevention of congenital malformations in infants of insulin-dependent diabetic mothers. *Diabetes Care* **6**, 219-223.

Fujii H, Sato T, Kaneko S, Gotoh O, Fujii-Kuriyama Y, Osawa K, Kato S & Hamada H (1997) Metabolic inactivation of retinoic acid by a novel P450 differentially expressed in developing mouse embryos. *EMBO J* **16**, 4163-4173.

Galindo A, Burguillo AG, Azriel S & Fuente Pde L (2006) Outcome of fetuses in women with pregestational diabetes mellitus. *J Perinat Med* **34**, 323-331.

Gareskog M & Wentzel P (2004) Altered protein kinase C activation associated with rat embryonic dysmorphogenesis. *Pediatr Res* **56**, 849-857.

Gareskog M & Wentzel P (2007) N-Acetylcysteine and alpha-cyano-4-hydroxycinnamic acid alter protein kinase C (PKC)-delta and PKC-zeta and diminish dysmorphogenesis in rat embryos cultured with high glucose in vitro. *J Endocrinol* **192**, 207-214.

Germain P, Iyer J, Zechel C & Gronemeyer H (2002) Co-regulator recruitment and the mechanism of retinoic acid receptor synergy. *Nature* **415**, 187-192.

Goldman AS, Baker L, Piddington R, Marx B, Herold R & Egler J (1985) Hyperglycemia-induced teratogenesis is mediated by a functional deficiency of arachidonic acid. *Proc Natl Acad Sci U S A* **82**, 8227-8231.

Goldstein R, Levy E & Shafrir E (1985) Increased maternal-fetal transport of fat in diabetes assessed by polyunsaturated fatty acid content in fetal lipids. *Biol Neonate* **47**, 343-349.

Gonzalez E, Rosello-Catafau J, Jawerbaum A, Vela J, Sinner D, Pustovrh C, White V, Xaus C, Peralta C & Gimeno MA (2001) Involvement of inducible isoforms of COX and NOS in streptozotocin-pancreatic damage in the rat: interactions between nitridergic and prostanoid pathway. *Prostaglandins Leukot Essent Fatty Acids* **64**, 311-316.

Goto MP, Goldman AS & Uhing MR (1992) PGE2 prevents anomalies induced by hyperglycemia or diabetic serum in mouse embryos. *Diabetes* **41**, 1644-1650.

Goto Y, Kakizaki M & Masaki N (1976) Production of spontaneous diabetic rats by repetition of selective breeding. *Tohoku J Exp Med* **119**, 85-90.

Goulding MD, Chalepakis G, Deutsch U, Erselius JR & Gruss P (1991) Pax-3, a novel murine DNA binding protein expressed during early neurogenesis. *EMBO J* **10**, 1135-1147.

Graham TE, Yang Q, Bluher M, Hammarstedt A, Ciaraldi TP, Henry RR, Wason CJ, Oberbach A, Jansson PA, Smith U & Kahn BB (2006) Retinol-binding protein 4 and insulin resistance in lean, obese, and diabetic subjects. *N Engl J Med* **354**, 2552-2563.

Greene ND, Stanier P & Copp AJ (2009) Genetics of human neural tube defects. *Hum Mol Genet* **18**, R113-129.

Guleria RS, Pan J, Dipette D & Singh US (2006) Hyperglycemia inhibits retinoic acid-induced activation of Rac1, prevents differentiation of cortical neurons, and causes oxidative stress in a rat model of diabetic pregnancy. *Diabetes* **55**, 3326-3334.

Gundersen TE & Blomhoff R (2001) Qualitative and quantitative liquid chromatographic determination of natural retinoids in biological samples. *J Chromatogr A* **935**, 13-43.

Hagay ZJ, Weiss Y, Zusman I, Peled-Kamar M, Reece EA, Eriksson UJ & Groner Y (1995) Prevention of diabetes-associated embryopathy by overexpression of the free radical scavenger copper zinc superoxide dismutase in transgenic mouse embryos. *Am J Obstet Gynecol* **173**, 1036-1041.

Haines H, Hackel DB & Schmidt-Nielsen K (1965) Experimental Diabetes Mellitus Induced by Diet in the Sand Rat. *Am J Physiol* **208**, 297-300.

Halilagic A, Ribes V, Ghyselinck NB, Zile MH, Dolle P & Studer M (2007) Retinoids control anterior and dorsal properties in the developing forebrain. *Dev Biol* **303**, 362-375.

Hawthorne G, Robson S, Ryall EA, Sen D, Roberts SH & Ward Platt MP (1997) Prospective population based survey of outcome of pregnancy in diabetic women: results of the Northern Diabetic Pregnancy Audit, 1994. *BMJ* **315**, 279-281.

Herrera E, Palacin M, Martin A & Lasuncion MA (1985) Relationship between maternal and fetal fuels and placental glucose transfer in rats with maternal diabetes of varying severity. *Diabetes* **34 Suppl 2**, 42-46.

Hill AL, Phelan SA & Loeken MR (1998) Reduced expression of pax-3 is associated with overexpression of cdc46 in the mouse embryo. *Dev Genes Evol* **208**, 128-134.

Hollemann T, Chen Y, Grunz H & Pieler T (1998) Regionalized metabolic activity establishes boundaries of retinoic acid signaling. *EMBO J* **17**, 7361-7372.

Hornnes PJ, Kuhl C & Lauritsen KB (1981) Gastrointestinal insulinotropic hormones in normal and gestational-diabetic pregnancy: response to oral glucose. *Diabetes* **30**, 504-509.

Huang HZ, Lu BH, Chen YY & Liao GQ (2003) [Study on etiology of retinoic acid-induced cleft palate in mouse]. *Zhonghua Kou Qiang Yi Xue Za Zhi* **38**, 185-187.

Iessi IL, Bueno A, Sinzato YK, Taylor KN, Rudge MV & Damasceno DC (2010) Evaluation of neonatally-induced mild diabetes in rats: Maternal and fetal repercussions. *Diabetol Metab Syndr* **2**, 37.

Isken A, Golczak M, Oberhauser V, Hunzelmann S, Driever W, Imanishi Y, Palczewski K & von Lintig J (2008) RBP4 disrupts vitamin A uptake homeostasis in a STRA6-deficient animal model for Matthew-Wood syndrome. *Cell Metab* **7**, 258-268.

Iulianella A, Beckett B, Petkovich M & Lohnes D (1999) A molecular basis for retinoic acid-induced axial truncation. *Dev Biol* **205**, 33-48.

Iulianella A & Lohnes D (1997) Contribution of retinoic acid receptor gamma to retinoid-induced craniofacial and axial defects. *Dev Dyn* **209**, 92-104.

Jawerbaum A, Sinner D, White V, Pustovrh C, Capobianco E & Gonzalez E (2002) Modulation of nitric oxide concentration and lipid metabolism by 15-deoxy Delta12,14prostaglandin J2 in embryos from control and diabetic rats during early organogenesis. *Reproduction* **124**, 625-631.

Jensen DM, Korsholm L, Ovesen P, Beck-Nielsen H, Moelsted-Pedersen L, Westergaard JG, Moeller M & Damm P (2009) Peri-conceptional A1C and risk of serious adverse pregnancy outcome in 933 women with type 1 diabetes. *Diabetes Care* **32**, 1046-1048.

Jiang B, Kumar SD, Loh WT, Manikandan J, Ling EA, Tay SS & Dheen ST (2008) Global gene expression analysis of cranial neural tubes in embryos of diabetic mice. *J Neurosci Res* **86**, 3481-3493.

Junod A, Lambert AE, Orci L, Pictet R, Gonet AE & Renold AE (1967) Studies of the diabetogenic action of streptozotocin. *Proc Soc Exp Biol Med* **126**, 201-205.

Junod A, Lambert AE, Stauffacher W & Renold AE (1969) Diabetogenic action of streptozotocin: relationship of dose to metabolic response. *J Clin Invest* **48**, 2129-2139.

Kan O, Baldwin SA & Whetton AD (1994) Apoptosis is regulated by the rate of glucose transport in an interleukin 3 dependent cell line. *J Exp Med* **180**, 917-923.

Kawaguchi R, Yu J, Honda J, Hu J, Whitelegge J, Ping P, Wiita P, Bok D & Sun H (2007) A membrane receptor for retinol binding protein mediates cellular uptake of vitamin A. *Science* **315**, 820-825.

Kay TW, Thomas HE, Harrison LC & Allison J (2000) The beta cell in autoimmune diabetes: many mechanisms and pathways of loss. *Trends Endocrinol Metab* **11**, 11-15.

Kennedy KA, Porter T, Mehta V, Ryan SD, Price F, Peshdary V, Karamboulas C, Savage J, Drysdale TA, Li SC, Bennett SA & Skerjanc IS (2009) Retinoic acid enhances skeletal muscle progenitor formation and bypasses inhibition by bone morphogenetic protein 4 but not dominant negative beta-catenin. *BMC Biol* **7**, 67.

Kessel M & Gruss P (1991) Homeotic transformations of murine vertebrae and concomitant alteration of Hox codes induced by retinoic acid. *Cell* **67**, 89-104.

Khan NA (2007) Role of lipids and fatty acids in macrosomic offspring of diabetic pregnancy. *Cell Biochem Biophys* **48**, 79-88.

Khoury MJ, Becerra JE, Cordero JF & Erickson JD (1989) Clinical-epidemiologic assessment of pattern of birth defects associated with human teratogens: application to diabetic embryopathy. *Pediatrics* **84**, 658-665.

Kim YK, Wassef L, Hamberger L, Piantedosi R, Palczewski K, Blaner WS & Quadro L (2008) Retinyl ester formation by lecithin: retinol acyltransferase is a key regulator of retinoid homeostasis in mouse embryogenesis. *J Biol Chem* **283**, 5611-5621.

Kitzmiller JL, Gavin LA, Gin GD, Jovanovic-Peterson L, Main EK & Zigrang WD (1991) Preconception care of diabetes. Glycemic control prevents congenital anomalies. *JAMA* **265**, 731-736.

Kochhar DM (2000) Teratogenicity of retinoic acid. *Teratology* **62**, 178-180.

Kolterman OG, Insel J, Saekow M & Olefsky JM (1980) Mechanisms of insulin resistance in human obesity: evidence for receptor and postreceptor defects. *J Clin Invest* **65**, 1272-1284.

Koo SH, Cunningham MC, Arabshahi B, Gruss JS & Grant JH, 3rd (2001) The transforming growth factor-beta 3 knock-out mouse: an animal model for cleft palate. *Plast Reconstr Surg* **108**, 938-948; discussion 949-951.

Koubova J, Menke DB, Zhou Q, Capel B, Griswold MD & Page DC (2006) Retinoic acid regulates sex-specific timing of meiotic initiation in mice. *Proc Natl Acad Sci U S A* **103**, 2474-2479.

Krumlauf R (1994) Hox genes in vertebrate development. *Cell* **78**, 191-201.

Kucera J (1971) Rate and type of congenital anomalies among offspring of diabetic women. *J Reprod Med* **7**, 73-82.

Kumar SD, Dheen ST & Tay SS (2007) Maternal diabetes induces congenital heart defects in mice by altering the expression of genes involved in cardiovascular development. *Cardiovasc Diabetol* **6**, 34.

Lambin S, van Bree R, Caluwaerts S, Vercruysse L, Vergote I & Verhaeghe J (2007) Adipose tissue in offspring of Lepr(db/+) mice: early-life environment vs. genotype. *Am J Physiol Endocrinol Metab* **292**, E262-271.

Lammer EJ, Chen DT, Hoar RM, Agnish ND, Benke PJ, Braun JT, Curry CJ, Fernhoff PM, Grix AW, Jr., Lott IT & et al. (1985) Retinoic acid embryopathy. *N Engl J Med* **313**, 837-841.

Lan MS, Wasserfall C, Maclaren NK & Notkins AL (1996) IA-2, a transmembrane protein of the protein tyrosine phosphatase family, is a major autoantigen in insulin-dependent diabetes mellitus. *Proc Natl Acad Sci U S A* **93**, 6367-6370.

Langer O & Conway DL (2000) Level of glycemia and perinatal outcome in pregestational diabetes. *J Matern Fetal Med* **9**, 35-41.

Lee AT, Reis D & Eriksson UJ (1999) Hyperglycemia-induced embryonic dysmorphogenesis correlates with genomic DNA mutation frequency in vitro and in vivo. *Diabetes* **48**, 371-376.

Lee MY (2008) A study on dysregulation of retinoic acid catabolism by Cyp26a1 in increasing the risk of caudal regression in diabetic pregnancy. *MPhil thesis submitted to The Chinese University of Hong Kong.*

Lee SJ, Kim DC, Choi BH, Ha H & Kim KT (2006) Regulation of p53 by activated protein kinase C-delta during nitric oxide-induced dopaminergic cell death. *J Biol Chem* **281**, 2215-2224.

Leid M, Kastner P, Lyons R, Nakshatri H, Saunders M, Zacharewski T, Chen JY, Staub A, Garnier JM, Mader S & et al. (1992) Purification, cloning, and RXR identity of the HeLa cell factor with which RAR or TR heterodimerizes to bind target sequences efficiently. *Cell* **68**, 377-395.

Lenzen S & Panten U (1988) Alloxan: history and mechanism of action. *Diabetologia* **31**, 337-342.

Leroy I, de Thonel A, Laurent G & Quillet-Mary A (2005) Protein kinase C zeta associates with death inducing signaling complex and regulates Fas ligand-induced apoptosis. *Cell Signal* **17**, 1149-1157.

Leung BW (2005) Cellular and molecular mechanisms of increased embryonic susceptibiliy to retinoic acid teratogenicity in diabetic pregnancy. *PhD thesis submitted to The Chinese University of Hong Kong.*

Leung MB, Choy KW, Copp AJ, Pang CP & Shum AS (2004) Hyperglycaemia potentiates the teratogenicity of retinoic acid in diabetic pregnancy in mice. *Diabetologia* **47**, 515-522.

Li R, Chase M, Jung SK, Smith PJ & Loeken MR (2005) Hypoxic stress in diabetic pregnancy contributes to impaired embryo gene expression and defective development by inducing oxidative stress. *Am J Physiol Endocrinol Metab* **289**, E591-599.

Loeken MR (2006) Advances in understanding the molecular causes of diabetes-induced birth defects. *J Soc Gynecol Investig* **13**, 2-10.

Lohnes D, Kastner P, Dierich A, Mark M, LeMeur M & Chambon P (1993) Function of retinoic acid receptor gamma in the mouse. *Cell* **73**, 643-658.

Lohnes D, Mark M, Mendelsohn C, Dolle P, Decimo D, LeMeur M, Dierich A, Gorry P & Chambon P (1995) Developmental roles of the retinoic acid receptors. *J Steroid Biochem Mol Biol* **53**, 475-486.

Lohnes D, Mark M, Mendelsohn C, Dolle P, Dierich A, Gorry P, Gansmuller A & Chambon P (1994) Function of the retinoic acid receptors (RARs) during development (I). Craniofacial and skeletal abnormalities in RAR double mutants. *Development* **120**, 2723-2748.

Loudig O, Babichuk C, White J, Abu-Abed S, Mueller C & Petkovich M (2000) Cytochrome P450RAI(CYP26) promoter: a distinct composite retinoic acid response element underlies the complex regulation of retinoic acid metabolism. *Mol Endocrinol* **14**, 1483-1497.

Loudig O, Maclean GA, Dore NL, Luu L & Petkovich M (2005) Transcriptional co-operativity between distant retinoic acid response elements in regulation of Cyp26A1 inducibility. *Biochem J* **392**, 241-248.

Lufkin T, Lohnes D, Mark M, Dierich A, Gorry P, Gaub MP, LeMeur M & Chambon P (1993) High postnatal lethality and testis degeneration in retinoic acid receptor alpha mutant mice. *Proc Natl Acad Sci U S A* **90**, 7225-7229.

Luo J, Sucov HM, Bader JA, Evans RM & Giguere V (1996) Compound mutants for retinoic acid receptor (RAR) beta and RAR alpha 1 reveal developmental functions for multiple RAR beta isoforms. *Mech Dev* **55**, 33-44.

MacLean G, Abu-Abed S, Dolle P, Tahayato A, Chambon P & Petkovich M (2001) Cloning of a novel retinoic-acid metabolizing cytochrome P450, Cyp26B1, and comparative expression analysis with Cyp26A1 during early murine development. *Mech Dev* **107**, 195-201.

MacLean G, Li H, Metzger D, Chambon P & Petkovich M (2007) Apoptotic extinction of germ cells in testes of Cyp26b1 knockout mice. *Endocrinology* **148**, 4560-4567.

Maden M & Holder N (1992) Retinoic acid and development of the central nervous system. *Bioessays* **14**, 431-438.

Maden M, Sonneveld E, van der Saag PT & Gale E (1998) The distribution of endogenous retinoic acid in the chick embryo: implications for developmental mechanisms. *Development* **125**, 4133-4144.

Mangelsdorf DJ & Evans RM (1995) The RXR heterodimers and orphan receptors. *Cell* **83**, 841-850.

Martin M, Gallego-Llamas J, Ribes V, Kedinger M, Niederreither K, Chambon P, Dolle P & Gradwohl G (2005) Dorsal pancreas agenesis in retinoic acid-deficient Raldh2 mutant mice. *Dev Biol* **284**, 399-411.

Martinez-Frias ML (1994) Epidemiological analysis of outcomes of pregnancy in diabetic mothers: identification of the most characteristic and most frequent congenital anomalies. *Am J Med Genet* **51**, 108-113.

Martinoli L, Di Felice M, Seghieri G, Ciuti M, De Giorgio LA, Fazzini A, Gori R, Anichini R & Franconi F (1993) Plasma retinol and alpha-tocopherol concentrations in insulin-dependent diabetes mellitus: their relationship to microvascular complications. *Int J Vitam Nutr Res* **63**, 87-92.

McCaffery P & Drager UC (1997) A sensitive bioassay for enzymes that synthesize retinoic acid. *Brain Res Brain Res Protoc* **1**, 232-236.

McCaffery P, Evans J, Koul O, Volpert A, Reid K & Ullman MD (2002) Retinoid quantification by HPLC/MS(n). *J Lipid Res* **43**, 1143-1149.

McCaffery P & Simons C (2007) Prospective teratology of retinoic acid metabolic blocking agents (RAMBAs) and loss of CYP26 activity. *Curr Pharm Des* **13**, 3020-3037.

Mendelsohn C, Batourina E, Fung S, Gilbert T & Dodd J (1999) Stromal cells mediate retinoid-dependent functions essential for renal development. *Development* **126**, 1139-1148.

Mendelsohn C, Lohnes D, Decimo D, Lufkin T, LeMeur M, Chambon P & Mark M (1994) Function of the retinoic acid receptors (RARs) during development (II). Multiple abnormalities at various stages of organogenesis in RAR double mutants. *Development* **120**, 2749-2771.

Mendelsohn C, Ruberte E, LeMeur M, Morriss-Kay G & Chambon P (1991) Developmental analysis of the retinoic acid-inducible RAR-beta 2 promoter in transgenic animals. *Development* **113**, 723-734.

Mestman JH (1980) Outcome of diabetes screening in pregnancy and perinatal morbidity in infants of mothers with mild impairment in glucose tolerance. *Diabetes Care* **3**, 447-452.

Mey J, McCaffery P & Klemeit M (2001) Sources and sink of retinoic acid in the embryonic chick retina: distribution of aldehyde dehydrogenase activities, CRABP-I, and sites of retinoic acid inactivation. *Brain Res Dev Brain Res* **127**, 135-148.

Mic FA, Haselbeck RJ, Cuenca AE & Duester G (2002) Novel retinoic acid generating activities in the neural tube and heart identified by conditional rescue of Raldh2 null mutant mice. *Development* **129**, 2271-2282.

Mic FA, Molotkov A, Benbrook DM & Duester G (2003) Retinoid activation of retinoic acid receptor but not retinoid X receptor is sufficient to rescue lethal defect in retinoic acid synthesis. *Proc Natl Acad Sci U S A* **100**, 7135-7140.

Michael Weindling A (2009) Offspring of diabetic pregnancy: short-term outcomes. *Semin Fetal Neonatal Med* **14**, 111-118.

Moglia BB & Phelps DS (1996) Changes in surfactant protein A mRNA levels in a rat model of insulin-treated diabetic pregnancy. *Pediatr Res* **39**, 241-247.

Moley KH (2001) Hyperglycemia and apoptosis: mechanisms for congenital malformations and pregnancy loss in diabetic women. *Trends Endocrinol Metab* **12**, 78-82.

Moley KH, Chi MM & Mueckler MM (1998) Maternal hyperglycemia alters glucose transport and utilization in mouse preimplantation embryos. *Am J Physiol* **275**, E38-47.

Moley KH, Vaughn WK, DeCherney AH & Diamond MP (1991) Effect of diabetes mellitus on mouse pre-implantation embryo development. *J Reprod Fertil* **93**, 325-332.

Moss JB, Xavier-Neto J, Shapiro MD, Nayeem SM, McCaffery P, Drager UC & Rosenthal N (1998) Dynamic patterns of retinoic acid synthesis and response in the developing mammalian heart. *Dev Biol* **199**, 55-71.

Nakhooda AF, Like AA, Chappel CI, Murray FT & Marliss EB (1977) The spontaneously diabetic Wistar rat. Metabolic and morphologic studies. *Diabetes* **26**, 100-112.

Nelson DR (1999) A second CYP26 P450 in humans and zebrafish: CYP26B1. *Arch Biochem Biophys* **371**, 345-347.

Niederreither K, Abu-Abed S, Schuhbaur B, Petkovich M, Chambon P & Dolle P (2002a) Genetic evidence that oxidative derivatives of retinoic acid are not involved in retinoid signaling during mouse development. *Nat Genet* **31**, 84-88.

Niederreither K & Dolle P (2008) Retinoic acid in development: towards an integrated view. *Nat Rev Genet* **9**, 541-553.

Niederreither K, McCaffery P, Drager UC, Chambon P & Dolle P (1997) Restricted expression and retinoic acid-induced downregulation of the retinaldehyde dehydrogenase type 2 (RALDH-2) gene during mouse development. *Mech Dev* **62**, 67-78.

Niederreither K, Subbarayan V, Dolle P & Chambon P (1999) Embryonic retinoic acid synthesis is essential for early mouse post-implantation development. *Nat Genet* **21**, 444-448.

Niederreither K, Vermot J, Schuhbaur B, Chambon P & Dolle P (2002b) Embryonic retinoic acid synthesis is required for forelimb growth and anteroposterior patterning in the mouse. *Development* **129**, 3563-3574.

Notkins AL & Lernmark A (2001) Autoimmune type 1 diabetes: resolved and unresolved issues. *J Clin Invest* **108**, 1247-1252.

Nugent P, Sucov HM, Pisano MM & Greene RM (1999) The role of RXR-alpha in retinoic acid-induced cleft palate as assessed with the RXR-alpha knockout mouse. *Int J Dev Biol* **43**, 567-570.

Olmedilla B, Granado F, Gil-Martinez E, Blanco I & Rojas-Hidalgo E (1997) Reference values for retinol, tocopherol, and main carotenoids in serum of control and insulin-dependent diabetic Spanish subjects. *Clin Chem* **43**, 1066-1071.

Otani H, Tanaka O, Tatewaki R, Naora H & Yoneyama T (1991) Diabetic environment and genetic predisposition as causes of congenital malformations in NOD mouse embryos. *Diabetes* **40**, 1245-1250.

Oyama K, Sugimura Y, Murase T, Uchida A, Hayasaka S, Oiso Y & Murata Y (2009) Folic acid prevents congenital malformations in the offspring of diabetic mice. *Endocr J* **56**, 29-37.

Padmanabhan R & al-Zuhair AG (1990) Ultrastructural studies on the placentae of streptozotocin induced maternal diabetes in the rat. *Z Mikrosk Anat Forsch* **104**, 212-230.

Pani L, Horal M & Loeken MR (2002) Rescue of neural tube defects in Pax-3-deficient embryos by p53 loss of function: implications for Pax-3-dependent development and tumorigenesis. *Genes Dev* **16**, 676-680.

Pappas RS, Newcomer ME & Ong DE (1993) Endogenous retinoids in rat epididymal tissue and rat and human spermatozoa. *Biol Reprod* **48**, 235-247.

Pavlinkova G, Salbaum JM & Kappen C (2009) Maternal diabetes alters transcriptional programs in the developing embryo. *BMC Genomics* **10**, 274.

Perez-Castro AV, Toth-Rogler LE, Wei LN & Nguyen-Huu MC (1989) Spatial and temporal pattern of expression of the cellular retinoic acid-binding protein and the cellular retinol-binding protein during mouse embryogenesis. *Proc Natl Acad Sci U S A* **86**, 8813-8817.

Phelan SA, Ito M & Loeken MR (1997) Neural tube defects in embryos of diabetic mice: role of the Pax-3 gene and apoptosis. *Diabetes* **46**, 1189-1197.

Piddington R, Joyce J, Dhanasekaran P & Baker L (1996) Diabetes mellitus affects prostaglandin E2 levels in mouse embryos during neurulation. *Diabetologia* **39**, 915-920.

Pinter E, Reece EA, Leranth CZ, Garcia-Segura M, Hobbins JC, Mahoney MJ & Naftolin F (1986) Arachidonic acid prevents hyperglycemia-associated yolk sac damage and embryopathy. *Am J Obstet Gynecol* **155**, 691-702.

Polonsky KS (2006) Retinol-binding protein 4, insulin resistance, and type 2 diabetes. *N Engl J Med* **354**, 2596-2598.

Powers RW, Chambers C & Larsen WJ (1996) Diabetes-mediated decreases in ovarian superoxide dismutase activity are related to blood-follicle barrier and ovulation defects. *Endocrinology* **137**, 3101-3110.

Quadro L, Blaner WS, Salchow DJ, Vogel S, Piantedosi R, Gouras P, Freeman S, Cosma MP, Colantuoni V & Gottesman ME (1999) Impaired retinal function and vitamin A availability in mice lacking retinol-binding protein. *EMBO J* **18**, 4633-4644.

Quadro L, Hamberger L, Gottesman ME, Colantuoni V, Ramakrishnan R & Blaner WS (2004) Transplacental delivery of retinoid: the role of retinol-binding protein and lipoprotein retinyl ester. *Am J Physiol Endocrinol Metab* **286**, E844-851.

Quadro L, Hamberger L, Gottesman ME, Wang F, Colantuoni V, Blaner WS & Mendelsohn CL (2005) Pathways of vitamin A delivery to the embryo: insights from a new tunable model of embryonic vitamin A deficiency. *Endocrinology* **146**, 4479-4490.

Ray WJ, Bain G, Yao M & Gottlieb DI (1997) CYP26, a novel mammalian cytochrome P450, is induced by retinoic acid and defines a new family. *J Biol Chem* **272**, 18702-18708.

Reece EA & Eriksson UJ (1996) The pathogenesis of diabetes-associated congenital malformations. *Obstet Gynecol Clin North Am* **23**, 29-45.

Reece EA, Ji I, Wu YK & Zhao Z (2006) Characterization of differential gene expression profiles in diabetic embryopathy using DNA microarray analysis. *Am J Obstet Gynecol* **195**, 1075-1080.

Reece EA, Leguizamon G & Wiznitzer A (2009) Gestational diabetes: the need for a common ground. *Lancet* **373**, 1789-1797.

Reijntjes S, Blentic A, Gale E & Maden M (2005) The control of morphogen signaling: regulation of the synthesis and catabolism of retinoic acid in the developing embryo. *Dev Biol* **285**, 224-237.

Reijntjes S, Gale E & Maden M (2003) Expression of the retinoic acid catabolising enzyme CYP26B1 in the chick embryo and its regulation by retinoic acid. *Gene Expr Patterns* **3**, 621-627.

Reijntjes S, Gale E & Maden M (2004) Generating gradients of retinoic acid in the chick embryo: Cyp26C1 expression and a comparative analysis of the Cyp26 enzymes. *Dev Dyn* **230**, 509-517.

Ribes V, Otto DM, Dickmann L, Schmidt K, Schuhbaur B, Henderson C, Blomhoff R, Wolf CR, Tickle C & Dolle P (2007) Rescue of cytochrome P450 oxidoreductase (Por) mouse mutants reveals functions in vasculogenesis, brain and limb patterning linked to retinoic acid homeostasis. *Dev Biol* **303**, 66-81.

Rieutort M, Farrell PM, Engle MJ, Pignol B & Bourbon JR (1986) Changes in surfactant phospholipids in fetal rat lungs from normal and diabetic pregnancies. *Pediatr Res* **20**, 650-654.

Roberts C, Ivins S, Cook AC, Baldini A & Scambler PJ (2006) Cyp26 genes a1, b1 and c1 are down-regulated in Tbx1 null mice and inhibition of Cyp26 enzyme function produces a phenocopy of DiGeorge Syndrome in the chick. *Hum Mol Genet* **15**, 3394-3410.

Rosenmann E, Yanko L & Cohen AM (1984) Female sex hormone and nephropathy in Cohen diabetic rat (genetically selected sucrose-fed). *Horm Metab Res* **16**, 11-16.

Ross SA, McCaffery PJ, Drager UC & De Luca LM (2000) Retinoids in embryonal development. *Physiol Rev* **80**, 1021-1054.

Rossant J, Zirngibl R, Cado D, Shago M & Giguere V (1991) Expression of a retinoic acid response element-hsplacZ transgene defines specific domains of transcriptional activity during mouse embryogenesis. *Genes Dev* **5**, 1333-1344.

Rosselot C, Spraggon L, Chia I, Batourina E, Riccio P, Lu B, Niederreither K, Dolle P, Duester G, Chambon P, Costantini F, Gilbert T, Molotkov A & Mendelsohn C (2010) Non-cell-autonomous retinoid signaling is crucial for renal development. *Development* **137(2)**, 283-292.

Rossetti L, Smith D, Shulman GI, Papachristou D & DeFronzo RA (1987) Correction of hyperglycemia with phlorizin normalizes tissue sensitivity to insulin in diabetic rats. *J Clin Invest* **79**, 1510-1515.

Sadler TW, Hunter ES, 3rd, Wynn RE & Phillips LS (1989) Evidence for multifactorial origin of diabetes-induced embryopathies. *Diabetes* **38**, 70-74.

Sakai Y, Meno C, Fujii H, Nishino J, Shiratori H, Saijoh Y, Rossant J & Hamada H (2001) The retinoic acid-inactivating enzyme CYP26 is essential for establishing an uneven distribution of retinoic acid along the anterio-posterior axis within the mouse embryo. *Genes Dev* **15**, 213-225.

Sakhi AK, Gundersen TE, Ulven SM, Blomhoff R & Lundanes E (1998) Quantitative determination of endogenous retinoids in mouse embryos by high-performance liquid chromatography with on-line solid-phase extraction, column switching and electrochemical detection. *J Chromatogr A* **828**, 451-460.

Sandell LL, Sanderson BW, Moiseyev G, Johnson T, Mushegian A, Young K, Rey JP, Ma JX, Staehling-Hampton K & Trainor PA (2007) RDH10 is essential for synthesis of embryonic retinoic acid and is required for limb, craniofacial, and organ development. *Genes Dev* **21**, 1113-1124.

Santiago-Walker AE, Fikaris AJ, Kao GD, Brown EJ, Kazanietz MG & Meinkoth JL (2005) Protein kinase C delta stimulates apoptosis by initiating G1 phase cell cycle progression and S phase arrest. *J Biol Chem* **280**, 32107-32114.

Schaefer-Graf UM, Buchanan TA, Xiang A, Songster G, Montoro M & Kjos SL (2000) Patterns of congenital anomalies and relationship to initial maternal fasting glucose levels in pregnancies complicated by type 2 and gestational diabetes. *Am J Obstet Gynecol* **182**, 313-320.

Schaefer-Graf UM, Heuer R, Kilavuz O, Pandura A, Henrich W & Vetter K (2002) Maternal obesity not maternal glucose values correlates best with high rates of fetal macrosomia in pregnancies complicated by gestational diabetes. *J Perinat Med* **30**, 313-321.

Schaefer-Graf UM, Pawliczak J, Passow D, Hartmann R, Rossi R, Buhrer C, Harder T, Plagemann A, Vetter K & Kordonouri O (2005) Birth weight and parental BMI predict overweight in children from mothers with gestational diabetes. *Diabetes Care* **28**, 1745-1750.

Schaffer EM, Ritter SJ & Smith JE (1993) N-(4-hydroxyphenyl)retinamide (fenretinide) induces retinol-binding protein secretion from liver and accumulation in the kidneys in rats. *J Nutr* **123**, 1497-1503.

Schmidt CK, Brouwer A & Nau H (2003) Chromatographic analysis of endogenous retinoids in tissues and serum. *Anal Biochem* **315**, 36-48.

Schoenfeld A, Erman A, Warchaizer S, Ovadia J, Bonner G & Hod M (1995) Yolk sac concentration of prostaglandin E2 in diabetic pregnancy: further clues to the etiology of diabetic embryopathy. *Prostaglandins* **50**, 121-126.

Schranz DB & Lernmark A (1998) Immunology in diabetes: an update. *Diabetes Metab Rev* **14**, 3-29.

Shenefelt RE (1972) Morphogenesis of malformations in hamsters caused by retinoic acid: relation to dose and stage at treatment. *Teratology* **5**, 103-118.

Shepard TH, Tanimura T & Park HW (1997) Glucose absorption and utilization by rat embryos. *Int J Dev Biol* **41**, 307-314.

Shum AS, Poon LL, Tang WW, Koide T, Chan BW, Leung YC, Shiroishi T & Copp AJ (1999) Retinoic acid induces down-regulation of Wnt-3a, apoptosis and diversion of tail bud cells to a neural fate in the mouse embryo. *Mech Dev* **84**, 17-30.

Siman CM & Eriksson UJ (1997a) Vitamin C supplementation of the maternal diet reduces the rate of malformation in the offspring of diabetic rats. *Diabetologia* **40**, 1416-1424.

Siman CM & Eriksson UJ (1997b) Vitamin E decreases the occurrence of malformations in the offspring of diabetic rats. *Diabetes* **46**, 1054-1061.

Siman CM, Gittenberger-De Groot AC, Wisse B & Eriksson UJ (2000) Malformations in offspring of diabetic rats: morphometric analysis of neural crest-derived organs and effects of maternal vitamin E treatment. *Teratology* **61**, 355-367.

Simeoni U & Barker DJ (2009) Offspring of diabetic pregnancy: long-term outcomes. *Semin Fetal Neonatal Med* **14**, 119-124.

Singh SK, Singh RD & Sharma A (2005) Caudal regression syndrome--case report and review of literature. *Pediatr Surg Int* **21**, 578-581.

Sivan E, Lee YC, Wu YK & Reece EA (1997) Free radical scavenging enzymes in fetal dysmorphogenesis among offspring of diabetic rats. *Teratology* **56**, 343-349.

Smith JE, Lawless DC, Green MH & Moon RC (1992) Secretion of vitamin A and retinol-binding protein into plasma is depressed in rats by N-(4-hydroxyphenyl)retinamide (fenretinide). *J Nutr* **122**, 1999-2009.

Soprano DR, Gyda M, 3rd, Jiang H, Harnish DC, Ugen K, Satre M, Chen L, Soprano KJ & Kochhar DM (1994) A sustained elevation in retinoic acid receptor-beta 2 mRNA and protein occurs during retinoic acid-induced fetal dysmorphogenesis. *Mech Dev* **45**, 243-253.

Soprano DR & Soprano KJ (1995) Retinoids as teratogens. *Annu Rev Nutr* **15**, 111-132.

Srinivasan K & Ramarao P (2007) Animal models in type 2 diabetes research: an overview. *Indian J Med Res* **125**, 451-472.

Starkey JM, Zhao Y, Sadygov RG, Haidacher SJ, Lejeune WS, Dey N, Luxon BA, Kane MA, Napoli JL, Denner L & Tilton RG (2010) Altered retinoic acid metabolism in diabetic mouse kidney identified by O isotopic labeling and 2D mass spectrometry. *PLoS One* **5**, e11095.

Stoppie P, Borgers M, Borghgraef P, Dillen L, Goossens J, Sanz G, Szel H, Van Hove C, Van Nyen G, Nobels G, Vanden Bossche H, Venet M, Willemsens G & Van Wauwe J (2000) R115866 inhibits all-trans-retinoic acid metabolism and exerts retinoidal effects in rodents. *J Pharmacol Exp Ther* **293**, 304-312.

Strieleman PJ, Connors MA & Metzger BE (1992) Phosphoinositide metabolism in the developing conceptus. Effects of hyperglycemia and scyllo-inositol in rat embryo culture. *Diabetes* **41**, 989-997.

Strieleman PJ & Metzger BE (1993) Glucose and scyllo-inositol impair phosphoinositide hydrolysis in the 10.5-day cultured rat conceptus: a role in dysmorphogenesis? *Teratology* **48**, 267-278.

Suh MJ, Tang XH & Gudas LJ (2006) Structure elucidation of retinoids in biological samples using postsource decay laser desorption/ionization mass spectrometry after high-performance liquid chromatography separation. *Anal Chem* **78**, 5719-5728.

Sun X, Meyers EN, Lewandoski M & Martin GR (1999) Targeted disruption of Fgf8 causes failure of cell migration in the gastrulating mouse embryo. *Genes Dev* **13**, 1834-1846.

Swindell EC, Thaller C, Sockanathan S, Petkovich M, Jessell TM & Eichele G (1999) Complementary domains of retinoic acid production and degradation in the early chick embryo. *Dev Biol* **216**, 282-296.

Tahayato A, Dolle P & Petkovich M (2003) Cyp26C1 encodes a novel retinoic acid-metabolizing enzyme expressed in the hindbrain, inner ear, first branchial arch and tooth buds during murine development. *Gene Expr Patterns* **3**, 449-454.

Taimi M, Helvig C, Wisniewski J, Ramshaw H, White J, Amad M, Korczak B & Petkovich M (2004) A novel human cytochrome P450, CYP26C1, involved in metabolism of 9-cis and all-trans isomers of retinoic acid. *J Biol Chem* **279**, 77-85.

Takada S, Stark KL, Shea MJ, Vassileva G, McMahon JA & McMahon AP (1994) Wnt-3a regulates somite and tail bud formation in the mouse embryo. *Genes Dev* **8**, 174-189.

Takao Y, Akazawa S, Matsumoto K, Takino H, Akazawa M, Trocino RA, Maeda Y, Okuno S, Kawasaki E, Uotani S & et al. (1993) Glucose transporter gene expression in rat conceptus during high glucose culture. *Diabetologia* **36**, 696-706.

Teerlink T, Copper MP, Klaassen I & Braakhuis BJ (1997) Simultaneous analysis of retinol, all-trans- and 13-cis-retinoic acid and 13-cis-4-oxoretinoic acid in plasma by liquid chromatography using on-column concentration after single-phase fluid extraction. *J Chromatogr B Biomed Sci Appl* **694**, 83-92.

Tesone M, Ladenheim RG, Oliveira-Filho RM, Chiauzzi VA, Foglia VG & Charreau EH (1983) Ovarian dysfunction in streptozotocin-induced diabetic rats. *Proc Soc Exp Biol Med* **174**, 123-130.

Thaller C & Eichele G (1987) Identification and spatial distribution of retinoids in the developing chick limb bud. *Nature* **327**, 625-628.

Tran S, Chen YW, Chenier I, Chan JS, Quaggin S, Hebert MJ, Ingelfinger JR & Zhang SL (2008) Maternal diabetes modulates renal morphogenesis in offspring. *J Am Soc Nephrol* **19**, 943-952.

Trocino RA, Akazawa S, Takino H, Takao Y, Matsumoto K, Maeda Y, Okuno S & Nagataki S (1994) Cellular-tissue localization and regulation of the GLUT-1 protein in both the embryo and the visceral yolk sac from normal and experimental diabetic rats during the early postimplantation period. *Endocrinology* **134**, 869-878.

Tse HK, Leung MB, Woolf AS, Menke AL, Hastie ND, Gosling JA, Pang CP & Shum AS (2005) Implication of Wt1 in the pathogenesis of nephrogenic failure in a mouse model of retinoic acid-induced caudal regression syndrome. *Am J Pathol* **166**, 1295-1307.

Tuitoek PJ, Ritter SJ, Smith JE & Basu TK (1996a) Streptozotocin-induced diabetes lowers retinol-binding protein and transthyretin concentrations in rats. *Br J Nutr* **76**, 891-897.

Tuitoek PJ, Ziari S, Tsin AT, Rajotte RV, Suh M & Basu TK (1996b) Streptozotocin-induced diabetes in rats is associated with impaired metabolic availability of vitamin A (retinol). *Br J Nutr* **75**, 615-622.

Uehara M, Yashiro K, Mamiya S, Nishino J, Chambon P, Dolle P & Sakai Y (2007) CYP26A1 and CYP26C1 cooperatively regulate anterior-posterior patterning of the developing brain and the production of migratory cranial neural crest cells in the mouse. *Dev Biol* **302**, 399-411.

Ulven SM, Gundersen TE, Weedon MS, Landaas VO, Sakhi AK, Fromm SH, Geronimo BA, Moskaug JO & Blomhoff R (2000) Identification of endogenous retinoids, enzymes, binding proteins, and receptors during early postimplantation development in mouse: important role of retinal dehydrogenase type 2 in synthesis of all-trans-retinoic acid. *Dev Biol* **220**, 379-391.

Viana M, Herrera E & Bonet B (1996) Teratogenic effects of diabetes mellitus in the rat. Prevention by vitamin E. *Diabetologia* **39**, 1041-1046.

Vilar J, Lalou C, Duong VH, Charrin S, Hardouin S, Raulais D, Merlet-Benichou C & Lelievre-Pegorier M (2002) Midkine is involved in kidney development and in its regulation by retinoids. *J Am Soc Nephrol* **13**, 668-676.

Vlangos CN, O'Connor BC, Morley MJ, Krause AS, Osawa GA & Keegan CE (2009) Caudal regression in adrenocortical dysplasia (acd) mice is caused by telomere dysfunction with subsequent p53-dependent apoptosis. *Dev Biol* **334**, 418-428.

Wagner M, Han B & Jessell TM (1992) Regional differences in retinoid release from embryonic neural tissue detected by an in vitro reporter assay. *Development* **116**, 55-66.

Wagner E, McCaffery P & Drager UC (2000) Retinoic acid in the formation of the dorsoventral retina and its central projections. *Dev Biol* **222**, 460-470.

Wako Y, Suzuki K, Goto Y & Kimura S (1986) Vitamin A transport in plasma of diabetic patients. *Tohoku J Exp Med* **149**, 133-143.

Wang Q & Moley KH (2010) Maternal diabetes and oocyte quality. *Mitochondrion* **10**, 403-410.

Wang Y, Zolfaghari R & Ross AC (2002) Cloning of rat cytochrome P450RAI (CYP26) cDNA and regulation of its gene expression by all-trans-retinoic acid in vivo. *Arch Biochem Biophys* **401**, 235-243.

Weigensberg MJ, Garcia-Palmer FJ & Freinkel N (1990) Uptake of myo-inositol by early-somite rat conceptus. Transport kinetics and effects of hyperglycemia. *Diabetes* **39**, 575-582.

Weksler-Zangen S, Yaffe P & Ornoy A (2003) Reduced SOD activity and increased neural tube defects in embryos of the sensitive but not of the resistant Cohen diabetic rats cultured under diabetic conditions. *Birth Defects Res A Clin Mol Teratol* **67**, 429-437.

Wendler CC, Schmoldt A, Flentke GR, Case LC, Quadro L, Blaner WS, Lough J & Smith SM (2003) Increased fibronectin deposition in embryonic hearts of retinol-binding protein-null mice. *Circ Res* **92**, 920-928.

Wentzel P, Gareskog M & Eriksson UJ (2005) Folic acid supplementation diminishes diabetes- and glucose-induced dysmorphogenesis in rat embryos in vivo and in vitro. *Diabetes* **54**, 546-553.

Wentzel P, Thunberg L & Eriksson UJ (1997) Teratogenic effect of diabetic serum is prevented by supplementation of superoxide dismutase and N-acetylcysteine in rat embryo culture. *Diabetologia* **40**, 7-14.

Wentzel P, Welsh N & Eriksson UJ (1999) Developmental damage, increased lipid peroxidation, diminished cyclooxygenase-2 gene expression, and lowered prostaglandin E2 levels in rat embryos exposed to a diabetic environment. *Diabetes* **48**, 813-820.

Wentzel P, Wentzel CR, Gareskog MB & Eriksson UJ (2001) Induction of embryonic dysmorphogenesis by high glucose concentration, disturbed inositol metabolism, and inhibited protein kinase C activity. *Teratology* **63**, 193-201.

Werner EA & DeLuca HF (2001) Metabolism of a physiological amount of all-trans-retinol in the vitamin A-deficient rat. *Arch Biochem Biophys* **393**, 262-270.

White JA, Beckett-Jones B, Guo YD, Dilworth FJ, Bonasoro J, Jones G & Petkovich M (1997) cDNA cloning of human retinoic acid-metabolizing enzyme (hP450RAI) identifies a novel family of cytochromes P450. *J Biol Chem* **272**, 18538-18541.

White JA, Guo YD, Baetz K, Beckett-Jones B, Bonasoro J, Hsu KE, Dilworth FJ, Jones G & Petkovich M (1996) Identification of the retinoic acid-inducible all-trans-retinoic acid 4-hydroxylase. *J Biol Chem* **271**, 29922-29927.

White JA, Ramshaw H, Taimi M, Stangle W, Zhang A, Everingham S, Creighton S, Tam SP, Jones G & Petkovich M (2000a) Identification of the human cytochrome P450, P450RAI-2, which is predominantly expressed in the adult cerebellum and is responsible for all-trans-retinoic acid metabolism. *Proc Natl Acad Sci U S A* **97**, 6403-6408.

White JC, Highland M, Kaiser M & Clagett-Dame M (2000b) Vitamin A deficiency results in the dose-dependent acquisition of anterior character and shortening of the caudal hindbrain of the rat embryo. *Dev Biol* **220**, 263-284.

White JC, Shankar VN, Highland M, Epstein ML, DeLuca HF & Clagett-Dame M (1998) Defects in embryonic hindbrain development and fetal resorption resulting from vitamin A deficiency in the rat are prevented by feeding pharmacological levels of all-trans-retinoic acid. *Proc Natl Acad Sci U S A* **95**, 13459-13464.

Wilkinson DG, Bhatt S & Herrmann BG (1990) Expression pattern of the mouse T gene and its role in mesoderm formation. *Nature* **343**, 657-659.

World Health Organisation DoNDS (1999) Definition, Diagnosis and Classification of Diabetes Mellitus and its Complications.

Wyman A, Pinto AB, Sheridan R & Moley KH (2008) One-cell zygote transfer from diabetic to nondiabetic mouse results in congenital malformations and growth retardation in offspring. *Endocrinology* **149**, 466-469.

Yamaguchi TP, Takada S, Yoshikawa Y, Wu N & McMahon AP (1999) T (Brachyury) is a direct target of Wnt3a during paraxial mesoderm specification. *Genes Dev* **13**, 3185-3190.

Yamamoto Y, Zolfaghari R & Ross AC (2000) Regulation of CYP26 (cytochrome P450RAI) mRNA expression and retinoic acid metabolism by retinoids and dietary vitamin A in liver of mice and rats. *FASEB J* **14**, 2119-2127.

Yamashita H, Shao J, Qiao L, Pagliassotti M & Friedman JE (2003) Effect of spontaneous gestational diabetes on fetal and postnatal hepatic insulin resistance in Lepr(db/+) mice. *Pediatr Res* **53**, 411-418.

Yang Q, Graham TE, Mody N, Preitner F, Peroni OD, Zabolotny JM, Kotani K, Quadro L & Kahn BB (2005) Serum retinol binding protein 4 contributes to insulin resistance in obesity and type 2 diabetes. *Nature* **436**, 356-362.

Yang X, Borg LA & Eriksson UJ (1995) Altered mitochondrial morphology of rat embryos in diabetic pregnancy. *Anat Rec* **241**, 255-267.

Yang X, Borg LA & Eriksson UJ (1997) Altered metabolism and superoxide generation in neural tissue of rat embryos exposed to high glucose. *Am J Physiol* **272**, E173-180.

Yashiro K, Zhao X, Uehara M, Yamashita K, Nishijima M, Nishino J, Saijoh Y, Sakai Y & Hamada H (2004) Regulation of retinoic acid distribution is required for proximodistal patterning and outgrowth of the developing mouse limb. *Dev Cell* **6**, 411-422.

Ybot-Gonzalez P, Cogram P, Gerrelli D & Copp AJ (2002) Sonic hedgehog and the molecular regulation of mouse neural tube closure. *Development* **129**, 2507-2517.

Yoshikawa Y, Fujimori T, McMahon AP & Takada S (1997) Evidence that absence of Wnt-3a signaling promotes neuralization instead of paraxial mesoderm development in the mouse. *Dev Biol* **183**, 234-242.

Yu J, Yu L, Bugawan TL, Erlich HA, Barriga K, Hoffman M, Rewers M & Eisenbarth GS (2000) Transient antiislet autoantibodies: infrequent occurrence and lack of association with "genetic" risk factors. *J Clin Endocrinol Metab* **85**, 2421-2428.

Yu Y, Singh U, Shi W, Konno T, Soares MJ, Geyer R & Fundele R (2008) Influence of murine maternal diabetes on placental morphology, gene expression, and function. *Arch Physiol Biochem* **114**, 99-110.

Zaken V, Kohen R & Ornoy A (2001) Vitamins C and E improve rat embryonic antioxidant defense mechanism in diabetic culture medium. *Teratology* **64**, 33-44.

Zhang M, Chen W, Smith SM & Napoli JL (2001) Molecular characterization of a mouse short chain dehydrogenase/reductase active with all-trans-retinol in intact cells, mRDH1. *J Biol Chem* **276**, 44083-44090.

Zhang Y, Zolfaghari R & Ross AC (2010) Multiple retinoic acid response elements cooperate to enhance the inducibility of CYP26A1 gene expression in liver. *Gene* **464**, 32-43.

Figures

Figure 3.1 Expression of 3 subtypes of *Cyp26* in E9.0 embryos of non-diabetic and diabetic mice detected by whole mount *in situ* hybridization.

A *Cyp26a1* expression in E9.0 embryo of non-diabetic mouse. *Cyp26a1* expression is observed anteriorly in the cranial mesenchyme (CrM), cervical mesenchyme (CeM), maxillary and mandibular component of the first branchial arch (FBA) and the epithelial lining of the maxillo-mandibular cleft (MMC). Posteriorly, strong expression is found in the tail bud region (TB) of the embryo.

B *Cyp26a1* expression in E9.0 embryo of diabetic mouse. There is prominent down-regulation of *Cyp26a1* in all expression domains in the embryo of diabetic mouse in comparison to the embryo of non-diabetic mouse as shown in Figure A.

C *Cyp26a1* expression in E9.0 embryo of non-diabetic mouse. *Cyp26b1* is strongly expressed in the entire rhombomere (r) 5 to 6 and in the basal part of rhombomeres 2 to 4 in the embryo. Weak expression is also observed in the heart (Ht), caudal branchial arch (BA) and in tissues between the developing somites (S).

D *Cyp26b1* expression in E9.0 embryo of diabetic mouse. There is no observable difference in *Cyp26b1* expression in the embryo of diabetic mouse in comparison to the embryo of non-diabetic mouse as shown in Figure C.

E *Cyp26c1* expression in E9.0 embryo of non-diabetic mouse. Anteriorly, *Cyp26c1* expression pattern is similar to that of *Cyp26a1*, with strong expression in the cranial mesenchyme, cervical mesenchyme, first branchial arch and maxillo-mandibular cleft. Prominent signal is also observed in rhombomere 2 of the embryo. However, there is no detectable expression in the tail bud region.

F *Cyp26c1* expression in E9.0 embryo of non-diabetic mouse. There is no observable difference in *Cyp26c1* expression in the embryo of diabetic mouse in comparison to the embryo of non-diabetic mouse as shown in Figure E.

Labels:				
	BA	Branchial arch	CeM	Cervical mesenchyme
	CrM	Cranial mesenchyme	FBA	First branchial arch
	Ht	Heart	MMC	Maxillo-mandibular cleft
	r	Rhombomere	S	Somite
	TB	Tail bud region		

Scale bar: A-F 0.4 mm

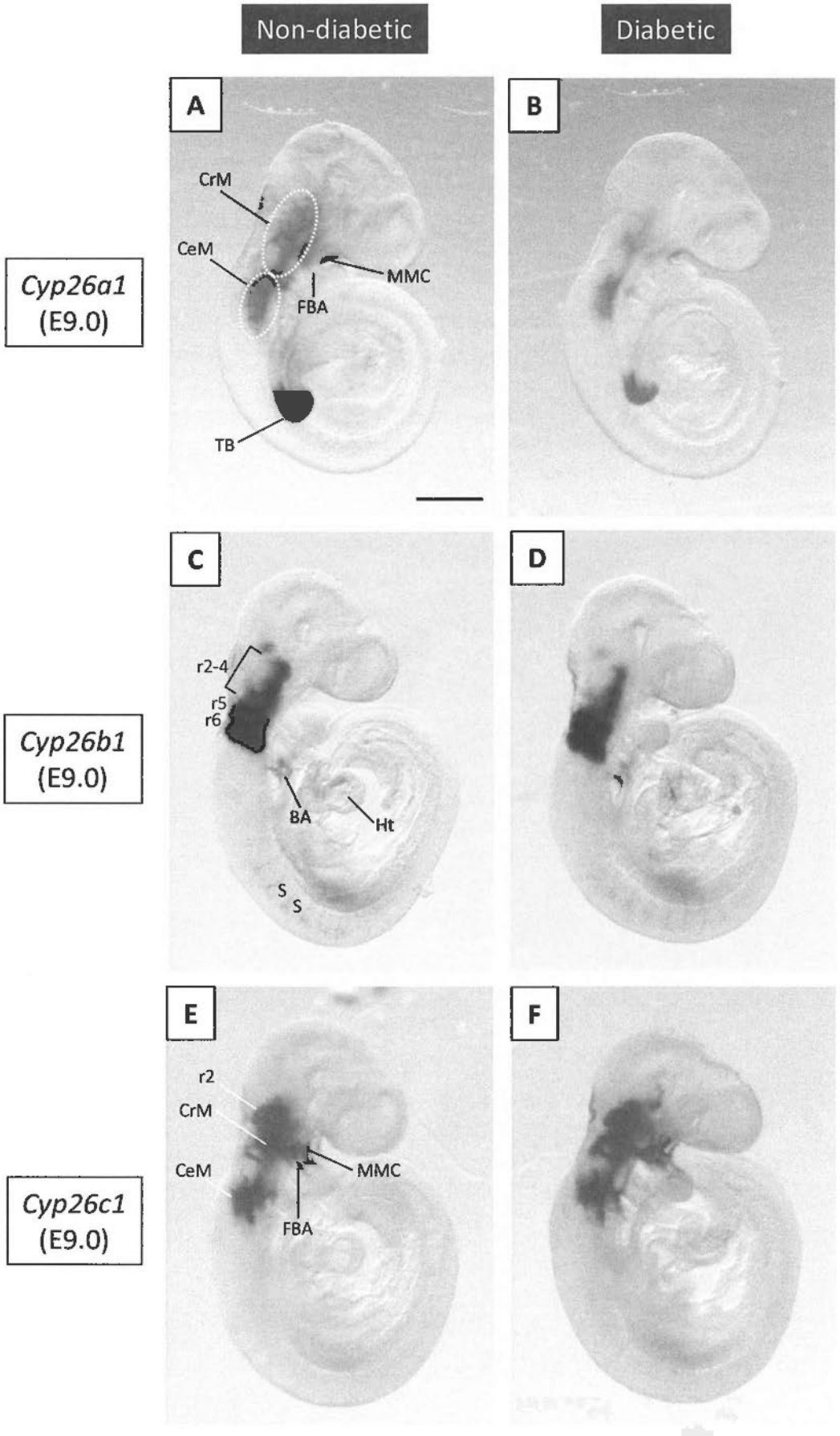
Non-diabetic
Diabetic
A
B
C
D
E
F
Cyp26a1 (E9.0)
Cyp26b1 (E9.0)
Cyp26c1 (E9.0)
CrM
CeM
MMC
FBA
TB
r2-4
r5
r6
BA
Ht
S
S
r2
CrM
CeM
MMC
FBA

Figure 3.2 Expression of *Cyp26a1* in E7.0 and E8.0 embryos of non-diabetic and diabetic mice detected by whole mount *in situ* hybridization.

A *Cyp26a1* expression in E7.0 embryo of non-diabetic mouse. *Cyp26a1* is highly expressed in the headfold region (HF) and the yolk sac (YS) endoderm layer of the embryo.

B *Cyp26a1* expression in E7.0 embryo of diabetic mouse. There is prominent down-regulation of *Cyp26a1* in all expression domains in the embryo of diabetic mouse in comparison with the embryo of non-diabetic mouse as shown in Figure A.

C *Cyp26a1* expression in E8.0 embryo of non-diabetic mouse. *Cyp26a1* is expressed in the anterior neural fold (ANF), posterior neural plate (PNP) and tail bud at the caudal extremity of the embryo.

D *Cyp26a1* expression in E8.0 embryos of diabetic mouse. There is prominent down-regulation of *Cyp26a1* in all expression domains in the embryo of diabetic mouse in comparison with the embryo of non-diabetic mouse as shown in Figure C.

Labels:	ANF	Anterior neural fold
	HF	Headfold
	PNP	Posterior neural plate
	TB	Tail bud
	YS	Yolk sac endoderm

Scale bar:	A-B	0.1 mm
	C-D	0.2 mm

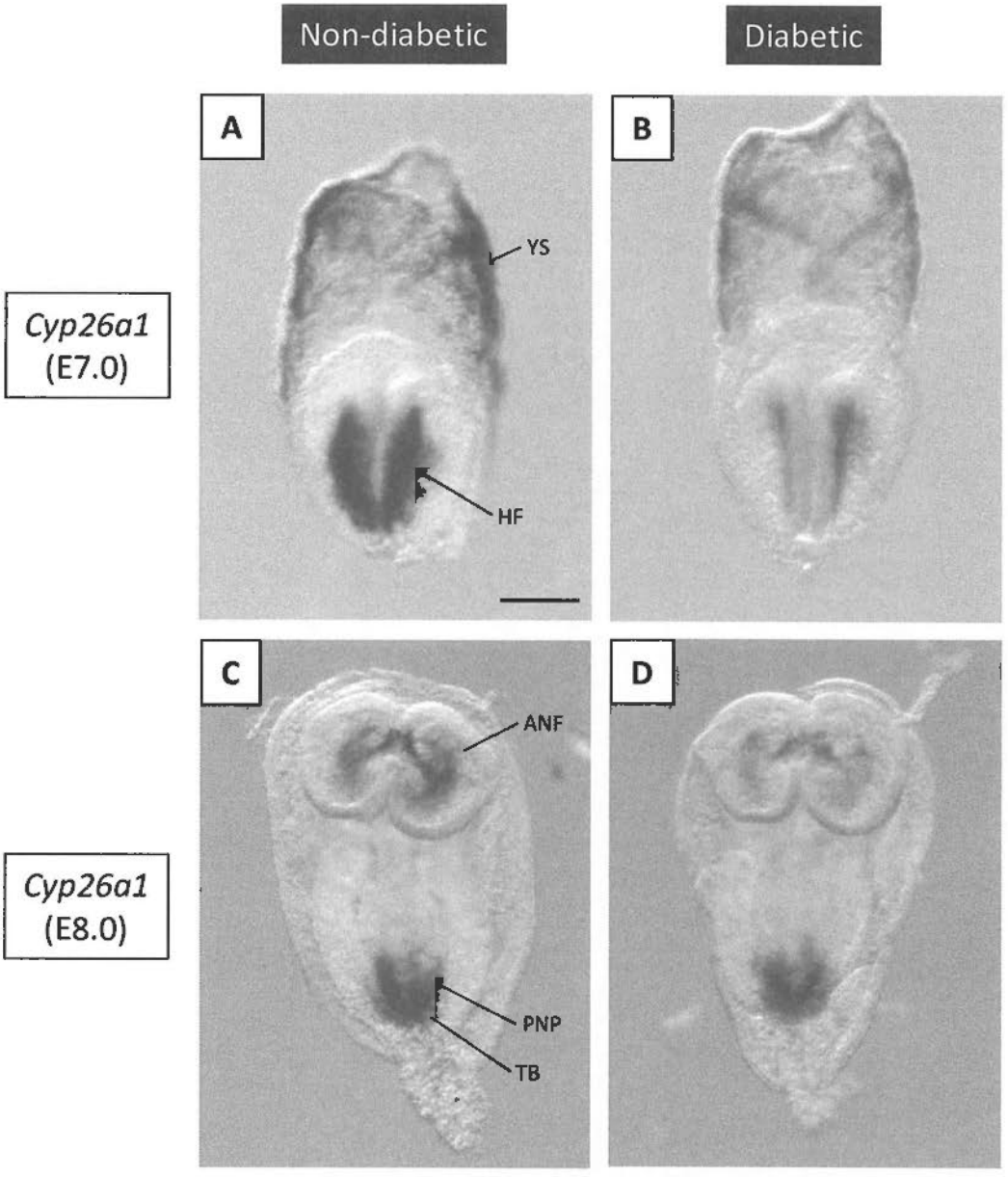
Non-diabetic
Diabetic
A
B
C
D
YS
HF
ANF
PNP
TB
Cyp26a1
(E7.0)
Cyp26a1
(E8.0)

Figure 3.3 Expression of *Cyp26a1* detected by whole mount *in situ* hybridization in embryos of non-diabetic and diabetic mice at different time points (0, 2, 4, 8 and 12 hr) after treatment with 50 mg/kg RA on E9.0.

A *Cyp26a1* expression in the embryo of non-diabetic mouse prior to RA treatment. *Cyp26a1* was expressed in the cranial mesenchyme (CrM), cervical mesenchyme (CeM), maxillary and mandibular component of the first branchial arch (FBA), maxillo-mandibular cleft (MMC) and the tail bud region (TB) of the embryo.

B *Cyp26a1* expression in the embryo of non-diabetic mouse at 2 hr after RA treatment. There was prominent increase in the expression level and expansion of the expression domains of *Cyp26a1* to multiple sites, such as the dorsal part of the neural tube (NT), the heart (Ht) and the body wall (BW) in the trunk region of the embryo. Expression at the posterior region had expanded from the tail bud to presomitic tissues and the allantois (Al).

C *Cyp26a1* expression in the embryo of non-diabetic mouse at 4 hr after RA treatment. The expression domain of *Cyp26a1* was similar to the embryo at 2 hr, with the expression level further intensified at this time point.

D *Cyp26a1* expression in the embryo of non-diabetic mouse at 8 hr after RA treatment. The up-regulation of *Cyp26a1* reached the peak at this time point, with high levels of expression in almost all domains.

E *Cyp26a1* expression in the embryo of non-diabetic mouse at 12 hr after RA treatment. The expression of *Cyp26a1* had dramatically reduced to basal levels, with complete switching off of *Cyp26a1* in ectopic sites. The expression domain was similar to the embryo without RA treatment as shown in Figure A.

F *Cyp26a1* expression in the embryo of diabetic mouse prior to RA treatment. Reduced expression of *Cyp26a1* in all expression domains, particularly easily noticeable in the anterior region, in comparison with the embryo of non-diabetic mouse as shown in Figure A.

G-I *Cyp26a1* expression in embryos of diabetic mice at 2 (G), 4 (H) and 8 hr (I) respectively after RA treatment. The extent of up-regulation of *Cyp26a1* in the embryo of diabetic mouse was not as high as the embryo of the non-diabetic group at the same time point.

J *Cyp26a1* expression in the embryo of diabetic mouse at 12 hr RA treatment. Similar down-regulation of *Cyp26a1* was found, but the extent of reduction was not as much as the embryo of non-diabetic group as shown in Figure E.

Labels:	Al	Allantois
	BW	Body wall
	CeM	Cervical mesenchyme
	CrM	Cranial mesenchyme
	FBA	First branchial arch
	Ht	Heart
	MMC	Maxillo-mandibular cleft
	NT	Neural tube
	TB	Tail bud

Scale bar:	A-J	0.45 mm

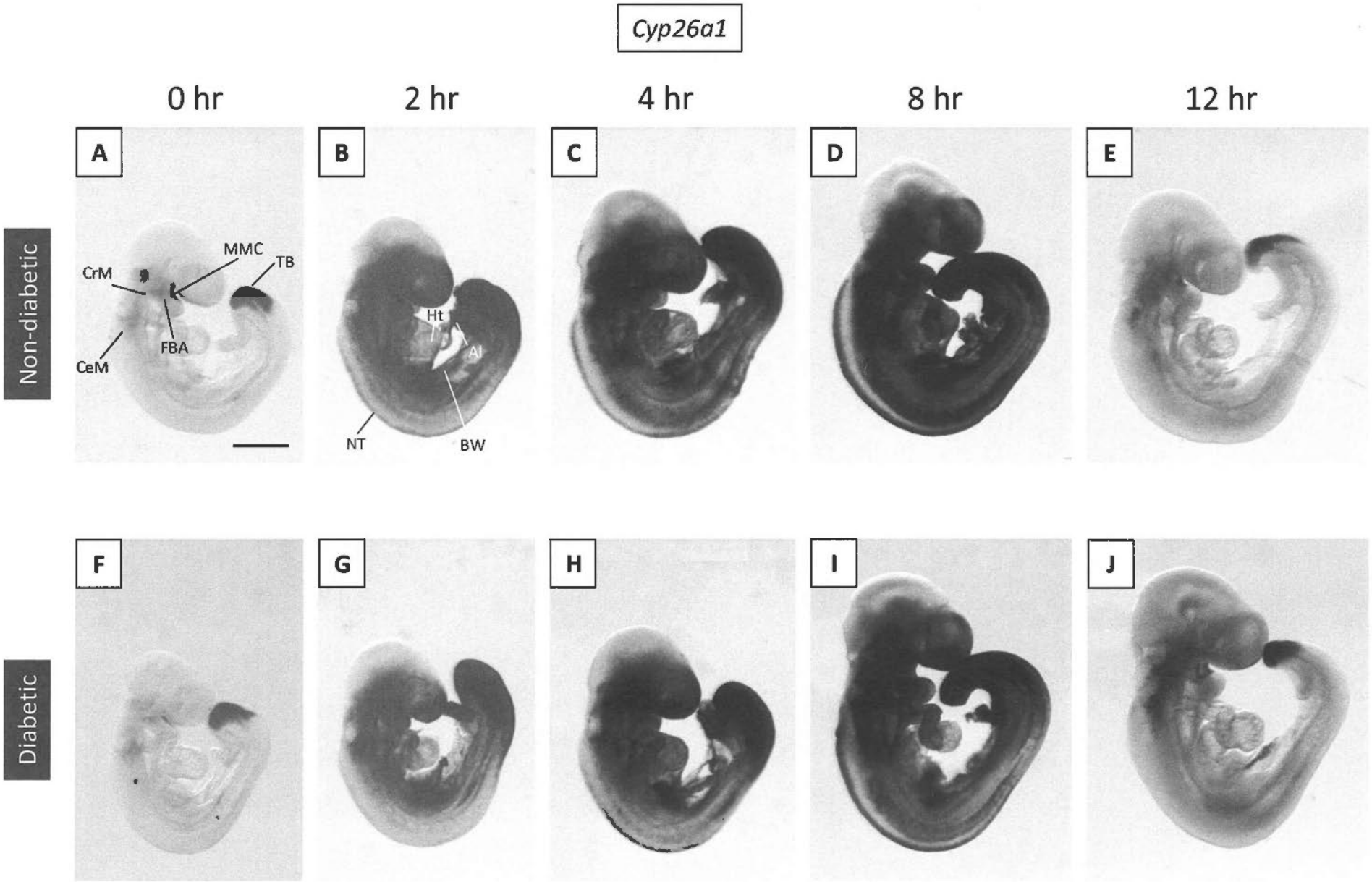
Cyp26a1
0 hr
2 hr
4 hr
8 hr
12 hr
Non-diabetic
Diabetic
A
B
C
D
E
F
G
H
I
J
MMC
TB
CrM
FBA
CeM
Ht
AI
NT
BW

Figure 3.4 Vibratome sections of the embryo of non-diabetic mouse at 2 hr after treatment with 50 mg/kg RA on E9.0 that had been subjected to whole mount *in situ* hybridization to detect *Cyp26a1*.

A Embryo for showing the level of sections.

B Section of the embryo cut at the level of the optic vesicle (Level B as shown in Figure 3.4A). There was so signal in the forebrain (FB), hindbrain (HB) and optic vesicle (OpV). However, intense signal was found in the surface ectoderm (SE) overlying these structures and weak signal in the cranial mesenchyme (CrM) surrounding these structures.

C Section of the embryo cut at the level of the maxillary component of the first branchial arch (Level C as shown in Figure A). Other than the surface ectoderm overlying the forebrain, intense expression was found in the epithelial lining of the maxillo-mandibular cleft (red arrowhead) of the first branchial arch (FBA) and the lining of the foregut diverticulum (FGD). Weak expression was observed in the cranial mesenchyme surrounding the forebrain and hindbrain, and in the mesodermal component of the first branchial arch.

D Section of the embryo cut at the level of the heart (Level D as shown in Figure A). High level of expression was found on the body wall (blue arrowhead) overlying the pericardial cavity of the heart (Ht) but not within the heart of the embryo. Weak staining was also found in the mesenchyme surrounding the neural tube (NT) and the foregut. Again, no staining was observed in the neural tube.

E Section of the embryo cut at the level of the mid-trunk (Level E as shown in Figure A). Low level of expression was detected at the midgut diverticulum (MGD). Stronger signal was found in the lateral body wall.

F Section of the embryo cut at the level of the lower trunk (Level F as shown in Figure A). Low level of expression was found within patches of cells in the neural tube and the dorsal aorta (DA), and around the umbilical vein (UV). Intense signal was observed in the hindgut diverticulum (HGD) and in the ventral body wall.

G Section of the embryo cut at the level just caudal to the allantois (Level G as shown in Figure A). Very strong expression was observed in the dorsal structures including the posterior neural plate (PNP) and the underlying mesenchyme. Within the caudal extremity of the hindgut diverticulum, the signal in the dorsal half was strong, whereas the ventral half was much weaker. Weak expression was also found in the tissue surrounding the dorsal aorta (DA), caudal diverticulum of intra-embryonic coelomic cavity (CC) and the vitelline artery (VA).

H Section of the embryo cut at the level of the tail bud (Level H as shown in Figure A). Intense homogenous staining was found in the entire tail bud.

Labels:	CC	Coelomic cavity
	CrM	Cranial mesenchyme
	DA	Dorsal aorta
	FB	Forebrain
	FBA	First branchial arch
	FGD	Foregut diverticulum
	HB	Hindbrain
	Ht	Heart
	HGD	Hindgut diverticulum
	MGD	Midgut diverticulum
	NT	Neural tube
	OpV	Optic vesicle
	PNP	Posterior neural plate
	SE	Surface ectoderm
	TB	Tail bud
	UV	Umbilical vein
	VA	Vitelline artery

Symbols:	Blue arrowhead	Body wall
	Red arrowhead	Epithelial lining of the maxillo-mandibular cleft

Cyp26a1 (2 hr)

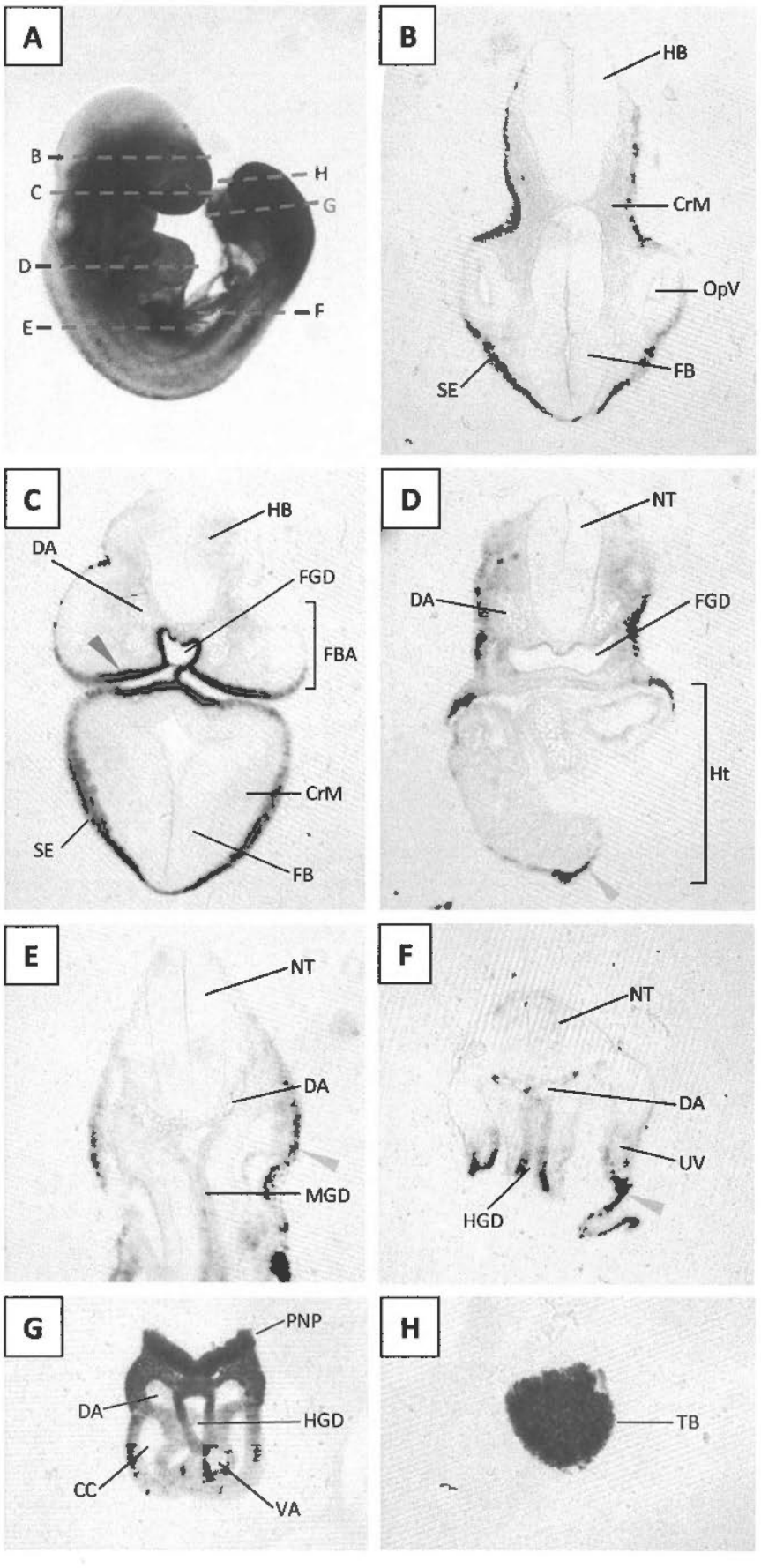
A
B
C
D
E
F
G
H
B
HB
CrM
OpV
FB
SE
C
HB
DA
FGD
FBA
CrM
SE
FB
D
NT
DA
FGD
Ht
E
NT
DA
MGD
F
NT
DA
UV
HGD
G
PNP
DA
HGD
CC
VA
H
TB

Figure 3.5 Vibratome sections of the embryo of non-diabetic mouse at 8 hr after treatment with 50 mg/kg RA on E9.0 that had been subjected to whole mount *in situ* hybridization to detect *Cyp26a1*.

A Embryo for showing the level of sections.

B Section of the embryo cut at the level of the optic vesicle (Level B as shown in Figure A). There was so signal in the forebrain (FB), hindbrain (HB) and optic vesicle (OpV). However, *Cyp26a1* was expressed in the cranial mesenchyme (CrM) surrounding these structures.

C Section of the embryo cut at the level of the otic vesicle (Level C as shown in Figure A). There was no signal in the hindbrain and otic vesicle (OtV). However, *Cyp26a1* was highly expressed in the mesenchyme surrounding these structures and also in the mesodermal component of the first branchial arch (FBA). Intense expression was found in the epithelial lining of the first branchial pouch (FBP).

D Section of the embryo cut at the level of the heart (Level D as shown in Figure A). Intense signal was found in the body wall (blue arrowhead) overlying the pericardial cavity of the heart while weak expression was found in the ventricular chamber (VC) of the heart of the embryo. High level of staining was also found in the mesenchyme. Signal was detected at the dorsal midline of the neural tube (NT).

E Heart covered with body wall. High level of expression of *Cyp26a1* in the body wall covering the heart tube.

F Heart with body wall removed. Intense expression was only found in the aortic sac (AS) and bulbus cordis (BC) region, while weak expression was found it the ventricular chamber (VC) of the heart.

G Section of the embryo cut at the level of the forelimb bud (Level G as shown in Figure A). Strong expression was detected at the neural crest (NC) and in patches of cells in the middle and ventral portion of the neural tube. Intense signal was also found in the dermomyotome (DM), and in the lateral and ventral body wall, and in tissue surrounding the umbilical vein (UV). Very low level of expression could be detected in the midgut (MG). No signal was observed in the forelimb bud (FLB) mesenchyme.

H Section of the embryo cut at the level of the allantois (Level H as shown in Figure A). Strong but non-uniform expression of *Cyp26a1* was observed in the neural tube. Intense signal was also detected in the body wall, in tissues surrounding the umbilical vein and vitelline artery (VA) and in the allantois (Al). No signal was detected in the somitic mesoderm.

I Section of the embryo cut at the level of the tail bud (Level I as shown in Figure A). Intense staining was found in the posterior neuropore (PNP) and the tail bud (TB).

Labels:	Al	Allantois
	AS	Aortic sac
	BC	Bulbus cordis
	CrM	Cranial mesenchyme
	DA	Dorsal aorta
	DM	Dermomyotome
	FB	Forebrain
	FBA	First branchial arch
	FBP	First branchial pouch
	FLB	Forelimb bud
	FGD	Foregut diverticulum
	HB	Hindbrain
	Ht	Heart
	HGD	Hindgut diverticulum
	MGD	Midgut diverticulum
	NC	Neural crest
	NT	Neural tube
	OpV	Optic vesicle
	OtV	Otic vesicle
	PNP	Posterior neuropore
	TB	Tail bud
	UV	Umbilical vein
	VC	Ventricular chamber
	VA	Vitelline artery

Symbol: Blue arrowhead Body wall

Cyp26a1 (8 hr)

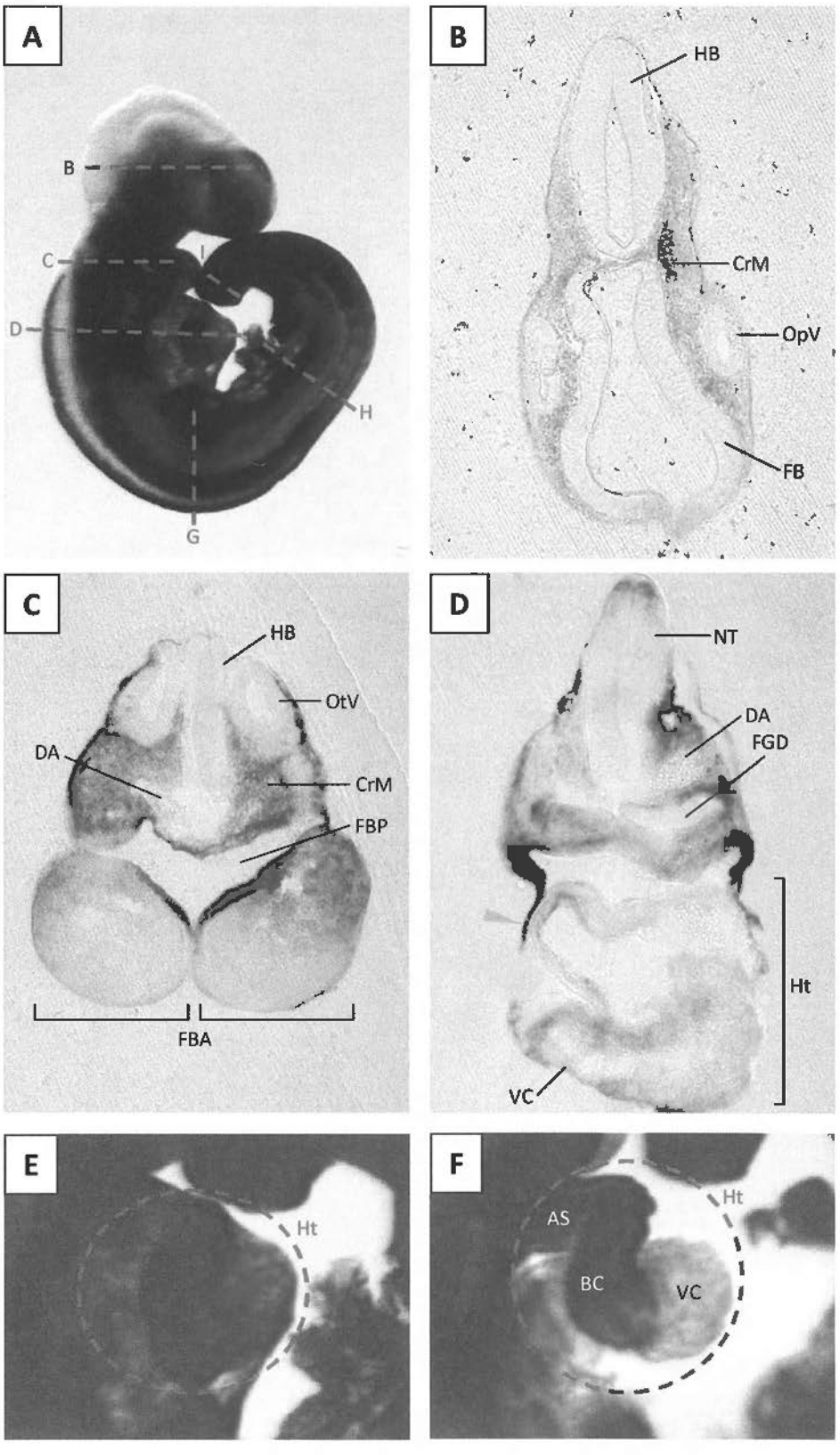
A
B
C
D
H
G
B
HB
CrM
OpV
FB
C
HB
OtV
DA
CrM
FBP
FBA
D
NT
DA
FGD
Ht
VC
E
Ht
F
Ht
AS
BC
VC

Cyp26a1 (8 hr)

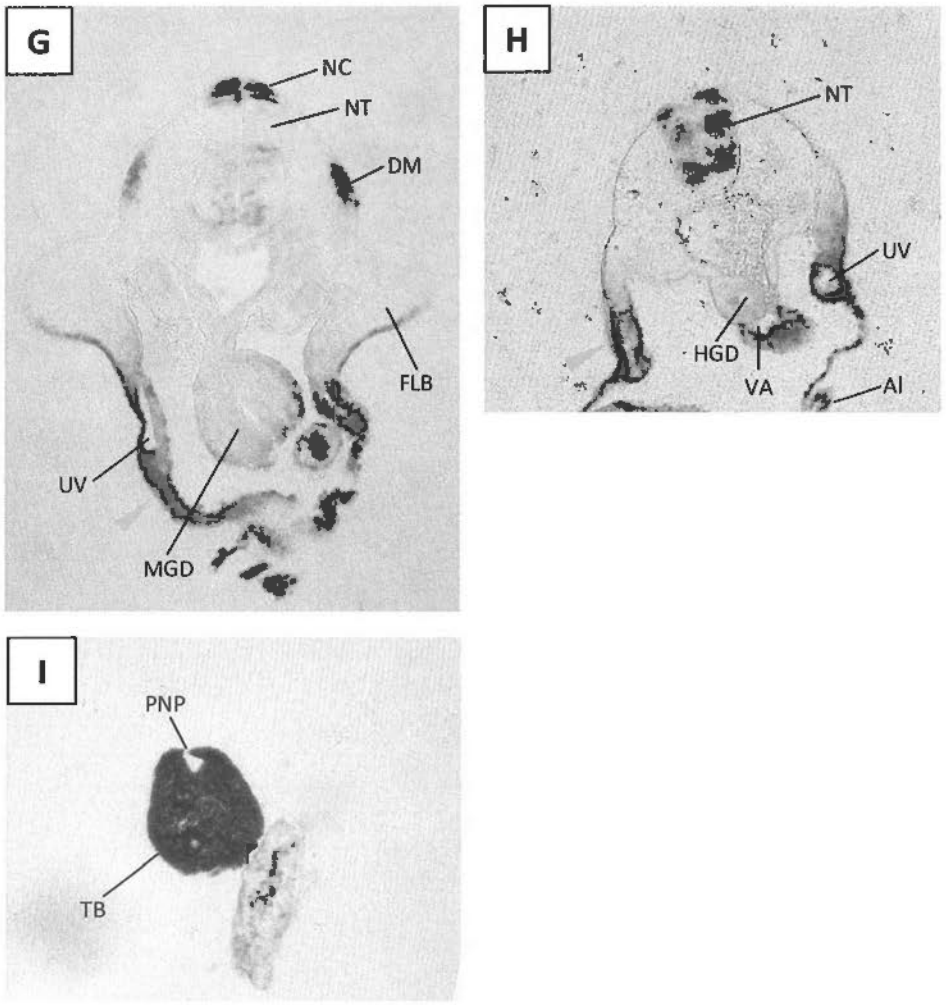

Figure 3.6 Expression of *Cyp26b1* detected by whole mount *in situ* hybridization in embryos of non-diabetic and diabetic mice at different time points (0, 2, 4, 8 and 12 hr) after treatment with 50 mg/kg RA on E9.0.

A *Cyp26b1* expression in the embryo of non-diabetic mouse prior to RA treatment. High level of expression was found in the hindbrain region at rhombomere (r)2 to 6. While expression spanned the entire rhombomeres 5 and 6, expression in rhombomeres 2-4 was restricted to the basal part. Weak signal was also detectable in the caudal branchial arch (BA), the heart (Ht) and in the tissue in between the somites (s). No signal was detected in the tail bud (TB) and the allantois (Al).

B *Cyp26b1* expression in the embryo of non-diabetic mouse at 2 hr after RA treatment. *Cyp26b1* expression was significantly up-regulated. Low level of expression was observed in the cranial mesenchyme (CrM) of the embryo. Intense expression was observed in the heart (Ht), along the ventral body. For the posterior region, obvious expression was found in the allantois (Al) of the embryo. On the other hand, the signal intensity and the domains in rhombomeres 2-4 appeared to have reduced.

C *Cyp26b1* expression in the embryo of non-diabetic mouse at 4 hr after RA treatment. The expression was further up-regulated, especially in the cranial mesenchymal tissue, the first branchial arch, in the entire trunk and also at the region connecting the allantois. Intense expression was found at the posterior presomitic (PS) region.

D *Cyp26b1* expression in the embryo of non-diabetic mouse at 8 hr after RA treatment. The expression generally was further intensified.

E *Cyp26b1* expression in the embryo of non-diabetic mouse at 12 hr after RA treatment. The expression had dramatically reduced, with complete switching off of *Cyp26b1* in ectopic sites. Rhombomeric expression was prominently decreased.

F *Cyp26b1* expression in the embryo of diabetic mouse prior to RA treatment. There was no observable difference in comparison with the embryo of non-diabetic mouse as shown in Figure 3.6A.

G-H *Cyp26b1* expression in the embryo of diabetic mouse at 2 (G) and 4 hr (H) after RA treatment. The extent of up-regulation of *Cyp26b1* was not as high as the embryo of non-diabetic group as shown in Figures B and C respectively.

I *Cyp26b1* expression in embryos of diabetic mice at 8 hr after RA treatment. Expression in embryos of diabetic pregnancy was very similar to the embryo of non-diabetic mouse as shown in Figure D.

J *Cyp26b1* expression in the embryo of non-diabetic mouse at 12 hr after RA treatment. Similar down-regulation of *Cyp26b1* was found, but the extent of reduction was not as much as the embryo of non-diabetic group as shown in Figure E.

Labels:	Al	Allantois
	CrM	Cranial mesenchyme
	Ht	Heart
	PS	Presomitic region
	r	rhombomere
	S	Somite
	TB	Tail bud

Scale bar:	A-J	0.45 mm

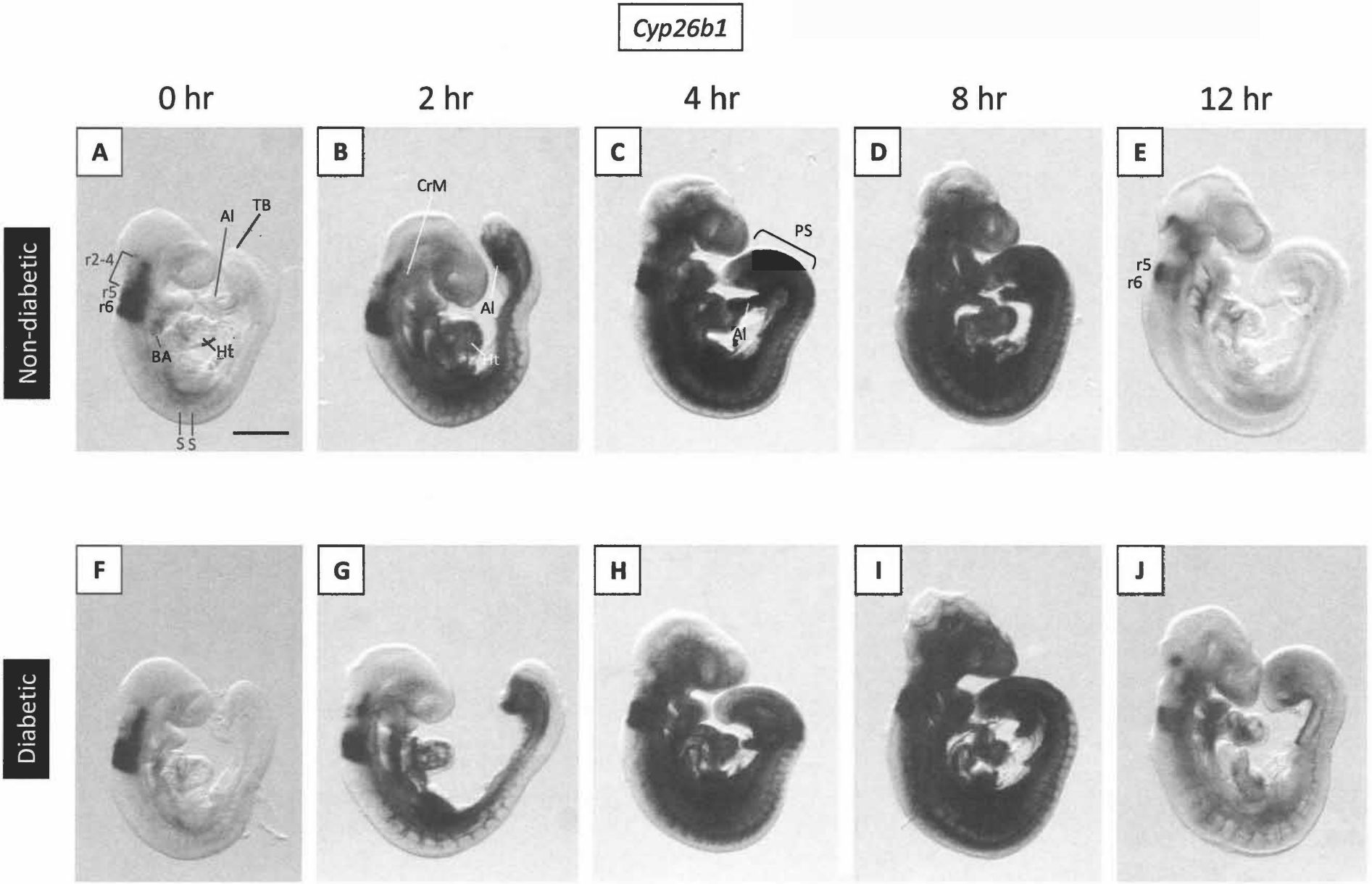
Cyp26b1
0 hr
2 hr
4 hr
8 hr
12 hr
Non-diabetic
Diabetic
A
B
C
D
E
F
G
H
I
J
TB
Al
r2-4
r5
r6
BA
Ht
S S
CrM
Al
Ht
PS
Al
r5
r6

Figure 3.7 Vibratome sections of the embryo of non-diabetic mouse at 2 hr after treatment with 50 mg/kg RA on E9.0 that had been subjected to whole mount *in situ* hybridization to detect *Cyp26b1*.

A Embryo for showing the level of sections.

B Section of the embryo cut at the level of the optic vesicle (Level B as shown in Figure A). Only weak expression was found in the cranial mesenchyme (CrM) surrounding the optic vesicle (OpV), and the forebrain (FB) and hindbrain (HB), which were devoid of any signal except in a band of cells in the mid-ventral region of rhombomere (r) 2.

C Section of the embryo cut at the level of rhombomere 5 (Level C as shown in Figure A). High level of expression was detected in the entire rhombomere 5 except the roof plate and floor plate. Signal was also observed in the endothelial lining of the dorsa aorta (DA) and the epithelial lining of the first branchial pouch (FBP). The mesodermal component of the first branchial arch (FBA) and the cranial mesenchyme did not have much signal.

D Section of the embryo cut at the level of heart (Level D as shown in Figure A). Intense signal was observed in the endothelial lining of dorsal aorta, and in the endocardial lining of the bulbus cordis (BC) and ventricular chamber (VC) of the heart (Ht). Signal was also readily observed in the mesenchyme surrounding the dorsal aorta and the foregut diverticulum (FGD). No signal can be detected in the neural tube (NT).

E Section of the embryo cut at the level just caudal to the heart (Level E as shown in Figure A). Intensive signal was found in the endothelial lining of the dorsal aorta and the cardinal vein (CV), and some patches of cells surrounding the neural tube.

F Section of the embryo cut at the level of the allantois (Level F as shown in Figure A). Posteriorly, high level of expression was observed in the ventral half of the body containing the vitelline artery (VA) and the coelomic cavity (CC), and also intense signal was detected in the allantois (Al). However, the neural tube and the underlying mesoderm, and the hindgut diverticulum was devoid of any signal.

Labels:	Al	Allantois
	BC	Bulbus cordis
	CrM	Cranial mesenchyme
	CV	Cardinal vein
	CC	Coelomic cavity
	DA	Dorsal aorta
	FB	Forebrain
	FBA	First branchial arch
	FBP	First branchial pouch
	FGD	Foregut diverticulum
	HB	Hindbrain
	HGD	Hindgut diverticulum
	Ht	Heart
	MGD	Midgut diverticulum
	NT	Neural tube
	OpV	Optic vesicle
	r	Rhombomere
	VA	Vitelline artery
	VC	Ventricular chamber

Cyp26b1 (2 hr)

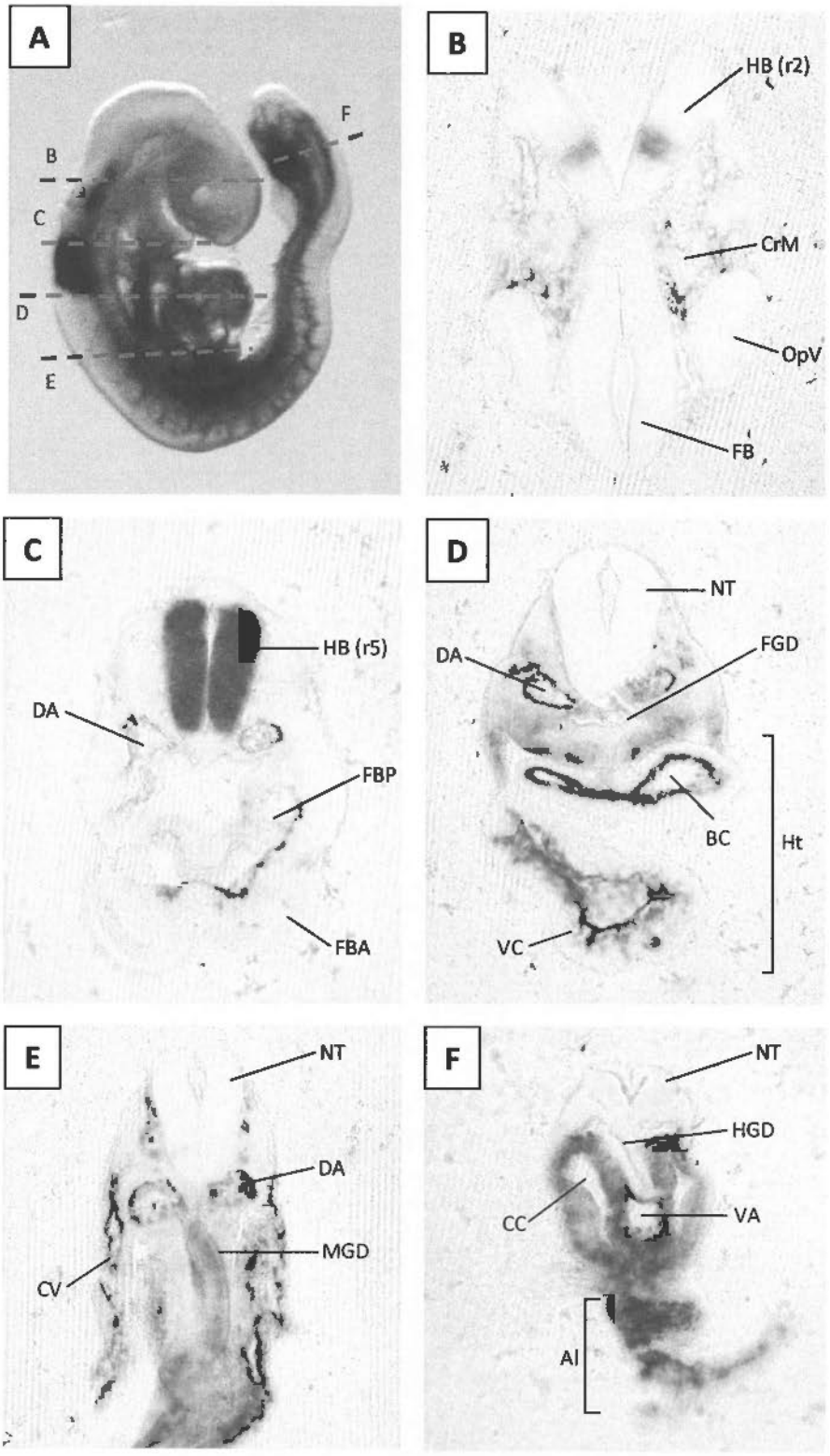
A
B
C
D
E
F
B
HB (r2)
CrM
OpV
FB
C
HB (r5)
DA
FBP
FBA
D
NT
DA
FGD
BC
Ht
VC
E
NT
DA
MGD
CV
F
NT
HGD
CC
VA
AI

Figure 3.8 Vibratome sections of the embryo of non-diabetic mouse at 8 hr after treatment with 50 mg/kg RA on E9.0 that had been subjected to whole mount *in situ* hybridization to detect *Cyp26b1*.

A Embryo for showing the level of sections.

B Section of the embryo cut at the level of the optic vesicle (Level B as shown in Figure A). Low level of expression was observed in the cranial mesenchyme (CrM) surrounding the forebrain (FB), hindbrain (HB) and optic vesicle (OpV). Within the mesenchyme, patches of cells, which appeared like developing blood vessels, were intensely stained.

C Section of the embryo cut at the level of the first branchial arch (Level C as shown in Figure A). Intense signal was observed in the endothelial lining of the dorsal aorta (DA) and in the developing blood vessels in the mesodermal layer surrounding the hindbrain and in the first branchial arch (FBA). Specific domains within rhombomere (r) 5 expressed low levels of *Cyp26b1*.

D Section of the embryo cut at the level of otic vesicle (Level D as shown in Figure A). There was high level of expression in the entire rhombomere 5 except the dorsal and ventral midline regions. Otic vesicle (Otv) lying adjacent to rhombomere 5 showed no signal. Strong signal was also observed in the endodermal layer of the foregut diverticulum (FGD) and also in discrete regions within the heart (Ht).

E Section of the embryo cut at the level of the forelimb bud (Level E as shown in Figure A). Specific cells in the ventrolateral region of the neural tube expressed high levels of *Cyp26b1*. High level of expression was also observed in the mesodermal layer of the forelimb bud (FLB) and endodermal layer of the midgut diverticulum (MGD). However, signal was not homogenous, with patches of cells showing intense signal.

F Section of the embryo cut at the level of the allantois (Level F as shown in Figure A). High level of expression was found in the somite (S). Intense signal was observed in the endothelial lining of the dorsal aorta, vitelline artery (VA) and the allantois (Al).

G Section of the embryo cut at the level of the tail bud (Level G as shown in Figure A). Only weak expression was observed in patches of cells within the tail bud.

Labels:	Al	Allantois
	CC	Coelomic cavity
	CrM	Cranial mesenchyme
	DA	Dorsal aorta
	FB	Forebrain
	FBA	First branchial arch
	FGD	Foregut diverticulum
	FLB	Forelimb bud
	Ht	Heart
	HB	Hindbrain
	HGD	Hindgut diverticulum
	MGD	Midgut diverticulum
	NT	Neural tube
	OpV	Optic vesicle
	OtV	Otic vesicle
	r	Rhombomere
	S	Somite
	TB	Tail bud
	VA	Vitelline artery

Cyp26b1 (8 hr)

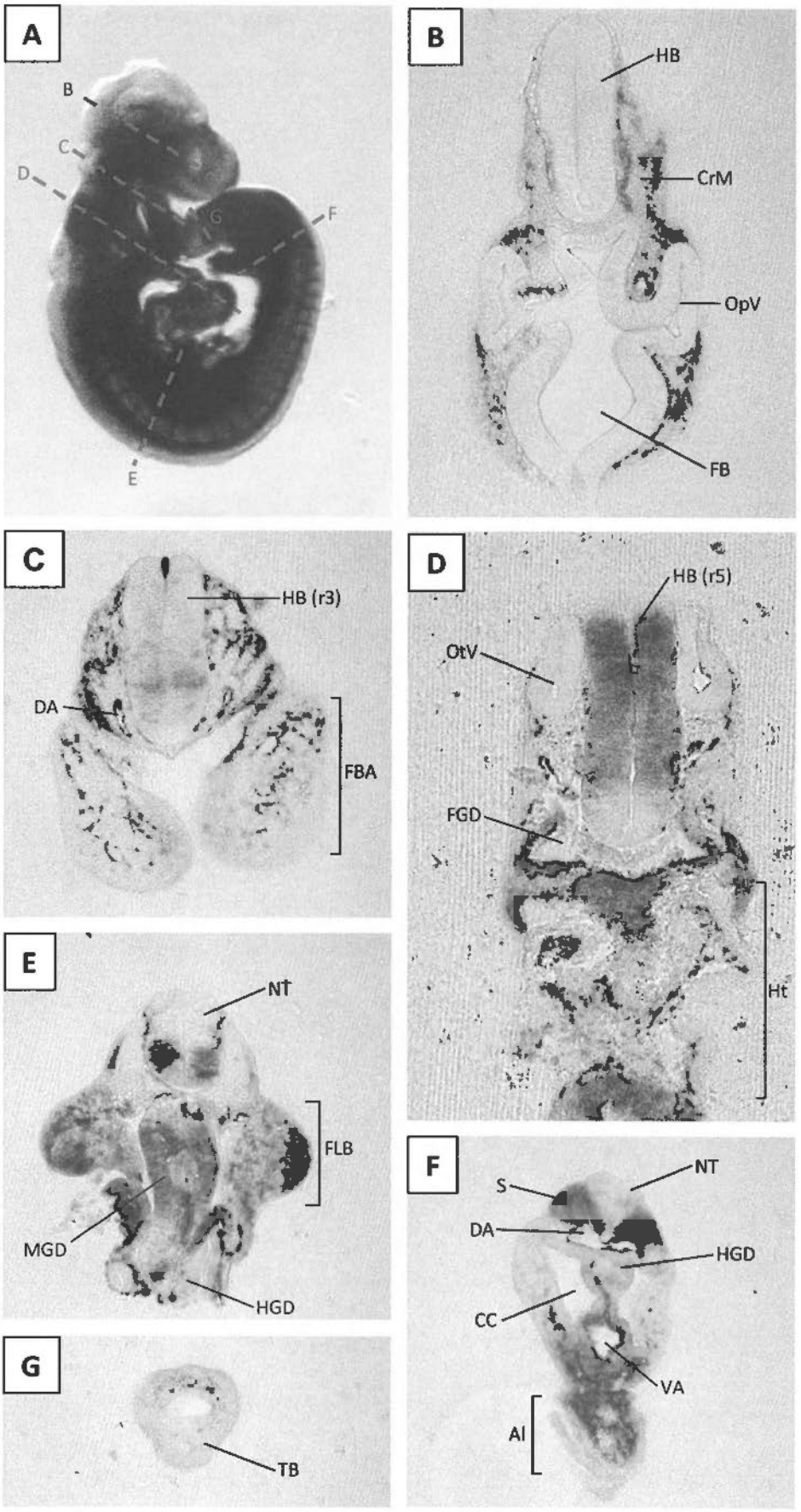
A
B
C
D
E
F
G
B
HB
CrM
OpV
FB
C
HB (r3)
DA
FBA
D
HB (r5)
OtV
FGD
Ht
E
NT
FLB
MGD
HGD
F
S
NT
DA
HGD
CC
VA
AI
G
TB

Figure 3.9 Expression of *Cyp26c1* detected by whole mount *in situ* hybridization in embryos of non-diabetic and diabetic mice at different time points (0, 2, 4, 8 and 12 hr) after treatment with 50 mg/kg RA on E9.0.

A *Cyp26c1* expression in the embryo of non-diabetic mouse prior to RA treatment. The expression pattern of *Cyp26c1* is similar to that of *Cyp26a1*. It was strongly expressed in the cranial mesenchyme (CrM), cervical mesenchyme (CeM), first branchial arch (FBA), maxillo-mandibular cleft (MMC). Strong signal was also observed in rhombomere (r) 2. However, it was not expressed in the tail bud (TB).

B *Cyp26c1* expression in the embryo of non-diabetic mouse at 2 hr after RA treatment. There was slight reduction in *Cyp26c1* expression.

C *Cyp26c1* expression in the embryo of non-diabetic mouse at 4 hr after RA treatment. There was prominent down-regulation of *Cyp26c1* in most expression domains except in rhombomere 2. Expression in the cervical mesenchyme had nearly switched off.

D *Cyp26c1* expression in the embryo of non-diabetic mouse at 8 hr after RA treatment. *Cyp26c1* had reduced to very low level in all expression domains, except at rhombomere 2, strong signal was still observed.

E *Cyp26c1* expression in the embryo of non-diabetic mouse at 12 hr after RA treatment. Expression of *Cyp26c1* in rhombomere 2 was prominently reduced. Only low level of expression was observed in the epithelial lining of the maxillo-mandibular and in patches of cells in the first branchial arch.

F *Cyp26c1* expression in the embryo of diabetic mouse prior to RA treatment. There was no observable difference in comparison with the embryo of non-diabetic mouse as shown in Figure E.

G *Cyp26c1* expression in the embryo of diabetic mouse at 2 hr after RA treatment. No observable change in *Cyp26c1* expression in comparison to embryo of diabetic mice prior to RA treatment as shown in Figure F.

H-J *Cyp26c1* expression in the embryo of diabetic mouse at 4 (H), 8 (I) and 12 hr (J) after RA treatment. There was increased level of down-regulation of *Cyp26c1* as time proceeded. However, no observable difference from embryos of non-diabetic mice at the corresponding time points could be detected.

Labels:	CeM	Cervical mesenchyme	CrM	Cranial mesenchyme
	FBA	First branchial arch	MMC	Maxillo-mandibular cleft
	r	Rhombomere	TB	Tail bud

Scale bar: A-J 0.45 mm

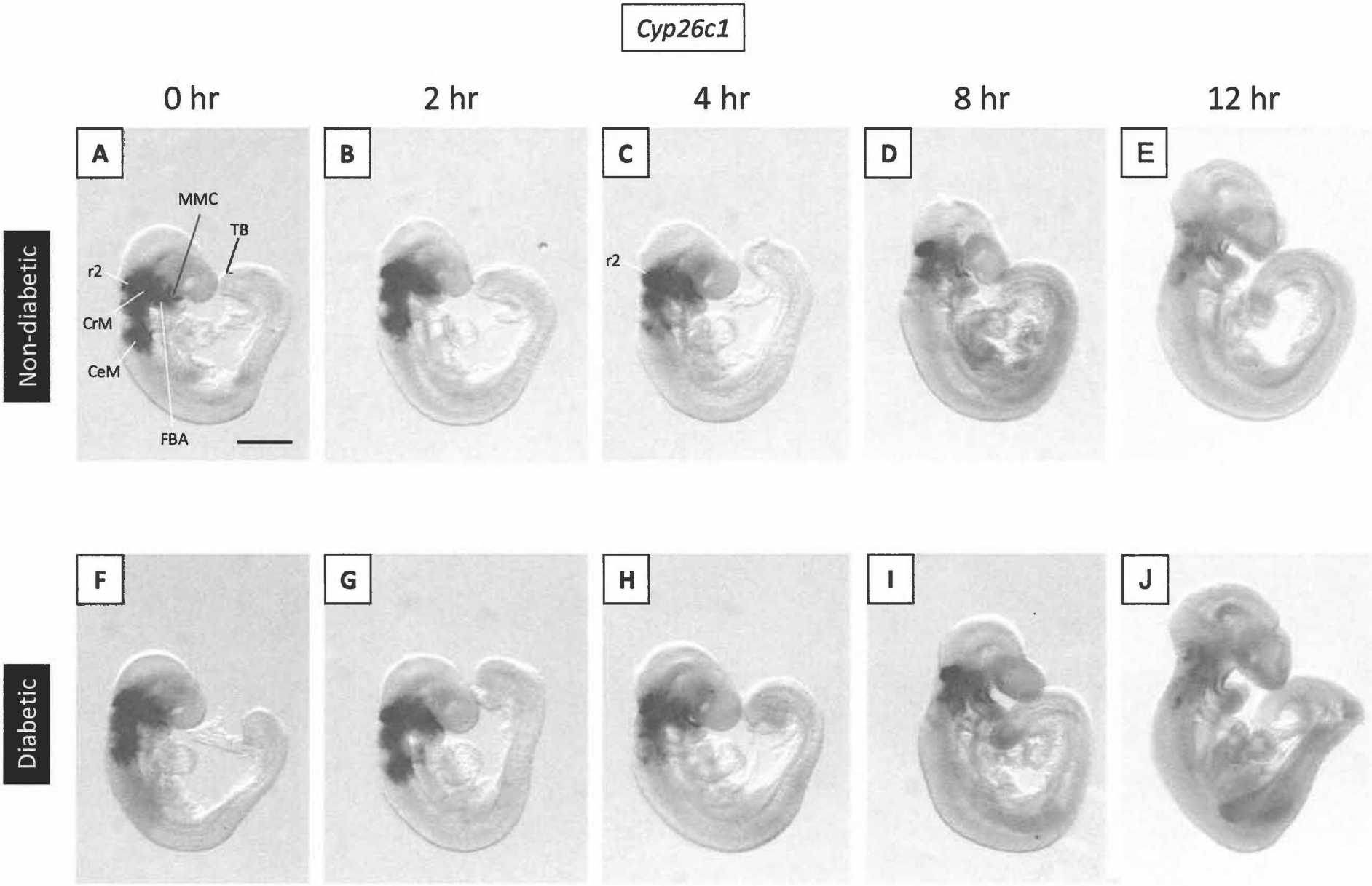
Cyp26c1
0 hr
2 hr
4 hr
8 hr
12 hr
Non-diabetic
Diabetic
A
B
C
D
E
F
G
H
I
J
MMC
TB
r2
CrM
CeM
FBA
r2

Figure 4.1 Expression of *Cyp26a1* in *Cyp26a1* heterozygous (+/-) and wild-type (+/+) embryos of non-diabetic (ND) and diabetic (SD) mice at E9.0 detected by whole mount *in situ* hybridization.

A-C The *Cyp26a1* wild-type embryo in non-diabetic pregnancy ($ND^{+/+}$) shows the highest expression level of *Cyp26a1*, anteriorly in the cranial (CrM) and cervical (CeM) mesenchyme, and posteriorly in the posterior neural plate (PNP) and tail bud mesoderm (TBM) in the tail bud region of the embryo.

D-F The *Cyp26a1* heterozygous embryo in non-diabetic pregnancy ($ND^{+/-}$) shows obvious reduction in expression level of *Cyp26a1*, especially in the anterior domains, and also in the tail bud mesoderm in comparison with $ND^{+/+}$ embryo.

G-I The *Cyp26a1* wild-type embryo in diabetic pregnancy ($SD^{+/+}$) shows obvious reduction in expression level of *Cyp26a1* in comparison with $ND^{+/+}$ embryo. Expression is more comparable with $ND^{+/-}$ embryo.

J-L The *Cyp26a1* heterozygous embryo in diabetic pregnancy ($SD^{+/-}$) shows the lowest expression level of *Cyp26a1* with expression in the anterior domains almost completely switched off and the expression in the tail bud region prominently reduced.

Labels:		
	CeM	Cervical mesenchyme
	CrM	Cervical mesenchyme
	PNP	Posterior neural plate
	TBM	Tail bud mesoderm

Scale bar:		
	A, D, G and J	0.7 mm
	B, E, H and K	0.15 mm
	C, F, I and L	0.35 mm

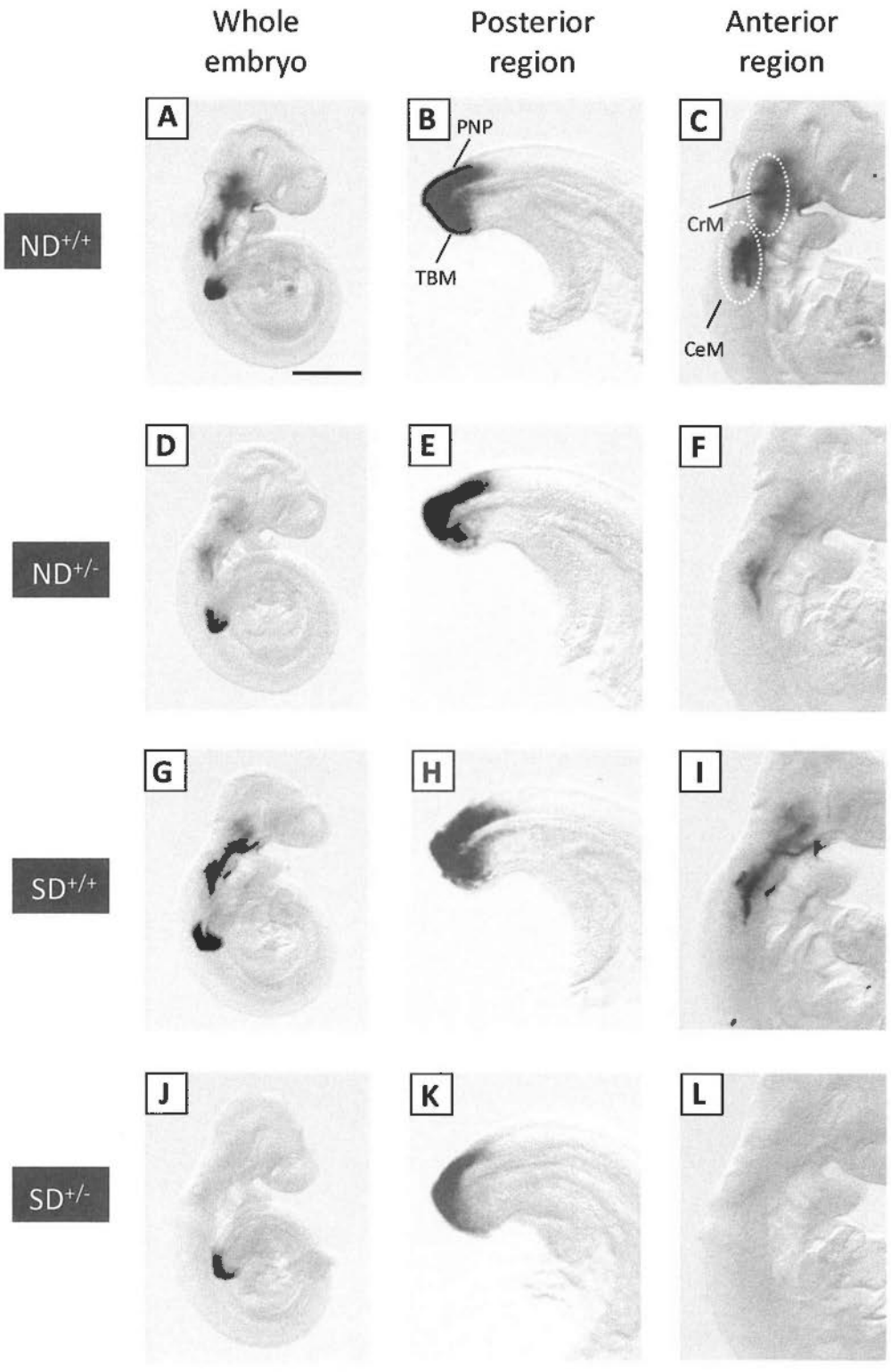
Whole embryo
Posterior region
Anterior region
A
B
PNP
TBM
C
CrM
CeM
ND+/+
D
E
F
ND+/-
G
H
I
SD+/+
J
K
L
SD+/-

Figure 5.1 Illustration of how the tail length and crump-rump length of a E13 mouse embryo were measured.

A Crump-rump length (CRL) is the maximum length of the body from the top of the head to the bottom of the buttock as indicated by the blue double arrow. The original position of the hindlimb bud was outlined with yellow dotted line. The hindlimb bud was removed for showing the entire caudal region of the embryo.

B Tail length (TL) is defined as the length of the caudal region from the posterior limit of the hindlimb bud (original position was outlined with yellow dotted line) to the tail tip as indicated by the white double arrow. The tail region was straightened during measurement.

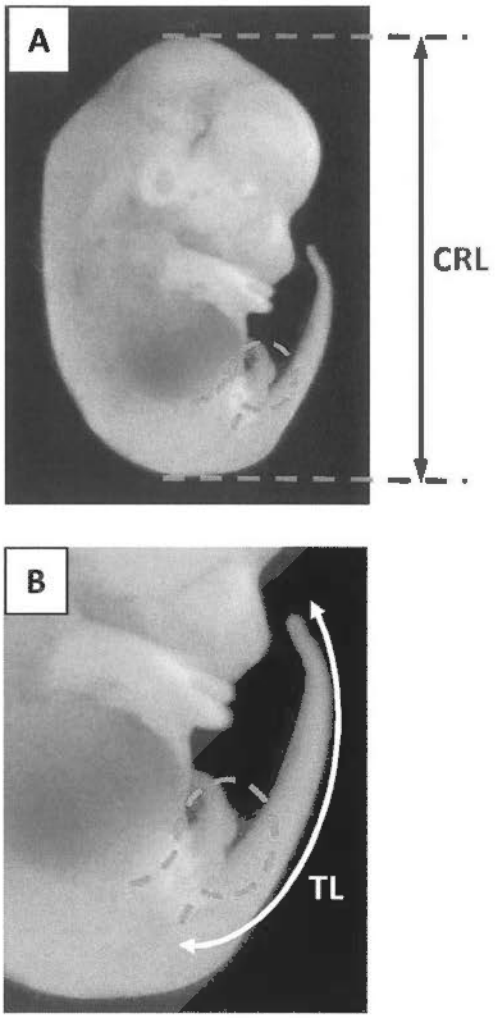
A
CRL
B
TL

Figure 5.2 Gross morphology of E13 embryos of non-diabetic and diabetic mice supplemented with 1.25 mg/kg RA (1.25RA) or vehicle as control (CON).

A Embryo of control non-diabetic mouse.

B Embryo of control diabetic mouse.

C Embryo of RA-supplemented non-diabetic mouse. No observable difference in gross morphology from embryo of control non-diabetic mouse as shown in Figure A, showing that the dose of RA supplemented probably did not cause any teratogenic effect.

D Embryo of RA-supplemented diabetic mouse. No observable difference in gross morphology from embryo of control diabetic mouse as shown in Figure C, showing that the dose of RA supplemented probably did not cause any teratogenic effect.

Scale bar: A-D 2 mm

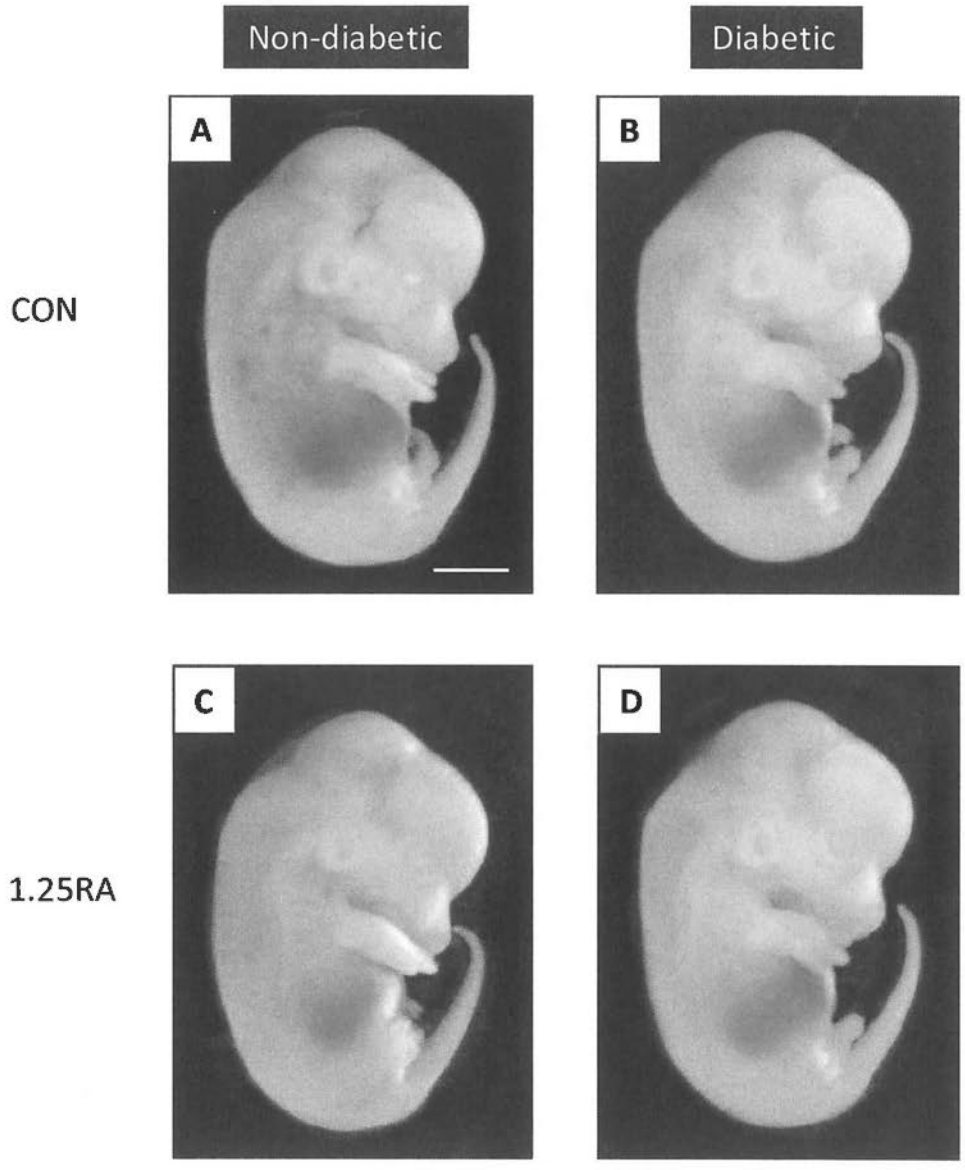
Non-diabetic
Diabetic
A
B
C
D
CON
1.25RA

Figure 6.1 Illustration of how the tail length and crump-rump length of a E18 fetus were measured.

Crump-rump length (CRL) is the maximum length of the body from the top of the head to the bottom of the buttock as indicated by the red double arrow. Tail length (TL) is defined as the length of the caudal region from the base to the tail tip as indicated by the white double arrow. The tail region was straightened during measurement.

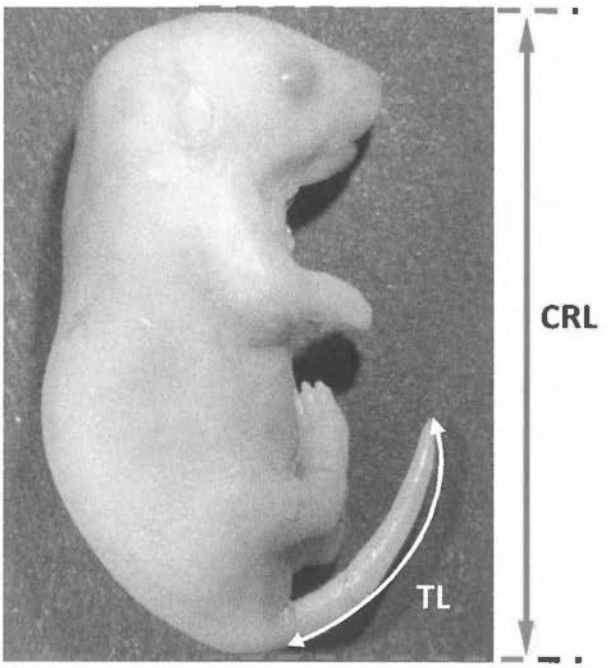
CRL
TL

Figure 6.2 **Expression of *Cyp26a1* detected by whole mount *in situ* hybridization in E9.0 embryos of non-diabetic (ND) and diabetic (SD) mice treated with phlorizin (PHZ) or vehicle as control (CON).**

A-B Anterior (A) and posterior (B) region of embryo of control non-diabetic mouse. Anteriorly, Cyp26a1 was expressed in the cranial mesenchyme (CrM), cervical mesenchyme (CeM), first branchial arch (FBA) and maxillo-mandibular cleft. Posteriorly, *Cyp26a1* was highly expressed in the posterior neural plate (PNP) and tail bud mesoderm (TBM).

C-D Anterior (C) and posterior (D) region of embryo of PHZ-treated non-diabetic mouse. There was no observable difference in *Cyp26a1* expression in comparison to embryo of control non-diabetic mice as shown in Figures A and B.

E-F Anterior (E) and posterior (F) region of embryo of control diabetic mouse. There was prominent reduction in *Cyp261* expression in comparison to embryo of control diabetic mice as shown in Figures A and B, which was most easily noticeable in the anterior region.

G-H Anterior (G) and posterior (H) region of embryo of PHZ-treated diabetic mouse. There was prominent increase in *Cyp26a1* expression in comparison to embryo of control diabetic mouse as shown in Figures E and F.

Labels:	CeM	Cervical mesenchyme
	CrM	Cranial mesenchyme
	FBA	First branchial arch
	MMC	Maxillo-mandibular cleft

Scale bar:	A, C, E and G	0.5 mm
	B, D, F and H	0.1 mm

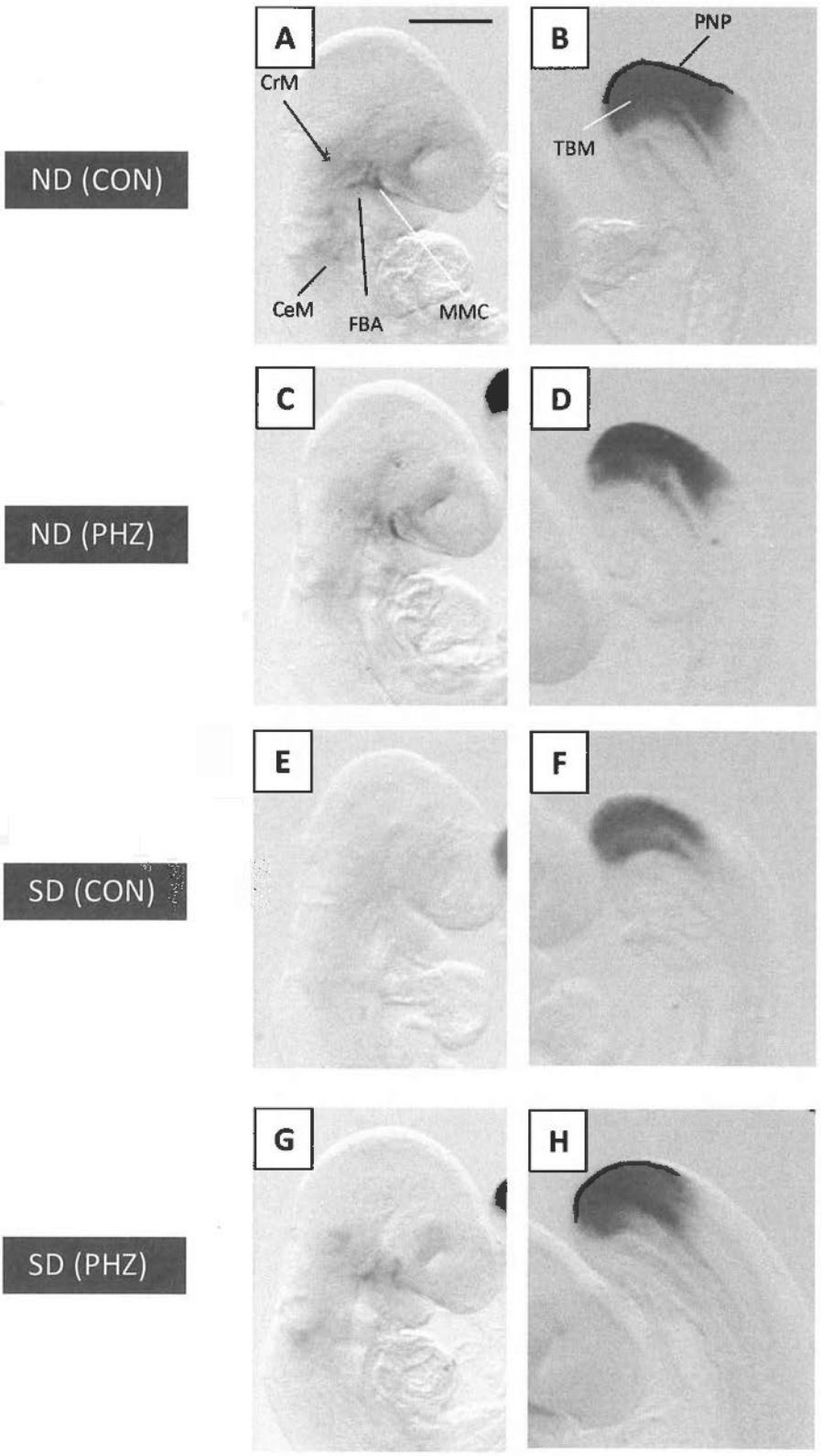
ND (CON)
ND (PHZ)
SD (CON)
SD (PHZ)
A
B
C
D
E
F
G
H
CrM
CeM
FBA
MMC
PNP
TBM

Figure 6.3 **Expression of *Cyp26a1* detected by whole mount *in situ* hybridization in rat embryos that had been cultured from head-fold stage at E9.5 for 24 hr in medium supplemented with varying concentrations of D-glucose (2, 3 and 4 mg/ml) or the solvent as control (CON).**

A-B Whole embryo (A) and posterior region (B) of rat embryo cultured in control medium. Anteriorly, *Cyp26a1* was only expressed in the optic primordium (arrowhead). Posteriorly, *Cyp26a1* was expressed in the posterior neural plate (PNP) and tail bud mesoderm (TBM).

C-D Whole embryo (C) and posterior region (D) of rat embryo cultured in medium supplemented with 2 mg/ml D-glucose. Expression in the optic primordium was reduced to very low level. Reduction of *Cyp26a1* expression was also observed in the tail bud region.

E-F Whole embryo (E) and posterior region (F) of rat embryo cultured in medium supplemented with 3 mg/ml D-glucose. *Cyp26a1* expression was no longer detectable in the optic primordium and in the posterior neural plate. Expression was only observed in the ventral part of the tail bud

G-H Whole embryo (G) and posterior region (H) of rat embryo cultured in medium supplemented with 4 mg/ml D-glucose. Expression of *Cyp26a1* in the ventral part of the tail bud had further reduced.

Labels: PNP Posterior neural plate
TBM Tail bud mesoderm

Symbol: Arrowhead Optic primordium

Scale bar: A, C, E and G 0.5 mm
B, D, F and H 0.2 mm

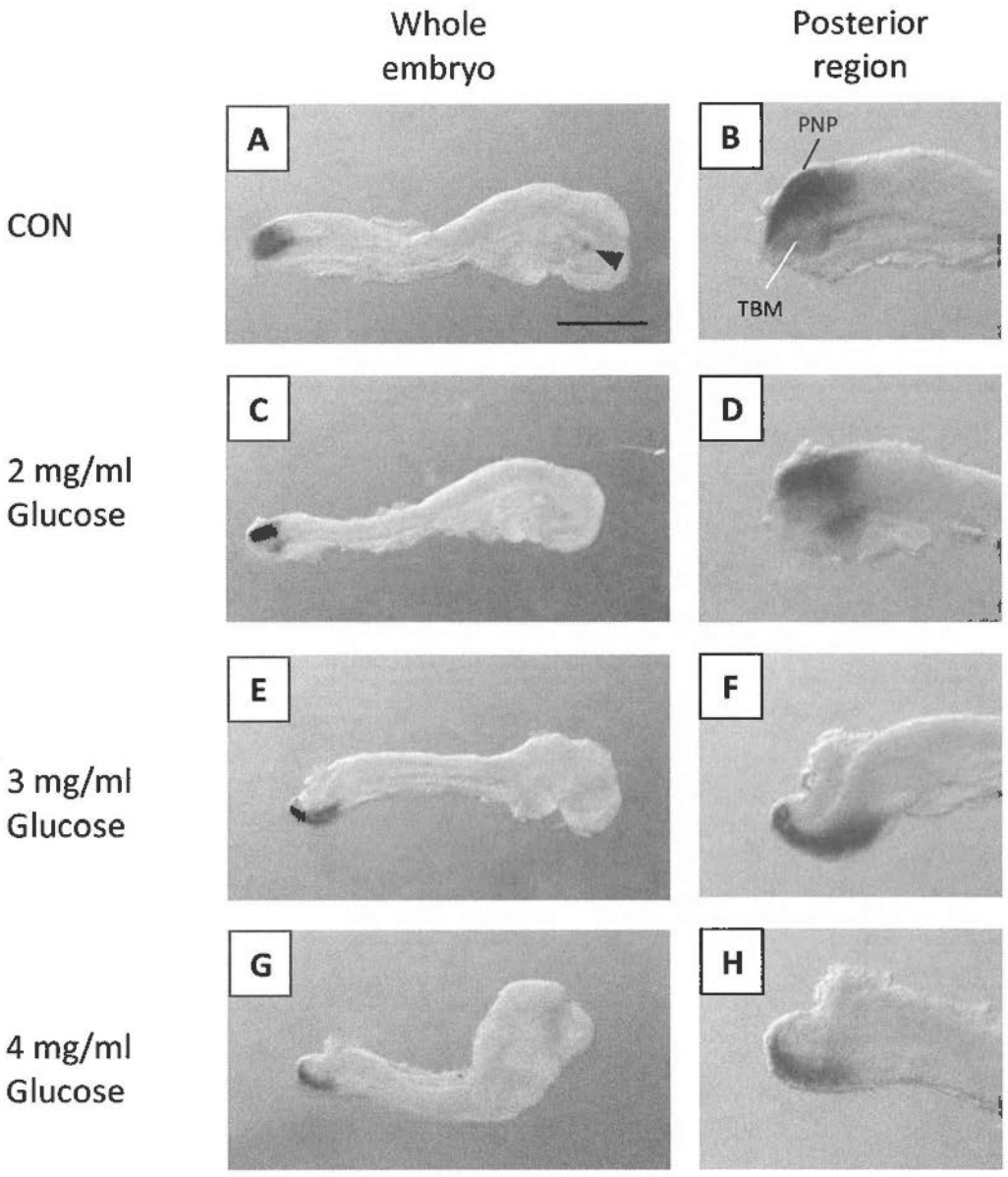
Whole embryo
Posterior region
CON
2 mg/ml Glucose
3 mg/ml Glucose
4 mg/ml Glucose
A
B
C
D
E
F
G
H
PNP
TBM

Figure 6.4 **Expression of *Cyp26a1* detected by whole mount *in situ* hybridization in rat embryos that had been cultured from head-fold stage at E9.5 for 48 hr in medium supplemented with varying concentrations of D-glucose (2, 3 and 4 mg/ml) or the solvent as control (CON).**

A-B Whole embryo (A) and posterior region (B) of rat embryo cultured in control medium. Anteriorly, *Cyp26a1* was expressed in the cranial and cervical mesenchyme (circled). Posteriorly, *Cyp26a1* was expressed in the posterior neural plate (PNP) and the tail bud (TB).

C-D Whole embryo (C) and posterior region (D) of rat embryo cultured in medium supplemented with 2 mg/ml D-glucose. Expression of *Cyp26a1* in the cranial domains had almost switched off. Expression in the tail bud region was noticeably reduced.

E-F Whole embryo (E) and posterior region (F) of rat embryo cultured in medium supplemented with 3 mg/ml D-glucose. Expression of *Cyp26a1* was only detectable in the caudal extremity of the embryo where the tail bud had reduced prominently in size.

G-H Whole embryo (G) and posterior region (H) of rat embryo cultured in medium supplemented with 4 mg/ml D-glucose. Expression of *Cyp26a1* in the caudal extremity of the embryo had further reduced.

Labels:	PNP	Posterior neural plate
	TBM	Tail bud mesoderm
Symbol:	Circle	Cranial and cervical mesenchyme
Scale bar:	A, C, E and G	0.5 mm
	B, D, F and H	0.25 mm

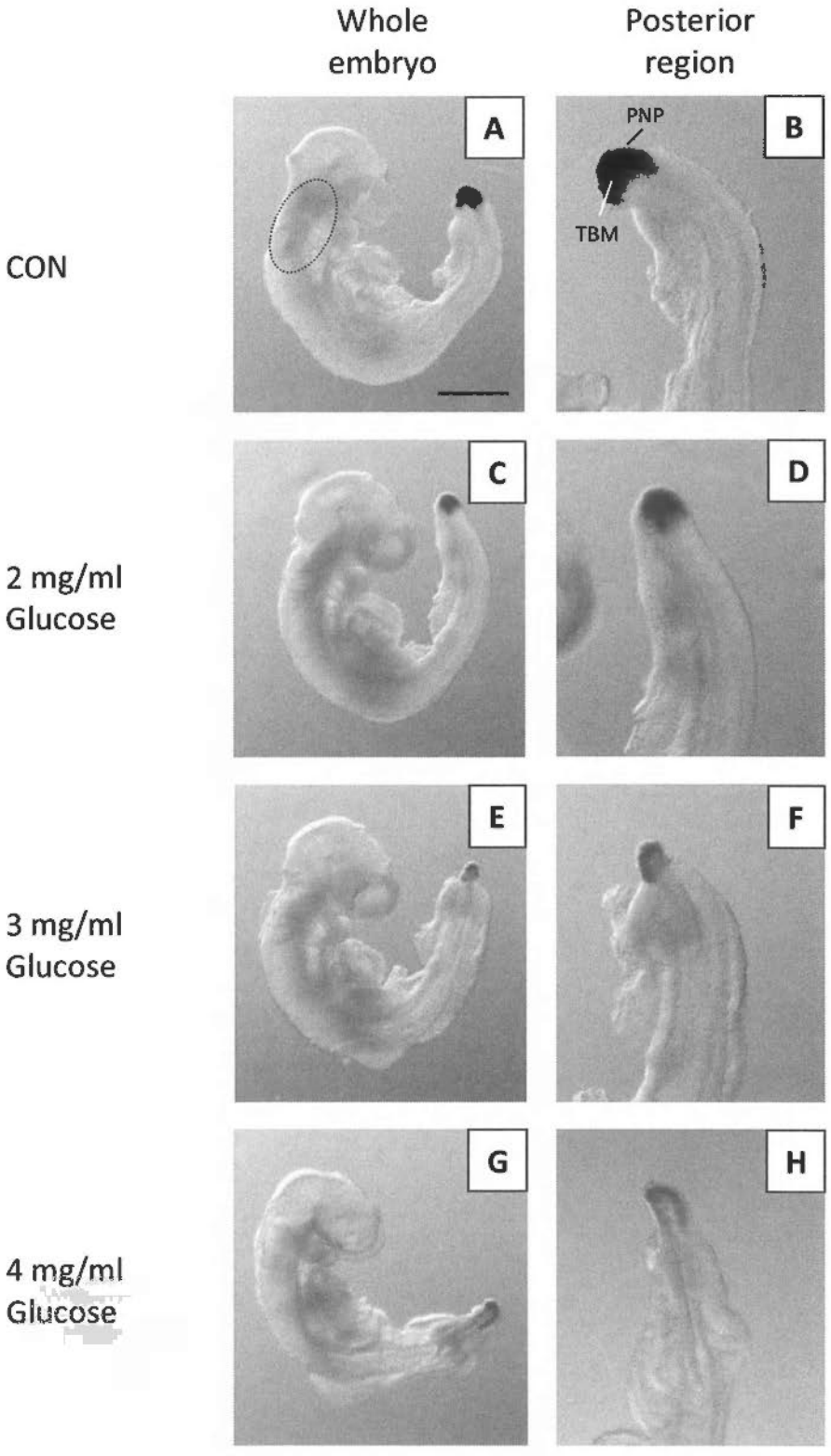
Whole embryo
Posterior region
CON
2 mg/ml Glucose
3 mg/ml Glucose
4 mg/ml Glucose
A
B
C
D
E
F
G
H
PNP
TBM

Graphs

Graph 3.1 Relative expression levels of (A) *Cyp26a1*, (B) *Cyp26b1* and (C) *Cyp26c1* in embryos of non-diabetic (ND) and diabetic (SD) mice at E9.0.

A. *Cyp26a1*

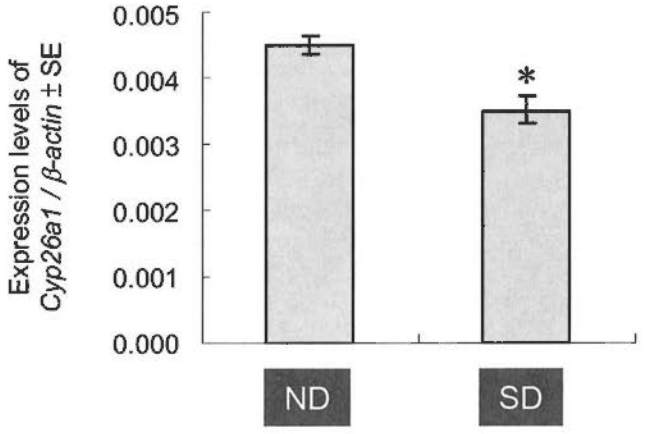

B. *Cyp26b1*

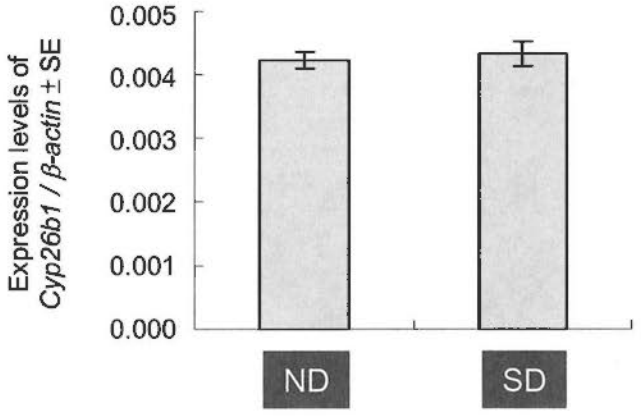

C. *Cyp26c1*

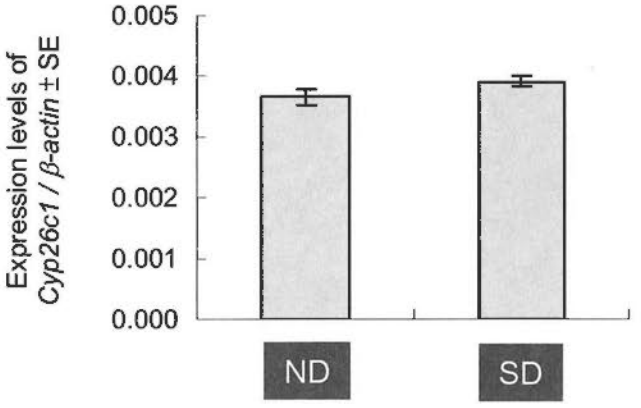

Sample size = 5 for all groups.

Data were analyzed by Independent Samples t-test.

* $p < 0.05$ vs. ND

Graph 3.2 Relative expression levels of *Cyp26a1* in embryos of non-diabetic (ND) and diabetic (SD) mice at (A) E7.0 and (B) E8.0.

A. E7.0

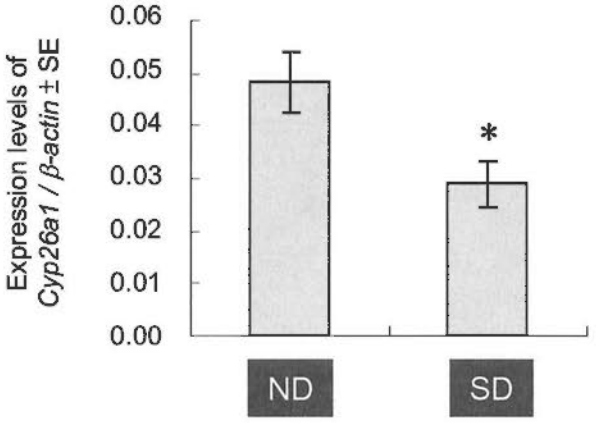

B. E8.0

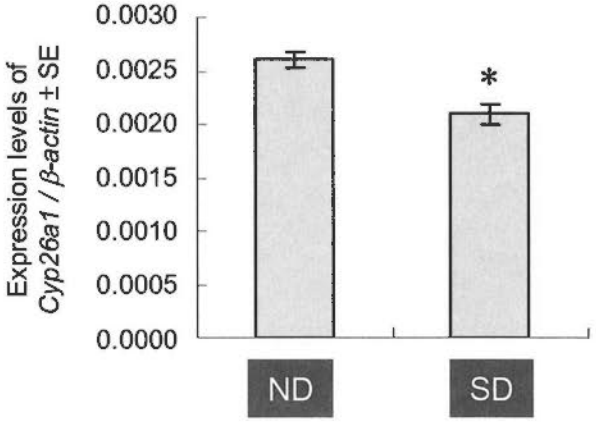

Sample size = 5 for all groups.

Data were analyzed by Independent Samples t-test.

* $p < 0.05$ vs. ND

Graph 3.3 Relative expression levels of *Cyp26a1* in embryos of non-diabetic (ND) and diabetic (SD) mice at different time points after maternal injection of 50 mg/kg RA (RA) or vehicle as control (CON) on E9.0.

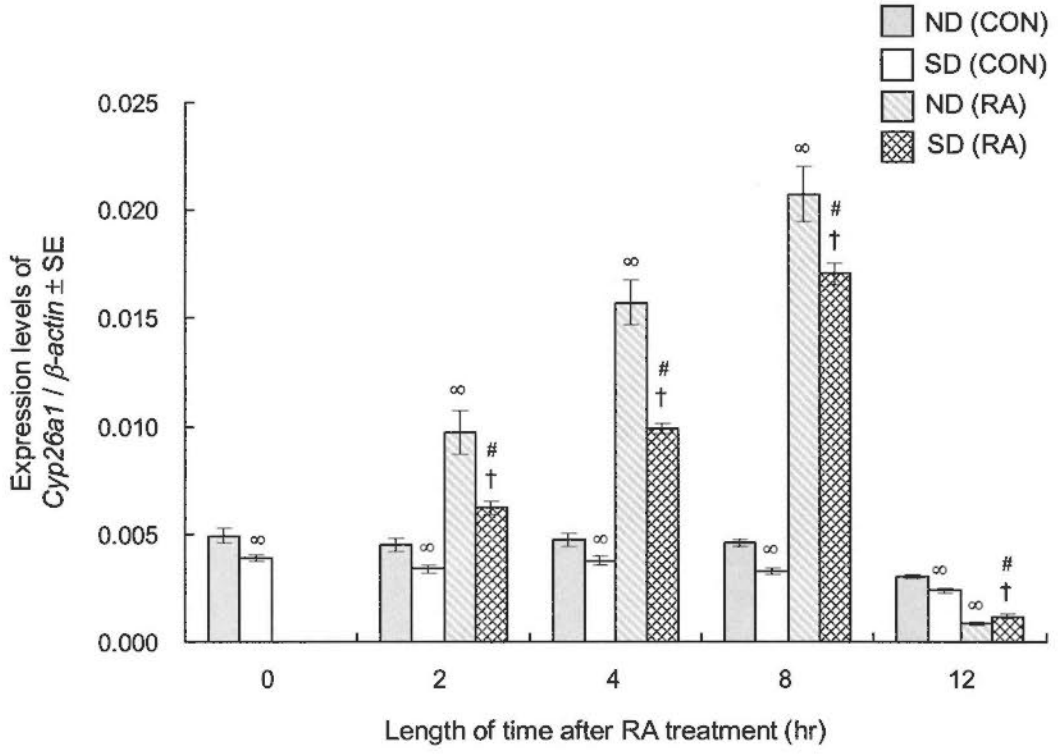

Sample size = 3 for all groups.

Data were analyzed by Independent Samples t-test.

$^{\infty}$ $p < 0.05$ vs. ND (CON) at the same time point

† $p < 0.05$ vs. SD (CON) at the same time point

$^{\#}$ $p < 0.05$ vs. ND (RA) at the same time point

Graph 3.4 Relative expression levels of *Cyp26b1* in embryos of non-diabetic (ND) and diabetic (SD) mice at different time points after maternal injection of 50 mg/kg RA (RA) or vehicle as control (CON) on E9.0.

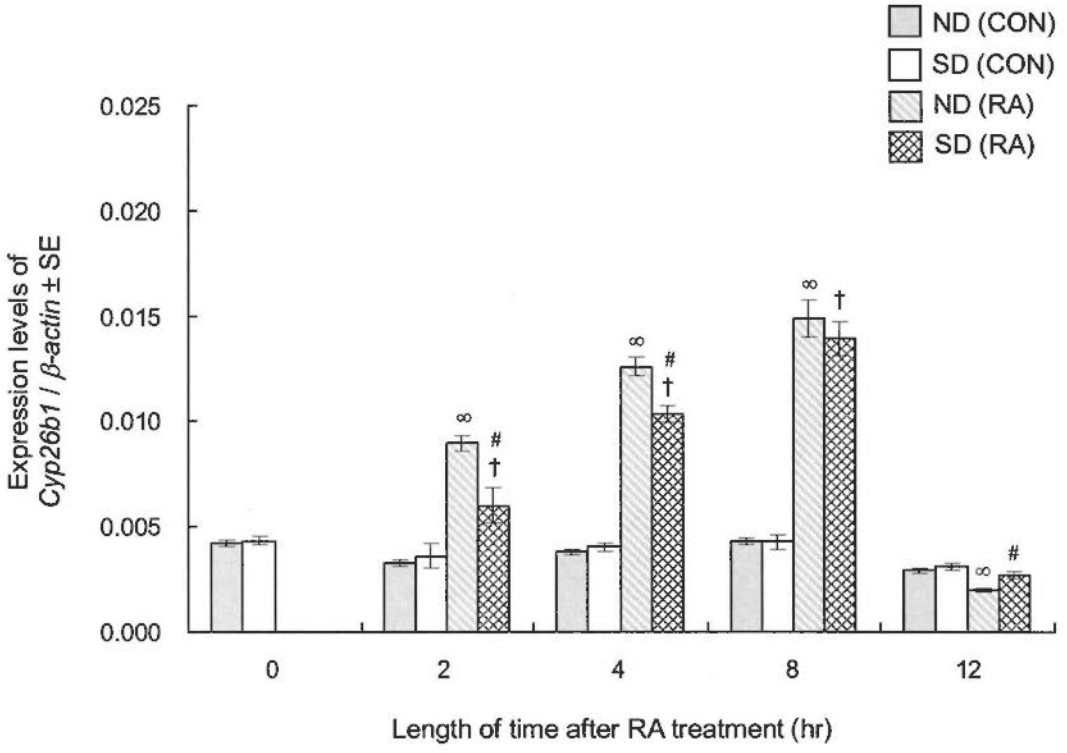

Sample size = 3 for all groups.

Data were analyzed by Independent Samples t-test.

$^{\infty}$ $p < 0.05$ vs. ND (CON) at the same time point

† $p < 0.05$ vs. SD (CON) at the same time point

$^{\#}$ $p < 0.05$ vs. ND (RA) at the same time point

Graph 3.5 Relative expression levels of *Cyp26c1* in embryos of non-diabetic (ND) and diabetic (SD) mice at different time points after maternal injection of 50 mg/kg RA (RA) or vehicle as control (CON) on E9.0.

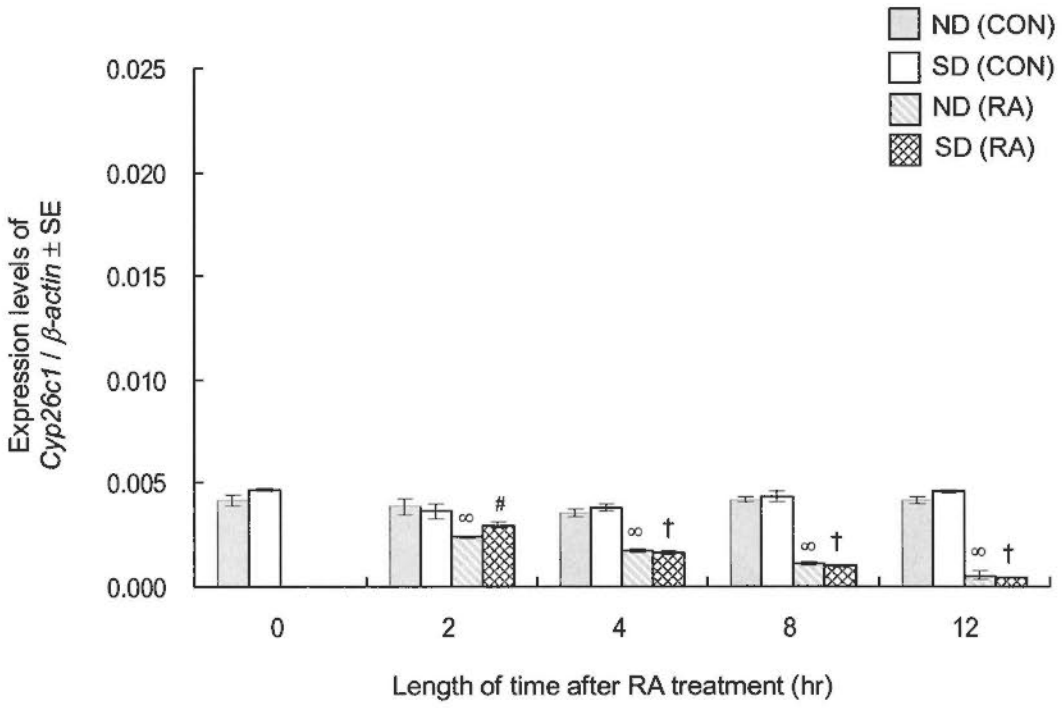

Sample size = 3 for all groups.

Data were analyzed by Independent Samples t-test.

$^{\infty}$ $p < 0.05$ vs. ND (CON) at the same time point

† $p < 0.05$ vs. SD (CON) at the same time point

$^{\#}$ $p < 0.05$ vs. ND (RA) at the same time point

Graph 4.1 Relative expression levels of *Cyp26a1* in the tail bud of *Cyp26a1* heterozygous (+/-) and wild-type (+/+) embryos of non-diabetic (ND) and diabetic (SD) mice at E9.0.

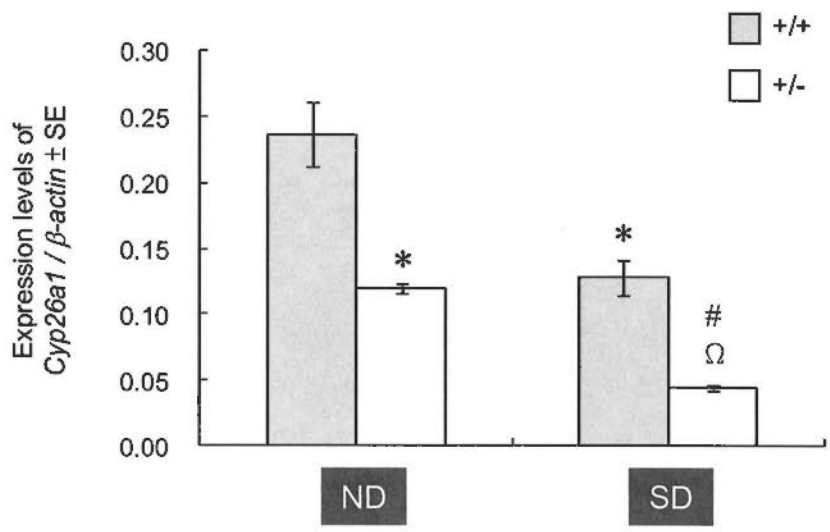

Sample size = 4 for all groups.

Data were analyzed by one-way ANOVA followed by Bonferroni test.

* $p < 0.001$ vs. $ND^{+/+}$

$^{\#}$ $p < 0.05$ vs. $SD^{+/+}$

$^{\Omega}$ $p < 0.05$ vs. $ND^{+/-}$

Graph 4.2 **Relative expression levels of *Cyp26a1* in the whole embryo (exclude tail bud) of *Cyp26a1* heterozygous (+/-) and wild-type (+/+) embryos of non-diabetic (ND) and diabetic (SD) mice at E9.0.**

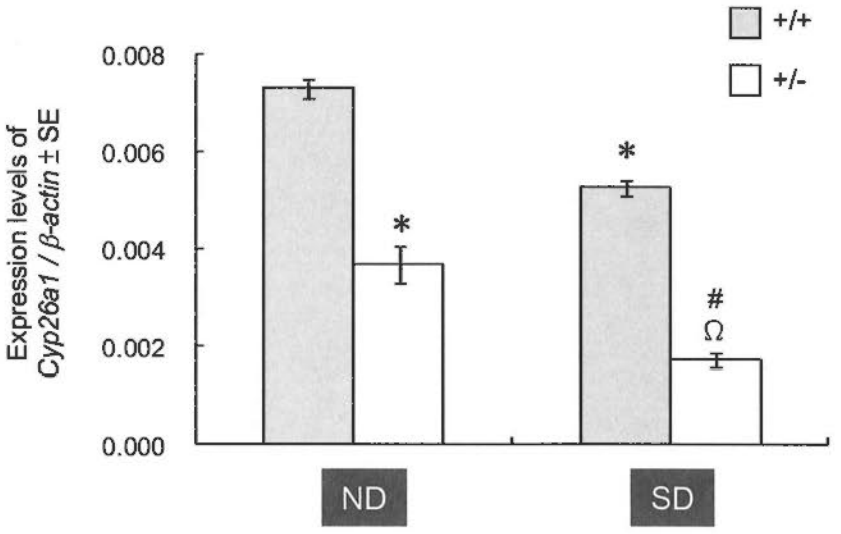

Sample size in parentheses.

Data were analyzed by one-way ANOVA followed by Bonferroni test.

* $p < 0.001$ vs. $ND^{+/+}$

\# $p < 0.001$ vs. $SD^{+/+}$

Ω $p < 0.001$ vs. $ND^{+/-}$

Graph 4.3 ***In vitro*** **assay of RA degrading activity in the tail bud of** ***Cyp26a1*** **heterozygous (+/-) and wild-type (+/+) embryos in non-diabetic (ND) and diabetic (SD) mice at E9.0.**

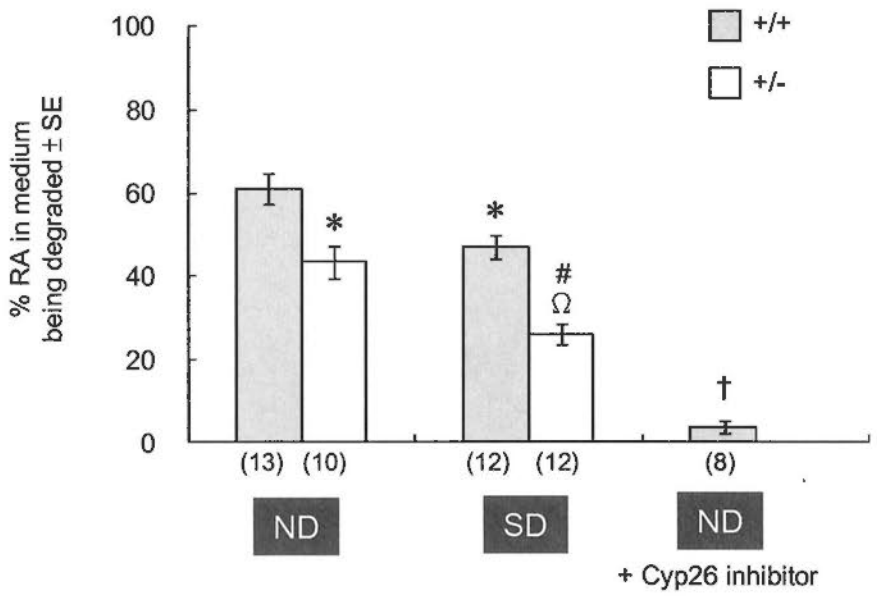

Sample size in parentheses.

Data were analyzed by one-way ANOVA followed by Bonferroni test.

* $p < 0.005$ vs. $ND^{+/+}$

\# $p < 0.001$ vs. $SD^{+/+}$

Ω $p < 0.005$ vs. $ND^{+/-}$

† $p < 0.005$ vs. $ND^{+/-}$

Graph 4.4 **RA levels in *Cyp26a1* heterozygous (+/-) and wild-type (+/+) embryos of non-diabetic (ND) and diabetic (SD) mice at 3 hr after maternal injection of 25 mg/kg RA on E9.0 as determined by HPLC.**

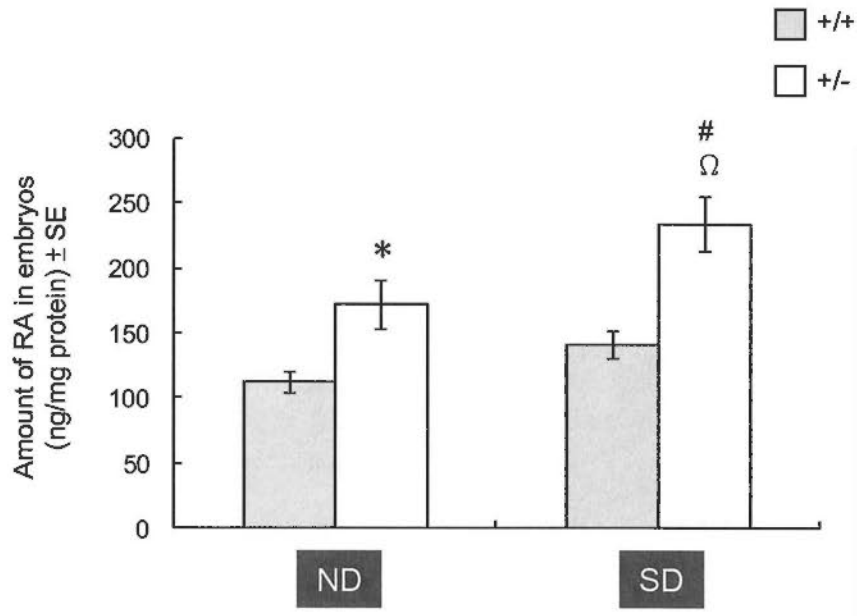

Sample size = 6 for all groups.

Data were analyzed by one-way ANOVA followed by Bonferroni test.

* $p < 0.01$ vs. $ND^{+/+}$

\# $p = 0.001$ vs. $SD^{+/+}$

Ω $p < 0.05$ vs. $ND^{+/-}$

Graph 4.5 **Incidence rates of (A) cleft palate and (B) renal malformations in E18 *Cyp26a1* heterozygous (+/−) and wild-type (+/+) fetuses of non-diabetic (ND) and diabetic (SD) mice induced by maternal injection of 40 mg/kg RA on E9.0.**

A. Cleft palate

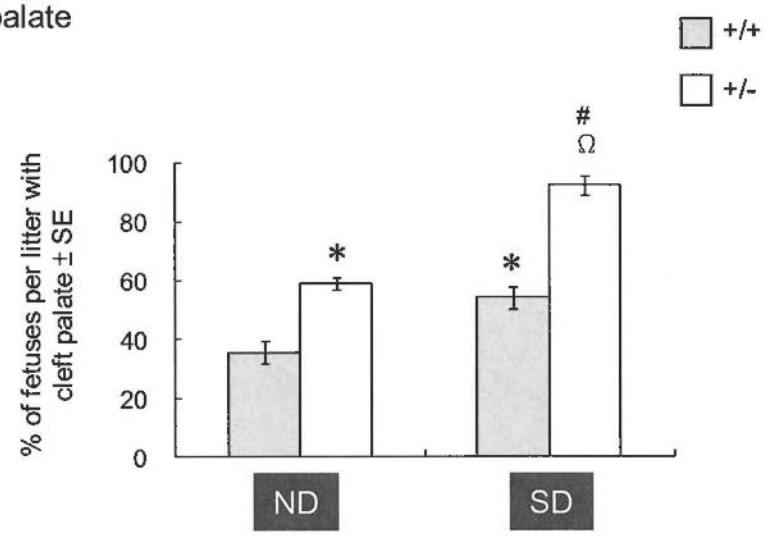

B. Renal malformations

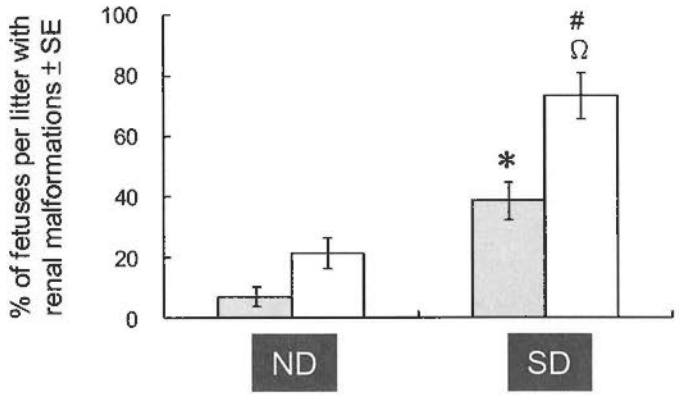

Sample size = 10 for all groups.

Data were analyzed by one-way ANOVA followed by Bonferroni test.

* $p < 0.005$ vs. $ND^{+/+}$

\# $p < 0.005$ vs. $SD^{+/+}$

Ω $p < 0.001$ vs. $ND^{+/-}$

Graph 4.6 Incidence rates of (A) exencephaly and (B) spina bifida in E13 *Cyp26a1* heterozygous (+/−) and wild-type (+/+) embryos of non-diabetic (ND) and diabetic (SD) mice induced by maternal injection of 25 mg/kg RA on E8.0.

A. Exencephaly

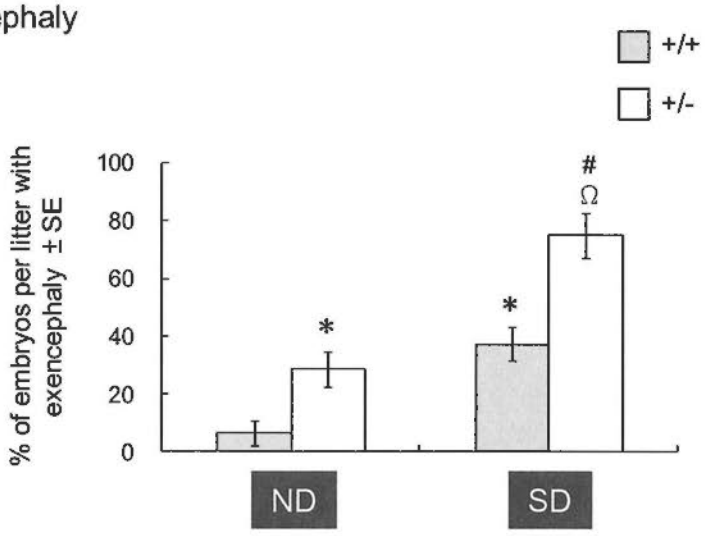

B. Spina bifida

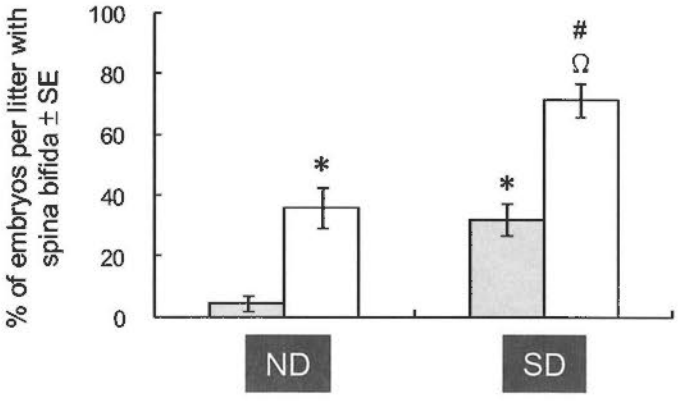

Sample size = 9 for all groups.

Data were analyzed by one-way ANOVA followed by Bonferroni test.

* $p < 0.05$ vs. $ND^{+/+}$

\# $p < 0.005$ vs. $SD^{+/+}$

Ω $p < 0.005$ vs. $ND^{+/-}$

Graph 5.1 Serum retinol levels in non-diabetic (ND) and diabetic (SD) mice under pregnant or non-pregnant (E9.0) status.

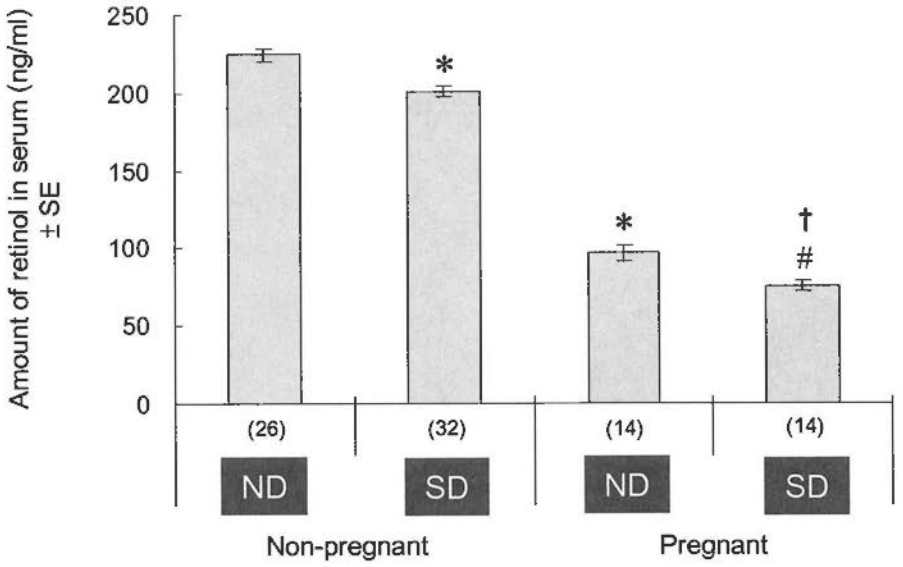

Sample size in parentheses.

Data were analyzed by Independent Samples t-test.

* $p < 0.001$ vs. ND (Non-pregnant)

# $p < 0.05$ vs. ND (Pregnant)

† $p < 0.001$ vs. SD (Non-pregnant)

Graph 5.2 Endogenous RA levels in embryos at E9.0 under non-diabetic (ND) and diabetic (SD) pregnancy.

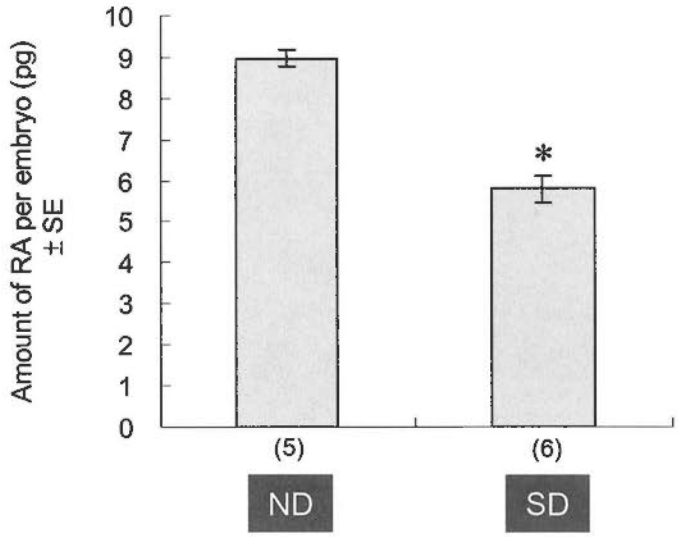

Sample size in parentheses.

Data were analyzed by Independent Samples t-test.

* $p < 0.005$ vs. ND

Graph 5.3 Relative expression levels of *Cyp26a1* in the tail bud of E9.0 embryos of non-diabetic (ND) and diabetic (SD) mice orally supplemented with 0.625 mg/kg RA (0.625RA) or 1.25 mg/kg RA (1.25RA) or vehicle as control (CON) on E8-22hr.

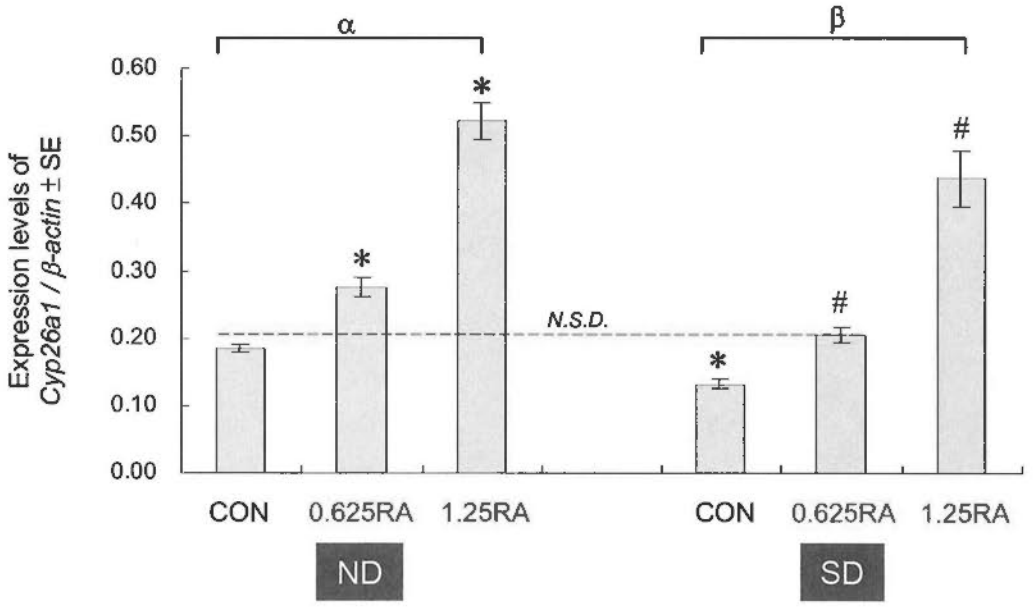

Sample size = 4 for each group.

Comparison between groups was analyzed by Independent Samples t-test.

$^{*}p < 0.05$ vs. ND (CON)

$^{\#}p < 0.01$ vs. SD (CON)

N.S.D. represents "No Significant Difference" between

SD (0.625RA) vs. ND (CON)

Correlation between dose of RA and *Cyp26a1* expression level was analyzed by Pearson's correlation.

$r = +0.943, {}^{\alpha}p < 0.001$

$r = +0.926, {}^{\beta}p < 0.001$

Graph 5.4 **The ratio of tail length (TL) to crown-rump length (CRL) in E13 embryos of non-diabetic (ND) and diabetic (SD) mice orally supplemented with 1.25 mg/kg RA (1.25RA) or vehicle as control (CON) on E8-22hr.**

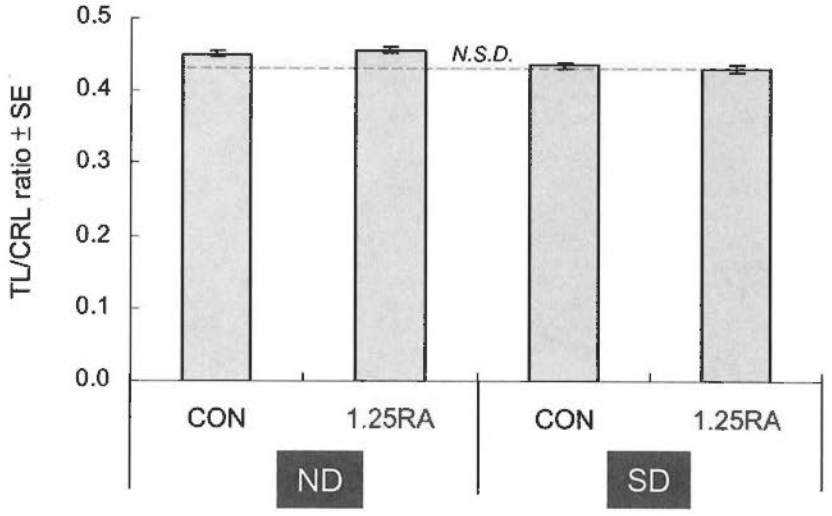

Sample size = 3 for all groups.

Data were analyzed by Independent Samples t-test.

N.S.D. represents "No Significant Difference" between SD (1.25RA) vs. ND (CON)

Graph 5.5 **RA levels in E9.0 embryos of non-diabetic (ND) and diabetic (SD) mice orally supplemented with 0.625 mg/kg RA (0.625RA) or vehicle as control (CON) on E8-22hr.**

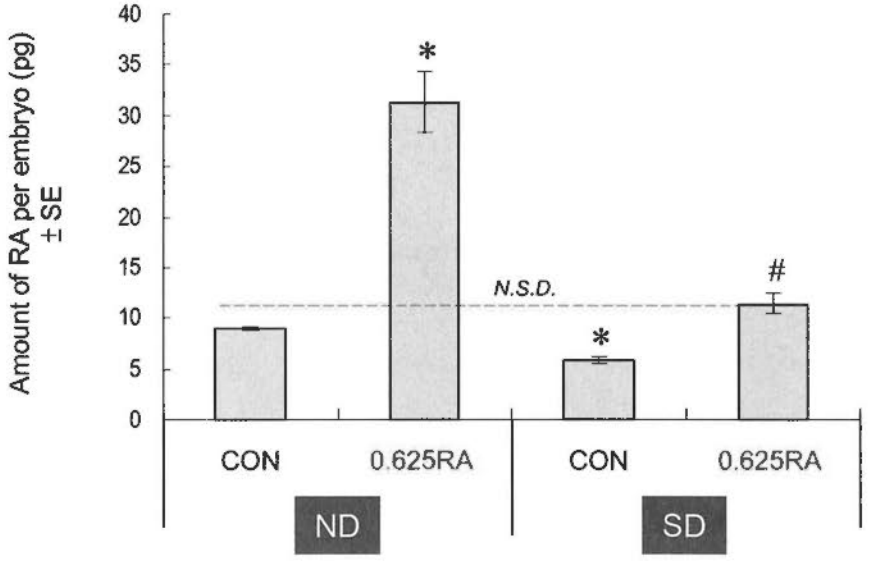

Sample size = 4 for all groups.

Data were analyzed by Independent Samples t-test.

* $p < 0.05$ vs. ND (CON)

# $p < 0.05$ vs. SD (CON)

N.S.D. represents "No Significant Difference" between SD (0.625RA) vs. ND (CON)

Graph 5.6 ***In vitro*** **RA degrading activity in the tail bud of E9.0 embryos of non-diabetic (ND) and diabetic (SD) mice orally supplemented with 0.625 mg/kg RA (0.625RA) or vehicle as control (CON) on E8-22hr.**

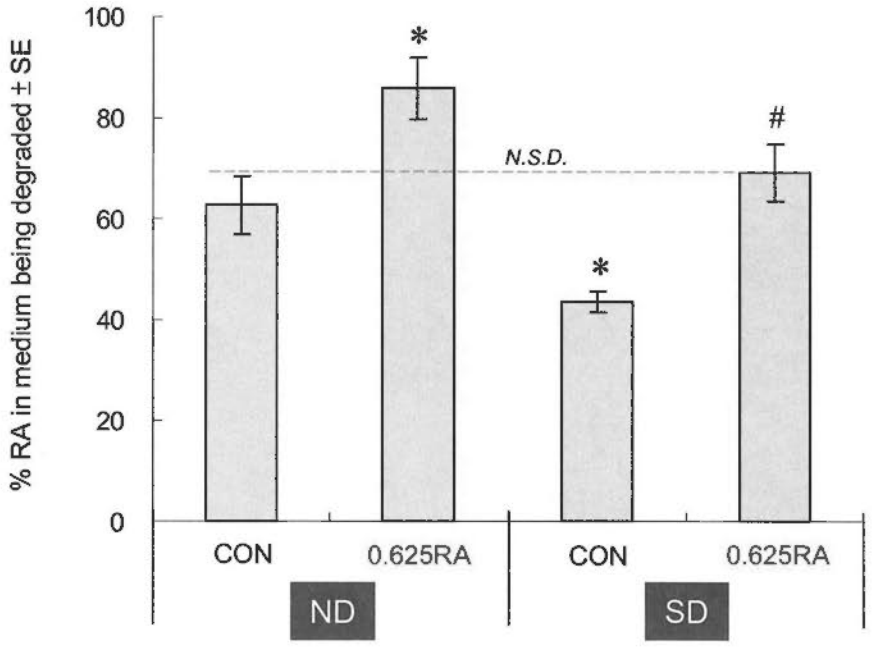

Sample size = 4 for all groups.

Data were analyzed by Independent Samples t-test.

* $p < 0.001$ vs. ND (CON)

# $p < 0.001$vs. SD (CON)

N.S.D. represents "No Significant Difference" between SD (0.625RA) vs. ND (CON)

Graph 5.7 The ratio of tail length (TL) to crown-rump length (CRL) in E13 embryos of vehicle-fed control (CON) or RA-supplemented [0.625 mg/kg RA (0.625RA) or 1.25 mg/kg RA (1.25RA)] non-diabetic (ND) and diabetic (SD) mice challenged with a teratogenic dose of 25 mg/kg RA (25RA) on E9.0.

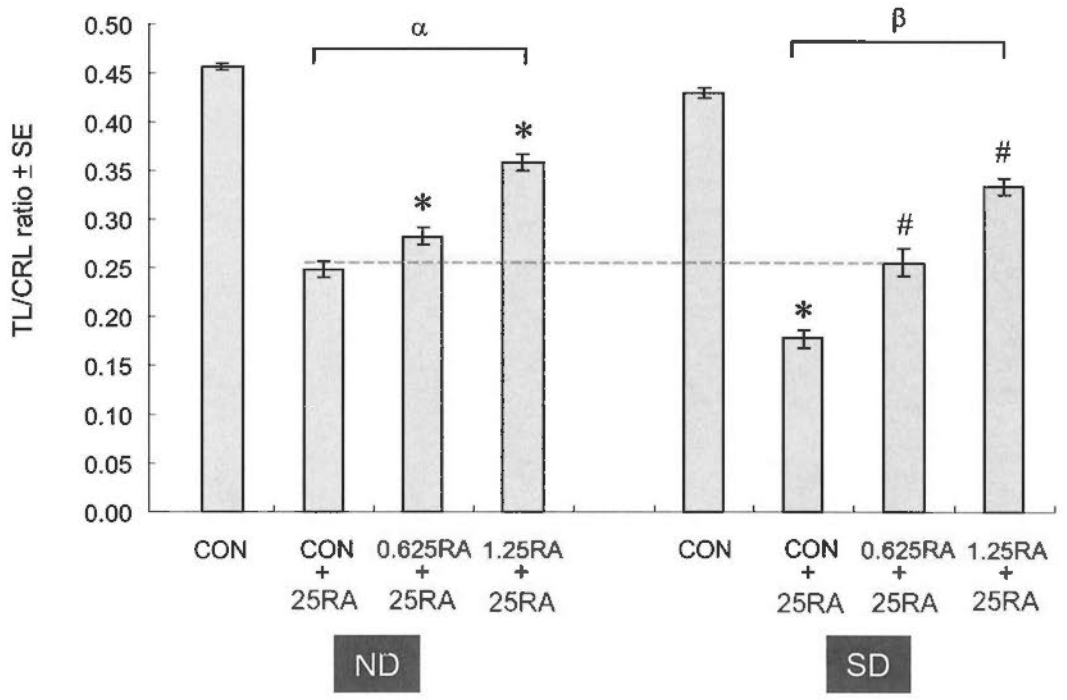

Sample size = 4 for all groups.

Comparison between groups was analyzed by Independent Samples t-test.

$^{*}p < 0.001$ vs. ND (CON+25RA)

$^{\#}p < 0.001$ vs. SD (CON+25RA)

N.S.D represents "No significant difference" between

SD (0.625RA+25RA) vs. ND (CON+25RA)

Correlation between dose of RA and TL/CRL ratio was analyzed by Pearson's correlation.

$r = +0.961, {}^{\alpha} p < 0.001$

$r = +0.945, {}^{\beta} p < 0.001$

Graph 5.8 **Relative expression levels of *Cyp26a1* in the tail bud of E9.0 *Cyp26a1* heterozygous (+/-) and wild-type (+/+) embryos of non-diabetic (ND) and diabetic (SD) mice orally supplemented with 0.625 mg/kg RA (0.625RA) or vehicle as control (CON) on E8-22hr.**

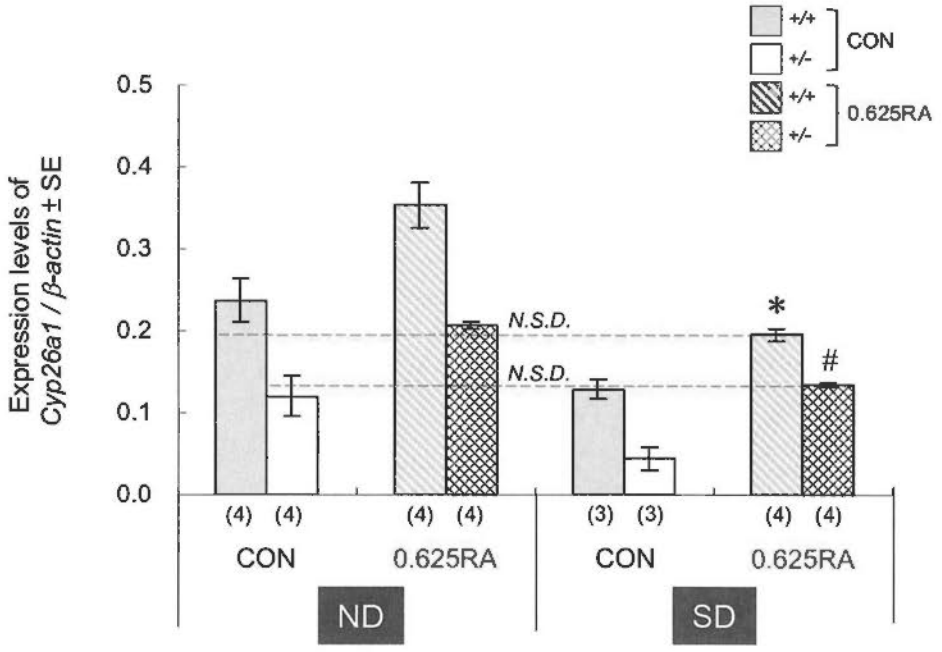

Sample size in parentheses.

Data were analyzed by one-way ANOVA followed by Bonferroni test.

* $p < 0.05$ vs. $SD^{+/+}$ (CON)

# $p < 0.05$ vs. $SD^{+/-}$ (CON)

N.S.D. represents "No significant difference" between

SD (0.625RA) vs. ND (CON) of the same genotype

Graph 5.9 **Relative expression levels of *Cyp26a1* in the whole embryo (exclude tail bud) of E9.0 *Cyp26a1* heterozygous (+/-) and wild-type (+/+) embryos of non-diabetic (ND) and diabetic (SD) mice orally supplemented with 0.625 mg/kg RA (0.625RA) or vehicle as control (CON) on E8-22hr.**

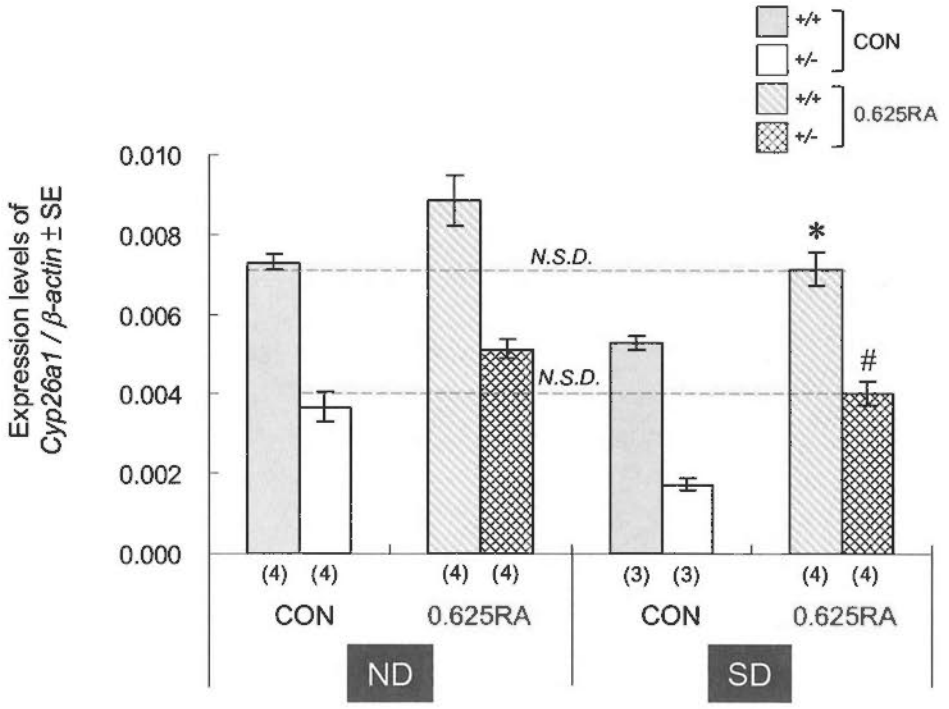

Sample size in parentheses.

Data were analyzed by one-way ANOVA followed by Bonferroni test.

* $p < 0.01$ vs. $SD^{+/+}$ (CON)

\# $p < 0.001$ vs. $SD^{+/-}$ (CON)

N.S.D. represents "No significant difference" between

SD (0.625RA) vs. ND (CON) of the same genotype

Graph 5.10 **Incidence rates of cleft palate in E18 *Cyp26a1* heterozygous (+/−) and wild-type (+/+) fetuses of control (CON) or RA-supplemented [0.625 mg/kg RA (0.625RA)] non-diabetic (ND) and diabetic (SD) mice induced by maternal injection of 40 mg/kg RA on E9.0.**

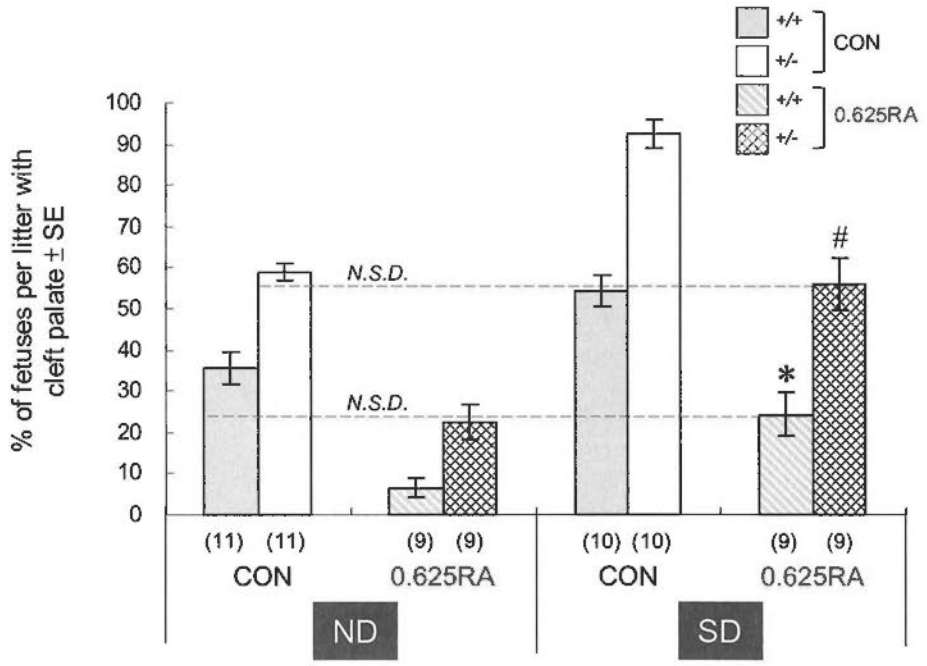

Sample size in parentheses.

Data were analyzed by one-way ANOVA followed by Bonferroni test.

* $p < 0.001$ vs. $SD^{+/+}$ (CON)

\# $p < 0.001$ vs. $SD^{+/-}$ (CON)

N.S.D. represents "No significant difference" between

SD (0.625RA) vs. ND (CON) of the same genotype

Graph 5.11 **Incidence rates of renal malformations in E18 *Cyp26a1* heterozygous (+/−) and wild-type (+/+) fetuses of control (CON) or RA-supplemented [0.625 mg/kg RA (0.625RA)] non-diabetic (ND) and diabetic (SD) mice induced by maternal injection of 40 mg/kg RA on E9.0.**

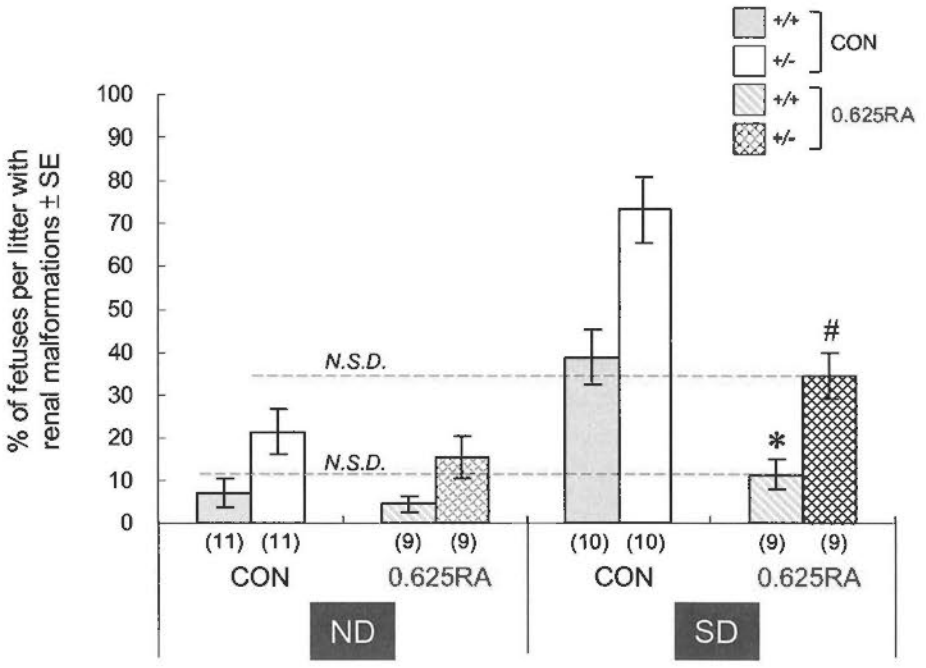

Sample size in parentheses.

Data were analyzed by one-way ANOVA followed by Bonferroni test.

* $p < 0.05$ vs. $SD^{+/+}$ (CON)

# $p < 0.001$ vs. $SD^{+/-}$ (CON)

N.S.D. represents "No significant difference" between

SD (0.625RA) vs. ND (CON) of the same genotype

Graph 5.12 **Incidence rates of exencephaly in E13 *Cyp26a1* heterozygous (+/−) and wild-type (+/+) embryos of control (CON) or RA-supplemented [0.625 mg/kg RA (0.625RA)] non-diabetic (ND) and diabetic (SD) mice induced by maternal injection of 25 mg/kg RA on E8.0.**

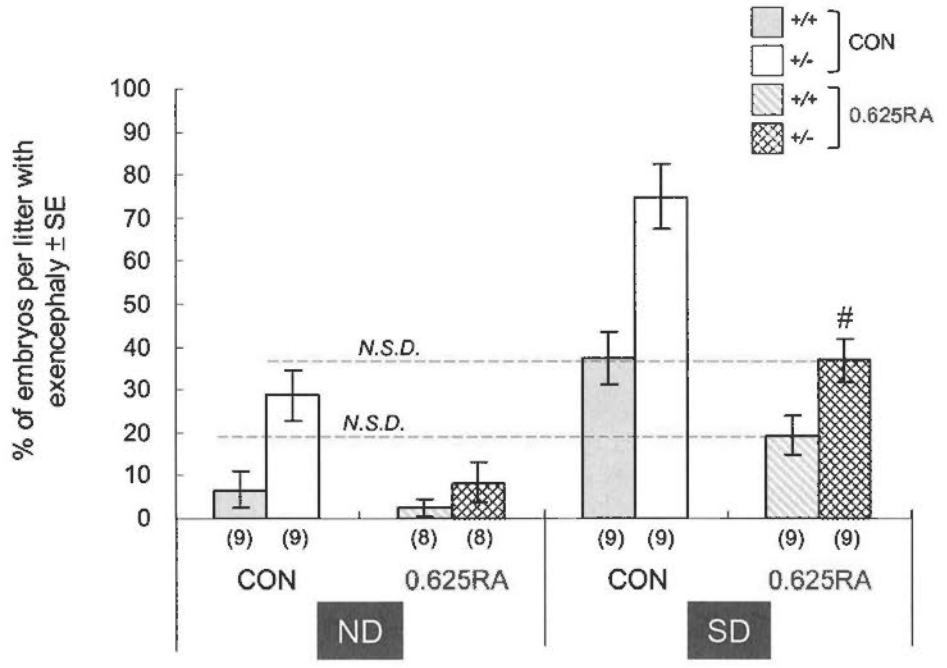

Sample size in parentheses.

Data were analyzed by one-way ANOVA followed by Bonferroni test.

$^{\#}p = 0.001$ vs. $SD^{+/-}$ (CON)

N.S.D. represents "No significant difference" between

SD (0.625RA) vs. ND (CON) of the same genotype

Graph 5.13 **Incidence rates of spina bifida in E13 *Cyp26a1* heterozygous (+/−) and wild-type (+/+) embryos of control (CON) or RA-supplemented [0.625 mg/kg RA (0.625RA)] non-diabetic (ND) and diabetic (SD) mice induced by maternal injection of 25 mg/kg RA on E8.0.**

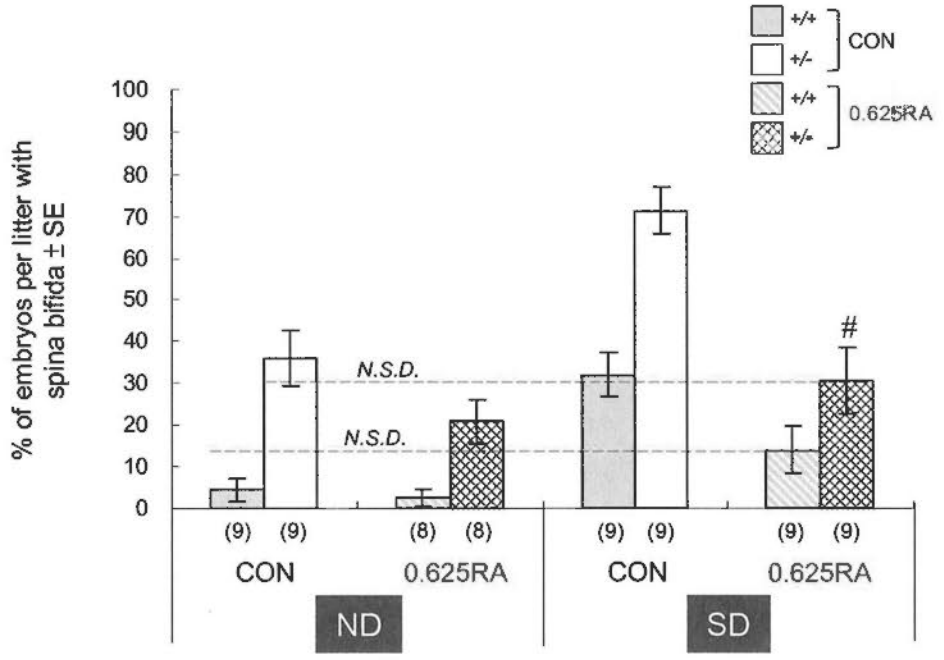

Sample size in parentheses.

Data were analyzed by one-way ANOVA followed by Bonferroni test.

$^{\#}p = 0.001$ vs. $SD^{+/-}$ (CON)

N.S.D. represents "No significant difference" between

SD (0.625RA) vs. ND (CON) of the same genotype

Graph 6.1 **Maternal blood glucose levels in non-diabetic (ND) and diabetic (SD) mice after treatment with phlorizin (PHZ) or vehicle as control (CON).**

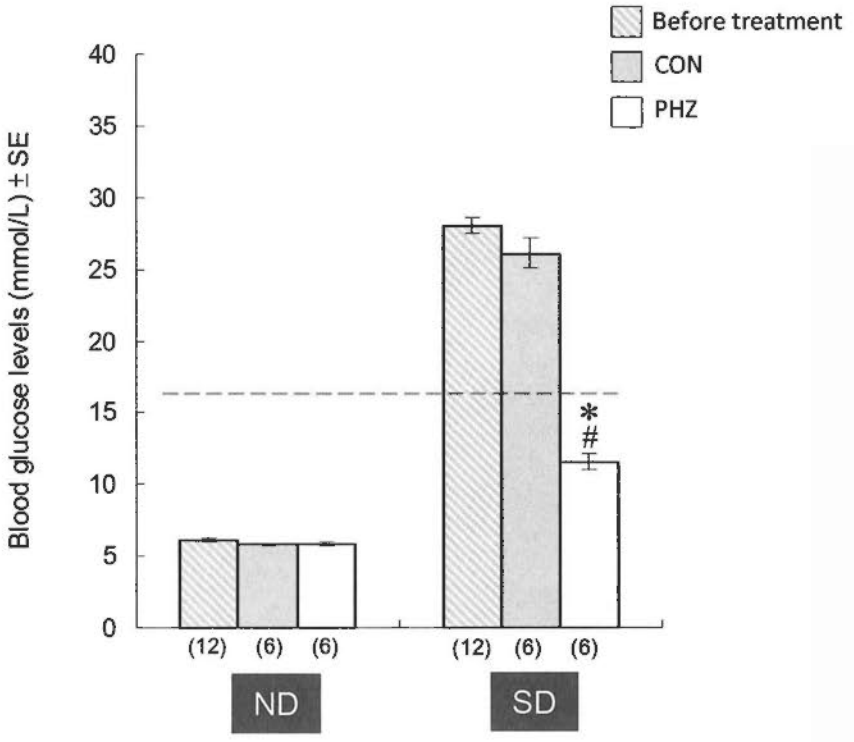

Sample size in parentheses.

Animal with blood glucose level over 16.5 mmol/L (dotted line) was defined as diabetic.

Data were analyzed by Independent Samples t-test.

* $p < 0.001$ vs. SD (CON)

Data were analyzed by Paired Samples t-test.

# $p < 0.001$ vs. SD (Before treatment)

Graph 6.2 **Relative expression levels of the 3 subtypes of *Cyp26* in (A) tail bud and (B) whole embryo (exclude tail bud) of E9.0 embryos of non-diabetic (ND) and diabetic (SD) mice treated with phlorizin (PHZ) or vehicle as control (CON).**

A. Tail bud

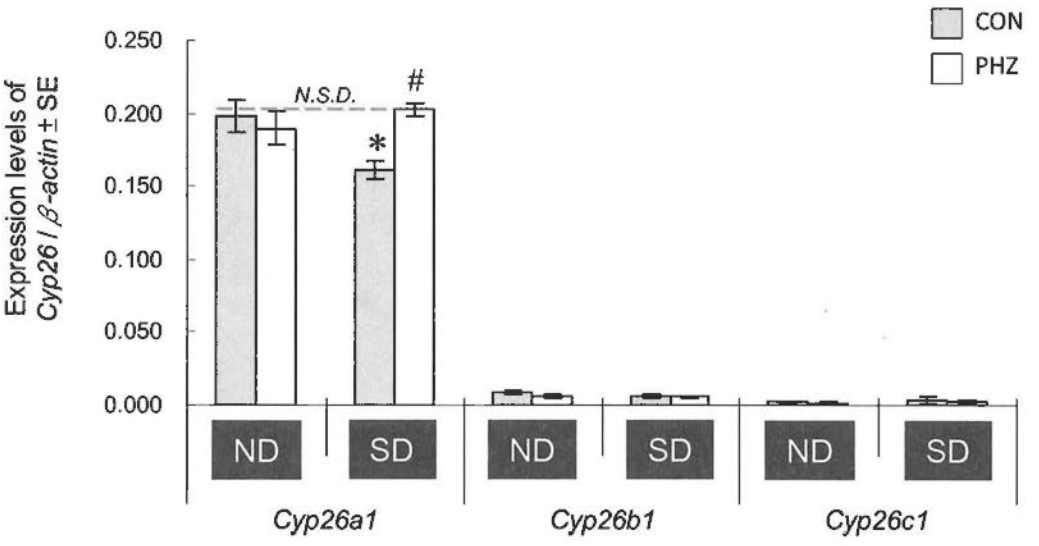

B. Whole embryo (exclude tail bud)

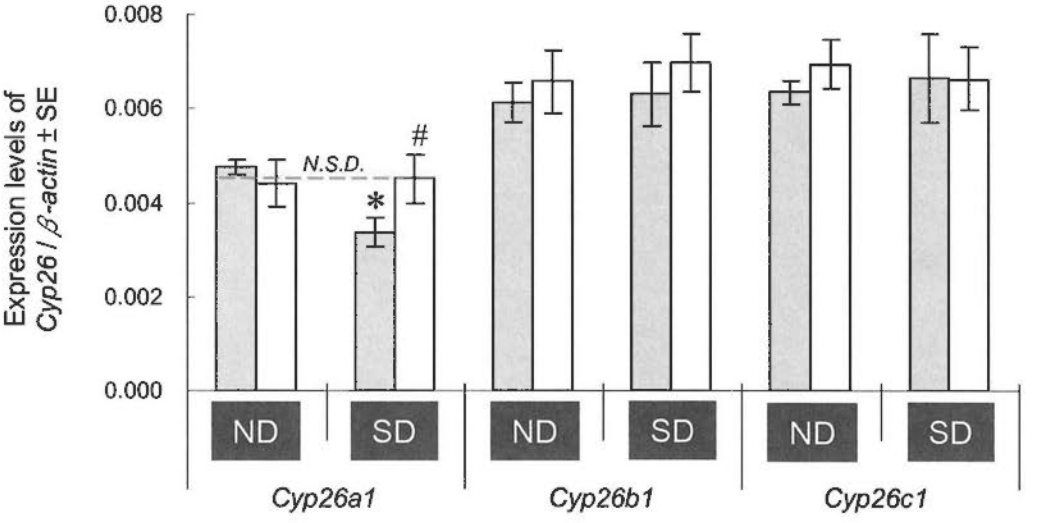

Sample size = 5 for all groups.

Data were analyzed by one-way ANOVA followed by Bonferroni test.

* $p < 0.01$ vs. ND (CON)

# $p < 0.005$ vs. SD (CON)

N.S.D. represents "No Significant Difference" between SD (PHZ) vs. ND (CON)

Graph 6.3 **Endogenous RA levels in E9.0 embryos of non-diabetic (ND) and diabetic (SD) mice treated with phlorizin (PHZ) or vehicle as control (CON) as determined by RA-responsive cell line.**

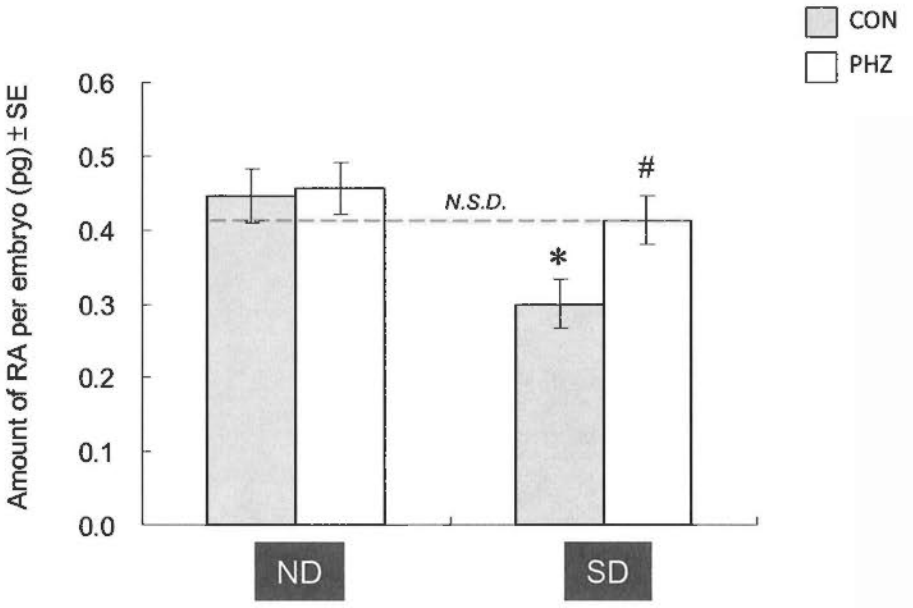

Sample size = 6 for all groups.

Data were analyzed by one-way ANOVA followed by Bonferroni test.

* $p = 0.005$ vs. ND (CON)

# $p < 0.05$ vs. SD (CON)

N.S.D. represents "No Significant Difference" between SD (PHZ) vs. ND (CON)

Graph 6.4 ***In vitro*** **RA degrading activity in (A) tail bud and (B) whole embryo (exclude tail bud) of E9.0 embryos of non-diabetic (ND) and diabetic (SD) mice treated with phlorizin (PHZ) or vehicle as control (CON).**

A. Tail bud

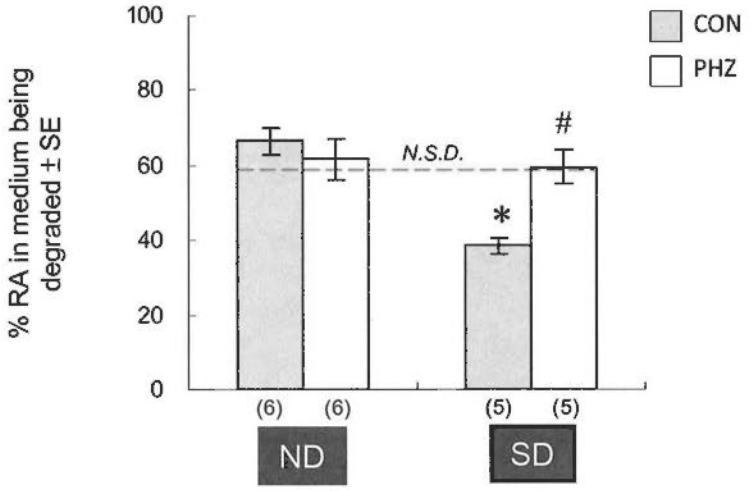

B. Whole embryo (exclude tail bud)

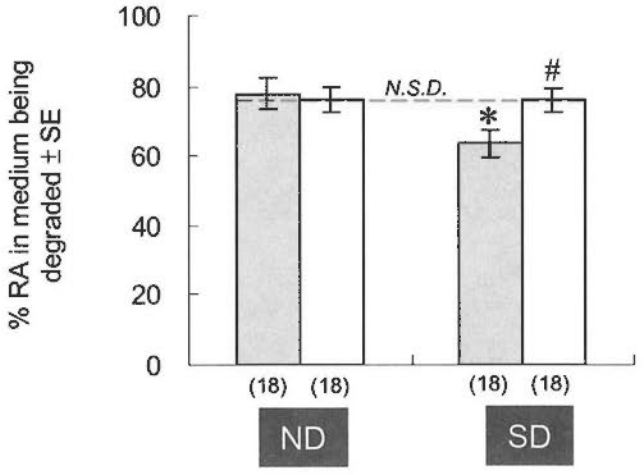

Sample size in parentheses.

Data were analyzed by one-way ANOVA followed by Bonferroni test.

* $p < 0.01$ vs. ND (CON)

# $p < 0.05$ vs. SD (CON)

N.S.D. represents "No Significant Difference" between SD (PHZ) vs. ND (CON)

Graph 6.5 **RA levels in (A) tail bud and (B) whole embryo (exclude tail bud) of embryos of control (CON) or phlorizin-treated (PHZ) non-diabetic (ND) and diabetic (SD) mice at 3 hr after maternal injection of 25 mg/kg RA on E9.0.**

A. Tail bud

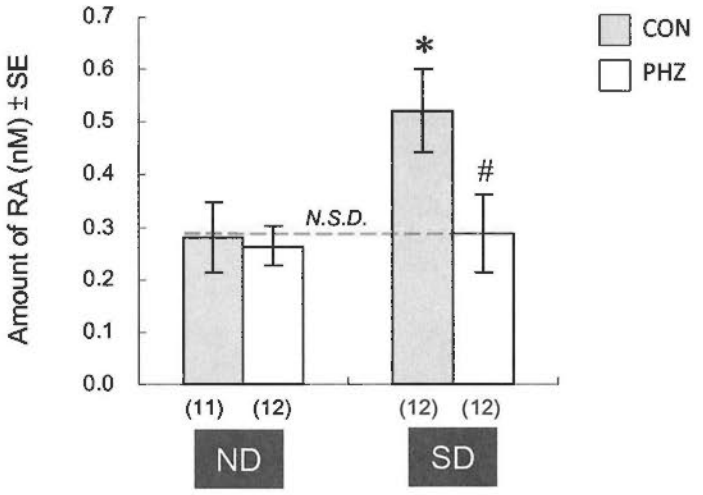

B. Whole embryo (exclude tail bud)

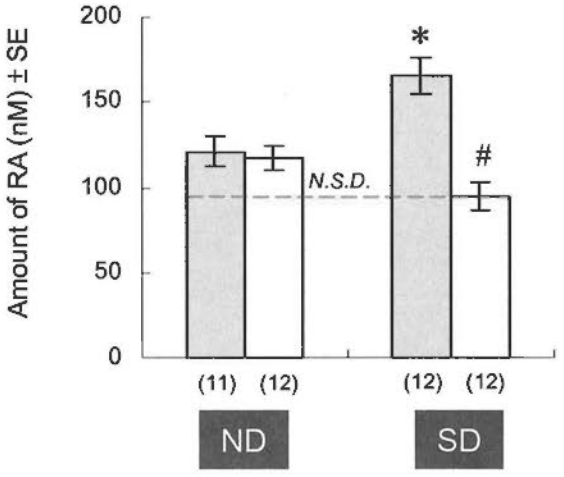

Sample size in parentheses.

Data were analyzed by one-way ANOVA followed by Bonferroni test.

* $p < 0.05$ vs. ND (CON)

# $p < 0.005$ vs. SD (CON)

N.S.D. represents "No Significant Difference" between SD (PHZ) vs. ND (CON)

Graph 6.6 **Incidence rates of (A) caudal regression, (B) cleft palate and (C) renal malformations in E18 fetuses of control (CON) or phlorizin-treated (PHZ) non-diabetic (ND) and diabetic (SD) mice induced by maternal injection of 25 mg/kg RA on E9.0.**

A. Caudal regression

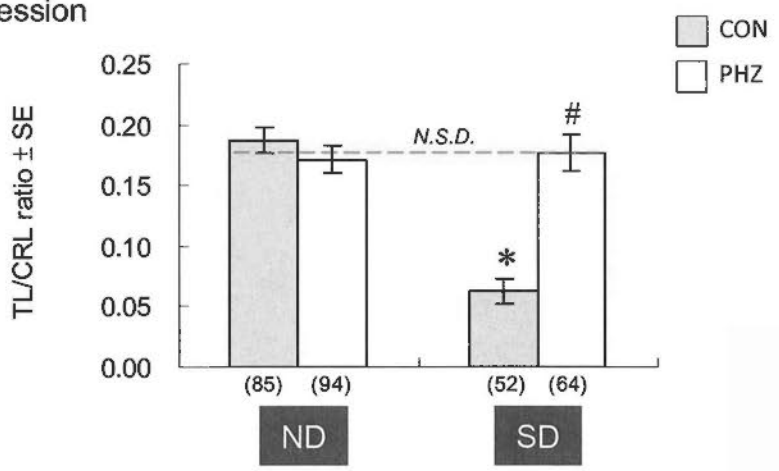

B. Cleft palate

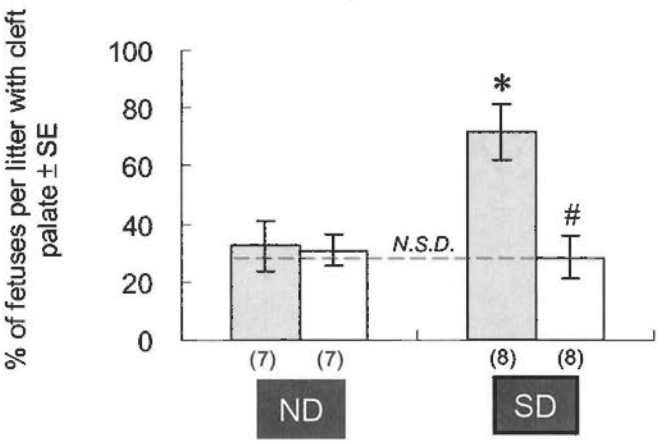

C. Renal malformations

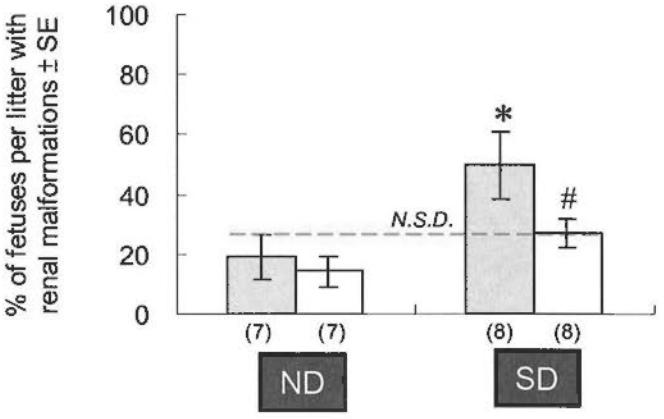

Sample size in parentheses.

Data were analyzed by one-way ANOVA followed by Bonferroni test.

* $p < 0.05$ vs. ND (CON)

# $p < 0.005$ vs. SD (CON)

N.S.D. represents "No Significant Difference" between SD (PHZ) vs. ND (CON)

Graph 6.7 **Relative expression levels of the 3 subtypes of *Cyp26* in (A) tail bud and (B) whole embryo (exclude tail bud) of rat embryos cultured for 24 hr in medium supplemented with varying concentrations of D-glucose or the solvent as control (CON).**

A. Tail bud

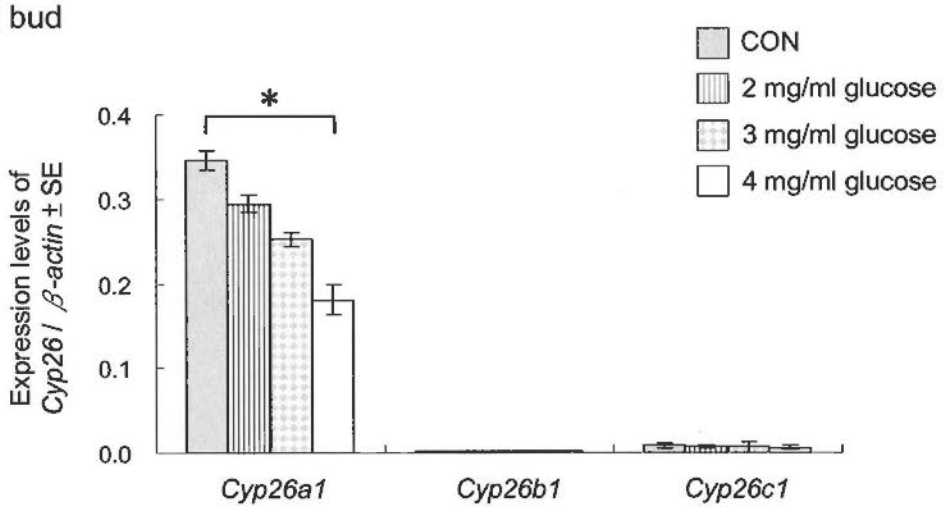

B. Whole embryo (exclude tail bud)

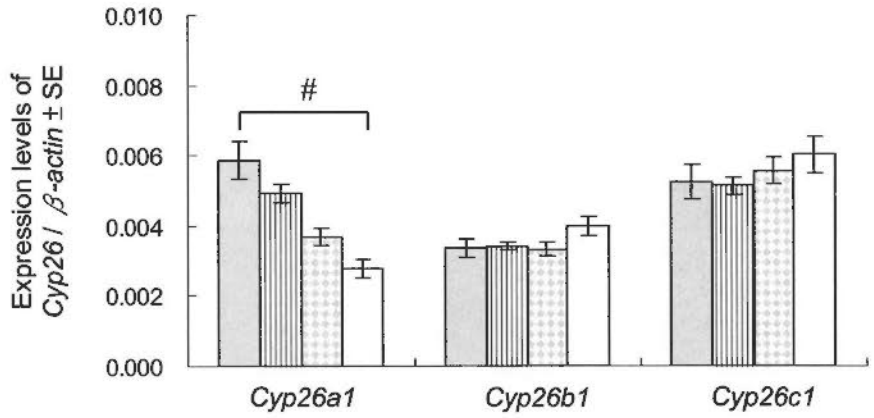

Sample size = 5 for all groups.

Correlation between glucose concentration and *Cyp26* expression level was analyzed by Pearson's correlation.

$r = -0.911$, $^{*} p < 0.001$

$r = -0.793$, $^{\#} p < 0.001$

Graph 6.8 **Relative expression levels of the 3 subtypes of *Cyp26* in (A) tail bud and (B) whole embryo (exclude tail bud) of rat embryos cultured for 48 hr in medium supplemented with varying concentrations of D-glucose or the solvent as control (CON).**

A. Tail bud

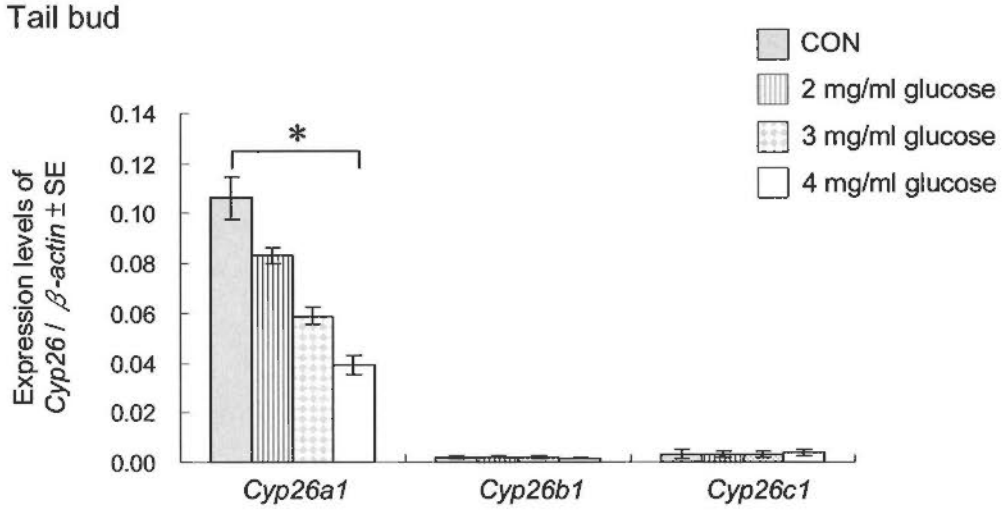

B. Whole embryo (exclude tail bud)

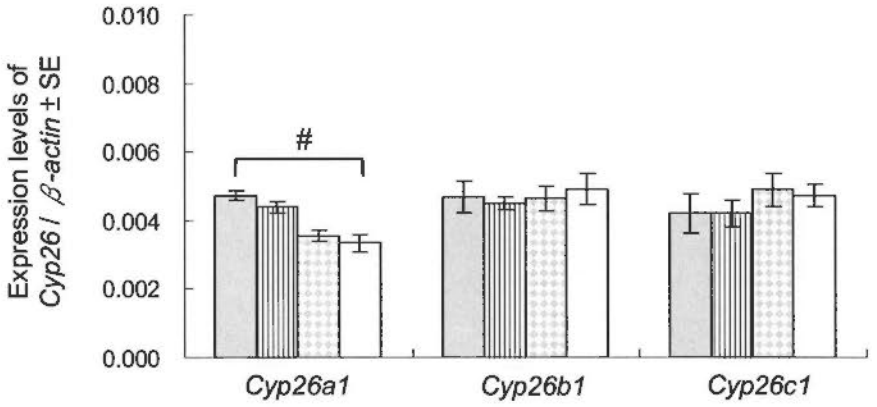

Sample size = 5 for all groups.

Correlation between glucose concentration and *Cyp26* expression level was analyzed by Pearson's correlation.

$r = -0.931$, $^{*}p < 0.001$

$r = -0.693$, $^{\#}p < 0.001$

Graph 6.9 **Endogenous RA levels in rat embryos cultured for 48 hr in medium supplemented with varying concentrations of D-glucose or the solvent as control (CON) as determined by the RA-responsive cell line.**

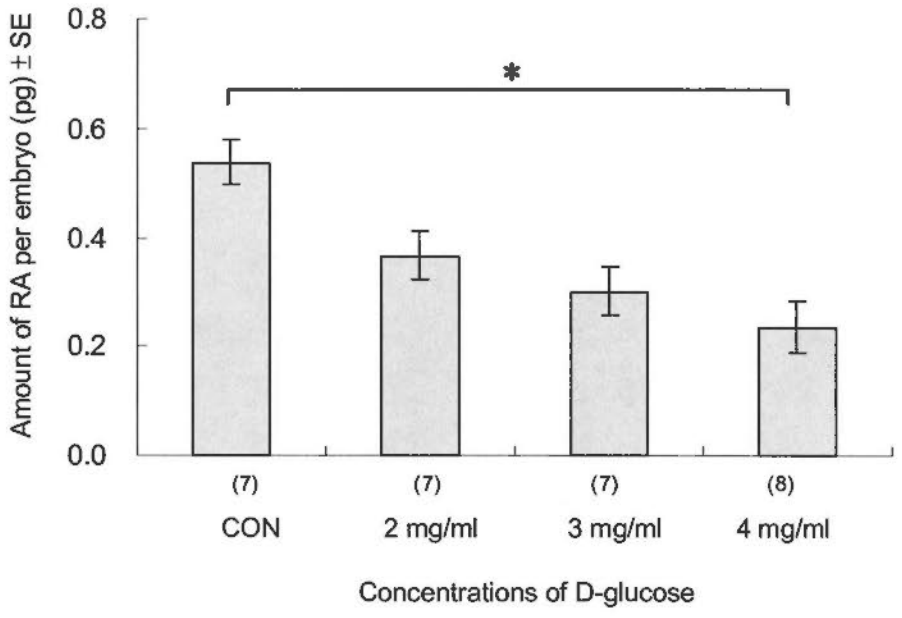

Sample size in parentheses.

Correlation between glucose concentration and endogenous A level was analyzed by Pearson's correlation.

$r = -0.700$, * $p < 0.001$